uOttawa

L'Université canadienne
Canada's university

FACULTÉ DES ÉTUDES SUPÉRIEURES ET POSTOCTORALES

uOttawa

L'Université canadienne
Canada's university

FACULTY OF GRADUATE AND POSDOCTORAL STUDIES

Indira Thapa

AUTEUR DE LA THÈSE / AUTHOR OF THESIS

M.Sc. (Chemistry)

GRADE / DEGREE

Department of Chemistry

FACULTÉ, ÉCOLE, DÉPARTEMENT / FACULTY, SCHOOL, DEPARTMENT

C-Linked AFGP Analogues Containing ß-Amino Acids: Preparation, Assessment and In Vitro Studies

TITRE DE LA THÈSE / TITLE OF THESIS

Dr. R. Ben

DIRECTEUR (DIRECTRICE) DE LA THÈSE / THESIS SUPERVISOR

CO-DIRECTEUR (CO-DIRECTRICE) DE LA THÈSE / THESIS CO-SUPERVISOR

EXAMINATEURS (EXAMINATRICES) DE LA THÈSE / THESIS EXAMINERS

Dr. T. Durst

Dr. N. Goto

Gary W. Slater

Le Doyen de la Faculté des études supérieures et postdoctorales / Dean of the Faculty of Graduate and Postdoctoral Studies

C – Linked AFGP Analogues Containing *β*-Amino Acids: Preparation, Assessment and *In Vitro* Studies

by
Indira Thapa

Thesis submitted to the
Faculty of Graduate & Postdoctoral Studies
University of Ottawa
in partial fulfillment of the requirements for the
M. Sc. degree in the
Ottawa-Carleton Chemistry Institute

Candidate

Indira Thapa

Supervisor

Professor Robert N.Ben

Your file Votre référence
ISBN: 978-0-494-18472-1
Our file Notre référence
ISBN: 978-0-494-18472-1

This work is dedicated to my mother and my late father who are always with me in every struggle of my life.

The most beautiful experience we can have is the mysterious – the fundamental emotion which stands at the cradle of true art and true science.

– Albert Einstein

ABSTRACT

Antifreeze Glycoproteins (AFGPs) are peptide-based compounds present in the blood serum of arctic and antarctic fish. These compounds inhibit the growth of ice and are key to their survival in icy cold water. The mechanism by which they inhibit the ice growth is regarded as an adsorption-inhibition process at the macromolecular level. However, the mechanism of action at the molecular level is still under debate among researchers. Our laboratory has been designing *C*-Linked AFGP analogues possessing enhanced chemical and biological stability for the purpose of structure-activity relationship studies. Towards this end, a series of AFGP analogues containing a β-amino acid in the polypeptide backbone have been synthesized. The requisite glycosylated β-amino acids in the building blocks were synthesized via a modified Arndt-Eistert homologation. These building blocks were then assembled into antifreeze analogues using standard solid phase synthesis protocols.

These analogues were evaluated for antifreeze-specific activity that is, for recrystallization inhibition (RI) and thermal hysterisis (TH). The analogues demonstrated a significant degree of TH, dynamic ice shaping and genuine RI activity attributed to biological antifreezes. Solution conformation of new analogues was performed using circular dichroism (CD) spectroscopy. Results showed that the overall conformation is mainly random coil.

In vitro cytotoxicity studies of these analogues at both physiological and cryogenic temperatures were performed on a human embryonic liver cell line. Except analogue **74**, the other analogues were found to be cytotoxic and cryotoxic at high analogue concentrations.

ACKNOWLEDGEMENTS

At this point of thesis completion, I shall be eternally indebted to my research advisor Professor Robert Ben for his highly inspiring and valuable guidance, continuous encouragement, advice and kindness of giving freedom during this research work. It was May the 10^{th} 2004, Rob demonstrated by himself my first reaction with diazomethane; That enthusiasm in science impressed me heartily and I was so deeply involved in my research that two years passed away like two days. I consider myself fortunate to have an ideal source of inspiration in him that will remain with me till the end of this life.

I am highly grateful to Vincent "Vinny" not only for science discussions but his helping attitude and sensitive nature was of great help for me to adjust in this entirely new environment. Liz and Roger deserve especial thanks for taking time to proof read my thesis from their busy schedule. I really appreciate you "Jenn" (Jennifer) for your help in my seminar preparation. I am also thankful to all the other members of the Ben lab, especially Frank, Suhuai, Pawel, Alex, Nicole, Gianni and Ferenc for your friendship.

Jessica, I truly appreciate your help in the cell studies. Our team with Matt (NRC) in the 'RI-project' (development of automatic RI-data processing technique) was really enjoyable and worthwhile. It would be unfair if I forget your friendship- Dr. Sara, Dr. Christophe, Dr. Park, Dr. Asim, Dr. Sharad, Dr. Melani, Alison and Lynn. I am also thankful to Dr. Glenn Facey and Ms. Cheryl for NMR support.

I would like to thank Dr. Gamboratta for letting me use his lab's IR facilities and Dr. Scaiano for CD spectroscopy. I owe all my mass spectrometry knowledge to Dr. Clem Kazakoff. His door was always open to me for discussion.

Most of all, my appreciation goes to my family for their good wishes and support to complete this study.

Finally, the University of Ottawa and financial agencies are acknowledged.

TABLE OF CONTENTS

LIST OF FIGURES

LIST OF GRAPHS

LIST OF SCHEMES

LIST OF TABLES

LIST OF ABBREVIATIONS

Ac	Acetyl
AFPs	Antifreeze proteins
AFGPs	Antifreeze glycoproteins
Ala	Alanine
Asn	Asparagine
Bn	Benzyl
Boc	*tert*-Butyloxycarbonyl
Cbz	benzyloxycarbonyl
CD	Circular dichroism
CDI	1,1-Carbonyldiimidazole
DCM	Dichloromethane
DIPEA	Diisopropylethylamine
DMAP	4-Dimethylamino pyridine
DMF	*N*, *N*-Dimethyl formamide
DMSO	Dimethyl sulfoxide
DPPA	Diphenylphosphorylazide
ESI	Electrospray Ionization
Fmoc	9-Fluorenylmethoxycarbonyl
Fmoc-OSu	Fmoc-succinimide
GalNAc	*N*-Acetyl-galactosamine
Gly	Glycine
HBTU	2-(1H-Benzotriazole-1-yl)-1,1,3,3-tetramethyluronium hexafluorophosphate
Hz	Hertz
*i*BUOCOCl	Isobutyl chloroformate
J	Coupling constant
kDa	KiloDalton

Lys	Lysine
M+	Parent molecular ion
MALDI	Matrix-assisted laser desorption ionization
MLGS	Mean largest grain size
mOsmos	MilliOsmos
MS	Mass Spectrometry
MTT	Methylthiazolydiphenyl-tetrazolium bromide
MeCN	Acetonitrile
NMM	N- methylmorpholine
OD	Optical density
Orn	Ornithine
PBS	Phosphate-buffered saline
Pfp	Pentaflourophenyl
PPII	Polyproline type II
ppm	Parts per million
RI	Recrystallization inhibition
SEM	Standard error of the mean
Ser	Serine
SPS	Solid phase synthesis
SAR	Structure-activity relationship
SM	Starting Material
TBDMS	*tert*-Butyldimethylsilyl
TFA	Trifluoroacetic acid
TH	Thermal hysteresis
Thr	Threonine
TMSOTf	Trimethylsilyltrifluoromethane sulfonate
TNBS	2,4,6-Trinitrobenzenesulfonic acid

Chapter 1

1.0 General Introduction

Darwinism explains that among the "organic beings" only those that can adapt to their changing environment survive. In the Earth's geological past when sea level glaciation occurred, a special protective mechanism evolved in various species of fish to prevent death due to the freezing temperatures.[1, 2] This mechanism utilizes antifreeze proteins and antifreeze glycoproteins. These fish proteins are one example of adaptation in the process of evolution.

1.1 Biological Antifreezes

One problem in biology is the survival of organisms at subzero conditions. Various studies suggest that the main causes of cell damage in living systems due to inter- or intra-cellular fluid freezing are i) by the physical abnormality of the cell membrane caused by contact with ice crystals and ii) by dehydration of the cell, which results in protein denaturation or electrolytic imbalance in the intracellular fluid. However, some cold-blooded organisms, including some species of fish that cannot increase their body temperature as warm-blooded animals can, can still survive in the polar Arctic and Antarctic sea, where the water temperature may drop down to approximately -1.9 ^{o}C.[3] The key to their survival in these conditions is their ability to lower the freezing point of their blood to -2.0 ^{o}C to -2.1 ^{o}C.[4] Scholander and co-workers (1953)[5,6] were the first to discover the abnormally low freezing temperature of blood serum from bullhead fish (*Pagahenia borchgrevinki*) and Antarctic cold icefish (*Dissostichus mawsoni*). This is not due to the presence of any colligatively acting substances present in the blood. A colligative effect depends on the number of moles of solute present in the solution rather

than on their chemical nature. It was found that the concentrations of colligative substances in the fish fluids are very low, such that they contribute to the freezing point depression only up to -0.86 °C. This 1 °C difference in temperature is attributed to the antifreeze glycoproteins (AFGPs) which are found in the sera of these fish.[7, 8, 9] Relative to colligative salts, AFGP is found to be 200-500 times more effective, on a molar basis, in lowering the freezing point of the intracellular fluid of a cell without increasing the osmotic pressure.[10] This is illustrated by comparing the freezing points of AFGPs, galactose, chicken lysozyme (a protein) and sodium chloride solution (Figure 1.1).[11] It has been shown that at low concentration, AFGPs are slightly more active than sodium chloride in lowering the freezing point of water but it is hundred times greater on a molar basis. The study suggested that the unique structural feature associated with AFGPs is attributed to their potent freezing point depression property rather than their high molecular weight. Neither the carbohydrate nor protein components are effective alone. As the concentration is increased, AFGPs show a point where its maximum activity is reached. This implies a non-linear relationship between activity and concentrations. In addition, the presence of NaCl in AFGP solution has been demonstrated to increase the observed freezing point depression. This suggests that colligative substances do not interact with the AFGPs, but rather, they show an additive effect.

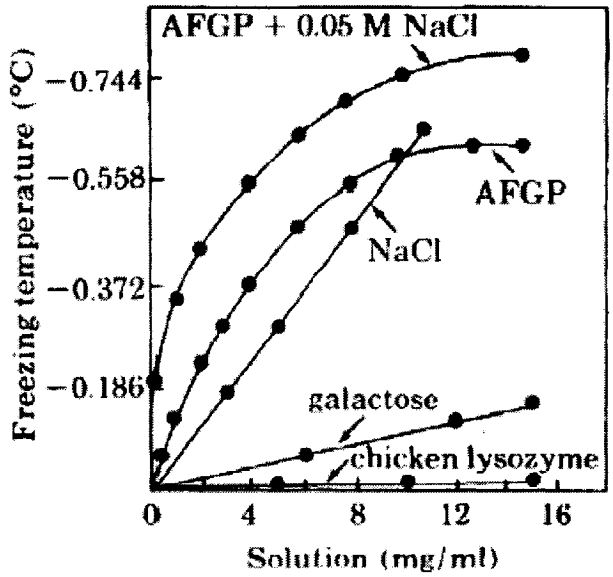

Figure 1.1: Illustration of freezing temperatures of chicken lysozyme, galactose, sodium chloride, AFGPs and AFGPs plus sodium chloride.[11]

1.1.1 "Antifreeze" Properties

1.1.1.1 Thermal Hysteresis (TH)

While they depress the freezing point, biological antifreezes exert a minimal effect on the melting point. This difference between the melting point and freezing point is termed *thermal hysteresis* (TH) and is a characteristic property of antifreezes.[10] Graph 1.1 illustrates that the melting temperature (T_m) is greater than the freezing temperature (T_f) in biological antifreezes whereas the melting and freezing temperatures of water are both equal to 0 °C.[12] The colligatively acting substances such as sodium chloride in water also depress the freezing point below 0 °C but the melting temperature (T_m) is equal to freezing temperature (T_f). The size of the TH gap induced by biological antifreezes is dependent upon the type and concentrations of biological antifreeze present. For instance, at physiological concentration, the TH gap of insect and fish antifreezes are ~5-

6 °C and ~2 °C, respectively, whereas plants have comparatively poor TH activity of only 0.1 to 0.5 °C.[13, 14] The narrow TH gap in fish is enough to protect them from cryoinjury and death. The TH gap is used to detect and quantify antifreeze activity.

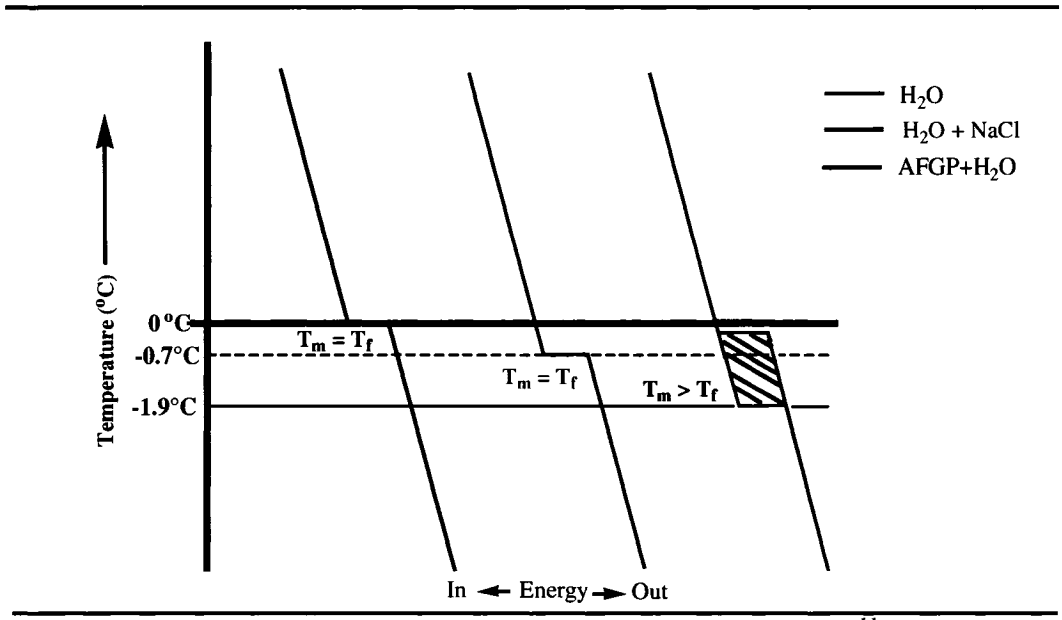

Graph 1.1: Qualitative illustration of thermal hysteresis (TH)[11]

1.1.1.2 Dynamic Ice Shaping

Within the TH gap ice crystal growth is inhibited. This occurs due to the adsorption of antifreeze onto specific faces of an ice crystal. This adsorption results in different polymorphic forms of the ice crystal.[15] This phenomenon is known as "dynamic ice shaping." Biological antifreezes are found to adsorb preferentially onto the prism faces of ice crystal (Figure 1.2b). Figure 1.2a, is an illustration of the basal faces ('c' axis) and prism faces ('a' axis) in an ice crystal.

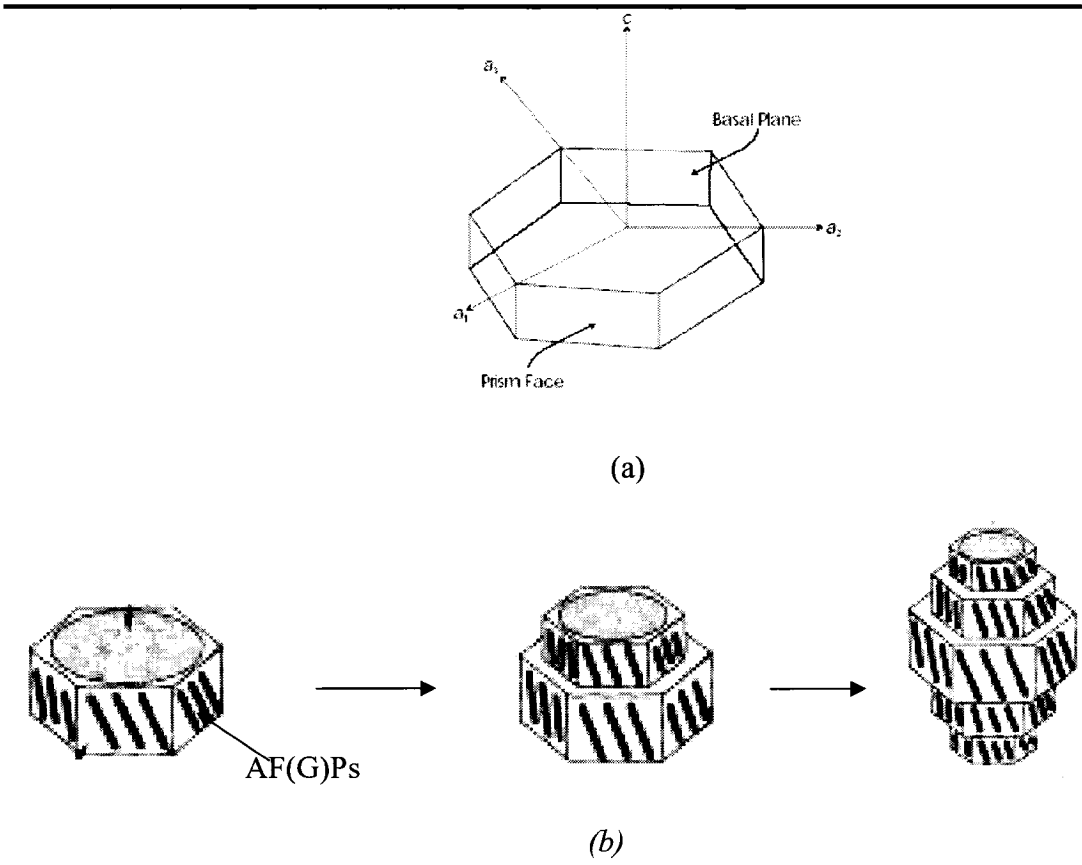

Figure 1.2: a) Hexagonal ice crystal showing basal ('c' axis) and prism faces ('a' axis) b) Dynamic ice shaping due to the adsorption of AFGPs on the prism faces resulting in the formation of bipyramidal ice crystal[16]

Adsorption of antifreeze molecules onto the normal ice growth plane restricts its growth along the 'a' axis (i.e prism faces) which eventually forces the addition of water molecules on the 'c' axis (i.e. basal faces) resulting in the formation of hexagonal bipyramidal ice crystals (Figure 1.2b).[16, 17, 18]

1.1.1.3 Recrystallization Inhibition (RI)

Another significant property of biological antifreezes is their ability to inhibit ice recrystallization. When a solution initially freezes, small crystals are formed, but during

the rewarming process ice crystals grow larger at the expense of smaller crystals.[19] In fact, this migration of ice boundaries occurs to minimize the overall energy of the system by decreasing the surface area in an enthalpically driven process. Antifreezes bind to the ice crystals at the ice–water interface and prevent ice boundary migration and consequently inhibit ice recrystallization.[20] This can be seen experimentally when a solution of antifreeze glycoprotein fraction 8 (AFGP 8) is compared with a PBS control solution (Figure 1.3).[21] Image A shows indistinguishable ice crystals in the presence of AFGP 8 solution whereas Image B Illustrates comparatively larger ice crystals in PBS control solution at the same magnification. This inhibitory property of antifreezes protects organisms against mechanical cell damage during ice grain boundary migration. RI is distinct from TH since it operates at much lower concentrations of biological antifreezes (100-500 times less) than the concentration required for TH activity.[22]

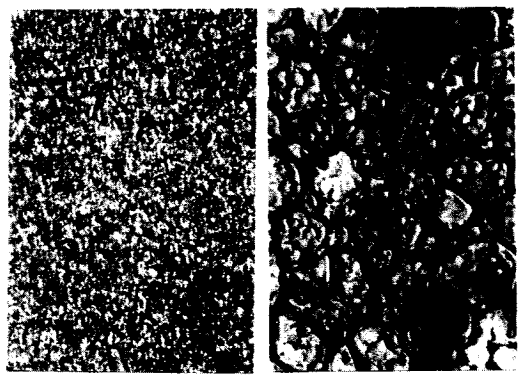

Image A: AFGP 8 **Image B: PBS**

Figure 1.3: Relative size of ice crystals in a solution of (A) AFGP 8 (B) PBS control at -6 °C after 30 minutes of annealing time[21]

1.1.1.4 Cell Membrane Stabilization

In addition to these physical properties (TH, RI, and dynamic ice shaping), biological antifreezes possess an interesting biological property which helps to protect cell membranes from the effect of cold temperature (non-freezing).[23, 24] It has been reported that cold-induced cell damage occurs during the lipid membrane thermotropic phase transition.[25, 26] During this transition, the liquid-crystalline phase is converted into a gel phase, and membrane permeability increases. This results in the leakage of cellular contents. It has been hypothesized by Wu and Fletcher that biological antifreezes bind to the lipid membrane during the cooling/rewarming process and thereby prevent leakage of the lipid membrane.[27]

1.2 Structures of Biological Antifreezes

Biological antifreezes are a diverse class of proteins found in species of fish inhabiting polar regions, as well as amphibians, trees, plants and insects.[28] In all organisms antifreezes are thought to be localized *in vivo* in the extracellular space. In the case of polar fish, biological antifreezes are synthesized in the liver, and are secreted into the blood and circulated to all fluid compartments except secreted fluids and brain.[29] Conversely, antifreezes in insects are located in the epidermal layer.[30] Plant antifreezes are secreted into the xylem, cell walls, and intracellular spaces in tissues.[31] Despite their different tissue locations in different species as well as the diverse structures, antifreezes share similar properties among the different groups. Biological antifreezes are classified mainly into two groups based on their structures. They are 1) Antifreeze Proteins (AFPs) and 2) Antifreeze Glycoproteins (AFGPs)

1.2.1 Antifreeze Proteins (AFPs)

Antifreeze proteins are further subdivided into four different types (I to IV). Each of these types possesses different primary, secondary and tertiary structures. It is hypothesized that the different types found among the different species and even within the same family are a result of independent evolution of AFPs.[32]

1.2.1.1 Type I

Duman and DeVries[33] and Hew and Yip[34] were the first to report type I AFP in the winter flounder (*Pseudopleuronectus americanus*). Since these AFPs are rich in alanine (approximately 65 %), the secondary structure is predominantly α-helix (Figure 1.4). The molecular weight ranges from 3.3 to 4.5 kDa.

Figure 1.4: Illustration of α-helix in type I AFP[35]

1.2.1.2 Type II

Natural sources of type II AFPs are the Sea Raven, the Smelt and the Atlantic herring.[36] The molecular weight of this type of protein ranges from 11 to 24 kDa, and these are rich in cysteine (8.3 mol % for Sea Rraven and 9.1 mol % for Atlantic herring).[37] They display greater TH compared to type I AFP (but it is still lower based on molecular weight). The presence of disulfide a bond is important for its activity. The type II is a globular protein and the secondary structure is a mixtures of α-helix, β-sheet and random coil[38] (Figure 1.5).

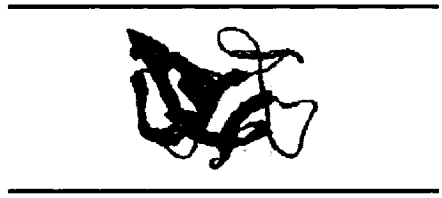

Figure 1.5: Illustration of a mixture of α-helix, β-sheets and random coil in type II AFP[35]

1.2.1.3 Type III

Type III AFP is found in the Ocean Pout (*Macrozoarces americanus*) and is composed of globular proteins.[39] It has a molecular weight of 6.5 kDa. The secondary structure is β-sandwich (Figure 1.6).

Figure 1.6: Illustration of β-sandwich in type III AFP[35]

1.2.1.4 Type IV

Type IV AFP is found in Longhorn Sculpin (*Myox ocephalus octodecimsponosis*)[40] and is composed of alanine rich helical bundles (Figure 1.7). The molecular weight is approximately 12 kDa.

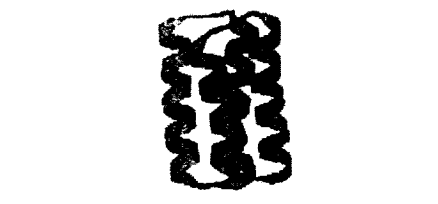

Figure 1.7: Illustration of helical bundles in type IV AFP[35]

1.2.2 Antifreeze Glycoproteins (AFGPs)

AFGPs constitute a major fraction of protein in the blood serum of Arctic cod and Antarctic notothenioid.[12] In contrast to AFPs, AFGPs show less variation in structure. The first structural evidence of AFGP was reported by DeVries in 1960.[41] A typical structure of AFGP is composed of an (L-alanine-L-alanine-L-threonine) tripeptide repeat unit in which the secondary hydroxyl group of the L-threonine residue is attached to the disaccharide β-D-galactosyl-(1,3)-α-D-N-acetylgalactosamine (Figure 1.8).[36] AFGPs can consist of 4 to 55 glycosylated tripeptide repeat units.

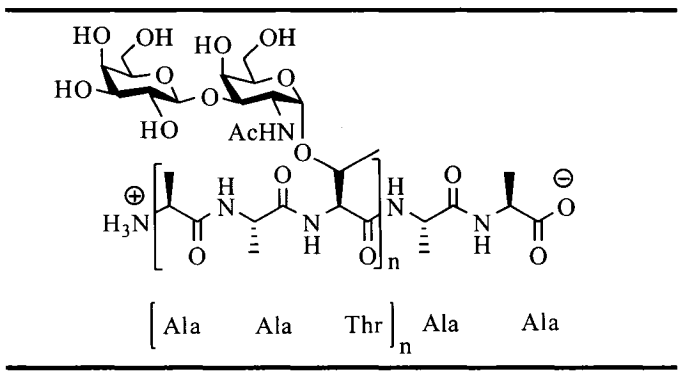

Figure 1.8: A typical structure of AFGP where n = 4 - 55

On the basis of the relative rate of electrophoretic mobility (which depends on the relative molecular weight), eight different fractions of AFGPs have been isolated.[42] The corresponding molecular weight ranges from 33 kDa to 2.6 kDa (Table 1.1).[43]

AFGP 1-2	33.7-28.8 kDa
AFGP 3-5	21.5-10.5 kDa
AFGP 6-7	5-3.8 kDa
AFGP 8	**2.6 kDa**

Table 1.1: Classification of AFGPs on the basis of molecular weight

AFGP 8 is the smallest fraction of AFGPs and is the working model for structure-function relationship studies performed in our laboratory. In some low molecular weight AFGPs, it has been found that L-alanine can be substituted by L-proline (Figure 1.9a) and L-threonine can be substituted by L-arginine (Figure 1.9b).[36]

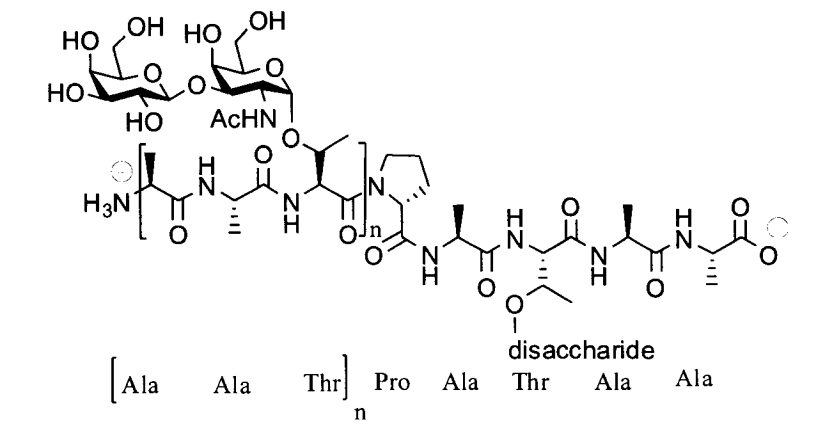

(a)

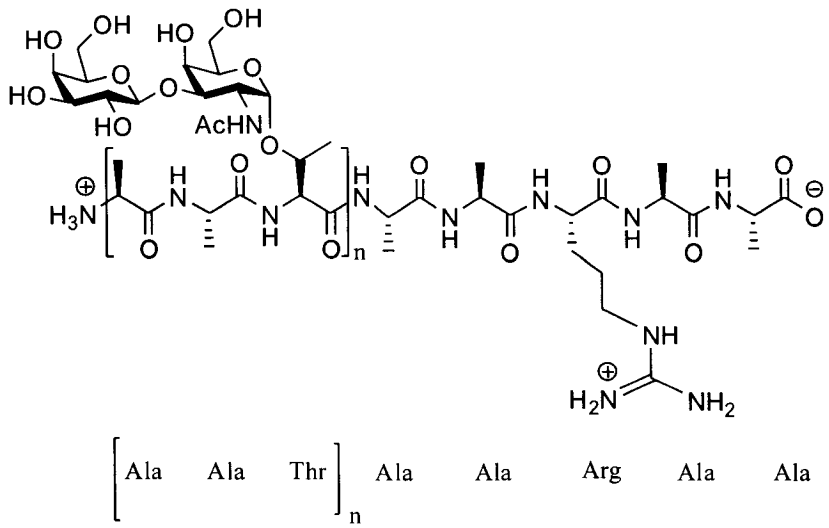

(b)

Figure 1.9: (a) AFGPs with L-proline that replaces L-alanine after L-threonine (b) AFGPs with L-arginine that replaces L-threonine

Regardless of the modification on the peptide backbone, each AFGP contains both hydrophilic disaccharide unit and hydrophobic L-alanine residues (almost 67 %).

1.3 Structure-Activity Relationships

Early structure-activity relationship studies have been performed on native AFGP via enzymatic and chemical modifications (Figure 1.10).[36] These early studies provided some valuable information about the importance of the carbohydrate moeity on antifreeze activity.[28, 44, 45] Antifreeze activity was found to be lost when AFGP was treated with 0.5N NaOH, due to β-elimination of the disaccharide component. Acetylation of the hydroxyl groups on the disaccharide as well as periodate oxidation to give aldehyde derivative both resulted in loss of TH activity. This implies that the hydroxyl groups in the disaccharide moiety are important for TH activity. Oxidation of the C-6 hydroxyl groups to produce the bis-aldehyde did not give any change in TH activity, suggesting that the C-6 hydroxyl groups do not play a role in TH activity. However, further oxidation to give the carboxylate derivative or conversion into a sulfite derivative removed all activity. This indicates that a negative charge on the disaccharide component is not favourable for TH activity. Further, information about the carbohydrate moiety was observed when borate derivates of disaccharide was formed by metal complexation at the C-3 and C-4 or C-4 and C-5 positions of the terminal galactose moiety. This result suggested that the cis-3,4 hydroxyl groups in carbohydrate are required for TH activity.

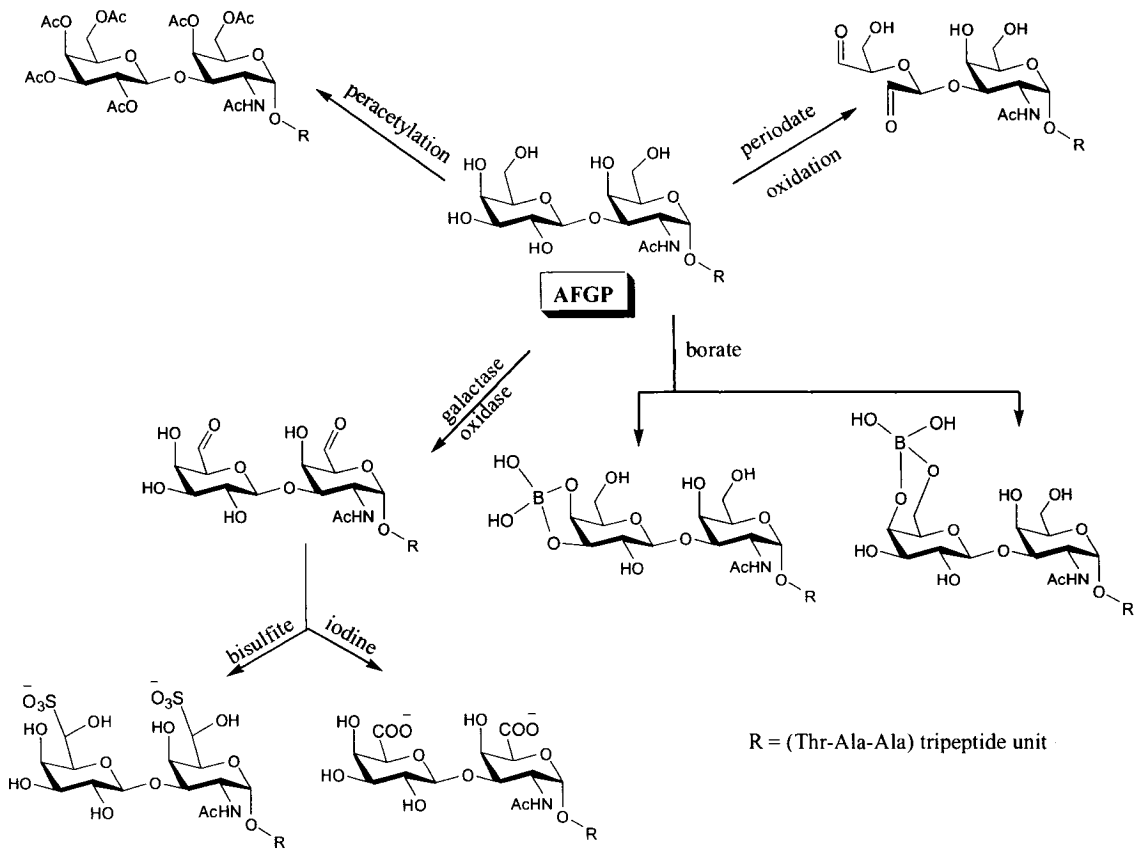

Figure 1.10: Structure- activity relationship studies on native AFGP[12]

However, these studies left some additional unanswered questions which were addressed by Nishimura.[46] They synthesized a series of AFGP analogues using a diphenylphosphorylazide (DPPA)-promoted polymerization. All of these analogues were tested for TH activity and laid out the findings as follows:

1. α-configuration of the *O*-glycosidic linkage is required for TH activity.
2. N-acetyl group at the C-2 position of the reducing sugar are essential for TH activity.
3. β-methyl group of the threonine residue also plays a role in TH activity.

Thus, in addition to the hydrophilic carbohydrate, the hydrophobic amino acid side chain likely also plays a role in determining antifreeze specific-activity of AFGPs.[41] However, the influence of the amino acid backbone on TH activity has yet to be fully explored.

1.4 Mechanism of Action

The current generally accepted working hypothesis for mechanistic studies was put forth by Raymond and DeVries in 1977. According to this hypothesis, the antifreeze molecules adsorb onto the surface of the growing ice front.[47] This event restricts the growth of ice in between the adsorbed AFGP molecules. As the temperature continues to decrease, these ice fronts grow with a large radius of curvature (Figure 1.11). Further addition of water molecules to this convex surface is thermodynamically unfavorable. This results in a non-equilibrium freezing point depression known as the **Kelvin effect**.[48]

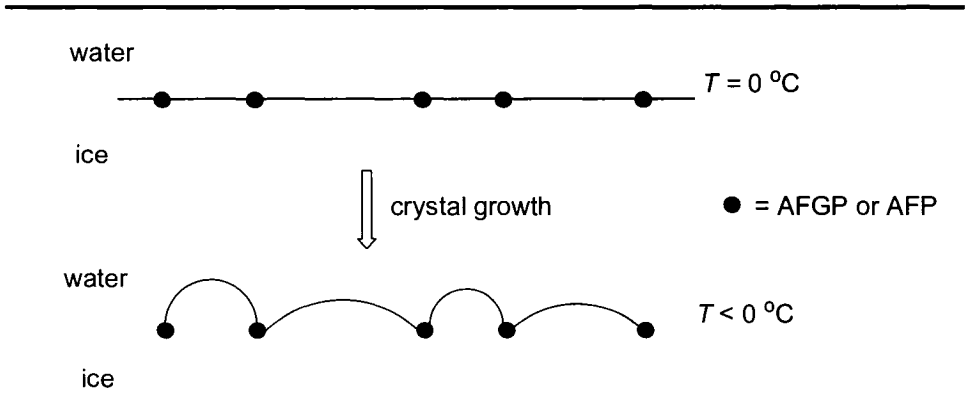

Figure 1.11: Schematic representation of the adsorption- inhibition mechanism

Given the hypothesis that the ice-water interface is static, the adsorption of AFGPs and AFPs onto the ice surface is thought to be irreversible. The irreversible

binding concept is supported by 3D models proposed by Knight[49] and Wilson.[50] However, Kuroda[51] doubted the irreversible binding of ice and put forth a reversible binding concept. Still another hypothesis is proposed by Hall and Lips.[52] Their hypothesis depends on the ability of AFGPs and AFPs to lower the energy of the system by lowering the nucleation temperature. Thus, there is continued controversy over the mode of ice-binding.

The adsorption-inhibition mechanism explains the ice binding affinity of AFGPs on a macromolecular level; however, the mechanism at the molecular level remains under debate.[53] Researchers are divided in support of either a hydrophilic or hydrophobic interaction to explain AFGP-ice binding.[54, 55]

1.4.1 The Proposed Role of Hydrophilic Interactions in Binding to Ice

It has been proposed that hydrogen bonding between the hydroxyl groups of the carbohydrate and the ice surface is responsible for ice binding. However, studies have shown that the number of potential hydrogen bonds contributed by AFGPs is insufficient for adequate binding with the ice lattice.[56] Previous studies revealed that only two hydroxyl groups in a disaccharide are in a suitable position to form hydrogen bonds with the ice surface. As shown in Figure 1.12A, if one hydroxyl group is presumed to form only one hydrogen bond and as AFGP 8 is composed of four glycosylated amino acid tripeptide repeat units then there can only be eight hydrogen bonds with the ice surface per molecule of AFGP 8.[28] The above mentioned theory of hydrophilic interaction between the hydroxyl group of the disaccharide unit and the water molecule on the ice

surface was revised by Knight and co-workers.[56] They proposed that the hydroxyl groups of the disaccharide are in fact incorporated into the ice lattice as shown in Figure 1.12B.

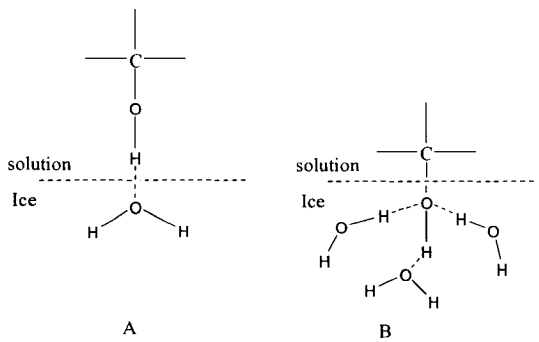

Figure 1.12: Hydrophilic interaction between ice surface and AFGP 8:

A) Hydrogen bonding interaction on the ice surface

B) Hydrogen bonding interaction within the ice lattice

Thus, each hydroxyl group forms three hydrogen bonds inside the ice lattice and this therefore makes a total of twenty-four hydrogen bonds per molecule of AFGP 8. This model supports the hydrogen-bonding hypothesis which has dominated the discussion among researchers.

The hydrogen bond hypothesis was studied for AFP I primarily by DeVries[57] (Figure 1.13a) and was later revised by Wen & Laursen (Figure 1.13b).[58] According to DeVries original model the hydroxyl group of the threonine and the carboxyl group of the aspartates form hydrogen bonds to oxygen atoms on the prism faces of ice crystals as illustrated in Figure 1.13a. The revised model by Wen and Laursen shows that the polar groups are within the hydrogen bonding range of the oxygen atoms in the ice lattice and bind to the pyramidal plane of prism faces on the ice as illustrates in Figure 1.13b.

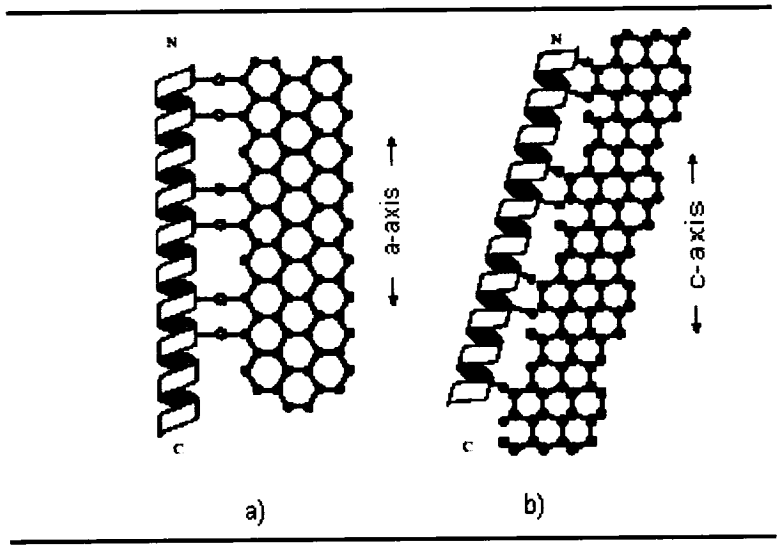

Figure 1.13: a) Original model for hydrogen bonding hypothesis for AFP I Proposed by DeVries, b) Revised model proposed by Wen & Laursen

The latter hypothesis is supported by the molecular modeling studies done by Madura and co-workers.[59] Their model suggests that polar groups of the amino acid side chains of Type I AFP are embedded into the ice lattice (Figure 1.14).

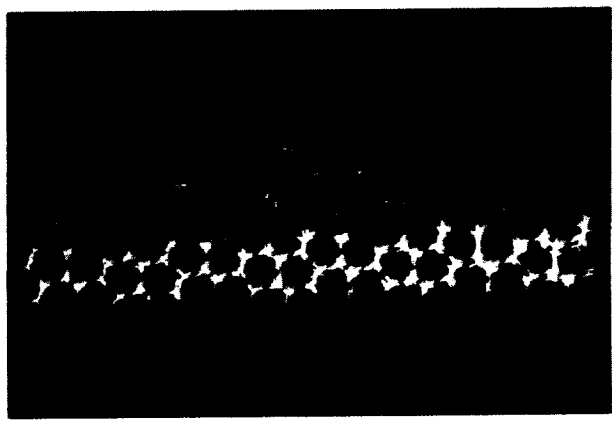

Figure 1.14: Molecular modeling of type I AFP

1.4.2 The Proposed Role of Hydrophobic Interactions in Binding to Ice

Structure-function studies performed on AFP I by the substitution of L-threonine residues with L-serine and L-valine residues indicate that hydrogen bonding may not be the key to ice binding.[54, 60, 61] These studies showed that when L-threonine residues were replaced with L-serine residues the TH activity of AFP I was lost. This was surprising since serine can form hydrogen bonds with the same affinity for ice binding as L-threonine can. However, replacement of L-threonine with L-valine showed only a small loss in activity. This indicated that the methyl group in L-threonine is important for ice binding. The recent studies done on AFGP by Nishimura and co-workers[46] have shown that the same hypothesis as for AFPs can hold true for the hydrophobic interaction between the AFGP molecules and the ice surface. They replaced L-threonine residues with L-serine residues to construct an (L-ala-L-ser-L-ala) AFGP analogue. When it was tested for TH, this analogue was found to be completely inactive. This demonstrated the importance of methyl group for the TH activity.

Despite these findings, a unified molecular mechanism that explains hydrophobic or hydrophilic interaction for the adsorption process between the protein and ice surface has not been postulated.[28]

1.5 Conformational Studies

One of the most important aspects for understanding the molecular mechanism of ice-binding is the conformational analysis of these complex polymers. Conformational analyses of AFGPs have focused mainly on the secondary structure. The conformation of AFGPs in solution may have a significant role in the interaction between the different

AFGP functional groups and the ice surface. Two main techniques are used to determine the AFGP conformation in solution; they are Circular Dichroism (CD) spectroscopy and Nuclear Magnetic Resonance (NMR).

Previous CD studies on AFGP demonstrated that random coil is the main contributor to secondary structure.[62, 63, 64] However, Franks and Morris[65] later reported an ordered three-fold left-handed helical conformation based on CD studies. The authors suggested that in such a conformation, disaccharide residues are aligned on only one side of the helix. Bush and co-workers[66] later proposed a three-fold left-handed helical conformation of the peptide backbone, and also showed that the carbohydrate component has negligible contribution to the CD measurements. Rao and Bush[67] also suggested that the three-fold left-handed helix is a low energy conformation based on coupling constant data (from NOE experiments) and semi-empirical molecular modeling calculations. Their calculation concluded that the length of the glycopolymer is important for antifreeze activity. This is in agreement with the kinetic model of antifreeze action that states the coefficient of adsorption increases with increasing molecular weight.[68] The larger AFGP 4 shows 25 times more activity compared to the smaller AFGP 8.

Variable temperature dependent NMR studies by Bush and Feeney[69] showed that low molecular weight AFGPs adopt a rod-shaped conformation similar to that of a three-fold polyproline type II helix at lower temperatures. However, the conformation of low molecular weight AFGPs changes to a flexible coil at higher temperatures. Solution conformations of AFGP 8 performed at various temperatures by Bouvet and Ben[70] using CD spectroscopy, showed interesting results. They showed that at room temperature, random coil is the main form of the glycopeptide conformations along with the other

conformations such as α-helix, β-sheet and β-turns. These results suggested that the solution conformation of the glycoprotein is flexible and can adopt different structures at various times. Similarly, temperatures as low as -5 °C, did not have any obvious impact on the conformations.

1.6 Applications

Unique cryoprotective properties make antifreeze proteins and antifreeze glycoproteins potentially important in everyday use. Their potential uses range from medical to commercial applications. Some of these important applications are outlined following.

1.6.1 Biological Antifreezes in Medicine

Amidst the large quantity of research being done in the medical field to improve the quality of life, the long term storage of human cells and organs has been a challenging one. Due to the lack of suitable preservation techniques, hypothermic storage of these human organs is limited to 12-20 hours (depending on the organ). As the temperature is lowered, cell death occurs due to inter- and intra-cellular ice formation.[71] This causes cell damage both through mechanical stress and osmotic imbalance. Some practical cryoprotectants such as DMSO and glycerol can keep the cells in a super-cooled state, but they cannot block extra cellular ice formation.[72] To overcome this problem, vitrification has been used for cryopreservation of biological systems.[73] Vitrification is a rapid cooling technique in which a highly concentrated solution of cryoprotectants is used and the samples are converted into a "glassy" state to avoid ice formation. The high

concentration of cryoprotectant in turn is associated with toxicity. Another limitation of vitrification is that it is only suitable for small sample volumes, since the cooling rate is not uniform for large volumes and therefore recrystallization will still occur during warming.[74] On the other hand, antifreeze glycoproteins stabilize the membrane during cooling, inhibit ice growth during freezing, and inhibit ice recrystallization during warming. These unique properties make it an attractive alternative to conventional cyoprotectants.[75]

Rubinsky and co-workers[71] have suggested that upon vitrification of pig oocytes (two-cell-stage embryos) with 40 mg/mL AFGPs, cell integrity is retained. However, freezing of red blood cells in the presence of 40 μg/mL of AFGPs reduced cell survival. Cell damage is thought to occur due to the formation of needle-shaped ice crystals (Figure 1.15) when the temperature is lowered below the TH gap.

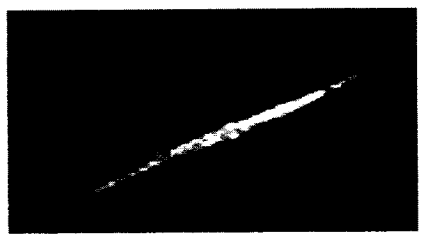

Figure 1.15: AFGP 8, ice spiculate below the TH gap

This destructive behaviour of biological antifreezes was utilized by Rubinsky for cryosurgery. Cryosurgery is a technique generally employed in oncology to destroy and prevent the undesired tissue by the help of freezing. A series of recent papers on cryosurgery[76, 77] have suggested that *in vivo* testing of AFP I solution to destroy tumor cell gave encouraging results as the mortality rate of cancer cells was found to be almost

100 %. This is the dual nature of antifreezes, they act as both cryoprotectants as well as chemical adjuvants in cryosurgery.

1.6.2 Antifreeze in Commerce

Another important potential application of biological antifreeze is its use in genetic engineering. Atlantic salmon does not possess biological antifreezes and is under constant threat of cryoinjury. This species could be protected by transferring the AFP gene responsible for antifreeze.[78] The AFP gene also imparts resistance to "White Pox" (a common disease for Salmon) as well as, it helps them to grow larger, up to four times their normal size, and this at a much faster rate. This is useful for salmon farming. Similarly, AFP genes were successfully introduced into potato leaves and other plants[79] to improve their resistance to frost damage. Crop damage from frost is a serious problem around the world.

1.6.3 Antifreeze in Industry

Antifreeze could be used in the food industry as an additive to improve quality and palatability of food by maintaining the smooth texture and taste (after freezing) through inhibition of recrystallization.[75]

1.7 Previous Syntheses of AFGPs and AFGP Analogues

Despite the enormous number of potential applications of AFGPs, these applications have not been fully realized due to the difficulty in accessing these compounds from their natural reservoirs. The chemical synthesis of AFGPs and their analogues could be viable alternative. Some of these endeavours are presented here.

1.7.1 Anderson's Synthesis of an Analogue for the Core Repeating AFGP Unit

The first approach to the synthesis of the structural core of an AFGP analogue was carried out by Anderson and co-workers.[80] As shown in Scheme 1.1, the β-D-galactosyl-(1,3)-α-D-N-acetylgalactosamine moiety of the native system was replaced with β-D-galactosyl-(1,3)-α-D-galactose. This convergent approach consisted of separate syntheses of the disaccharide and the tripeptide units.

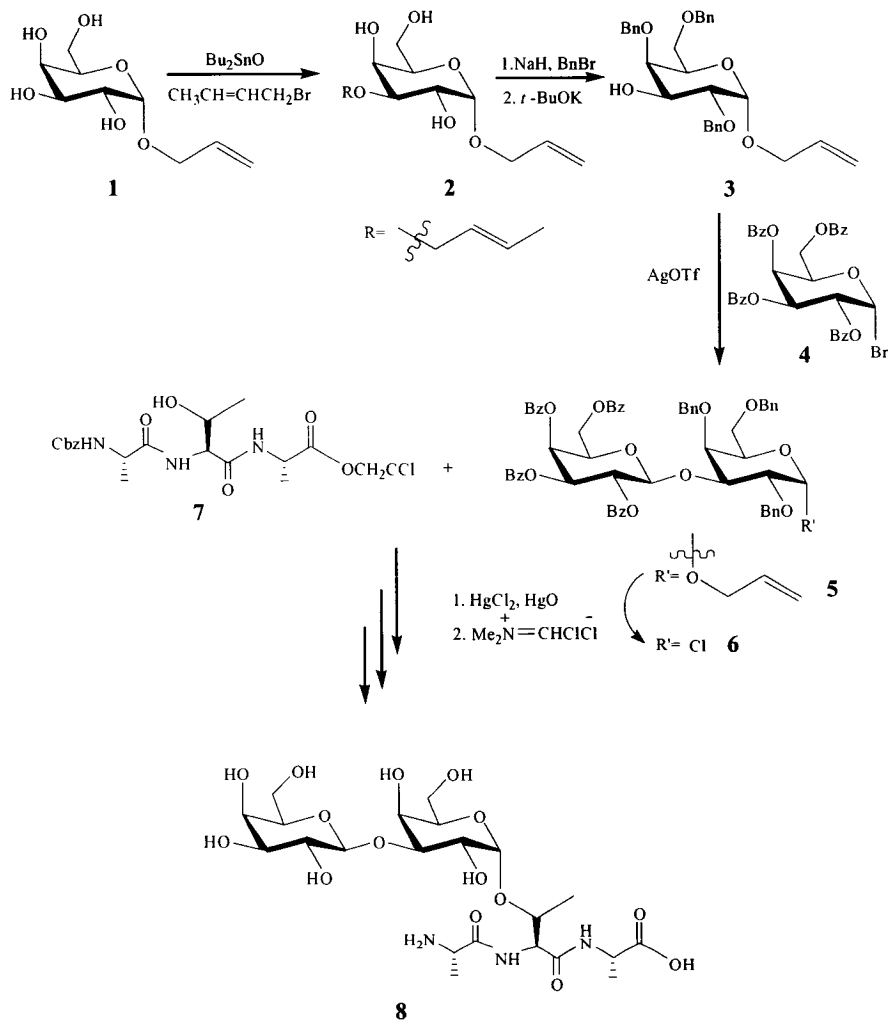

Scheme 1.1: Anderson's synthesis of AFGP analogues core unit

The two components were coupled together to afford the requisite glycosylated building block. The key step is the selective crotylation of compound **1** at the C-3 hydroxyl group to give compound **2**. The remaining hydroxyl groups were then benzylated to afford compound **3**. Selective removal of the crotyl functionality gave the free hydroxyl group at the C-3 position. Coupling of **3** with **4** afforded the disaccharide **5**. The glycosyl chloride **6** was prepared by treating **5** with Vilsmeier reagent. The desired building block **8** for the AFGP analogue was synthesized by coupling **6** with the tripeptide unit **7** and after removal of the protecting groups.

1.7.2 Filira's Continuous Solid Phase Synthesis of AFGP Analogues

The first AFGP analogue synthesized using a solid phase protocol was reported by Filira.[81] This is an example of a linear approach in which the AFGP analogue is synthesized in a stepwise manner (Scheme 1.2). The analogues prepared maintain the same sequence of amino acid in the tripeptide backbone as for native AFGP and the modification was made in the disaccharide component. The α-linked disaccharide was replaced with the monosaccharide β-linked galactose. This structural modification was made to mimic the β-1,3 linkage between the terminal galactose and GalNAc (galactosamine) in the native AFGP. The building block **12** was prepared by reaction of D-galactose pentaacetate **9** with both C- and N-termini protected L-threonine **10** in the presence of boron trifluoride diethyl etherate. This was followed by C-terminus deprotection and switching of protecting group at the N-terminus with Fmoc succinimide (Fmoc-OSu). Stepwise addition of the desired amino acids or building block afforded the polymer **13** composed of 2 to 7 tripeptide repeat units.

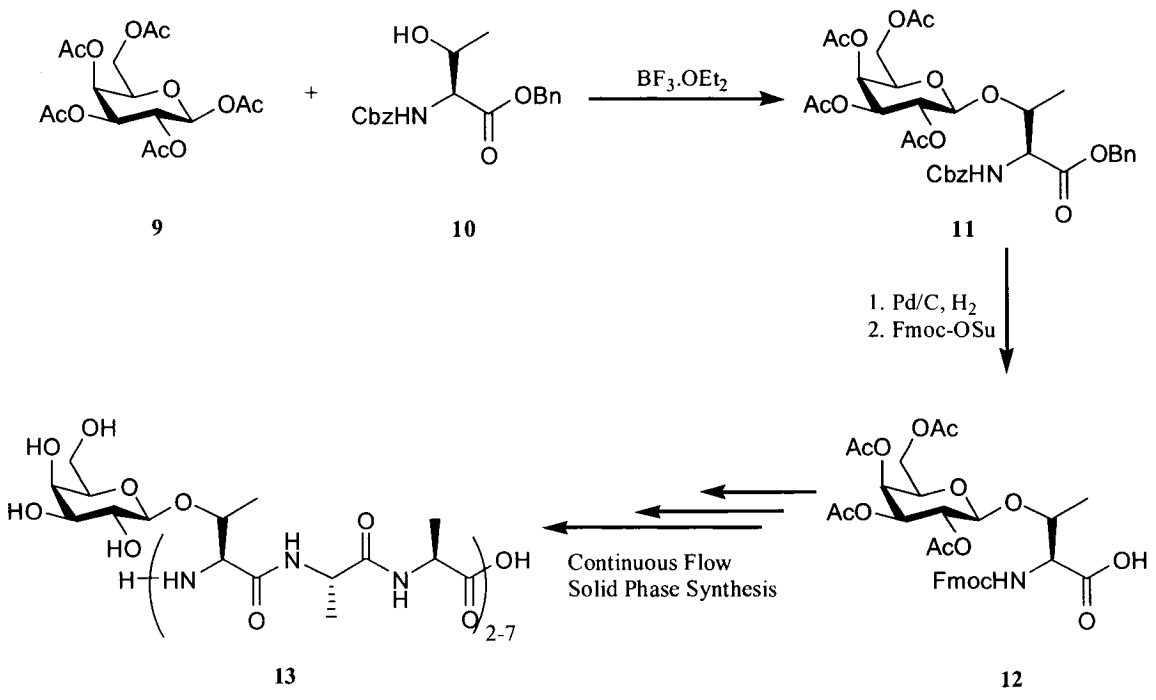

Scheme 1.2: Filira's synthesis of AFGP analogues

1.7.3 Meldal's Solid Phase Synthesis of AFGP Analogues

Meldal and Jensen reported a similar approach to Filira's for the solid phase synthesis of AFGP analogues (Scheme 1.3).[82] As with Filira's approach, they utilize the truncated version of the disaccharide but the L-threonine of native AFGP was replaced by L-serine. The use of pentafluorophenyl (Pfp) ester of fluoren-9-yl-methoxycarbonyl serine **15** to couple with the benzylated galactose bromide **14** greatly reduced the required steps for the building block synthesis. Building block **16** was ready for solid phase synthesis without further functional group manipulation due to the presence of the highly activated Pfp ester. The polypeptide **17** was prepared with 1 to 3 (L-serine-L-alanine-L-alanine) tripeptide repeat units with a continuous flow solid phase synthesis protocol.[83]

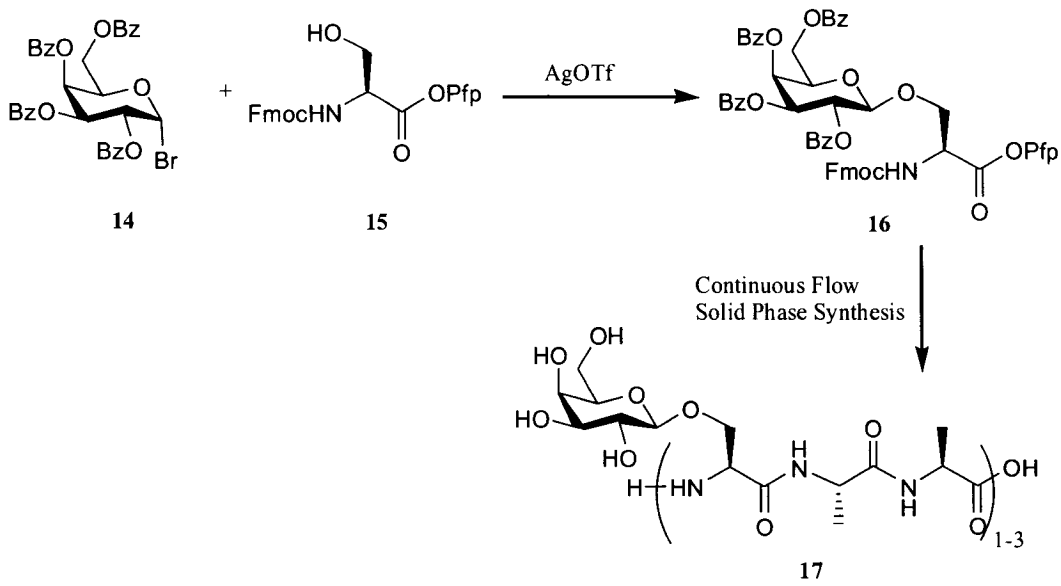

Scheme 1.3: Meldal's synthesis of serine AFGP analogues

1.7.4 Ben's Solid Phase Approach of *C*-linked AFGP Analogues

A new approach to synthesize AFGP analogues was reported by Ben and Eniade.[84] In this approach the labile carbon-oxygen linkage between the carbohydrate and the peptide backbone was replaced with a stable amide bond. Their approach utilized a commercially available monosaccharide unit instead of the native disaccharide system and the amino acid L-threonine was replaced by L-lysine (Scheme 1.4). The *C*-linked monosaccharide **18** was glycosylated with tripeptide **19** (L-lysine-L-glycine-L-glycine) by CDI mediated coupling. The amino acid L-lysine was chosen because the amide bond motif is structurally similar to the guanidinyl group in the L-arginine residue that is sometimes substituted for L-threonine in native AFGP.[85] In addition, in previous studies

AFP I analogues where L-lysine replaced L-threonine has exhibited antifreeze-specific activity.[86]

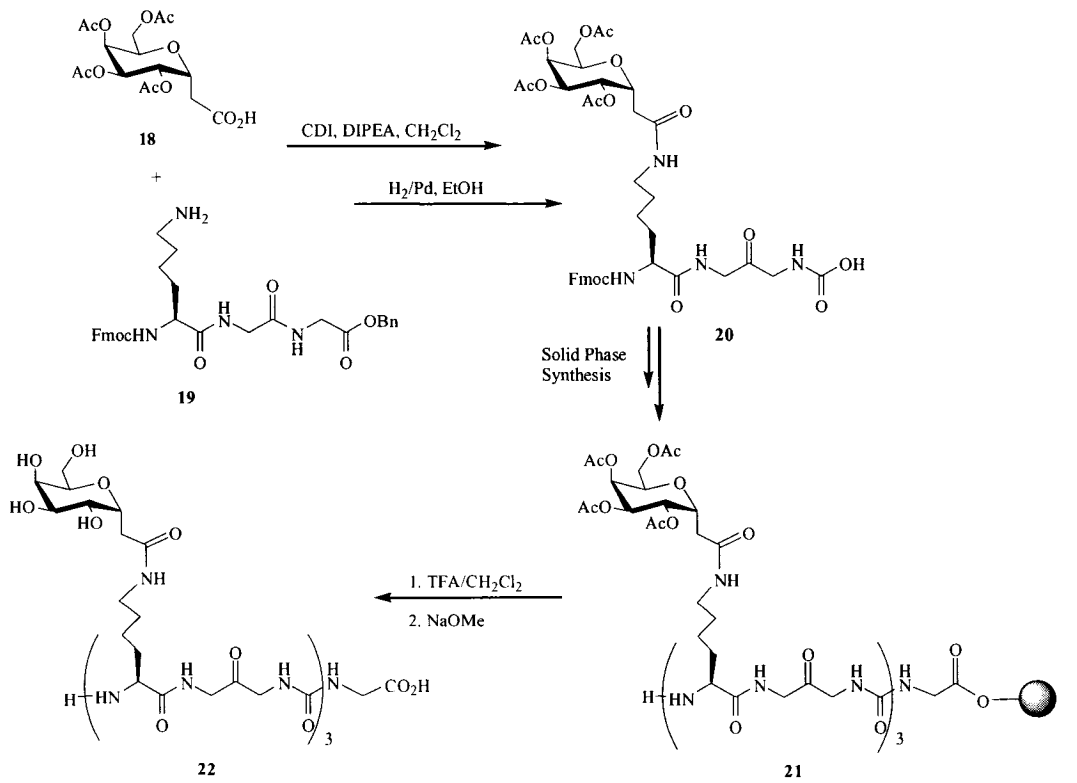

Scheme 1.4: Ben's solid phase synthesis of C-linked AFGP analogues

The glycosylated building block **20** afforded glycopeptide **22** via stepwise solid phase synthesis followed by cleavage from the resin and functional group deprotection.

1.7.5 Nishimura's Solution Phase Synthesis of Native AFGP

The first synthesis of native AFGP was reported by Nishimura and co-worker[87] in 1996 (Scheme 1.5). The disaccharide **25** was obtained by reaction of galactosyl

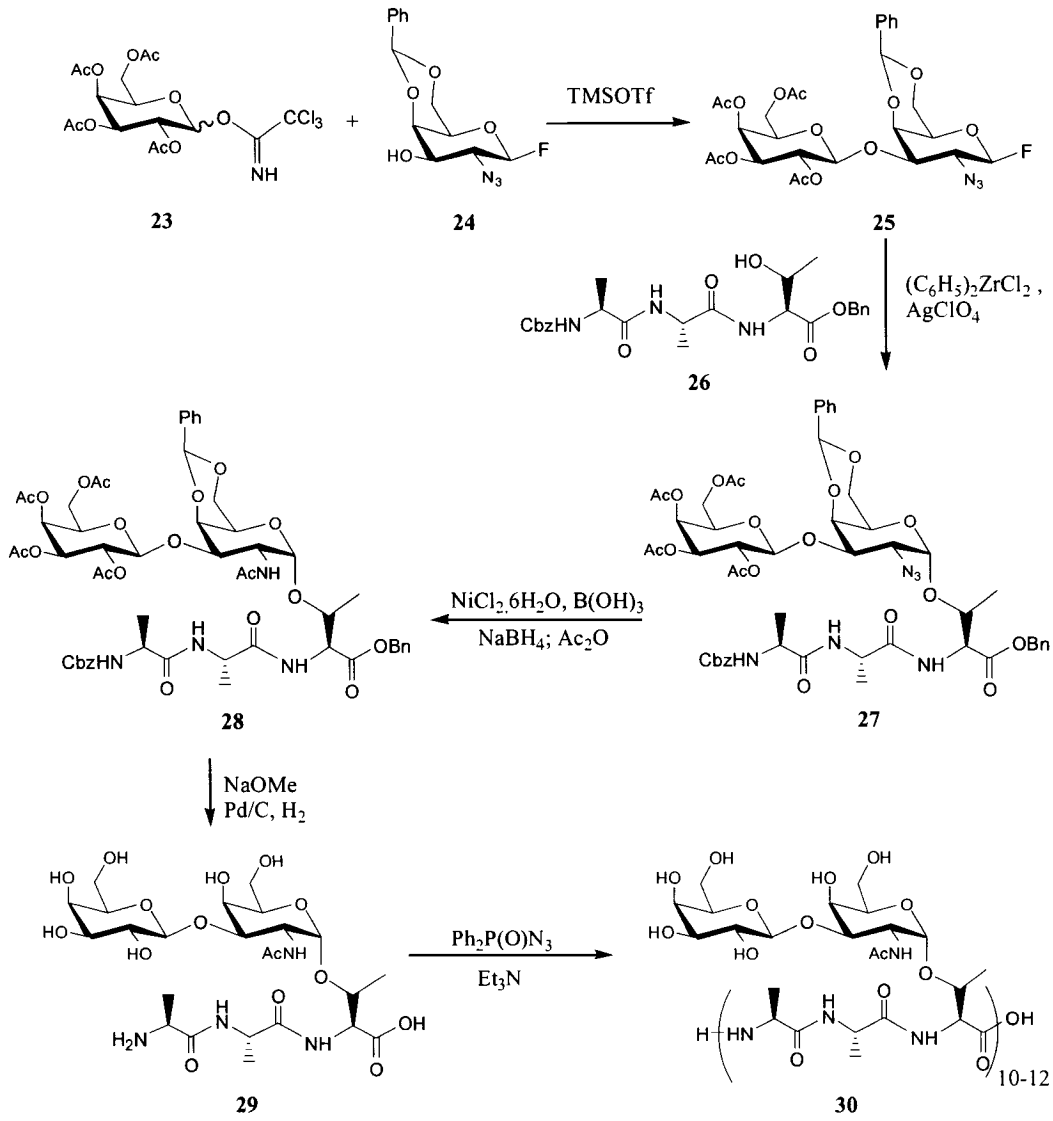

Scheme 1.5: Nishimura's solution phase synthesis of native AFGP 8

trichloroimidate **23** with **24** in the presence of trimethylsilyl trifluoromethanesulfonate (TMSOTf). To favour the formation of α-glycosidic linkage in **27**, coupling of the disaccharide with tripeptide **26** was performed in the presence of cyclopentadienylzirconium dichloride and silver perchlorate. The C-2 azide group was converted into the acetamido group by reduction of **27** with nickel chloride in sodium borohydride followed by acetylation to produce **28**. Polymer **30** with a tripeptide

(threonine-alanine-alanine) chain length of 10 to 12 was accomplished with diphenyl phosphoryl azide (DPPA) and triethyl amine from fully deprotected monomer **29**.

1.7.6 Chen's Solid Phase Synthesis of Native AFGP

Chen and co-workers[88] later reported the synthesis of native AFGP via the standard solid phase synthesis protocol (Scheme1.6). Their approach was based on the coupling of α-phenylselenyl glycoside **36** with the L-threonine residue **35** in the presence of silver triflate and tetramethyl urea to afford the mono glycosylated derivative **33**. Coupling of **33** with the glycoside donor **34** afforded disaccharide derivative **32**. The C-2 azide was converted into acetamide, which was then assembled into polymer **31** using solid support.

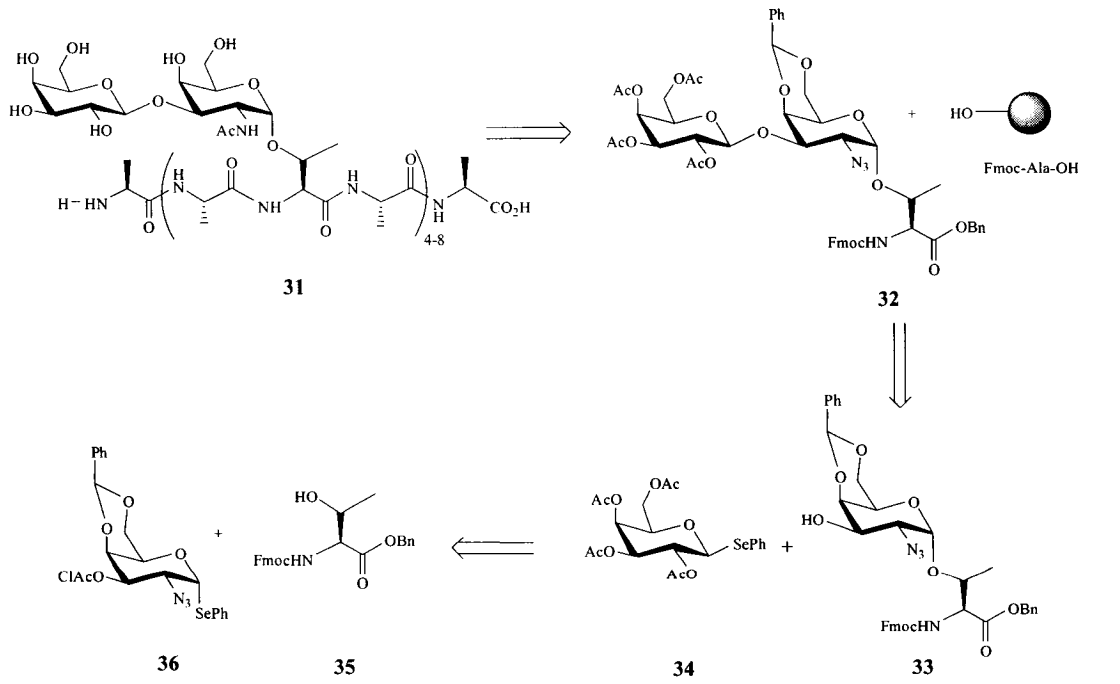

Scheme 1.6: Chen's approach to AFGP assembly

All of these strategies afforded viable routes for the synthesis of AFGPs and AFGP analogues. However, only a few of these methods especially those involving solid phase synthesis, have been used to prepare compounds for structure-activity relationship studies.

References:

[1] Cheng, C. H. *Curr. Opin. Genet. Dev.* **1998**, *8*, 715-720

[2] Scott, G. K., Davies, P. L., Shear, M. A., Fletcher, G. L. *Eur. J. Biochem.* **1987**, *168*, 629., Scott, G. K. *et al. Can. J. Fish. Aquat. Sci.* **1986**, *43*, 1028-1034

[3] Scholander, P. F., Dam, L. V., Kanwisher, J. W., Hammel, H. T., Gordon, M. S. *J. Cell. Comp. Physiol.* **1957**, *49*, 5 24.

[4] Feeney, R. E., Burcham, T. S., Yeh, Y *Ann. Rev. Biophys, Biophys. Chem.* **1986.** *15*:59-78

[5] Scholander, P.F., Flagg, W., walter, V., Irving, L. *physiol. Zool.* **1953**, *26*, 67

[6] Scholander, P.F., Van Dam, L., Kanwisher, J. W., Hammel, H. T. Gordon, M.S. *J. Cell Comp. Physiol.***1957**, *49*, 5.

[7] DeVries, A. L., Komatsu, S. K., Feeney, R. E. *J. Biol. Chem.* **1970**, *245*, 2901.

[8] DeVries, A. L., Vandenheede, J., Feeney, R. E. *J. Biol. Chem.* **1971,** *246*, 305.

[9] Komatsu, S. K., DeVries, A. L., Feeney, R.E. *J. Biol. Chem.* **1970**, *245*, 2909.

[10] Harding, M. M., Anderberg, P. I., Haymet, A. D. *J Eur. J. Biochem.* **2003**, *270*, 1381-1392

[11] Yeh, Y., Feeney, R. *Chem. Rev.* **1996**, *96*, 601.

[12] Fletcher, G. L., Hew, C. L., Devries, P. L. *Annu. Rev. Physiol.* **2001**, *63*, 359.

[13] Dumas, J. G. *Annu. Rev. Physiol.* **2001**, *63*, 327.

[14] Tysenko, M. G., Doucet, D., Davies, P. L., Walker, V. K. *Nat. Biotechnol.* **1997**, *15:* 887-890.

[15] Yang, D. S. C., Sax, M., Chakarbartty, A., Hew, C. L. *Nature* **1988,** *333*, 232-237.

[16] Tomimatsu, Y., Scherer, J., Yeh, Y., Feeney, R. E. *J. Biol. Chem.* **1976,** *251*, 2290-2298

[17] DeVries, A.L. *Science*, **1971**, *172*, 1152-1155

[18] Hew, C. L., Yang, S. C. D. *Eur. J. Biochem.* **1992**, *203*, 42

[19]. Kuiper, M. J., Davies, P.L., Walker, V.K. *Biophys. J.* **2001**, 81, 3560-3565

[20] Knight, C. A., Wen, D., Laursen, R. A. *Cryo biology* **1995**, *32,* 23-34

[21] Enaide, A., Ben, R. N. *Biomacromolecules* **2001**, *2,* 557

[22] Kuiper, J. M., Davies, L. P., Walker, K. V. *Biophys. J*, **2001**, *81*, 3560-3565

[23] Rubinsky, B.A., Arav, A., Mattioli, M., Devries, A. L.*Biochem. Biophys. Res. Comm.* **1990**, *173*, 1369-1374

[24] Tablin, F., Oliver, A. E., Walker, N. J., Crown, L. M., Crown, J. H. *J. Cell. Physiol.* **1996**, *168*, 305-313

[25] Quinn, P. J. *Cryobiology* **1985,** *22*, 128

[26] Clerc, S.G., Thompson, T. E. *Biophys. J.* **1995**, 68, 2323

[27] Wu, Y.; Fletcher, G. L. Biochem. Biophys. Acta **2000**, *11*, 1524

[28] Ben, R. N. *Chem. BioChem*, **2001**, *2*, 161-166

[29] O'Grady, S. M., Schrag, J. D., Raymond, J. A., DeVries, A. L. *exp. Zool.* **1982**, *224,* 177

[30] Duman, J. G., Howarth, K. L., Tomchney, A., Patterson, J. L.Comp. *Biochem.Physipol.* **1982,** *73,* 543.

[31] Griffith, M., Ala, P., Yang, D. S. C., Hon, W. C., Moffatt, B. A. *Plant Physiol.* **1992**, *100*: 593-596

[32] Cheng, C.H. *Curr. Opin. Genet. Dev.* **1998**, *8*, 715-720

[33] Duman, J. G., DeVries, A. L. *Nature* **1974,** *247*, 237

[34] Hew, C. L., Yip, C. C. *Biochem. Biophys. Res. Commun.* **1976**, *71*, 845

[35] Kelli, B., *et al. J. Mol. Rcognit.* **2000**, *13*, 101-113

[36] Harding, M. M., Anderberg, P. I. and. Haymet, A.D. *Eur. J. Biochem.*, **2003**, 270, 1381-1392

[37] Ewart, K. V., Fletcher, G. L. *Can. J. Zool.* **1990**, *68*, 1652.

[38] Sönnichsen, F. D., Sykes, B. D., Davies, P. L. *Protein Sci.* **1995**, *4*, 460.

[39] Hew, C.L., Slaughter, D., Joshi, S. B., Flecther, G. L., Ananthanarayanan, V. S. *J. Comp. Physiol.* **1984**, *155B*, 81.

[40] Deng, G.J., Andrews, D.W., Laursen, R. A. *FEBS Lett.* **1997**, *402*, 17.

[41] DeVries, A. L., Komatsu, S. K., Feeney, R. E. *J. Biol. Chem.* **1970**, *245*, 2901-2908.

[42] Raymond, J. A., DeVries, A. L. *Cryobiology* **1972**, *9*, 541

[43] DeVries, A. L., Vandenheede, J., Feeney, R. E. *J.Biol. Chem.* **1971**, *246*, 305

[44] DeVries, A. L., *Science,* **1971**, *172*, 1152

[45] Ahmed, A. I., Osuga, D. T., Feeney, R. E. *J. Biol. Chem* **1973**, *248*, 8524

[46] Nishimura, *Angew. Chem. Intl. Ed.* **2004**, 856-862

[47] Knight, C. A. *Nature* **2000,** *406,* 249.

[48] Bouvet, V., Ben, R. *Cell Biochemistry and Biophysics*, **2003**, *39*, 133.

[49] Knight, C. A., Cheng, C. H. C., DeVries, A. L. *Biophys. J.* **1991**, *59*: 409.

[50] Wilson, P. *Cryo-Letterl*, **1993**, *14,* 31.

[51] Kuroda, T. *Proc. 4th Topical Conference on Crystal Growth Mechanism; Hokkaido*

Press, **1991,** p 157.

[52] Hall, D.G., Lips, A. *Langmuir* **1999**, *15*, 1905.

[53] Haymet, A.D., Ward, J. L.G., Harding, M. M. *J. Am. Chem. Soc.* **1999,** *121*, 941-948

[54] Chao, H., Houston, M. E., Hodges, R. S., Key, C. M., Sykes, B. D., Loewen, M. C., Davies, P. L, Sönnichsen, F. D. *Biochemistry,* **1997,** *36*, 14652-14660

[55] Wierzbicki, A., Taylor, M. S., Knight, C. A., Madura, J. D.; Harrington, C. S., Sikes, C. S. *Biophys. J.* **1996**, *71*, 8-18.

[56] Knight, C.A., Driggers, E., DeVries, A. L. *Biophys. J.* **1993,** *64*, 252-259

[57] DeVries, A.L., A. *Rev. Physiol.* **1983**, *45*, 245-260.

[58] Wen, D. & Laursen, R.A., *Biophys. J.* **1992a**, *63,* 1659-1662

[59] Madura, J. D., *et al., J. Am. Chem. Soc.* **1994**, *116,* 417-418

[60] Haymet, A.D. J., Ward, L. G., Harding, M. M., Knight, C. A. *FEBS Lett.* **1998**, *430*, 301-306

[61] Zhang, W. & Laursen, R. A. *J. Biol. Chem.* **1998,** *273*, 34806-34812

[62] Franks, F., Morris, E.R. *Biochim. Biophys. Acta.* **1978,** *540*, 348-356

[63]Bush, C. A., Feeney, R. E., Osuga, D. T., Ralapati, S., Yeh, Y., *Int. J. Pept. Protein Res.* **1981**, *17,*125-129.

[64] Rao, B.N., Bush , C. A. *Biopolymers* **1987**, *26*, 1227-1244

[65] Franks, F., Morris, E.R. *Biochim. Biophys. Acta.* **1978,** *540*, 348-356

[66] Bush, C. A., Feeney, R. E., Osuga, D. T., Ralapati, S., Yeh, Y., *Int. J. Pept. Protein Res.* **1981**, *17,*125-129.

[67] Rao, B.N., Bush , C. A. *Biopolymers* **1987**, *26*, 1227-1244

[68] Burcham, T. S., Osuga, D. T., Rao, B. N. N., Bush, C. A., Feeney, R. E. *J. Biol. Chem.* **1986**, *261*, 6390

[69] Bush, C. A., Feeney, R.E. *Int. J.Pept. Protein Res.* **1986,** *28*, 386-397

[70] Bouvet, V. R., Lorello, G. R., Ben, R. N. *Biomacromolecules,* **2006**, *7(2),* 565-571

[71] Pegg, D. E. *Semin. Reprod. Med.* **2002** *20*, 5-13.

[72] Baust, J. M., Van Buskirk, R., and Baust, J. C. *In Vitro Cell Dev. Biol.* **2000** *36,* 262

[73] Meryman, H.T. *Cryobiology* , **1984,** *21*, 407-426

[74] Rubinski, B., Arav, B.A. DeVries, A. L. *Cryo-letters,* **1991**, 12, 93-106.

[75] Wang, J. H. *Cryobiology*, **2000**, *41*, 1-9

[76] Koushafar, H., Rubinsky, B. *Urology* **1997**, *49* ,421.

[77] Pham, L., Dahiya, R., Rubinsky, B. *Cryosurgery* **1999**, *38*, 169.

[78] Hew, C.L., Yang, D. S. C. *Eur.J.Biochem.* **1992**, *13*, 59.

[79] Griffith, M., Ewart,K.V. *Biotechnol. Adv.***1995,** *13,* 375

[80] Anisuzzaman, A. K. M., Anderson, L., Navia, J. L. *Carbohydr, Res.* **1988,** *174*, 265-278

[81] Filira, F. *Int . J. Biol. Macromol.* **1990**, *12*, 41

[82] Meldal, M., Jensen, K. J. *J.Chem. Soc. Chem. Commun.* **1990,** 483.

[83] Costa, J., Dutour, M. N., Pantaloni, A. Castro, B. *Tetrahedron Lett.* **1990,** *31*, 2905 208.

[84] Eniade, A., Ben, R. N. *Biomacromolecules* **2001**, *2*, 557-561.

[85] Kerr, W. L., Feeny, R. E., Osuga, D. S., Reid, D. S, *Cryo Lett.* **1985**, *6*, 371.

[86] Wierzbicki, A., Knight, C. A., Rutland, T. J., Muccio, D. D., Pybus, B. S., Sikes, C. S.

Biomacromolecules, **2000**, *1*, 268.

[87] Tsuda, T., Nishimura , S. I. *Chem. Commun.* **1996**, 2779-2780

[88] Tseng, P. H., Jiang, W. T., Chang, M.Y., Chen, S. T. *Chem. Eur. J.* **2001**, *7*, 585.

Chapter 2

2.0 Progress towards *C*-linked AFGP Analogues

2.1 Previous Syntheses of *C*-linked AFGP Analogues

Protein glycosylation has received considerable attention from the scientific community due to its role in various cellular recognization processes such as viral adhesion, infections, cancer metathesis, etc.[1] In general, glycosylation in natural glycoconjugates is through a nitrogen linkage between asparagine and the carbohydrate moiety, or an oxygen linkage between a serine or threonine and a sugar.[2] In native AFGPs, the latter type of linkage, termed "*O*-linked" is present. The *O*-linked glycopeptide is typically unstable and presents a challenge in synthesis due to the sensitive nature of the glycosidic linkage to both acidic and basic medium[3] (Figure 2.1).

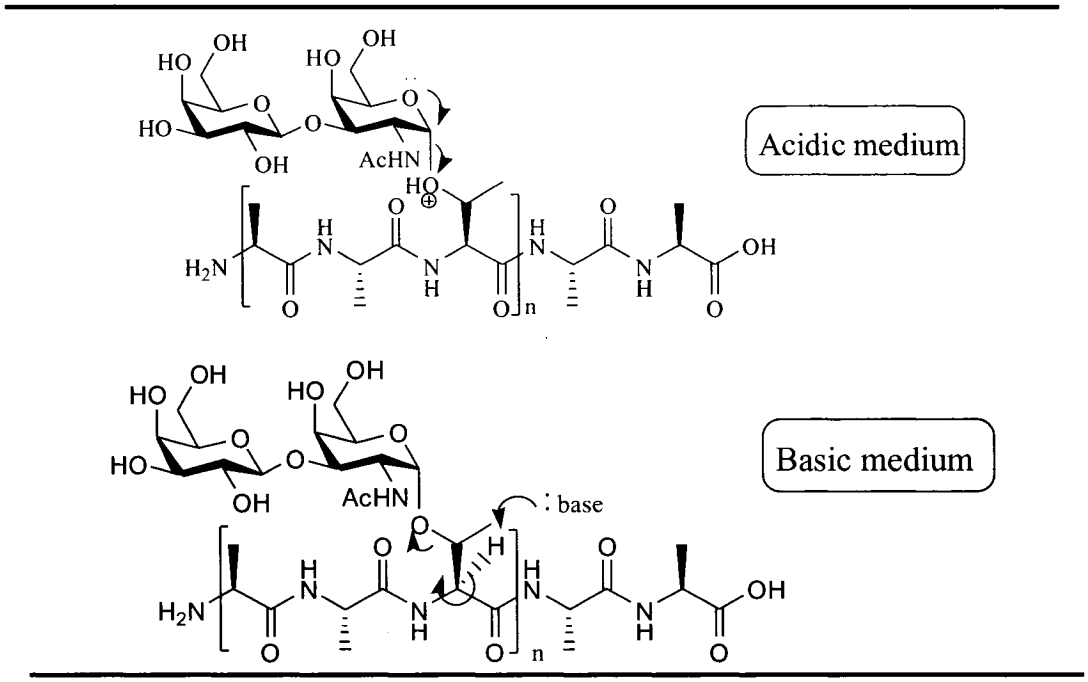

Figure 2.1: Cleavage of glycosidic bond in acidic and basic media

In acidic medium the glycocidic bond is readily hydrolyzed to form an oxocarbenium ion whereas in basic medium the polypeptide backbone is cleaved from the carbohydrate components due to the β-elimination. Another limitation of *O*-linked glycopeptides is their tendency to undergo enzymatic degradation *in vivo*.[4] However, organic chemists have the ability to create compounds that do not exist in nature. One example is the preparation of carbon linked or "*C*-linked" glycosides that mimic native *O*-linked glycosides. The *C*-linked glycosides have the advantage over *O*-linked glycosides in that they are stable under certain chemical (acidic or basic) and enzymatic conditions.[5, 6] Furthermore, *C*-linked glycosides adopt similar conformations as the native system, irrespective of the slight changes in bond length, bond angle and dihedral angle caused by substitution with a methylene group.[7]

Antifreeze glycoproteins are glycopeptides where the secondary hydroxyl group of the L-threonine residue is glycosylated with the disaccharide β-D-galactosyl-(1,3)-α-D-N-acetylgalactosamine.[8] Since they are present only in arctic and antarctic fish in small quantities of complex glycoprotein mixtures, a synthetic alternative is the only viable way to access these important compounds for the potential applications ranging from medical to commercial as well as for the purpose of structure-function relationship studies. This prompted the synthesis of our first generation of *C*-linked AFGP analogues (Figure 2.2).[9]

There are three differences between native AFGP and our first generation analogues. These are the replacement of the L-threonine side chain with the L-lysine, the replacement of the disaccharide with a single galactose moiety and the substitution of the L-alanine in the peptide backbone for L-glycine residues.

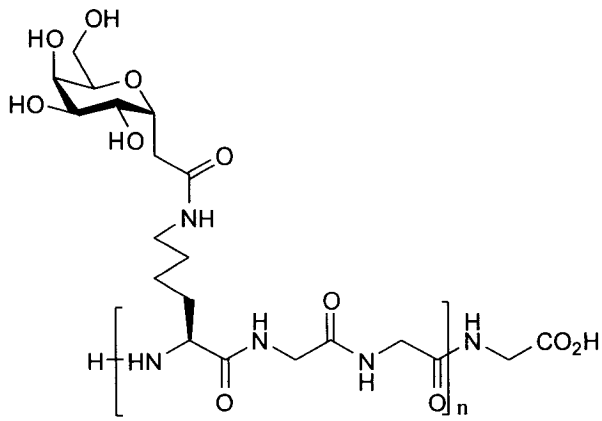

Figure 2.2: First generation C-linked AFGP analogues

L-lysine was an appropriate substitution since the L-lysine residue is structurally similarly to the L-arginine which is sometimes found as a substitute for the L-threonine in native AFGP 8.[10] The amide linkage between the carbohydrate and the amino acid backbone mimic the guanidinyl motif of arginine (Figure 2.3). In addition, studies performed on type I AFP where the L-threonine residues were replaced with

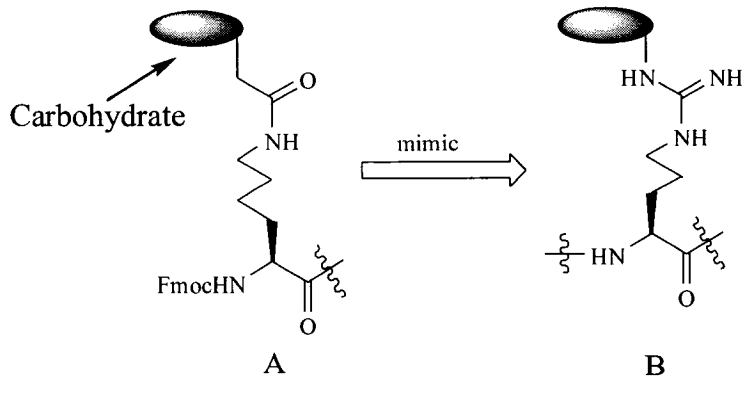

Figure 2.3: A) Amide bond in first generation C-linked analogues

B) Guanidinyl group in L-arginine of native AFGP

L-lysine showed thermal hysteresis activity.[11] Modifications to the carbohydrate moiety were based on the early structure-function relationship studies that showed the importance of the terminal galactose residue for antifreeze activity.[12] The replacement of the disaccharide in the native AFGP with a monosaccharide also simplifies the synthetic route. The final modification, the replacement of the L-alanine residues of the native system with L-glycine residues was done to avoid potential problem of racemization during solid phase synthesis. However, it was latter found that the solid phase synthesis of these analogues can be carried out without any unwanted racemization.

Three polymer lengths of first generation analogues were synthesized (Figure 2.2). Polymers with three tripeptide repeat units (3-mer) **37**, six tripeptide repeate units (6-mer) **38**, and nine tripeptide repeat units (9-mer) **39** were synthesized. This system was prepared as a proof of concept for the preparation of low molecular weight AFGP analogues.[6] However, when tested for activity (TH and RI), analogues **38** and **39** behaved only as weak antifreezes, whereas analogue **37** did not display any antifreeze-specific activity. By comparison, the potent native antifreeze AFGP 8 is a 4-mer. This study showed that there is a correlation between the length of the glycopolymer and antifreeze activity, with the suggestion that the minimum length requirement for activity might be a 4-tripeptide repeat unit (4-mer).

In the process of designing low molecular weight AFGP analogues, second generation analogues were synthesized possessing all the features of the first generation compounds, with the exception that the peptide backbone had only 4 tripeptide repeat units (Figure 2.4). Analogues **40** and **41**, both of which contained L-lysine residues in the side chain did not show any observable activities. In analogue **42** L-lysine was replaced

by an L-ornithine residue. Analogue **42** proved to be a potent recrystallization inhibitor (Figure 2.4).[13]

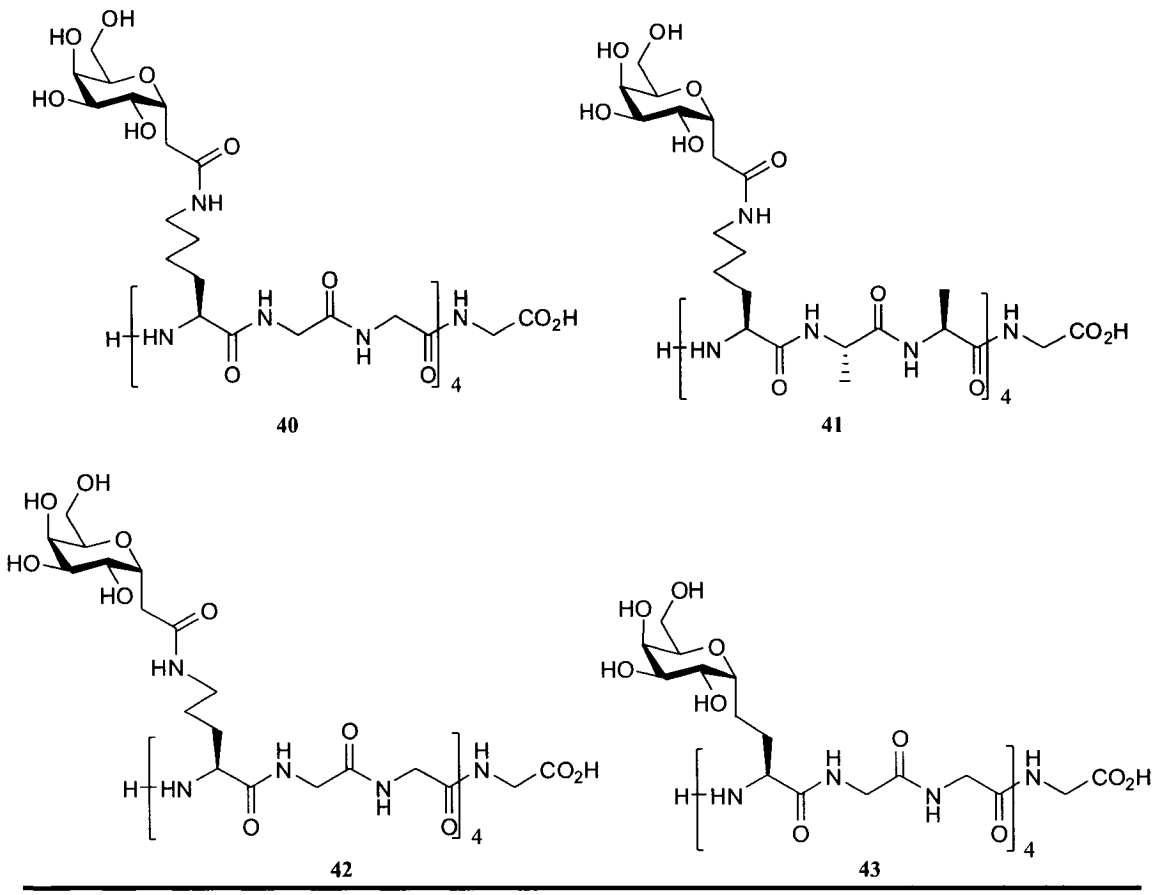

Figure 2.4: Structurally diverse Second generation analogues

The amino acid L-ornithine which had only one carbon less than L-lysine in its side chain, displayed much more RI activity. This result suggests that there exists a correlation between side chain length and RI activity. However, recent results from *C*-serine analogue **43** (Figure 2.4), which had only two carbons between the D-galactose moiety and peptide backbone, exhibited comparable RI activity to the L-ornithine analogue **42** which had a six atom linkage between the carbohydrate and the peptide

backbone.[14] The *C*-serine analogue **43** is a new generation analogue that has an all carbon linker (the amide bond has been removed altogether) in the side chain between the carbohydrate and the peptide backbone. This led us to hypothesize that the optimal side chain length is not the only requirement for enhanced RI activity. Further investigations into structure-function relationships are needed to explore this question.

2.2 Research Goals and Objectives

Our main research goal is to understand what properties of AFGPs allow them to bind to the surface of ice and inhibit the growth of ice crystals. Towards this end, structure-function relationship studies of AFGPs are needed. For these studies AFGP analogues possessing different structural features must be synthesized. This study should allow us to tailor the TH and RI activity of AFGP analogues, making them useful for different applications.

Based upon the interesting results described in the previous section we decided to investigate the importance of the polypeptide backbone for antifreeze activity. The peptide backbone was modified by the replacement of glycosylated α-amino acids with the corresponding β-amino acids. Replacement of a natural α-amino acid with an unnatural β-amino acid in AFGP analogues has not previously been explored. None of the biological AFPs or AFGPs known to date possesses β-amino acids in their peptide sequences. However, a number of other naturally occurring peptides are found to contain β-amino acids. For instance, it is reported that the dipeptide carnosine which contains β-glycine-histidine, is a naturally occurring mammalian peptide present in muscles and

other excitable tissues. It possesses strong and specific antioxidant properties.[15] It has been found that the cleavage of this β-glycine containing dipeptide is significantly slower than the cleavage of α-amino acid containing dipeptides.[16] Recently, a number of peptidomimetics containing β-amino acids have begun to emerge. Studies have shown that these β-peptides not only exhibit an increased metabolic resistance and potent biological activity, but are also able to form well-defined novel secondary structures similar to those found in nature; For instance, helices, turns, tubes and sheets.[17]

Based on these studies we hoped that the incorporation of β-amino acids in our new AFGP analogues would change the conformation of the peptide backbone such that it might have an impact on antifreeze-specific activity. We also hoped that the study of these unusual analogues would open up a new area into the molecular understanding of the mechanism of action. Taking advantage of the previous studies done in our lab we modeled our new analogues as shown in Figure 2.5.

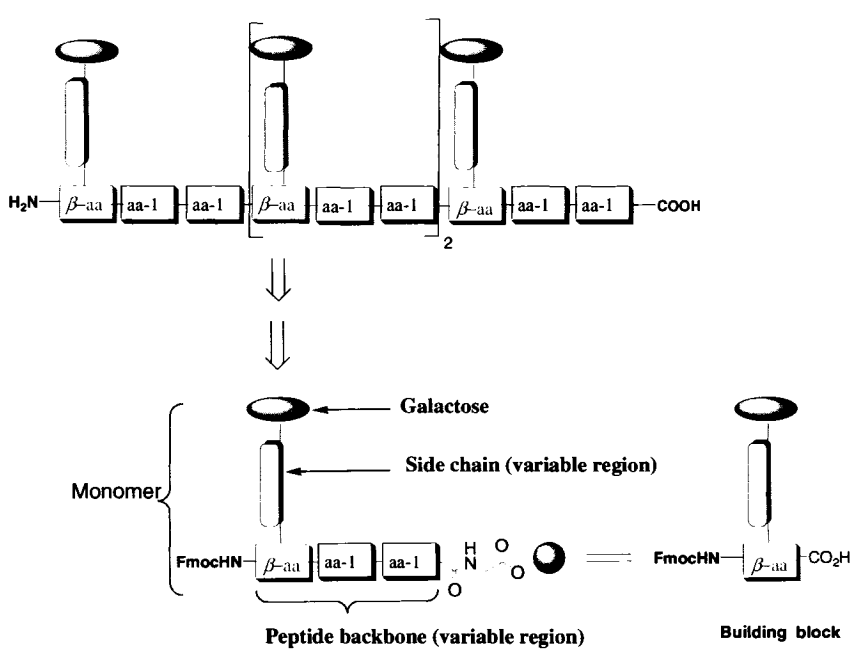

Figure 2.5: Model for new AFGP analogues containing β-amino acids

According to this model, we designed our new analogues to have a β-amino acid in the building block. As mentioned, the side chain of L-ornithine is one carbon shorter than that of L-lysine. Both of these amino acids were included in different peptides of the new analogues. Since the effect of the side chain length on activity has already been observed in the second generation analogues, this study will help us to understand the relationship between side chain length and peptide backbone variation for activity. Based upon the previous SAR studies on AFGPs[18] galactose was chosen as the carbohydrate component. We wanted to vary the other amino acids in the backbone to investigate the role of hydrophobic interactions and its impact on antifreeze activity. The amino acid L-alanine and L-glycine were chosen for this study.

To accomplish this goal, our first objective was to develop a synthetic strategy for the synthesis of building blocks containing β-amino acids. While a number of synthetic methodologies exist for the synthesis of β-amino acids none of them have described the synthesis of glycosylated β-amino acids. One of the most efficient methods for the synthesis of β-amino acids is via the Arndt-Eistert one carbon homologation.[19] The main attraction of this method is that the Wolff rearrangement of the diazoketone intermediate proceeds with retention of configuration, which forms the basis for the synthesis of optically active homologous carboxylic acids.[20, 21] Based on this principle a method for the homologation of glycosylated α-amino acids to β-amino acids was established (Scheme 2.1). The precursor for glycosylated β-amino acids, that is, the glycosylated α-amino acids was prepared in a convergent fashion starting from commercially available β-D-Galactose and an orthogonally protected (Fmoc at α-terminus and *t*-Boc at ε-terminus) commercially available α-amino acids. Previous studies suggested that the use

of fluoren-9-ylmethoxycarbonyl (Fmoc) for the protection of the α-amino group and acetyl protecting groups for the hydroxyl groups of the carbohydrate can work smoothly for preparation of the building block precursor. Further, selective deprotection of the Fmoc group can be achieved during solid phase synthesis without any harm to the carbohydrate component.

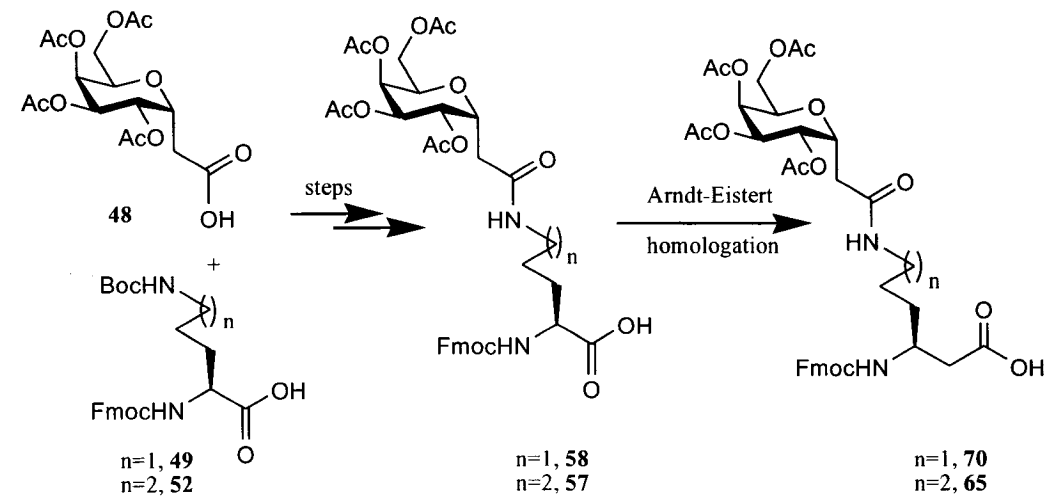

Scheme 2.1: Synthesis of glycosylated β-amino acids

An intermediate in the Arndt-Eistert homologation reaction was the diazoketone derivative of glycosylated α-amino acid. To ensure that the Fmoc protecting group remained intact during decomposition of diazoketone, base-free conditions were chosen. Thermal Wolff rearrangement with catalytic silver benzoate in dioxane and water was one choice for the purpose. The building blocks **70** and **65** (Scheme 2.1) were then assembled into the desired AFGP analogues **72**, **74**, and **76** (Figure 2.6) via a step-wise solid phase synthesis protocol. Analogue **72** incorporated L-alanine residues in the backbone whereas analogues **74** and **76** had L-glycine residues in the backbone. The

amino acid L-alanine can induce an α-helix conformation and this analogue can therefore be used to study the conformational effect on activity by comparison with the native system, since native AFGP 8 is composed of a high percentage of L-alanine residues. Conformational studies were done using circular dichroism (CD) spectroscopy.

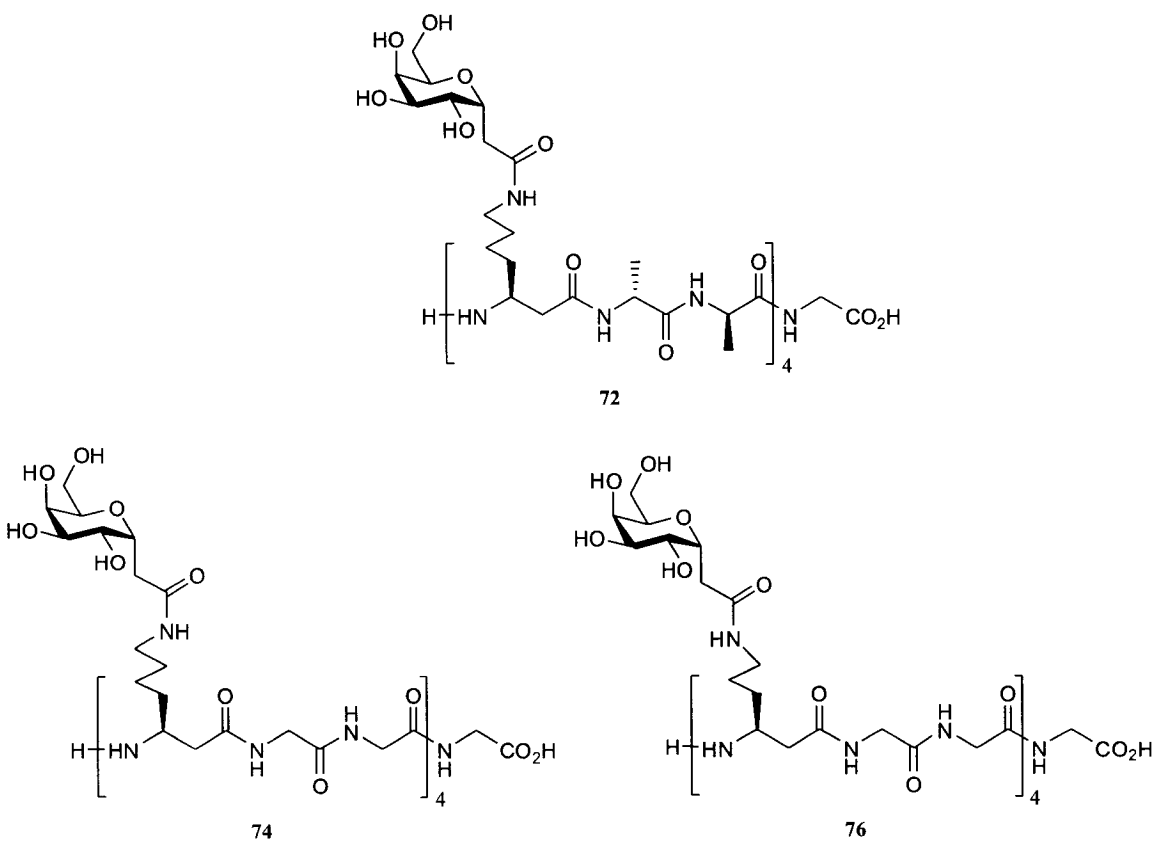

Figure 2.6: Structure of the new AFGP analogues

All of these analogues were tested for antifreeze-specific activity (TH and RI). Nanolitre osmometry was used to determine the TH activity. The measurement was conducted on a single ice crystal, making it possible to observe the change in ice crystal morphology within the TH gap. The RI assay provides a direct measurement of actual

ice crystal sizes. This assay demonstrates the ability of a compound to inhibit the ice growth during recrystallization below the TH gap, which is important for the cryopreservation of cells and tissues. In order to determine the potential cryoprotective properties for human applications, these analogues were tested for cytotoxicity and cryotoxicity in human embryonic liver cell line.

In summary, my research goal was to investigate the effect on antifreeze activity of integrating β-amino acids into the peptide backbone of AFGP 8 analogues. To achieve this goal, the followings objectives were laid out:

1. Synthesis of glycosylated L-lysine and L-ornithine building blocks containing β-amino acids;
2. Synthesis of new AFGP 8 analogues having β-amino acid building blocks and possessing the amino acids L-alanine and L-glycine in different peptide backbones;
3. Assessment of these analogues using thermal hysteresis (TH) assay, recrystallization inhibition (RI) assay and conformational analysis via circular dichroism (CD) spectroscopy;
4. Evaluation of cytotoxicity and cryotoxicity of these analogues using a human embryonic liver cell line.

References:

---

[1] (a) Bertozzi, C. R., Kiessling, L. L. *Science* **2001**, *291*, 2357. (b) Rudd, P. M., Elliot, T., Cresswell, P., Wilson, I. A. *Science* **2001**, *291*, 2370.

[2] Dwek, R. A. *Chem. Rev.* **1996**, *96*, 683.

[3] Sjolin, P., Kihlberg, J. *J. Org. Chem.* **2001**, *66*, 2957.

[4] Boon, G. J., Hale, K. J. *Organic synthesis with Carbohydrate*, Blackwell; science Malden, MA. **2000**, page 156 160

[5] Marcaurelle, L. A., Bertozzi, C. R. *Chem. Eur. J.* **1999,** *5*, 1384.

[6] Sparks, M. A.,Williams, K. W., Whitesides, G. M. *J. Med. Chem*, **1993**, *36*, 778 783.

[7] Jiménez-Barbero, J., Espinosa, J. F., Asensio, J. L., Canada, F. J., Poveda, A. *Adv. Carbohydrate Chem. Biochem.* **2001**, *56*, 235.

[8] Ben, R. N., *Chem. BioChem*, **2001**, *2*, 161-166l; Fletcher, G. L., Hew, C.L., Davies, P. L. *Annu. Rev. Physiol.* **2001**, *63*, 359.

[9] Eniade, A., Purushotham, M., Ben, N. R., Wang, J. B., Horwath, K. *Cell Biochemistry and Biophysics*, **2003,** *38*, 115.

[10] C. L. Hew, D. Slaughter, G. Fletcher, J. B. Shashikant, *Can. J. Zool.* **1981**, *59*, 2186-2192.

[11] A, Wierzbicki, C. A. Knight, T. J. Rutland, D. D. Muccio, B. S. Pybus, C. S. Sikes, *Biomacromolecules* **2000,** *1*, 268-274.

[12] Komatsu, S. K., DeVries, A. L., Feeney, R. E. *J. Biol. Chem.* **1970**, *245*, 2909-2913.

[13] Murphy, A. V. Ph. D Thesis. Binghamton University, New York.

[14] Liu, S., Ben, N. R. *Organic Letters*, **2005**, *7*, 2385-2388.

[15] Quinn, P. J., Boldyrev, A. A., Formazuyk, V. E. *Mol. Aspects Med.* **1992**, *13*, 379.

[16] Hanson, H. T., Smith, E. L. *J. Biol. Chem.* **1948**, *175*, 833.

[17] Hintermann, T., Seebach, D. *Chimia* **1997**. *51*, 244.

[18] Harding, M. M., Anderberg, P. I. and. Haymet, A.D. *Eur. J. Biochem.*, **2003**, 270, 1381-1392

[19] Liu, M., Sibi, M. P. *Tetrahedron*, **2002**, *58*, 7991-8035.

[20] Lane, J. F., Wallis, E. S. *J. Org. Chem.*, **1941**, *6*, 443.

[21] Wiberg,K. B., Hutton, T. W. *J. Amer. Chem. Soc.*, **1956**, *78*, 1640.

Chapter 3

3.0 Synthesis of *C*-linked AFGP Analogues Containing *β*-Amino Acids

Modification of the peptide backbone of AFGP analogues by replacement of *α*-amino acids with *β*-amino acids has not previously appeared in the literature. Towards this end, a new generation of *C*-linked AFGP analogues containing *β*-amino acids has been prepared. The requisite building blocks for solid phase synthesis were prepared in a convergent manner. The carbohydrate **48** and the amino acids **54** and **51** were coupled together to give the corresponding glycosylated *α*-amino acids which were then converted into the desired *β*-amino acids via Arndt-Eistert homologation to afford the building blocks **70** and **65**. The polypeptides **72, 74, 76** were then assembled (Figure 3.1).

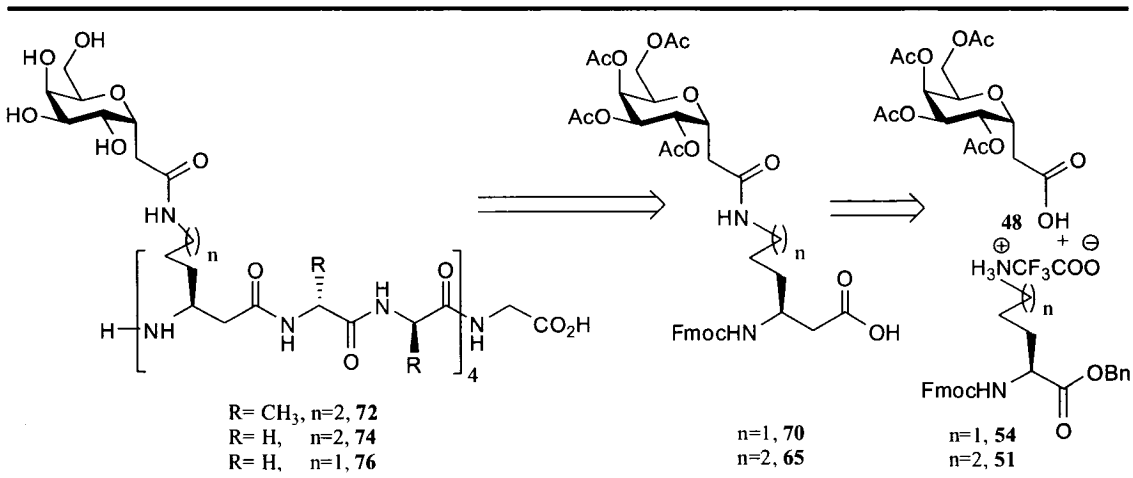

Figure 3.1: Retrosynthetic analysis of targeted analogues

3.1 Preparation of the Carbohydrate Component

SAR studies completed in our laboratory had suggested that D-galactose is the best monosaccharide for antifreeze activity.[1] Hence, we have decided to keep D-galactose for the carbohydrate component.

3.1.1 Preparation of *C*-linked Carboxylic Acid derivative from *β*-D-Galactose Pentaacetate.

The *C*-linked monosaccharide unit (i.e. *C*-linked allylated-galactose tetraacetate) **46** was prepared starting from commercially available *β*-D-galactose pentaacetate **44** as outlined in Scheme 3.1.

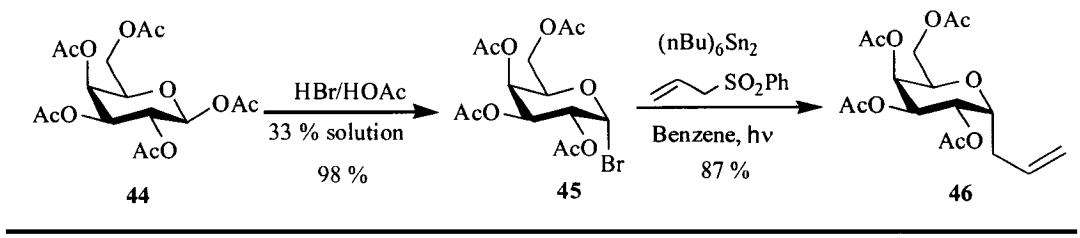

Scheme 3.1: Allylation of β-D-galactose pentaacetate

Reaction of **44** with hydrogen bromide in 33 % acetic acid solution produced *α*-bromo-D-galactose tetraacetate **45** in 98 % yield. This selectivity can be explained as illustrated in Scheme 3.2. The deacetylation at the anomeric position is assisted by a lone pair of electrons from the ring oxygen to form the intermediate oxocarbenium ion. The oxocarbenium ion is then attacked by bromine nucleophile either via either path "a" to produce the *α*-anomer, or it will follow route "b" to produce the *β*-anomer. Attack via path "b" is lower in energy but the *α*-product has added stabilization due to the anomeric effect[2] and is therefore lower in energy than the *β*-product; the *α*-anomer is the thermodynamic product. Since the reaction is reversible, the thermodynamically more stable product *α*-anomer is formed. Complicating the mechanism neighboring group participation from the acetate group at the C2 position is also occurred (not shown in the Scheme 3.2).[3]

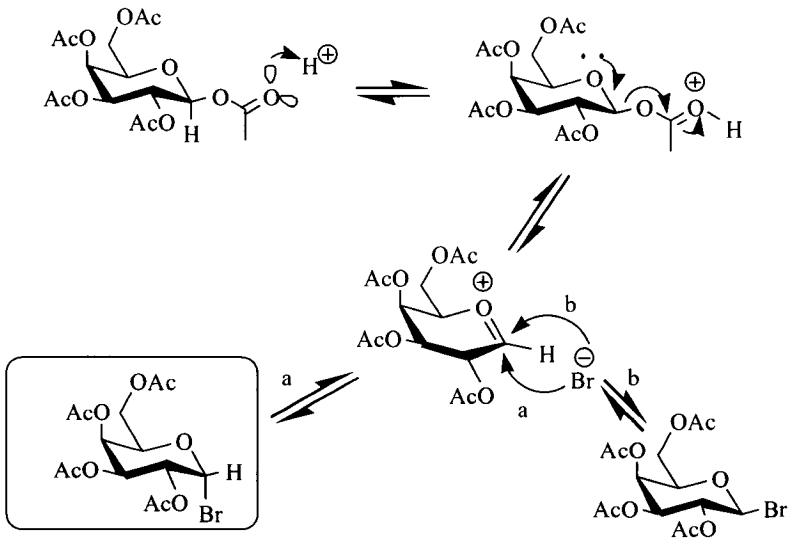

Scheme 3.2: Mechanism of α-bromopyranose synthesis

α-C-allyl-D-galactose tetraacetate **46** was synthesized from *α*-bromo-D-galactose tetraacetate **45** using a protocol developed by Magnusson and co-workers.[4] The photochemically mediated allylation required (1.4 equivalents of bis-tributyl tin, 3 equivalents of allyl-phenyl-sulfone, 55 equivalents of distilled benzene) and 12 hours exposure to a 450W mercury lamp. The longer reaction time (compared to the one stated in the literature), produced an improved yield of 87 % over the 71 % yield reported by Magnusson. The *C*-allylated-D-galactose derivative **46** was then oxidized via ozonolysis to the corresponding aldehyde derivative **47** in 95 % yield. Compound **47** was further oxidized to the carboxylic acid derivative **48** in 90 % yield via the Pinnick oxidation. 2-methyl-2-butene was used in excess as a scavenger. This high yielding reaction was previously implemented in the Ben lab (Scheme 3.3).

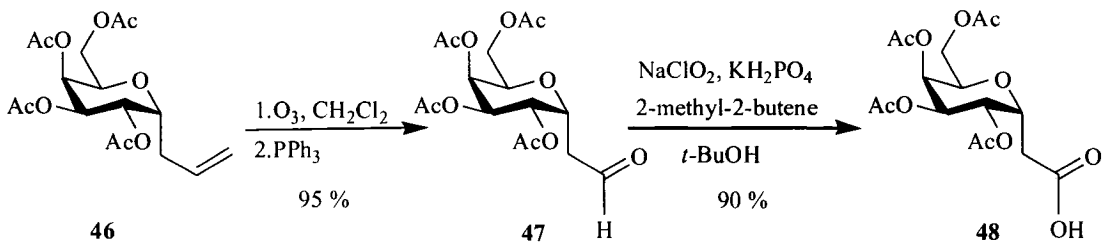

Scheme 3.3: Oxidation of C-allylated D-galactose

3.2 Preparation of the Amino Acid Components

Results from previous *C*-linked AFGP analogues studies suggested that a polypeptide with L-ornithine rather than L-lysine linking the carbohydrate to the peptide backbone have better RI activity. To study the effects of the side chain length on activity in the new analogues synthesized, the amino acids L-lysine and L-ornithine were coupled to the monosaccharide to prepare the building blocks for solid phase synthesis of new AFGP analogues

3.2.1 Preparation of Fmoc-L-Lysine-OBn

Commercial Fmoc-L-lysine(Boc)-OH **49** was activated *in situ* with 1,1-carbonyl diimidazole (CDI), and was subsequently reacted with benzyl alcohol to afford the fully protected benzyl ester of lysine **50** in 90 % yield. Selective deprotection of the acid-labile tertiary butoxycarbonyl (*t*-Boc) group was accomplished under acidic condition using 50% trifluoroacetic acid (TFA) in dichloromethane. The amino ester **51** with a free ε-amino terminus was recovered in 100 % yield as the TFA salt (Scheme 3.4).

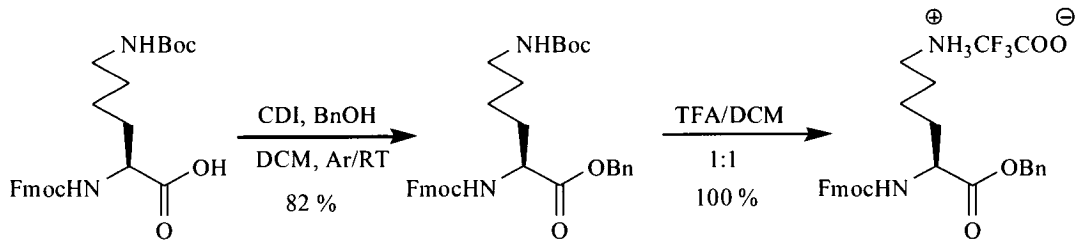

49 **50** **51**

Scheme 3.4: Synthesis of Fmoc-L-lysine-OBn

3.2.2. Preparation of Fmoc-L-Orn-OBn

Utilizing the same procedure as described in 3.2.1, commercial Fmoc-L-orn(Boc)-OH **52** was first benzylated to give the corresponding benzyl ester **53** in 90 % yield. Selective deprotection of the acid-labile *t*-Boc protecting group from the side chain amino acid was accomplished to afford **54** in 100 % yield (Scheme 3.5).

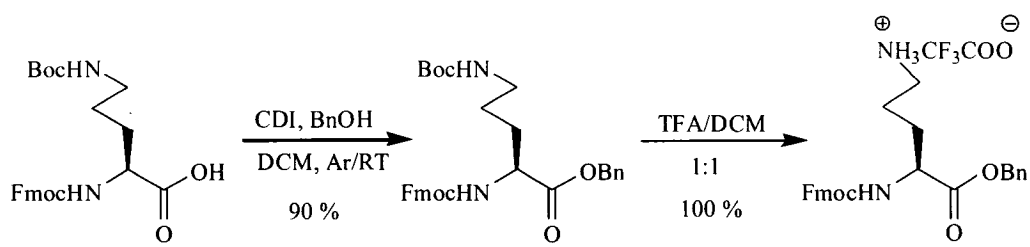

52 **53** **54**

Scheme 3.5: Synthesis of Fmoc-L-orn-OBn

3.3 Preparation of the Glycosylated Building Blocks

With both the carbohydrate and amino acid components in hand, coupling reactions were performed to prepare the glycosylated α-amino acids.

3.3.1 Synthesis of Glycosylated α-Amino Acids

The carbohydrate derivative **48** was directly coupled with the free ε-amino terminus of the amino acid L-lysine or L-ornithine (**51** or **54**) in the presence of the activating agent 2-(1H-Benzotriazole-1-yl)-1,1,3,3-tetramethyluronium hexafluorophosphate (HBTU) and diisopropyl ethylamine (DIPEA). After 12 hours reaction time, compound **55** was obtained in 83 % yield and compound **56** was obtained in 76 % yield (Scheme 3.6).

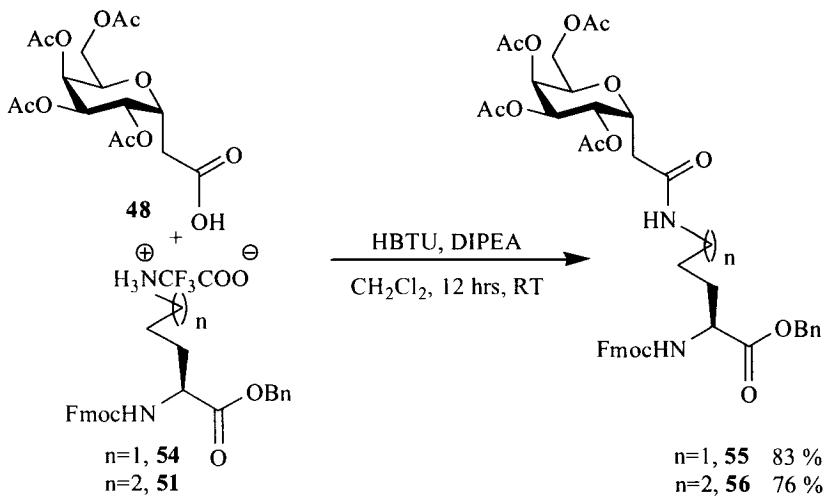

Scheme 3.6: Coupling of ornithine or lysine with the galactose derivative

The debenzylation of compound **55** and **56** was performed in the presence of 10% palladium on activated charcoal. With the use of methanol as the solvent, the undesirable cleavage of the Fmoc protecting group was detected for **56**. However, this side-product was greatly reduced when ethanol was used and **57** was obtained in 85 % yield. Compound **55** was found to have limited solubility in ethanol which resulted in a very poor yield of 10 % of **58**. To alleviate the problems of solubility in selective

hydrogenolysis for **55,** the solvent system was switched to 1:1 ethanol/ethylacetate, which produced compound **58** in 84 % yield (Scheme 3.7).

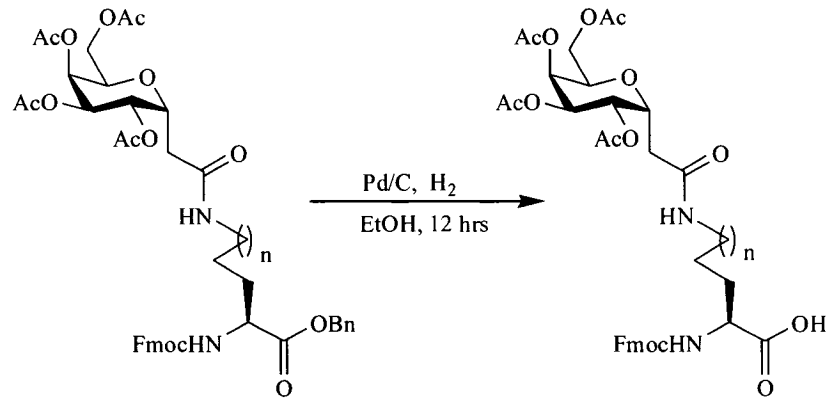

n=1, **55** 83 %
n=2, **56** 76 %

n=1, **58** 84 %
n=2, **57** 85 %

Scheme 3.7: Hydrogenolysis of glycosylated benzyl ester building blocks

3.3.2 Synthesis of β-Amino Acid Building Blocks via Arndt-Eistert Homologation

There was no precedent in the literature for the synthesis of glycosylated β-amino acids. However, given the significance of β-amino acids, numerous methodologies have emerged for the synthesis of optically pure β-amino acids.[5] Liguori and co-workers have reported the homologation of N-Fmoc protected α-amino acids to its corresponding β-amino acids in quantitative yields with the retention of configuration via the Arndt-Eistert reaction. The overall transformation is illustrated in Scheme 3.8.[6] It is based on the formation of N-Fmoc-aminoacyldiazoketone via the corresponding acyl chloride intermediate. The diazoketones formed in this reaction may be used in the rearrangement step without any purification. To ensure that the base-labile Fmoc protecting group

remained intact during decomposition of the diazoketone, base-free conditions (catalytic silver benzoate in dioxane and water at 70 °C) were used.

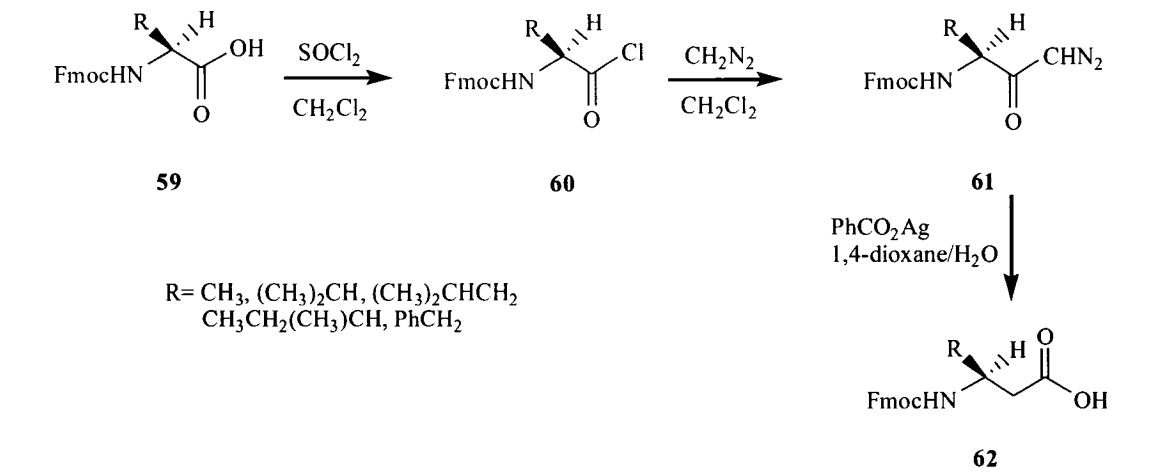

Scheme 3.8: Homologation of α-amino acids[6]

This approach was applied first to prepare diazoketone derivative **64** (Scheme 3.9). The intermediate acyl chloride derivative **63** was prepared using an excess of thionyl chloride, however, this product was not isolated because of its tendency to hydrolyze back to the starting material. The acid chloride formation was confirmed by IR spectroscopy. The corresponding diazoketone **64** was prepared after many failed attempts, by dropwise addition of acyl chloride **63** to an excess of a cold (0 °C) and dry solution of diazomethane in dichloromethane. Modification to the literature work-up procedure, afforded **64** as a yellow solid in 30 % yield. However, purification was tedious due to the formation of other products of close Rf values and the yield was not satisfactory.

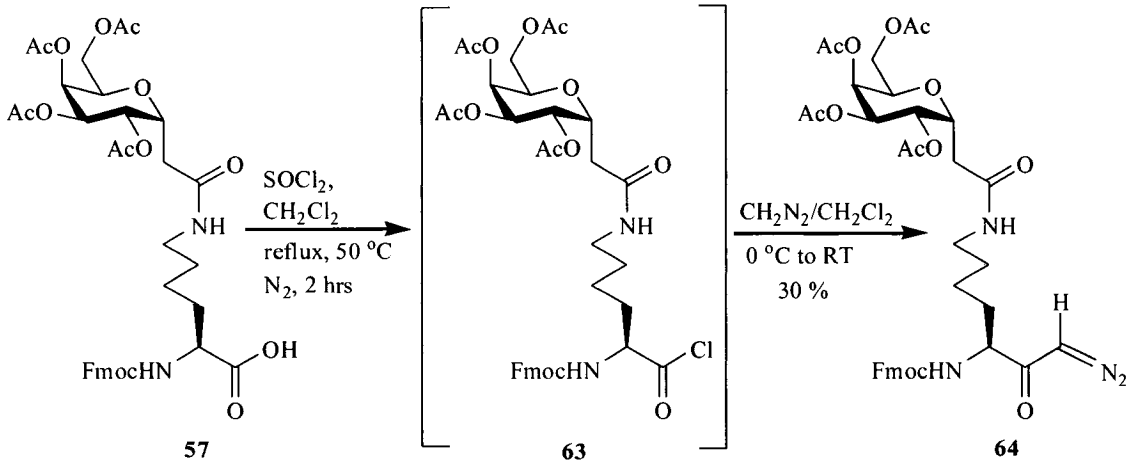

Scheme 3.9: Synthesis of diazoketone derivative of α-lysine

In an attempt to improve the synthesis of diazoketone derivative **64** from **57**, oxalyl chloride $(COCl)_2$ in the presence of catalytic dimethyl formamide (DMF) was employed. While the formation of acid chloride was confirmed by IR spectroscopy, the corresponding diazoketone was not detected.

Seebach and co-workers[7] have reported a modified version of the Arndt-Eistert reaction for use with N-Fmoc-protected α-amino acids to make the corresponding β-amino acids for solid phase synthesis applications. Their approach relies on the *in situ* formation of a mixed anhydride by the use of isobutyl chloroformate (*i*BuOCOCl) and N-methylmorpholine (NMM). The highly activated acid derivative was then converted into the corresponding diazoketone. This procedure was utilized to make diazoketone **64** (Scheme 3.10). The use of 1.05 equivalent of each of isobutyl chloroformate and N-methyl morpholine (NMM)) at low temperature (-20 °C) avoided the formation of unwanted side products. In addition, cleavage of base-labile Fmoc protecting group was

also not detected. 1-methyl-N-nitro-N-nirtoso-guanidine or N-methyl-N-nitrosourea was used as a precursor for the generation of diazomethane gas in diethyl ether. The reaction was started with 40 % aqueous potassium hydroxide. To ensure complete drying, the concentrated solution of diazomethane gas (0.7M) was stored over potassium hydroxide pellets overnight.

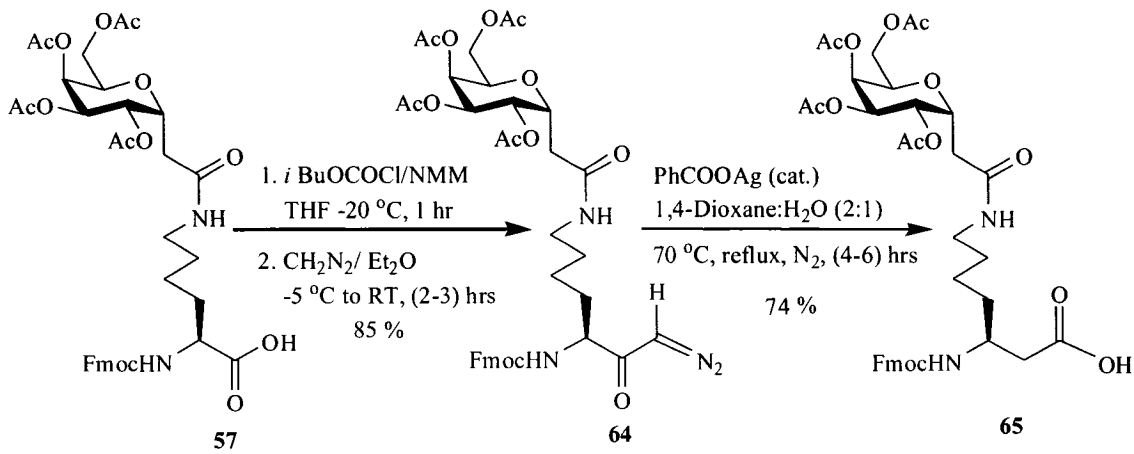

Scheme 3.10: Mixed anhydride- based approach for the synthesis of diazoketone derivative and synthesis of glycosylated β-lysine

The etheral solution of dry diazomethane was added at -5 °C to the reaction mixture containing the mixed anhydride until a rich yellow colour persisted. The reaction mixture was then allowed to warm up to room temperature until the reaction was complete by TLC (2-3 hours). Any excess diazomethane in the reaction mixture was removed by adding 5 % acetic acid. Aqueous work-up and evaporation of solvent at room temperature afforded the yellow solid of diazoketone **64** in 85 % yield after flash column chromatography through silica gel neutralized with triethylamine. Therefore, the mixed

anhydride-based procedure proved to be higher yielding and more efficient for our substrate as compared to the acyl chloride intermediate-based procedure described above.

Based on literature protocol,[6] compound **64** was allowed to undergo the Wolff rearrangement in the presence of catalytic silver benzoate in dioxane and water to afford **65** in 74 % yield (Scheme 3.10). Different reaction conditions used and the yields obtained for compounds **64** and **65** are summarized in table 3.1.

Entry	SM	Products	Reagents	Temperatures	Time	Yield (%)
1	**57**	**64**	1. $SOCl_2/CH_2Cl_2$ 2. CH_2N_2/Et_2O	50 °C 0 °C to RT	2 hrs 4 to 5 hrs	**30**
2	**57**	**64**	1. $(COCl)_2/CH_2Cl_2$ DMF 2. CH_2N_2/CH_2Cl_2	50 °C 0 °C to RT	2 hrs 4 to 5 hrs	**0**
3	**57**	**64**	1. *i* BuOCOCl/NMM 2. CH_2N_2/Et_2O	-20 °C -5 °C/RT	1 hrs 2 to 3 hrs	**85**
4	**64**	**65**	Cat. PhCOOAg, dioxane/H_2O (2:1)	70 °C	4 to 5 hrs	**74**

Table3.1: Summary of the different reaction conditions used and yields obtained

The above mentioned conditions for Arndt-Eistert homologation were optimized and applied to the synthesis of β-ornithine containing building block **70** to obtain a good yield (80 %) (Scheme 3.11). The building blocks containing β-amino acids were purified by HPLC before assembly into AFGP analogues via solid phase synthesis.

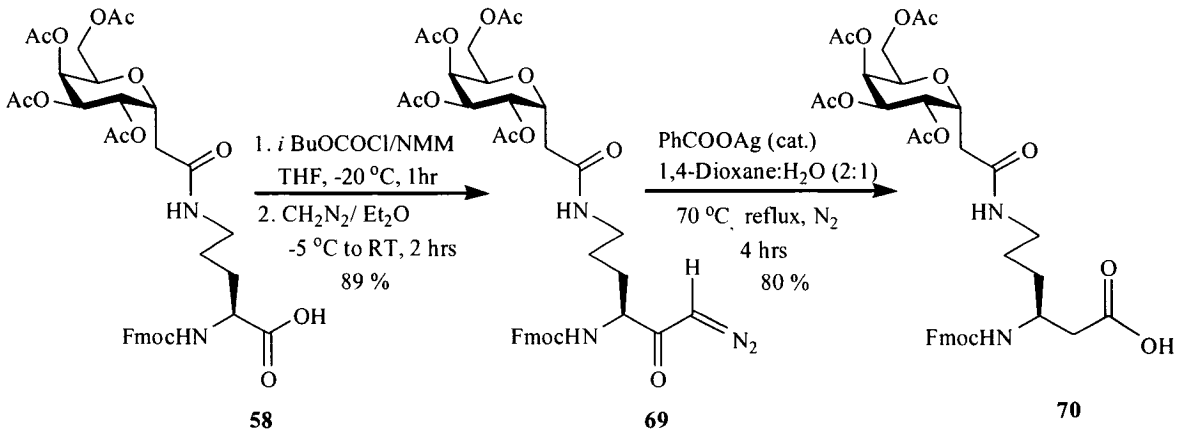

Scheme 3.11: Homologation of glycosylated α-ornithine

In summary, we have synthesized the glycosylated building blocks containing β-amino acids via standard and modified Arndt-Eistert homologation. The mixed anhydride-based modified Arndt-Eistert method proved to be high yielding and more efficient for the preparation of our desired glycosylated β-amino acid building blocks for solid phase assembly of our new AFGP analogues.

3.4 Solid Phase Synthesis

Solid phase chemistry began over forty years ago in 1963 with the elegant work of Merrifield.[8] Since then, the solid phase approach has been used in numerous areas for the synthesis of biopolymers,[9] polypeptides,[10] polysaccharides[11] and glycopolymers.[12] The main attraction of solid phase synthesis is its high yielding coupling steps and ease of purification which only involves washing of reagents with conventional solvents such as DMF, DCM, MeOH. Once the excess reagents are removed, the beads are ready for the

next coupling. The beads used are insoluble and provide a solid support for peptide synthesis.

3.4.1 General Strategy for Solid Phase Synthesis

The success of solid phase synthesis begins with the selection of a suitable solid support. Commercially available Fmoc-glycine pre-loaded Wang resin is used for the synthesis of glycopeptides. Wang resin (Figure 3.2) is made out of cross-linked polystyrene matrix and is functionalized with a *p*-benzyloxy benzylalcohol linker which facilitates the loading of the first amino acid by the C-terminus via an acid-labile ester bond.

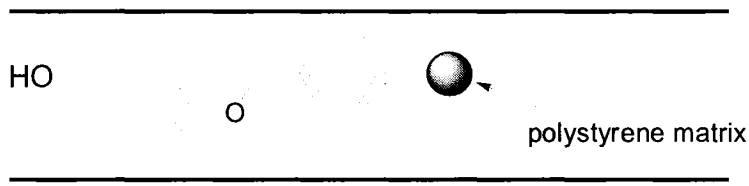

Figure 3.2: p-benzyloxy benzylalcohol (Wang) resin

In addition, the bead has a good swelling capacity. The resin is activated by soaking the resin in dry DMF for one hour. The glycopeptides are assembled using an Fmoc strategy.[13] The Fmoc strategy involves removal of the Fmoc protecting group at the α-terminus of the amino acid with a base such as piperidine to provide a free site for coupling to the next activated and Fmoc protected amino acid. The amino acid activation is done *in situ* using 1.1 to 3 equivalents of each of the activating agent 2-(1H-Benzotriazole-1-yl)-1,1,3,3-tetramethyluronium hexafluorophosphate (HBTU) and diisopropylethylamine (DIPEA) with respect to the amino acid that in turn is calculated in terms of resin loading. Resin loading varies in different batches from 0.6 to 0.65 g/mol.

The first amide bond is formed between the activated amino acid and the resin bound amino acid in basic media. The coupling of amino acids requires 24 to 48 hours depending on the type of amino acid. Excess reagents are washed off with N,N-dimethyl formamide (DMF) for 15 minutes, three times (3 x 10 mL), after each Fmoc deprotection and amino acid coupling step. The growth of the polymer chain is accomplished by the sequential Fmoc deprotection and coupling of new amino acids until the desired length of peptide is synthesized. After deprotection of the last Fmoc protecting group, the polymer is cleaved from the resin and remains in solution. It is subsequently precipitated out from diethyl ether as a solid product. Deacetylation is achieved in basic conditions and the product is neutralized with acid exchange resin (amberlite IR-120). The final AFGP analogues are obtained after lyophilization and purification by reverse phase HPLC. The presence or absence of free primary amine during Fmoc deprotection and amino acid coupling is tested primarily by visual colorimetric Kaiser[14] and TNBS[15] tests. In the Kaiser test, beads change colour from light yellow to blue for the positive test, which indicates the presence of free primary amine, whereas in the TNBS test, the orange/red colour of the beads is an indication of a positive test. The negative test in both cases is confirmed by the original colour of the beads.

A Summary for the general solid phase synthesis protocol is outlined in Scheme 3.12.

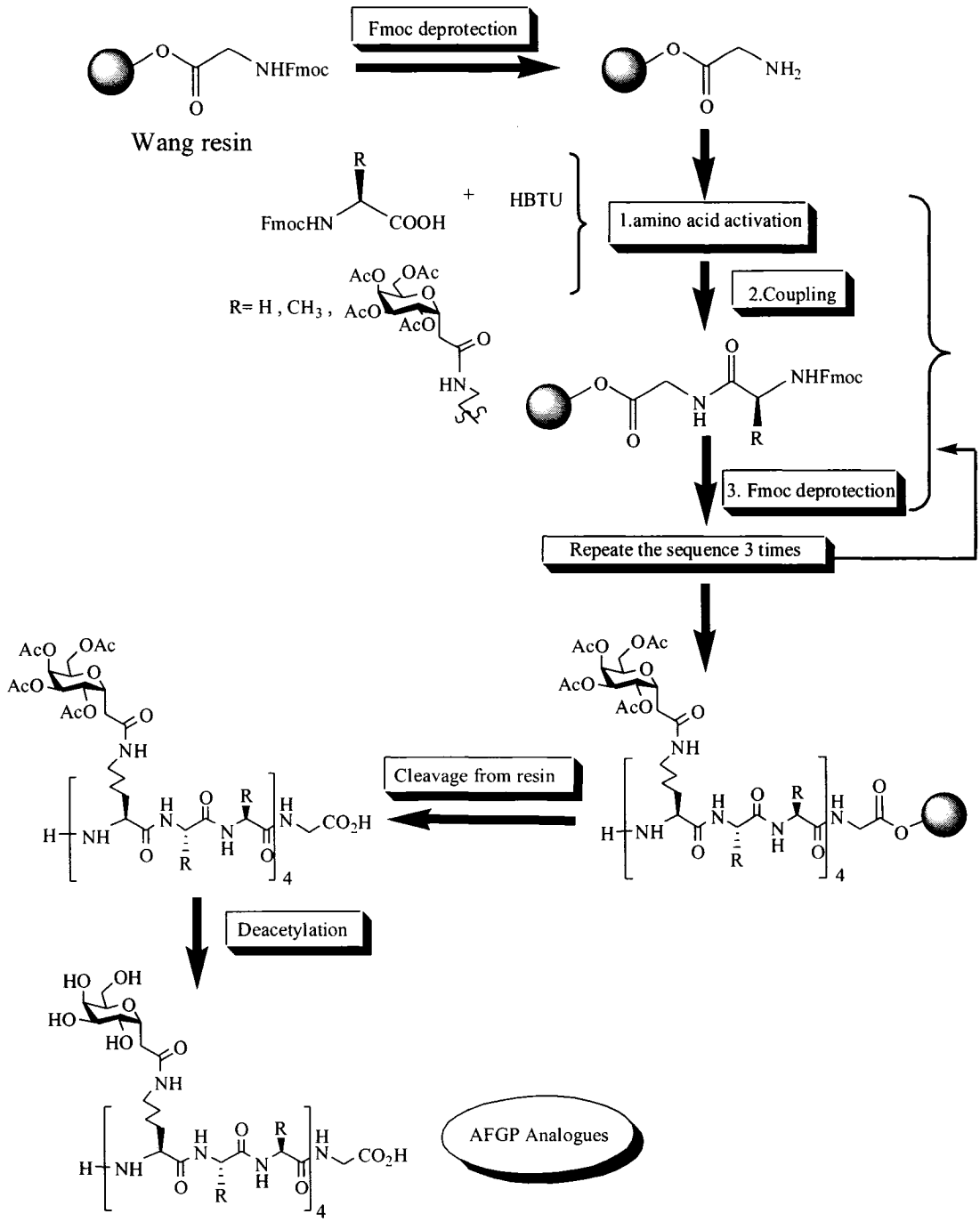

Scheme 3.12: General strategy for solid phase synthesis

3.4.2 Solid Phase Assembly of New Analogues

All of the new AFGP analogues were assembled via manual solid phase synthesis protocols. In previous studies, it was found that four tripeptide repeat units is the minimum peptide length requirement for antifreeze activity.[16] Given this finding, and to allow for a comparative study with the second generation analogues, we decided to prepare polymers with four tripeptide repeat units.

3.4.2.1 Synthesis of [β-Lysine (D-Galactose)-Alanine-Alanine]$_4$ Glycine

The Fmoc-glycine pre-loaded Wang resin with a loading capacity of 0.6 mmol/g was activated by swelling with dry DMF for 1 hour. The resin bound amino acid Fmoc deprotection was accomplished by treatment with 20 % piperidine in dry DMF. Gentle shaking for 2 hours was done in a spinner to ensure minimum mechanical damage to the resin. Excess reagents were washed off with DMF and Fmoc deprotection was confirmed with positive Kaiser (ninhydrin) and 2,4,6-trinitrobenzenensulfonic acid (TNBS) tests. The first amino acid coupling with free amine bound to the resin was performed with commercial alanine (3 equivalents) pre-activated with HBTU (3 equivalents) in DMF in the presence of DIPEA (3 equivalents). The solution was allowed to shake for 24 hours in a manual solid phase synthesizer. Excess reagents were washed off with DMF. Completion of reaction was ensured with negative Kaiser and TNBS tests. The whole process was repeated for the second amino acid coupling with commercial alanine. The third coupling was performed with building block **65** to complete the tripeptide. Building block coupling was done with 1.2 equivalents of each of the reagents. The entire sequence of tripeptide formation was repeated three more times to get four tripeptide

repeat units. The progress of the building block coupling was monitored every 24 hours. In contrast to commercial amino acids, the β-amino acid containing building block required longer coupling times (48 hours). Another important issue concerning β-amino acid building block is that the Kaiser ninhydrine test for the Fmoc deprotection failed. That is, beads did not change colour with the ninhydrin reagents despite the reaction having reached completion. Similar results have been reported by Seebach and co-workers[6] in the synthesis of β-peptides. Therefore, the completion of the reaction was monitored by TNBS tests only. After the final deprotection of the Fmoc protecting group, the resin was washed successively with DMF, DCM and MeOH to allow for the maximum swelling and contraction of the resin pockets. The resin was dried over KOH pellets for 6 hours under high vacuum. The desired product was cleaved from the resin by treatment with 50 % TFA in DCM. Evaporation and precipitation with diethyl ether afforded 90 % yield (on the basis of resin loading) of the brown sticky solid **71** (Scheme 3.13).

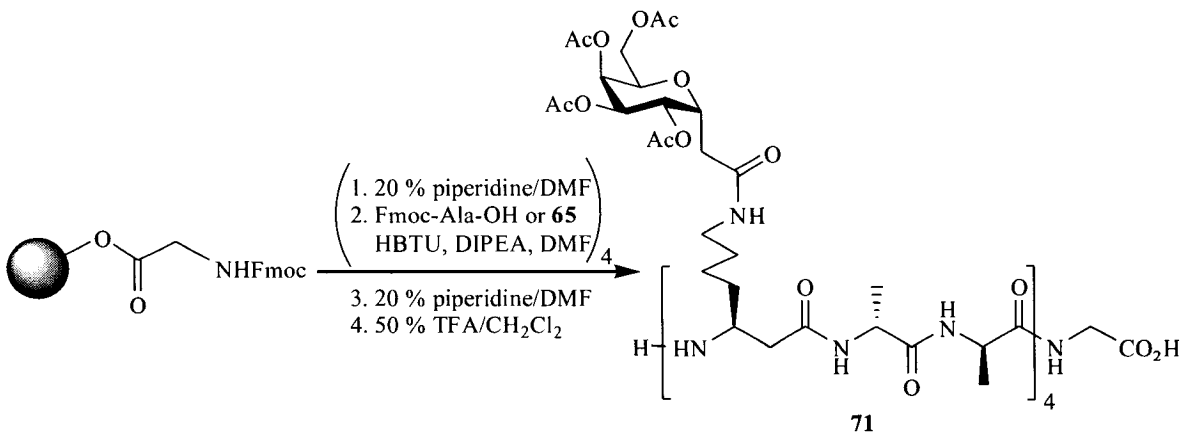

71

Scheme 3.13: Solid phase assembly of [β-lys (D-gal)-ala-ala]$_4$ gly

Deacetylation of **71** was performed in basic conditions in the presence of sodium methoxide (pH 10 to 11). The reaction mixture was neutralized with acidic Amberlite IR-120 resin, filtered, concentrated, lyophilized and purified by reverse phase HPLC using standard glycoprotein purification protocol with acetonitrile and water (0.1 % TFA in water and acetonitrile) to afford analogue **72** in quantative yield (Scheme 3.14).

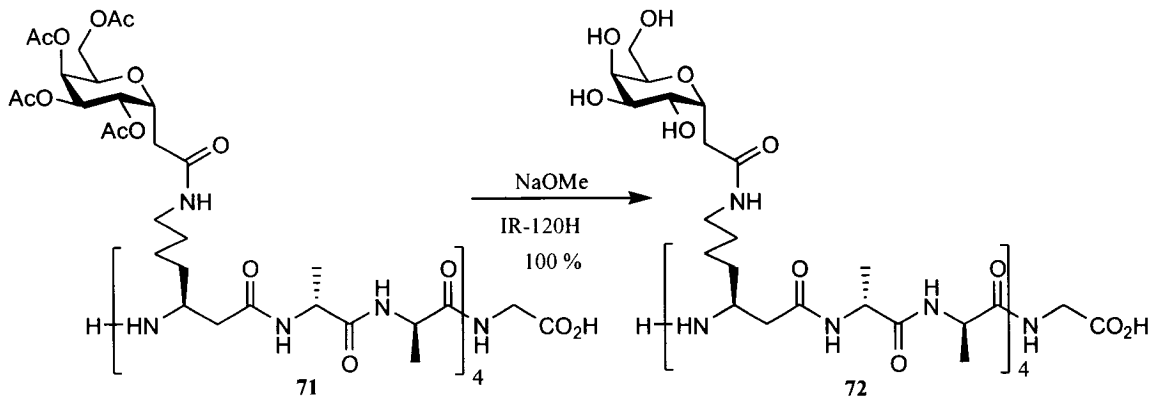

Scheme 3.14: Deacetylation of polymer obtained from solid phase synthesis

3.4.2.2 Synthesis of [β-Lysine (D-Galactose)-Glycine-Glycine]$_4$ Glycine

A similar protocol (as mentioned in 3.4.2.1) was used for the synthesis of **73**, although commercial L-alanine was substituted with commercial L-glycine and analogue **74** was isolated in 90 % yield after HPLC purification (Scheme 3.15).

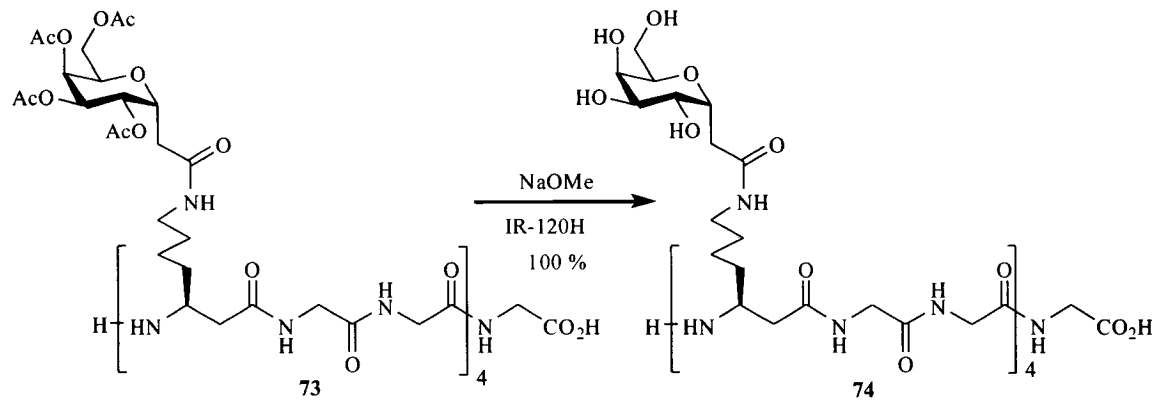

Scheme 3.15: Analogue [β-lys (gal)-gly-gly]$_4$ gly, synthesized via solid phase

3.4.2.3 Synthesis of [β-Ornithine (D-Galactose)–Glycine-Glycine]$_4$ Glycine

For the purpose of comparative study with the most RI active second generation analogue **42**, we prepared the corresponding analogue **76** containing β-ornithine. The above mentioned optimized manual solid phase synthesis protocol was applied to prepare the desired protected AFGP analogue **75** in 93 % yield. Deacetylation of **75** afforded a white solid of **76** in quantitative yield after purification by reverse phase HPLC (Scheme 3.16).

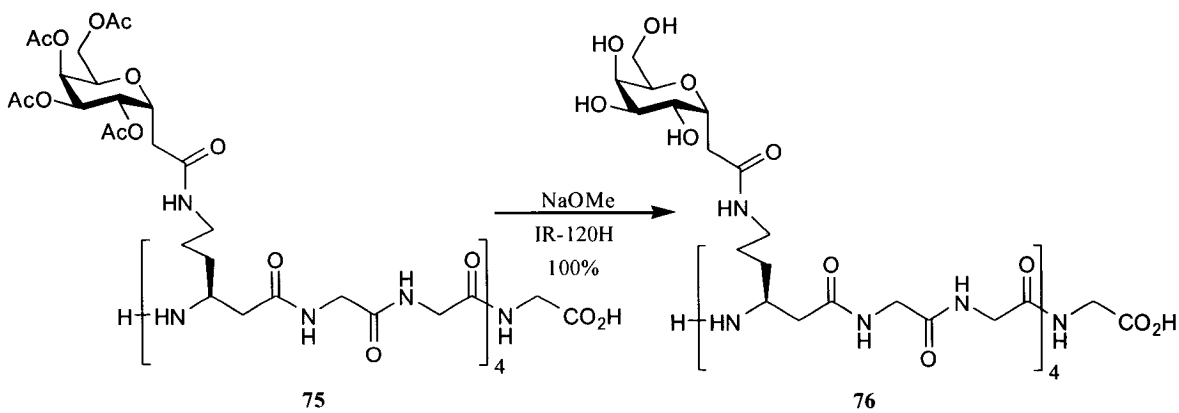

Scheme 3.16: Analogue [β-orn(gal)-gly-gly]$_4$ gly synthesized via solid phase

The results from solid phase synthesis were confirmed with MALDI spectrometry and are summarized in Table 3.2.

New AFGP Analogues containing β-Amino Acids		**Yield**
[β-lysine(D-galactose)-alanine-alanine]$_4$ glycine	**72**	90 %
[β-lysine(D-galacose)-glycine-glycine]$_4$ glycine	**74**	90 %
[β-ornithine(D-galactose)-glycine-glycine]$_4$ glycine	**76**	93 %

Table 3.2: Summary of new AFGP analogues prepared via solid phase synthesis

In conclusion, we have successfully synthesized all of the three targeted AFGP analogues containing glycosylated β-amino acid via manual solid phase synthesis protocol. The use of solid phase synthesis has been shown to be an efficient method to synthesize AFGP analogues containing β-amino acids. The syntheses were reproducible, high yielding and required only very little purification.

References:

[1] Liu, S., Ben, N. R. *Organic Letters*, **2005**, *7*, 2385-2388.

[2] Deslongchamps, P., *Streoelectronic effects in Organic Chemistry,* Pegamon Press, **1983**, p. 4 -8

[3] Stick. R. V. *Carbohydrate, The Sweet Molecules of Life*; Acedemic press 2001.

[4] Ponten, F., Magnusson, G. *J. Org. Chem.* **1996**, *61*, 7463

[5] Liu, M., Sibi, M. P. *Tetrahedron*, **2002**, *58*, 7991-8035.

[6] Liguori, A., Leggio, A.,Procopio, A. ,Sindona,G.*J. Chem. Soc., Perkin Trans. 1*, **1997**, 1969-1971

[7] Seebach, D., Abele, S., Guichard, G. *Helvita Chemica Acta.* **1998**, *81*, 187

[8] Merrifield, R.B. *J. Am. Chem. Soc.* **1963**, *85*, 2149.

[9] Farrall, M.J., Frechet, J.M.J. *J. Org. Chem.* **1976**, *46*, 3877

[10] Houghten, R. A., Pinilla, C., Blondelle, S. E., Appel, J. R., Dooley, C. T., Cuervo, J. H. *Nature* **2001**, *354*, 84.

[11] Ecker, D. J., Vickers, T. A., Hanecak, R., Driver, V., Anderson, K. *Nucleic Acid Res.* **1993**, *21*, 1853.

[12] Eniade, A., Ben, R. N. *Biomacromolecules* **2001**, *2*, 557.

[13] Fields, G. B., Noble, R. L. *Int. J. Pept. Protein Res.* **1990**, *35*, 161-214.

[14] Kaiser, E. *Anal. Biochem.* **1970**, *34*, 595

[15] Hancock, W. S., Battersby, J. E. *Anal. Biochem.* **1976**, *71*, 261.

[16] (a) Tsuda, T., Nishimura, S. T. *Chem. Commun.*, **1996**, 2779; (b) Shioiri, T., Ninomiya, K., Yamada, S. I. *J. Am. Chem. Soc.* **1972**, *94*, 6203.

Chapter 4

4.0 ANTIFREEZE ACTIVITY AND SOLUTION CONFORMATION OF NEW AFGP ANALOGUES 75

4.0 Antifreeze Activity and Solution Conformation of New AFGP Analogues

The antifreeze specific activity of both natural and synthetic analogues has been assessed by utilizing their unique properties: thermal hysteresis (TH), recrystallization inhibition (RI) and dynamic ice shaping.[1] Circular dichroism (CD) has been widely used to study the solution conformation of glycoproteins.

4.1 Assessing Thermal Hysteresis (TH) Activity and Dynamic Ice Shaping of Analogues 72, 74 and 76.

The test was performed by using nanoliter osmometer (Figure 4.1). This technique is regarded as the "golden standard" for antifreeze-specific activity assessment. This is one of the most important tests to quantify antifreeze-specific activity of biological antifreezes.

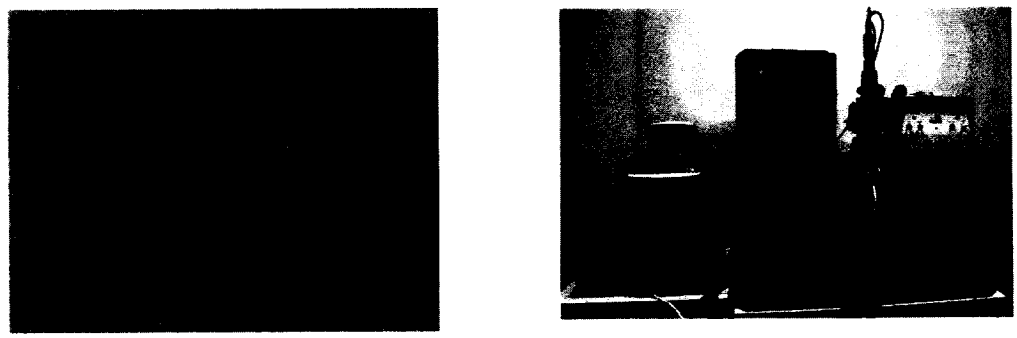

A B

Figure 4.1: A) Sample holder B) Clifton technical physics nanoliter osmometer: Instrument ranges 0 to 5,000 milliOsmos (1.0 Osmo = - 1.86 °C)

This technique not only allows the measurement of the TH gap, but it is also used to observe changes in the ice crystal morphology. These changes are known as "dynamic ice shaping." Dynamic ice shaping is the result of adsorption of antifreeze molecules onto the specific faces of ice crystals, which produces different polymorphic forms.[2] To perform the assay, the sample was prepared by dissolving 10 mg/mL of the analogues in double distilled water. A sample holder containing nanoholes was loaded with paraffin-oil. A nanoliter droplet of analyte was then submerged in the pre-cooled oil in the sample holder and flash-frozen at -40 °C. The temperature was then gradually increased until the sample was melted back to a single ice crystal. The melting point was then determined. The freezing point was determined by gradually decreasing the temperature. A degree of thermal hysteresis was determined by lowering 10 mOsmos (0.0186 °C) units of temperature every 15 seconds. The thermal hysteresis gap is the difference between freezing point and melting point.

Biological antifreezes have the unique ability to bind to the surface of an ice crystal and change the ice crystal morphology and the rate of growth within the TH gap. This can be visualized using nanolitre osmometry. AFGP 8 produces hexagonal bipyramidal ice crystals (Figure 4.2A) within the TH gap. The crystals grow explosively and burst (spiculate) when the temperature is lowered below the freezing point (Figure 4.2B).

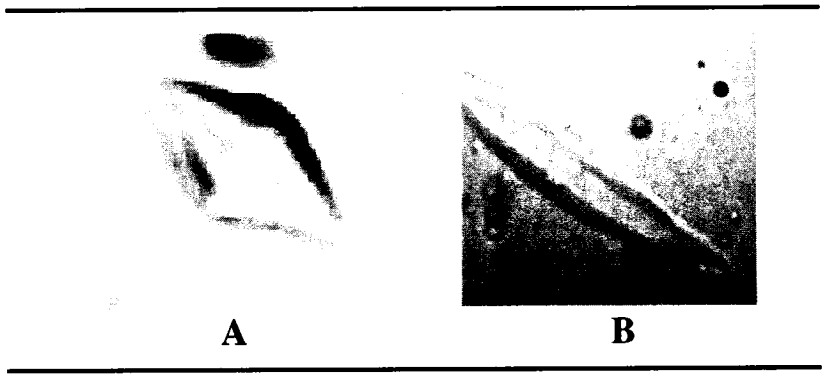

Figure 4.2: A) Ice crystal in the presence of AFGP 8 B) Ice spicule formation below TH gap

The ice spiculation effect is unique to biological antifreezes. In the absence of biological antifreezes, ice crystals are round and have no edges and facets (Figure 4.3).

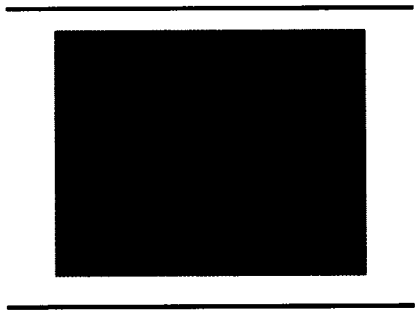

Figure 4.3: Ice crystal of distilled water (round shape)

Nanolitre osmometry assay results of all of our new AFGP analogues are presented in table 4.1. Interestingly, all of the analogues tested showed a significant degree of thermal hysteresis as well as dynamic ice shaping. The TH gap shown by these analogues were even higher than the TH gap reported for the synthetic AFGP 8 prepared by Nishimura and co-workers[3] at equimolar concentrations. Nishimura's synthetic AFGP 8 contains all the structural features of native AFGP 8 including the disaccharide moiety possessing the acetamide (-$NHCOCH_3$) group at the C-2 position of the reducing sugar as

well as the threonine residue in the peptide backbone. To identify the structural motif essential for the antifreeze activity they synthesized a series of AFGP analogues and tested for TH activity.

Compounds	Ice shaping	TH (°C)
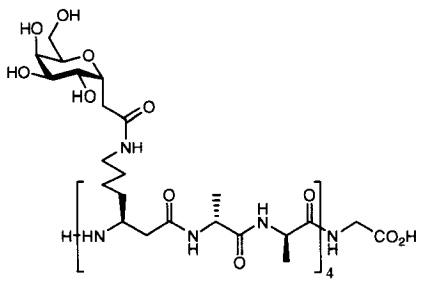 **72**	 Hexagonal bipyramidal	-0.17±0.002
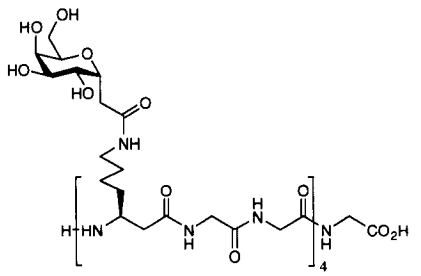 **74**	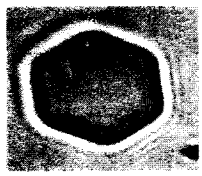 Hexagon	-0.12±0.002
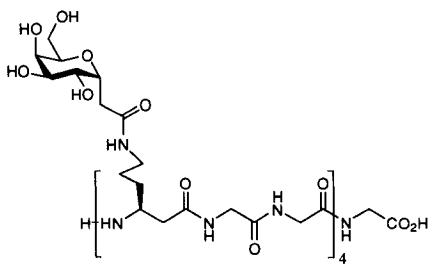 **76**	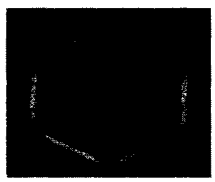 Hexagon	-0.10±0.002
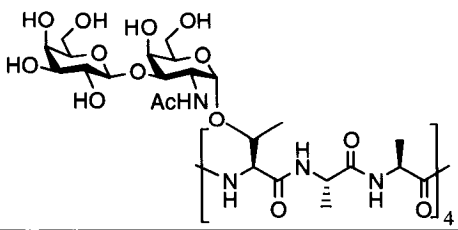 **AFGP 8**	 Hexagonal bipyramidal	-0.12 (Fletcher[4])

Table 4.1: Results from nanoliter osmometry: New analogues and AFGP 8

The findings from their work suggested that C-2 acetamide group is crucial for the TH activity.[3] However, our results showed that C-2 acetamide group is not a key functional group required for TH activity in our *C*-linked AFGP analogues since all of our new analogues (**72**, **74** and **76**) replaced the disaccharide with a single galactose moiety and no acetamide group at the C-2 position, and still displayed increased TH activity.

Among the three analogues, compound **72**, which contained *β*-(L-lysine)-L-alanine-L-alanine in the peptide backbone, displayed the largest TH gap of 0.17 °C at concentration 10 mg/mL. This TH gap is higher than the native AFGP 8 reported by Fletcher and co-workers[4] at the same concentrations (table 4.1). As mentioned, analogue **72** replaced disaccharide in native AFGP 8 with a single galactose moiety and L-threonine with the *β*-amino acid analogue of L-lysine. It is likely that despite the dramatic structural changes compared to the native AFGP 8, analogue **72** must contain a structural motif that is favourable for ice binding and for freezing point depression similar to that of native AFGP 8. Notably, the second generation analogue **41** that contained a α-(L-lysine)-L-alanine-L-alanine (Figure 4.4) backbone showed neither thermal hysteresis nor dynamic ice shaping.

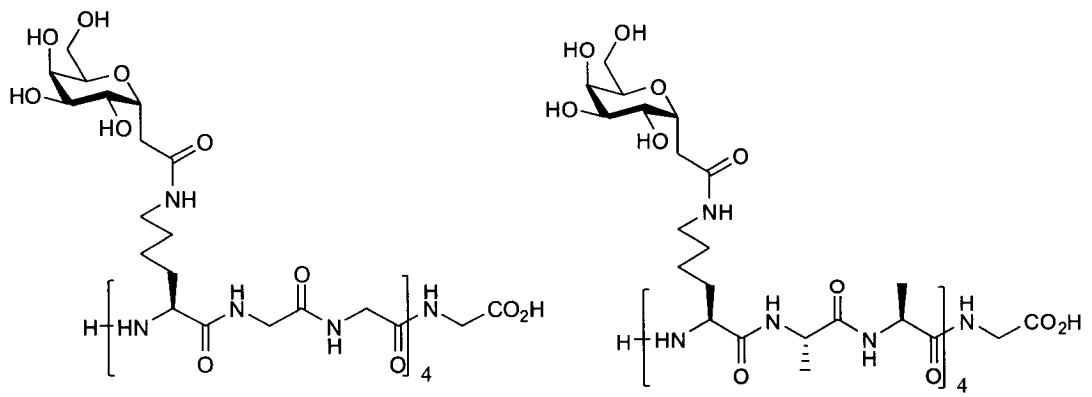

Figure 4.4: Structure of the second generation analogues

The only difference between the two compounds is one carbon atom per building block that is four per peptide. Thus, it seems likely that the β-amino acid in the peptide backbone is resulting in the increased TH activity. These results suggest that the modification of the polypeptide backbone may change the conformation of AFGP analogue to one that is favourable for ice lattice matching ultimately resulting an enhanced TH activity. In addition analogue **72**, displayed hexagonal bipyramidal ice shaping (Table 4.1), indicating that the analogue interacts with the ice surface. Interestingly, unlike AFGP 8 which forms ice spicules when the temperature is lowered below the freezing point, the analogue caused the ice to change shape from hexagonal bipyramidal to a hexagon until all the solution was frozen. The significance of different ice crystal morphologies has not been explained in the antifreeze literature.

Analogue **74** replaced L-alanine residues in the peptide backbone of analogue **72** with L-glycine residues to give β-(L-lysine)-L-glycine-L-glycine. The TH gap exhibited by analogue **74** was somewhat lower than the TH gap produced by analogue **72** (Table 4.1). The only difference between analogues **72** and **74** is the amino acid residues (L-alanine and L-glycine respectively) in the peptide backbone. From this series of experiments it is likely that L-alanine residues play some part in the TH activity.[5] In addition, the mode of ice interaction of analogue **74** seems to be different than analogue **72** as it produced a hexagonal ice crystal (table 4.1) that remained below the TH gap (Figure 4.5). It is reported that hexagonal ice shaping results from the binding of biological antifreezes to both the prism and basal planes.[6] However, the second generation analogue **40** containing the glycosylated α-(L-lysine)-L-glycine-L-glycine peptide backbone (Figure 4.4), did not display any of these antifreeze-specific activities.

Figure 4.5: Ice growth below freezing point in a solution of 74

This again suggests the possibility of favourable conformational change attributed to the β-amino acid incorporated polypeptide backbone for TH activity.

Analogue **76** showed comparable TH activity and hexagonal ice shaping (Table 4.1) to that of analogue **74**. This analogue incorporated β-(L-ornithine)-L-glycine-L-glycine in the peptide backbone. Therefore, the replacement of L-lysine with L-ornithine does not enhance the thermal hysteresis activity and thus indicates that the change in length of the side chain by one methylene group apparently has minimal effect on TH activity. The α-L-ornithine containing analogue **42** (Figure 4.6), on the other hand, did not display any observable TH activity but did show ice binding as demonstrated by the hexagonal shape of the ice crystal.[7] These results suggest that the modification of the peptide backbone by incorporating β-amino acid is important for the TH activity.

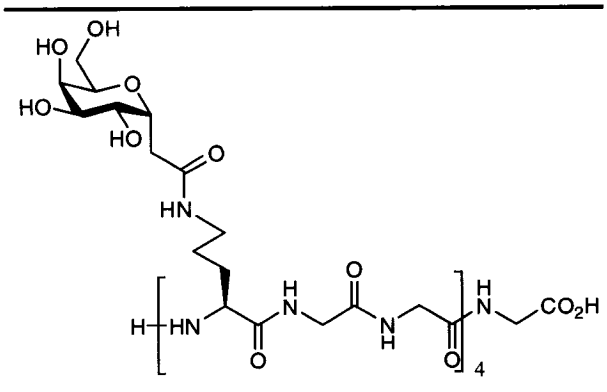

42

Figure 4.6: Structure of ornithine containing second generation analogue

In summary, all three of the new analogues, despite being drastically different in structures from native AFGP 8, displayed comparable thermal hysteresis activity as well as dynamic ice shaping. Analogue **72**, which contained L-alanine resides in the peptide backbone, showed the highest TH activity, suggesting that L-alanine residues are important for increased TH activity. On the other hand, a change in side chain length between the carbohydrate and the peptide backbone has minimal effect on antifreeze activity as shown by the comparable TH gaps of analogues **74** and **76**. The only structural difference between the new analogues (**72**, **74** and **76**) and the corresponding second generation analogues (**41**, **40** and **42**) is the presence of an extra methylene groups at every third amino acid in the peptide backbone. Hence, incorporation of β-amino acid seems to enhance TH activity of our peptides. This could be due to the dramatic conformational change attributed to the β-amino acids incorporated polypeptide backbone which might adopt the conformation that is favourable for the ice lattice matching and hence strong interaction to the ice surface. This results in an enhanced TH activity and lowering of freezing point. The study also suggests that C-2 acetamide group is not the key functional group for TH activity in our *C*-linked AFGP analogues.

4.2 Assessing Recrystallization Inhibition (RI) Activity of Analogues 72, 74 and 76.

Another technique to quantify antifreeze specific activity of biological antifreezes is the recrystallization inhibition (RI) assay.[8] This technique can detect antifreeze activity at very low sample concentrations compared to that required for observable TH activity.[9] Further, it also allows actual measurement of ice crystal sizes. To perform the RI assay, a stock solution at a concentration of 5.54 x 10^{-4} M was prepared by dissolving the analogue in a phosphate-buffered saline (PBS) solution at pH 7.4, followed by further dilution to various concentrations. A 10 µl droplet of the solution was dropped from a height of three meters onto a pre-cooled aluminum block at -78 °C. The droplet instantly freezes as a very thin wafer which was then immediately transferred to a microscope stage where the temperature was maintained at -6 °C. The wafer was then allowed to anneal for 30 minutes to facilitate the recrystallization process. Photographs were taken at three different areas of the wafer for each concentration and were analyzed.

The surface area of individual crystal was calculated via elliptical area using, $A = \pi ab$, where 'A' is the area, and 'a' and 'b' are the radii of the ellipse. After determination of the actual size of each grain, the mean largest grain sizes (MLGS) from 30 different largest grains were calculated for the particular sample. Figure 4.7 provides an example of the photograph taken from the particular area of a wafer and a table of average area calculated for the four largest crystals (**1**, **2**, **3** and **4**) selected directly from the photographs. Sides A and B represent the length and width of the ellipse of a crystal respectively. The average area for these largest grain sizes was calculated using

computer software "Photoshop." The value from "Photoshop" was then converted into millimeter square units from the known value of PBS control.

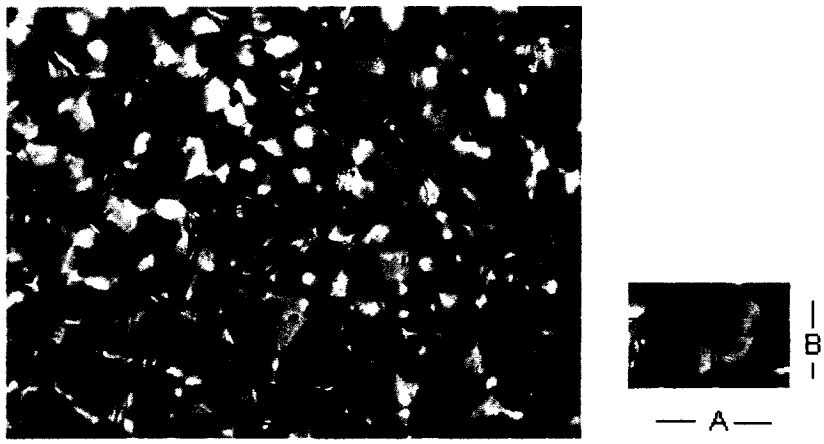

Photograph: Illustration of ten largest grains selected for MLGS calculation

(Magnification 20 x)

Ice crystal	Side	Diameter	Radius	Area	Average area(MLGS)	Average Area (MLGS) in mm^2
1	A	45.6	22.80	1167.54	1108.52	0.01
	B	32.6	16.30			
2	A	41.6	20.80	967.11		
	B	29.6	14.80			
3	A	38.7	19.35	1012.15		
	B	33.3	16.65			
4	A	41.6	20.80	1287.30		
	B	39.4	19.70			

Figure 4.7: Mean Largest Grain Size (MLGS) calculated from photograph

In actual calculation the ten largest grains from each particular area of a wafer were selected and it was done on triplicate. The error in calculation was propagated in terms of standard error of mean (SEM).[10] The mean largest grain size was then plotted

against the different concentrations of analogue in PBS solution serving as the negative control.

Graph 4.1 is a representation of the recrystallization inhibition assay performed on AFGP 8 at various concentrations ranging from 5.54 x 10^{-6} M to 5.54 x 10^{-12} M. Various concentrations were used to rule out the non-specific RI effect produced by antifreeze glycoprotein.[11] The MLGS at the highest concentration of 5.54 x 10^{-6} M was 1.56 x 10^{-3} mm^2 and at the lowest concentration 5.54 x 10^{-12} M was 1.24 x 10^{-2} mm^2. The relationship between concentration of the sample and MLGS is inverse. In other words, the average grain size increases with the decreasing sample concentrations. However, the relationship is not linear. This implies that AFGP 8 shows non-colligative behaviour of RI activity. From a previous study of the Ben lab[12] it was seen that colligatively-acting

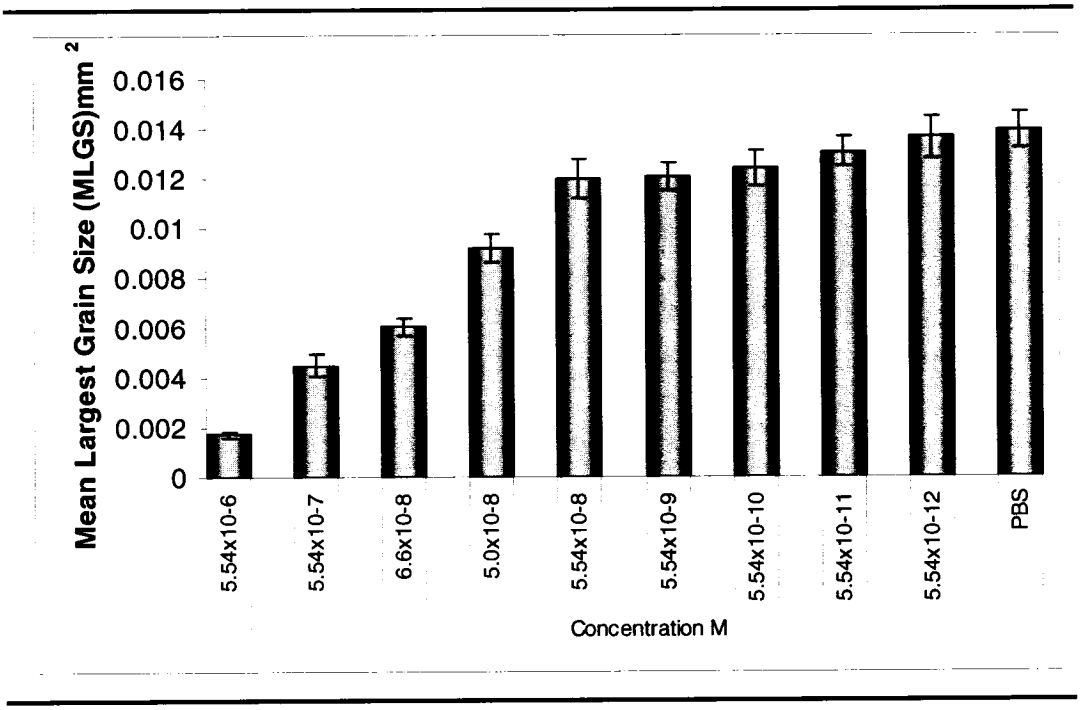

Graph 4.1: Recrystallization inhibition assay of AFGP 8

substances like sodium chloride and proteins (bovine serum albumen) had no effect on recrystallization inhibition and MLGS calculated were found to be comparable to those of PBS control (data not shown). The above graph shows that the AFGP 8 is a potent recrystallization inhibitor compared to the PBS control.

All of the new AFGP analogues (**72**, **74**, and **76**) were assayed for RI activity and compared with a PBS solution as a negative control. The results are presented in Graph 4.2. Results showed that the RI activity of these analogues were not as great as it was anticipated. Among the three new compounds (**72**, **74**, and **76**), compound **76** was the most active recrystallization inhibitor as the average mean largest grain size of the ice crystals observed with the most concentrated solution was smaller compared to compounds **72** and **74**.

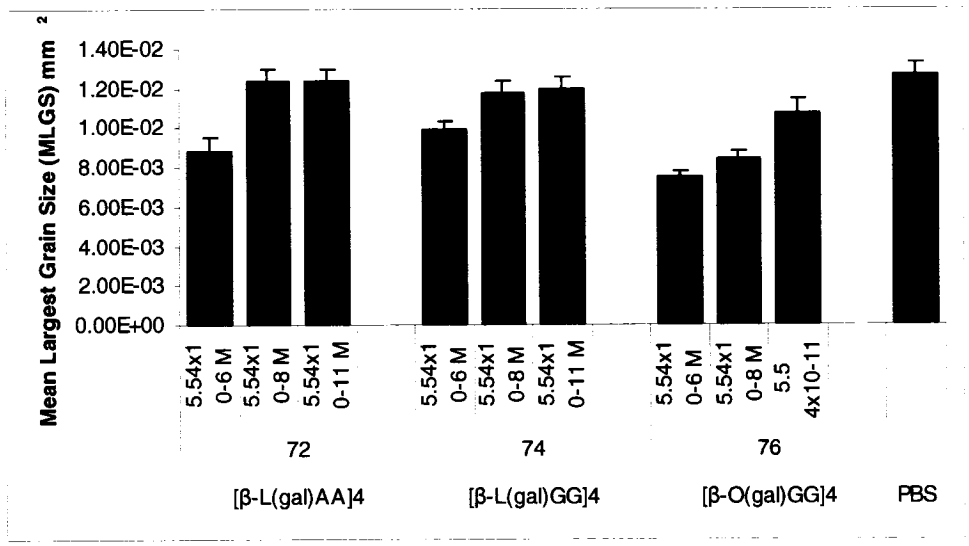

Graph 4.2: Recrystallization inhibition assay of new AFGP analogues

The MLGS value for ice crystals observed with compound **76** at a concentration of 5.54 x 10^{-6} M was 7.50 x 10^{-3} ± 3.3 x 10^{-4} mm^2. This value was 40 % smaller in grain size compared to the PBS solution (1.26 x 10^{-2} mm^2). Previous findings in our lab suggested that the analogue containing α-L-ornithine in the peptide backbone had greater RI activity compared to the analogue that contained an α-L-lysine side chain.[6] This was the same for analogues containing *β*-amino acids. Graph 4.2 showed that compound **76** with *β*-(L-ornithine)–L-glycine-L-glycine peptide backbone was more active than both compounds **74** *β*-(L-lysine)-L-glycine-L-glycine and **72** *β*-(L-lysine)-L-alanine-L-alanine. This suggests that there is a relationship between side chain length and RI activity. Graph 4.2 also showed the non-linear relationship between various concentrations ranging from 5.54 x 10^{-6} M to 5.54 x 10^{-11} M for all the analogues. This suggests that the RI activity was not due to colligative effects, but rather it is a non-colligative RI effect which is the property of biological antifreezes.

Among the compounds that contained L-lysine in the side chain, compound **72** containing L-alanine residue in the backbone had greater RI activity. It showed an 11 % decrease in the size of ice crystals compared to that of compound **74** containing L-glycine in the peptide backbone, at a concentration of 5.54 x 10^{-6} M. This result allows us to hypothesize that the presence of L-alanine residues in the polypeptide backbone could be important for RI activity.

The MLGS values of all the new analogues **72**, **74** and **76** containing with *β*-amino acids were compared with the corresponding *α*-analogues **41**, **40** and **42** respectively. This is shown in Graph 4.3. Results showed that MLGS for the second generation analogues **41** was 0.01325 mm^2 at a concentration of 5.54 x 10^{-6} M. It did not

have observable RI activity since this value was within the range of SEM error for PBS control (1.2 x 10^{-2} ± 6.33 x 10^{-4} mm^2). The corresponding β-analogue **72** had a MLGS value of 8.84 x 10^{-3} $mm.^2$ This value represents a 33 % decrease in crystal size indicating that **72** showed a genuine RI activity.

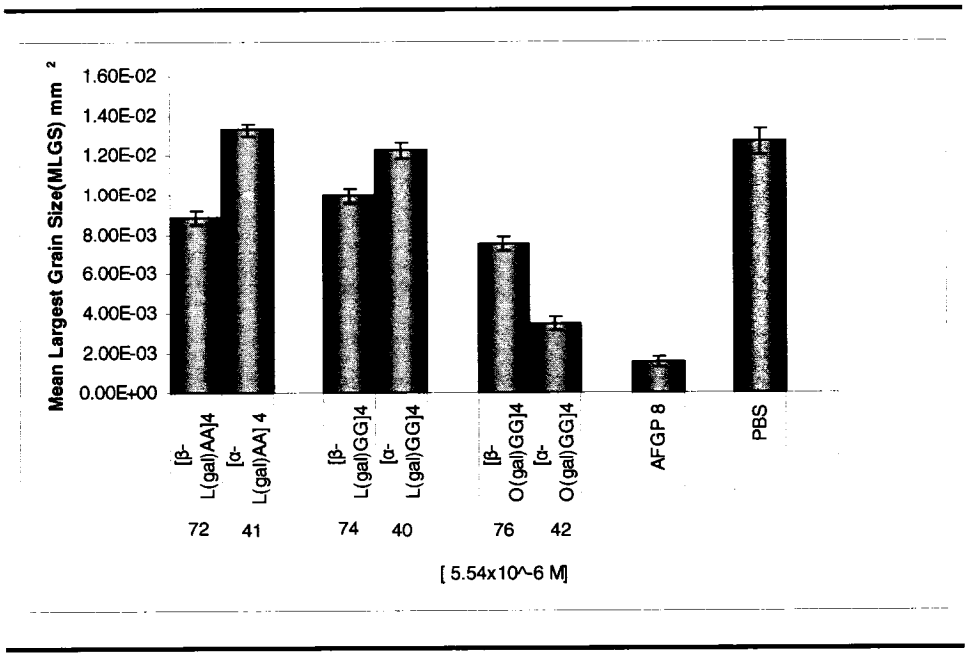

Graph 4.3: Comparative RI study of new β-analogues and corresponding second generation α-analogues

Similarly, the MLGS observed for second generation α-analogue **40** was 1.22 x 10^{-2} mm^2 which was within the error limit of PBS control and therefore, it had no RI activity. Analogue **74** on the other hand, showed observable RI activity (1.0 x 10^{-2} mm^2). However, this activity was limited compared to native AFGP 8. It implies the minimal influence of β-amino acid in the peptide backbone for RI activity in the L-lysine series. However, this trend does not hold for the L-ornithine containing compounds. Compound **76** containing β-L-ornithine had 3.4 times less RI activity than the corresponding second

generation compound **42** containing α-L-ornithine. This result was not expected since compound **42** showed no observable TH gap whereas **76** had an appreciable degree of TH activity and dynamic ice shaping indicating that there is a strong interaction between analogue **76** and ice lattice. This result allows us to hypothesize that peptide backbone modification with β-amino acid is important for increased TH activity but has minimal effect on RI activity. This result is in accordance with the literature[13] report that TH and RI are two independent phenomenon and are related qualitatively not quantitatively.

In conclusion, results from RI activity for new analogues are not as encouraging as it was anticipated. We can hypothesize that modification of the peptide backbone by incorporating β-amino acids may allow the polymer to adopt a conformation which is favourable only for TH activity but has minimal effect on RI activity. Even though these analogues are far less potent inhibitors of ice recrystallization compared to native AFGP 8 (Graph 4.3), they possess genuine RI activity. These are the only analogues synthesized so far in our lab which exhibited all the properties of native AFGP i.e. TH, RI and "dynamic ice shaping" despite having only four tripeptide repeat units (i.e.4-mer) in the polymer chain. These analogues demonstrated significant degree of TH and dynamic ice shaping but had limited RI activity. This study suggests that different structural motifs may have different influence on TH, RI and dynamic ice shaping activity. In addition, by imparting small variations in structure, it seems to be possible to develop antifreeze glycoprotein analogues with tailored antifreeze-specific activities such as RI, TH and dynamic ice shaping with required degree of potency for different applications.

4.3 Conformational Analysis of Analogues 72, 74 and 76.

The solution conformation of AFGP has always been an issue among the chemical community (refer section 1.5). However, it has become important in biological antifreeze research because of its importance in understanding the molecular mechanism of ice binding. Different techniques have been applied by different researchers to understand the solution conformation of AFGP. Circular dichroism (CD) spectroscopy data published by Franks and co-workers[14] and Bush and co-workers[15] is in favour of random coil solution conformation for AFGPs. This result supports the data recently published by Bouvet and Ben.[16] The studies performed at various temperatures and concentrations have shown that at higher concentrations appreciable amount of β-sheet and α-helix character is observed whereas random coil is the main conformation at lower concentrations. This suggests that AFGP is flexibile in solution. The vacuum ultraviolet CD study done by Bush and Feeney suggests a three-fold left-handed helix conformation.[17] On the other hand, Raman spectroscopy emphasizes a random coil conformation.[18] Bush and co-workers[15] have reported that the carbohydrate moiety has negligible contribution to the conformation of glycoprotein.

Towards this end, an analysis of the solution conformation of the new analogues containing β-amino acids has been performed. Circular dichroism (CD) spectroscopy was used to measure the conformations of these analogues. It is one of the most reliable techniques widely used to determine the secondary structures of proteins and glycoproteins.[19] Secondary structures like α-helix, β-sheet, β-turn and random coil produce distinctive CD signatures when circularly polarized light passes through optically active molecules in far-UV regions.[20]

Our new analogues and AFGP 8 were examined using *Jasco* Model J-810 automatic spectrophotometer interfaced with Acer Computer. A molar concentration of 43 μM of the analogue in double distilled water was used. All measurements were done at 22 °C. Data obtained from CD spectroscopy was converted into molar elipticity (deg. cm^2 $dmol^{-1}$) and was plotted against wavelength number (nm). Graph 4.4 depicts the CD spectrum of AFGP 8 and Graph 4.5 depicts the CD spectrum of analogues **72**, **74** and **76**.

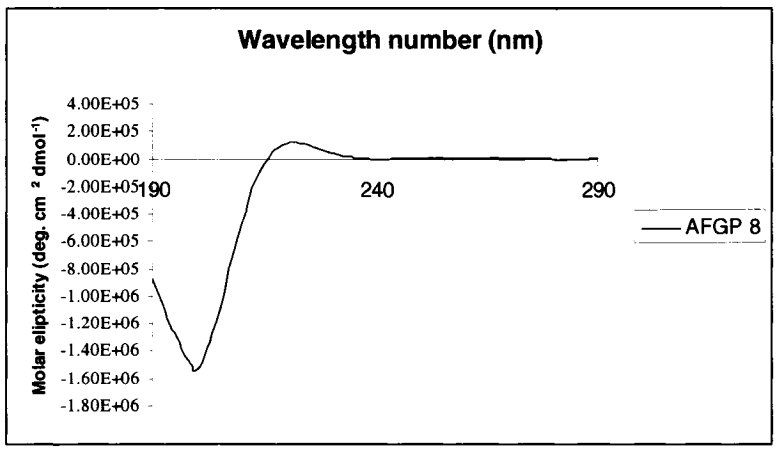

Graph 4.4: CD spectrum of AFGP8

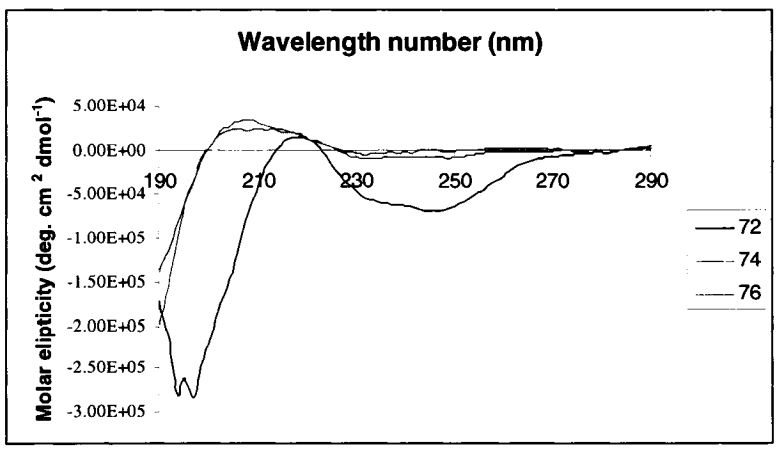

Graph 4.5: CD spectrum of new analogues

The data for the most prominent negative and positive band observed in the CD spectra are summarized in the in Table 4.2.

Compounds	**[θ] deg. cm^2 dmol^{-1} Positive Band**	***λ (nm)***	**[θ] deg. cm^2 dmol^{-1} Negative band**	***λ (nm)***
72	1.16 x 10^4	**216**	-2.86.84 x 10^4 -6.84 x 10^4	**197** **244**
74	3.25 x 10^4	**206**	-9.67 x 10^4	**231**
76	2.0 x 10^4	**204**	-4.75 x 10^3	**231**
AFGP 8	1.12 x 10^5	**220**	-1.51 x 10^6	**198**

Table 4.2: CD spectroscopy data for new analogues and AFGP 8

The secondary structures were estimated using the web-based program, CDPro.[21] Spectral data were deconvoluted using a self-consistent program (SELCON 3) prepare by Sreerama and Woody.[22] This method utilizes a known set of data base protein for comparison. Therefore, IBASIS5 was chosen as a set of 37 different reference proteins containing secondary structures like α-helix, β-sheet, β-turn, polyproline type II and unordered structures. The results are presented in the Table 4.3.

Compounds	α-helix	β-Sheet	B-Turn	PP II	Random Coil	Sum
72	0.102	0.133	0.116	0.098	0.513	**0.962**
74	-0.055	0.116	0.071	0.113	0.710	**0.954**
76	-0.047	0.252	0.071	0.094	0.444	**0.814**
AFGP 8	**0.134**	**0.201**	**0.146**	**0.115**	**0.404**	**0.999**

Table 4.3: CD deconvolution results for new analogues and AFGP 8

The CD spectrum of AFGP 8 (Graph 4.4), showed a strong negative band at 198 nm and a positive band at 220 nm. The strong negative band at 198 nm is typical of a random coil structure whereas the positive band at 220 is that of a polyproline type II helix. However, the positive band at 220 nm was not as pronounced as would be expected for helical structure. In addition, CD deconvolution results (Table 4.3) showed that AFGP 8 in solution exhibited 40 % of random coil conformation and only ~11 % of the polyproline type II structure. This data is consistent with the recent findings from Bouvet and Ben.[16]

The CD spectrum data for analogue **72** exhibited a strong negative band at 197 nm with the molar elipticity $[\theta] = -2.8684 \times 10^4$, which was similar to the negative band shown by AFGP 8 at 198 nm. In addition, it showed a less intense negative band at 244 nm. Similarly, a positive band appeared at 216 nm which is more typical of a random coil structure rather than polyproline type II. The CD deconvolution result (Table 4.3) showed that the solution conformation of analogue **72** was 51 % random coil structure

and 10 % α-helix. Among the other secondary structures β-sheet 13 %, β-turn 11 % and polyproline type II ~10 % were the next most significant contributors. It seems that this analogue existed as a flexible coil with different conformations in aqueous solution at room temperature and concentrations as low as 43 μM. An interesting correlation exists between compound **72** and AFGP 8. There was a similar ratio of α-helix and β-turn structures present in the solution, irrespective of other conformations. Interestingly, compound **72** contained a similar percentage of alanine residues in the peptide backbone as that of native AFGP 8.

The CD spectrum of analogue **74**, where L-alanine residues in the peptide backbone of compound **72** were replaced with L-glycines displayed a unique curve with a positive band at 206 nm. It is 2.8 orders of magnitude more intense than that exhibited by **72**. In contrast to **72**, a very weak negative band was observed around ~231 nm for this analogue. This suggests that no helical conformation was contributing to the overall structure of the polymer. This is not surprising, since L-glycine residues make up approximately 67 % of the analogue and these do not impart any conformational rigidity. The CD deconvolution result showed that the main fractional weight was composed of 71% unstructured random coil conformation, and β-sheet and polyproline type II were the second higher contributors (~11 %). In solution a small percentage of β-turn (~7 %) was also present.

The analogue **76**, in which L-lysine in analogue **74** was replaced with L-ornithine, also showed a similar pattern in the CD spectrum. A single positive band was seen at 204 nm but was 1.6 order of magnitude less intense in molar elipticity ($\theta = 2.0 \times 10^4$) than **74** ($\theta = 3.25 \times 10^4$). However, CD deconvolution result showed that the main fractional

weight was composed of 44 % random coil conformation. This is 37 % less than that of lysine side chain containing glycopolymer **74**. A small percentage of polyproline type II (~9 %) and β-turn (~7 %) was also present in the solution conformation along with the 25 % β-sheet structure. Notably, the α-L-ornithine containing analogue **42**, had only ~1 % β-sheet structure[7] in the solution which is negligible compared to the corresponding β-analogue **76** (25 %). Analogue **42** had potent RI activity but had no TH activity. On the other hand, analogue **76** had a significant degree of TH activity and had a minimal RI activity. This result suggests that difference in activity may be due to the difference in conformations between the compounds.

In conclusion, the overall solution conformations of these analogues are mainly random coil. The CD deconvolution results show that among the three analogues, compound **72** has comparable amounts of α-helix (~10 %) and β-turn (~11 %) structures in the solution to that of AFGP 8 (~13 % & ~14 % respectively). Similarly, the CD spectrum shows a similar curve and negative band in compound **72** and AFGP 8. Interestingly, compound **72** is the one which had higher TH activity among the three compounds. In addition, compounds **74** and **76** had comparable TH activity. Further, both have equal amounts of β-turn (~0.07 %) and negligible α-helix structures. Compared to AFGP 8, these ratios (β-turn and α-helix) are almost half. Compound **76** has high percentage of β-sheet (25%) structure which is comparable to the native AFGP 8 (~20 %). Similarly, compound **74** has equal amount of PP II (~11 %) structure with that of native AFGP 8 (~11 %). Based on the findings of CD spectroscopy and CD

deconvolution results, it is likely that small change in conformations might have a significant impact on antifreeze-specific activity.

References

[1] a) Haymet, A. D. J., Ward, L. G., Harding, M. M., *J.Am. Chem. Soc.* **1999**, *121*, 941; b) Chakrabarty, A., Ananthanarayanan, V. S., Hew, C.L. *J. Biol. Chem.***1989**, *264,* 11307; c) Houston, M. E., Chao, H., Hodges, R. S., Sykes, B. D., Kay, C. M., Sonnichsen, F. D., Loewen, M. C., Davis, P. L. *J.Biol. Chem.* **1998**, *273*, 11714.

[2] Yang, D. S. C., Sax, M., Chakarbartty, A., Hew, C. L. *Nature* **1988,** *333*, 232-237.

[3] Nishimura, S. I. *et al., Angew. Chem. Int. Ed.* **2004**, *43*, 856

[4] Wu, Y., Banoup, J., Goddard, V. S., Kao, H. M., Fletcher, G. L. *Comparative Biochemistry and Physiology Part B*, **2001,** *128,* 265-273

[5] Marshall, C. B., Chakbarty, A., Davies, P. L. *The Journal of Biological Chemistry*, **2005**, *280*, 17920-17929.

[6] Jia, Z., Davies, P. L *TRENDS in Biochemical Sciences* **2002**, *27*, 101.

[7] Murphy, A. V. Ph.D. thesis 2004, Binghamton, New York

[8] Eniade, A., Purushotham, M., Ben, R. N., Wang, J. B., Howath, K., *CellBiochem. CellBiophysics* **2003,** *38(2):*115-24

[9] Davies, P.L., et al., *Biophysics. J.* **2001**, *81*(6), 3560-3565

[10] Standard error of mean (SEM) sm=s/√lN s= standard deviation, N= number of data points collected

[11] Eniade,A., Purushottom, M., Ben, R. N., Wang, J. B., Horwarth, K. *Cell Biochem. Biophys,* **2003**, *38*, 115.

[12] Murphy, A. V. Ph.D thesis, 2004, Binghamton, New york.

[13] Eniade, A., purushottom, M., Ben, R. N., Wang, J. B., Horwath, K. Cell Biochem.

Biophys 2003, 38, 115.

[14] Franks, F. Morris, E. R. *Biochim. Biophys. Acta* **1978**, *540*, 346-356

[15] Rao, B. N., Bush, C. A. *Biopolymers* **1987**, *26*, 1227-1244.

[16] Bouvet, V. R., Lorello, G. R., Ben, R. N., *Biomacromolecules,* **2005**

[17] Bush, C. A., Feeney, R. E., Osuga, D. S. T., Talapati, S., Yeh, Y. *J. Peptide Protein Res.* **1981**, *17*, 125

[18] Yomimatsu, Y., Scherer, J. R., Yin, Y., Feeney, R. E. *J. Biol.Chem.* **1976,** *251*, 2290-2298.

[19] Franks, F., Morris, E. R. *Biochim. Biophys. Acta* **1978**, *540*, 346-356.

[20] Sreerama, N., Woody, R. W. *Method Enzymol.* **2004**, *383*, 318-35

[21] Program was downloaded from : http://lamar.colostate.edu/~sreeram/CDPro/

[22] Sreerama, N., Woody, R. W. *Biochemistry* **1994**, *33*, 10022

Chapter 5

5.0 *In Vitro* Cytotoxicity Assessment of New AFGP Analogues

5.1 Background

Biological antifreezes evolved as a cryo-adaptive strategy in organisms inhabiting subzero temperature environment. These compounds have the ability to inhibit ice crystal growth and thereby protect the organisms from cryoinjury and death.[1] This is an attractive property of biological antifreezes for medical applications such as organ transplantation that requires hypothermic storage of cells and tissues. In general, in the hypothermic storage of cells, cell damage occurs due to ice recrystallization during the freezing and thawing cycles.[2, 3] Before biological and synthetic antifreezes can be used as additives for low temperature preservation, their effects on cells and tissues should be examined. The cryo-additives are generally applied to the samples before cooling and after thawing. It is therefore necessary to examine the cytotoxicity at physiological temperatures. On the other hand, the surrounding environment of the organisms that utilize biological antifreezes can be below 0 ^{o}C. In addition, cryopreservation requires low temperature applications of the biological antifreezes. Consequently, cryotoxicity tests of biological as well as synthetic analogues are required.

The cytotoxicity and cryotoxicity testing was performed using human embryonic liver cells [WRL 68, ATCC] in conjunction with the MTT (Methylthiazolyldiphenyl-tetrazolium bromide) assay. The MTT assay was developed by Mosmann.[4] The MTT assay is a convenient and reliable measure for cytotoxicity and is a colorimetric test based on the colour change of yellow tetrazolium salt MTT into blue formazan. The tetrazolium ring present in the MTT is cleaved by the mitochondrial enzyme succinate-dehydrogenase[5] thereby giving the reduced product formazan, as shown in Figure 5.1.

This enzyme is active only in living cells and as a result, the amount of formazan produced is directly proportional to the number of viable cells, since cell viability is directly related to mitochondrial activity. Cell viability is quantified by measuring the optical density (OD) of viable cells at the UV-visible wavelength of 570 nm.

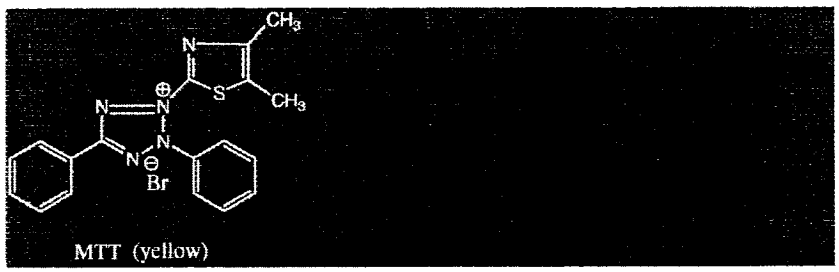

Figure 5.1: Reduction of MTT into formazan

The *in vitro* cytotoxicity and cryotoxicity studies were previously performed with native AFGP 8 on human embryonic liver cells.[6] The cytotoxicity data (Graph 5.1) showed that AFGP 8 was cytotoxic at the higher concentrations of 2 mg/mL and 4 mg/mL, whereas at lower concentrations 0.25, 0.5 and 1.0 mg/mL, AFGP 8 did not display any cytotoxicity.[6]

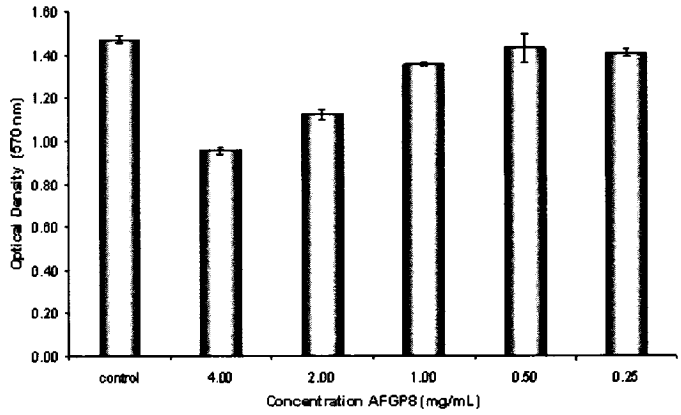

Graph 5.1: Cytotoxicity of AFGP 8 to human embryonic liver cells (WRL 68) at 37 °C[6]

These results show that AFGP 8 could still have potential for human applications if low concentrations of AFGP 8 are used.

Various studies performed on plant and mammalian cells have shown that biological antifreezes (AFPs and AFGPs) were not cryoprotective to cells at temperatures below the freezing point.[7, 8] The cryotoxicity of biological antifreezes is thought to be due to mechanical stress facilitated by ice spicule formation below the TH gap which results in intra-cellular ice formation caused by cell membrane rupture by ice spicule.[9, 10] This destructive property has been utilized by Rubinsky in cryosurgery to destroy the unwanted cells.[11] On the other hand, recrystallization-inhibition activity of biological antifreezes protect cells and their membranes at subzero temperatures. This is the dual nature of biological antifreezes. Therefore, an analogue of biological antifreeze could be developed as an effective cryoprotectant for human applications by tailoring these properties TH, RI and dynamic ice shaping. Cryotoxicity tests of AFGP 8 were performed in the Ben laboratory to understand the potential cryoprotective applications for human use, utilizing human embryonic liver cell line at –20 °C (Graph 5.2).[6]

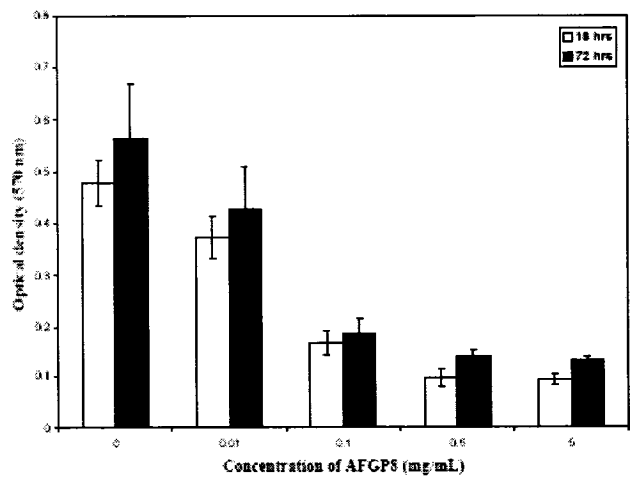

Graph 5.2: Cryotoxicity of AFGP 8 to human embryonic liver cells (WRL 68) at –20 °C[6]

Graph 5.2 shows that AFGP 8 was cryotoxic even at concentration as low as 0.01 mg/mL at –20 °C. This will limit its potential use as a cryoprotectant for human applications. Our new analogues (**72**, **74** and **76**), despite being radically different in structures from native AFGP 8, displayed a significant degree of thermal hysteresis, dynamic ice shaping and genuine recrystallization inhibition activity. These analogues changed ice crystal morphology within the TH gap but unlike AFGP 8, they did not form ice spicules below the freezing point. It was of interest to test our new analogues for their cytotoxic as well as cryotoxic effects to human cell lines. These analogues will not prove to be good cryoprotectants but will serve as a nice control to study the relationship between cryotoxicity, TH activity and dynamic ice shaping in *C*-linked AFGP analogues. A *C*-linked analogue (*C*-Serine) tested before in our laboratory had shown promise as a good cryoprotectant.[6] This analogue had potent RI activity and had no TH as well as dynamic ice shaping properties.

5.2 *In Vitro* Cytotoxicity Assessment of Analogues 72, 74, and 76 at Physiological Temperature.

The *in vitro* cytotoxicity of compounds **72**, **74** and **76** was performed in human embryonic liver cells (WRL 68) at a physiological temperature. Human embryonic liver cells were incubated with different concentrations of compounds **72, 74** and **76** at 37 °C for a period of 18 hours. The MTT assay was performed with the standard MTT protocol.[12] The results from the MTT assay for compounds **72, 74** and **76** are plotted in Graph 5.3, Graph 5.4 and Graph 5.5 respectively.

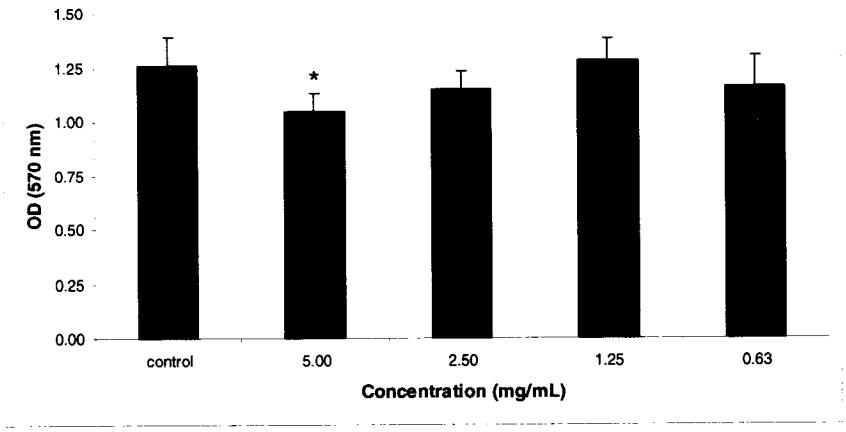

Graph 5.3: Cytotoxicity of analogue 72 to human embryonic liver cells at 37 °C.

The data was analyzed using Student's *t*-test. Data analysis showed that there was a significant difference ($P<0.05$) in cell viability between the control cells and cells treated with 5 mg/mL of compound **72.** At this concentration (5 mg/mL), the compound was apparently toxic to the cells, as cell viability was reduced to 80 %. However, at lower concentrations of 2.5 mg/mL, 1.25 mg/mL and 0.625 mg/mL there was no significant difference ($P>0.05$) in cell viability. Therefore, this compound is less toxic to this cell line than AFGP 8.

A similar analysis showed that there was no significant difference in cell viability when cells were incubated with compound **74** even at high concentrations of 5 mg/mL (Graph 5.4). Compound **74** is therefore not cytotoxic to the human liver cells at physiological temperature.

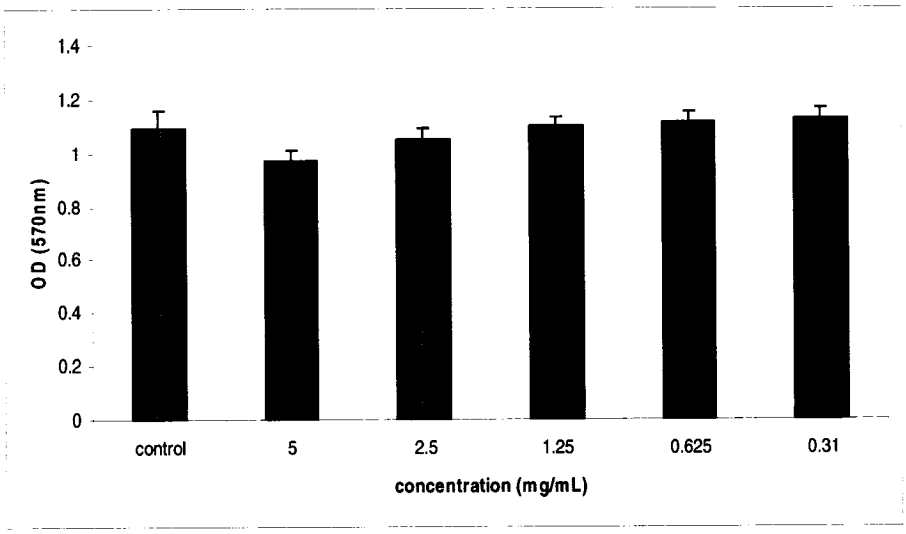

Graph 5.4: Cytotoxicity of analogue 74 to human embryonic liver cells at 37 °C.

In contrast, our data showed that there was a significant difference ($P<0.05$) in cell viability at higher concentrations of 5 mg/mL and 2.5 mg/mL of analogue **76**. As seen from the data, cell viability was reduced to 66 % at concentration of 5 mg/mL of compound **76** (Graph 5.5). However, at the lower concentrations of 1.25 mg/mL and 0.625 mg/mL this compound did not display any cytotoxic effects ($P>0.05$).

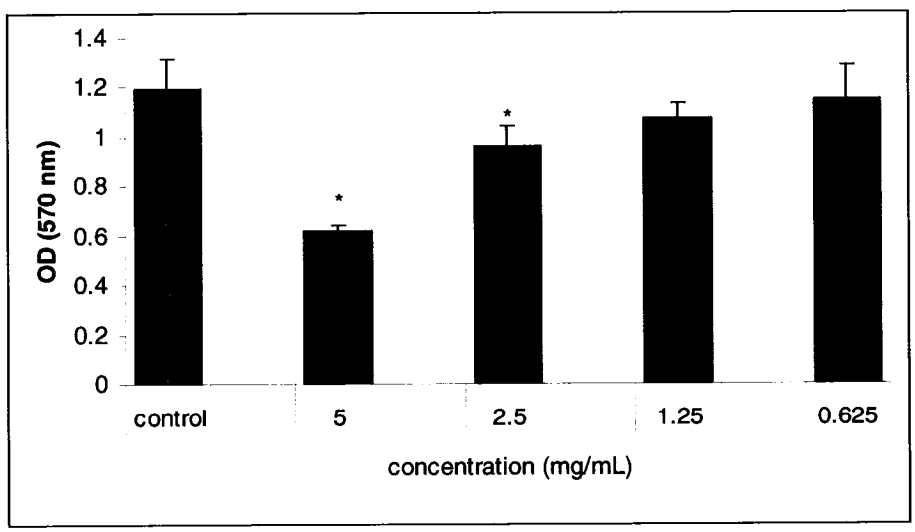

Graph 5.5: Cytotoxicity of analogue 76 to human embryonic liver cells at 37 °C

Despite the dramatic structural differences from native AFGP 8, compounds **72** and **76** showed similar cytotoxicity trends (with the analogue concentrations) towards human liver cell lines at physiological temperature as AFGP 8. However, compound **74** did not display any cytotoxicity to the human liver cells at physiological temperature. In order to gain an insight in the mode of cytotoxicity, further *in vitro* investigations such as internalization assay, caspase activity etc. of these analogues are required.

5.3 *In Vitro* Cryotoxicity Assessment of Analogues 72, 74, and 76

In order to examine the potential cyotoxicity of our new analogues at subzero temperatures, we performed a cryotoxicity assay using human liver cells at -25 °C.[6] In this assay, cells were submerged in a cryobath containing absolute ethanol at -25 °C for 18 hours. The MTT assay was then performed. The results are presented in Graph 5.6, Graph 5.7 and Graph 5.8 for compounds **72, 74** and **76** respectively. Cells at 4 % DMSO were used as a positive control since it is a common cryopreservative.

Similar to the results at 37 °C, a significant difference ($P<0.05$) in cell viability was seen for compound **72** at -25 °C for cells treated with 5 mg/mL of the analogue. Graph 5.6 showed that cell viability was reduced to 61 % at this concentration (5 mg/mL) relative to the control cells. However, no significant difference ($P>0.05$) in cell viability was seen at the lower concentrations of 2.25, 1.25 and 0.625 mg/mL. This result was encouraging, however, relative to the positive control (4 % DMSO treated cells) this analogue was not cryoprotective. Therefore, compound **72** was cryotoxic to human liver cells only at higher concentrations at cryogenic temperatures (-25 °C).

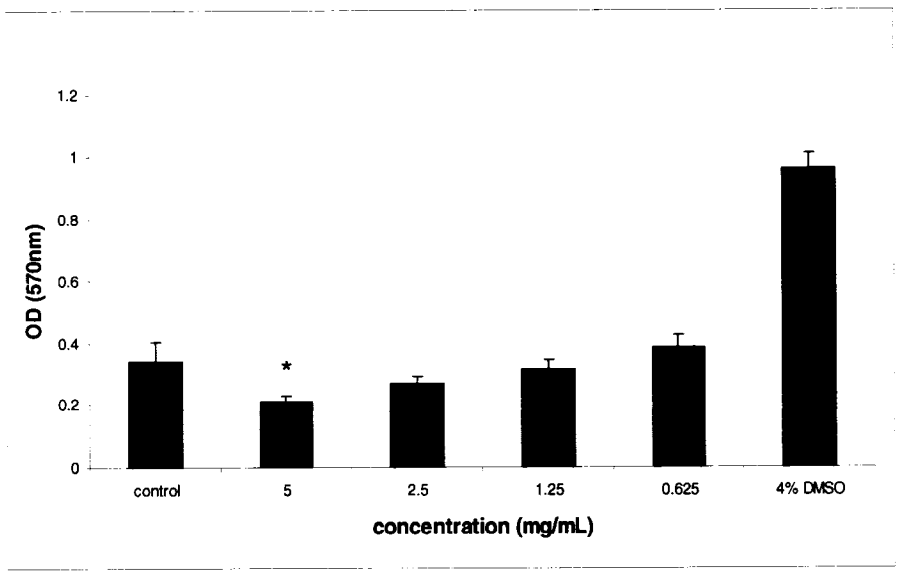

Graph 5.6: Cryotoxicity of analogue 72 to human embryonic liver cell line at -25 °C

Analogue **74** (Graph 5.7) showed that the cell viability was reduced to 89 % at the concentration of 5 mg/mL relative to control cells (untreated cells). At lower concentrations (2.25, 1.25, 0.625 mg/mL) analogue **74** did not display any significant difference in cell viability. However, this analogue was not cryoprotective relative to 4 % DMSO. Compared to analogue **72** (Graph 5.6) cell viability was high with analogue **74**. This result was expected because compound **72** had greater TH activity of 0.17 °C and hexagonal bipyramidal ice shaping whereas analogue **74** had TH activity of 0.12 °C and hexagonal ice shaping.

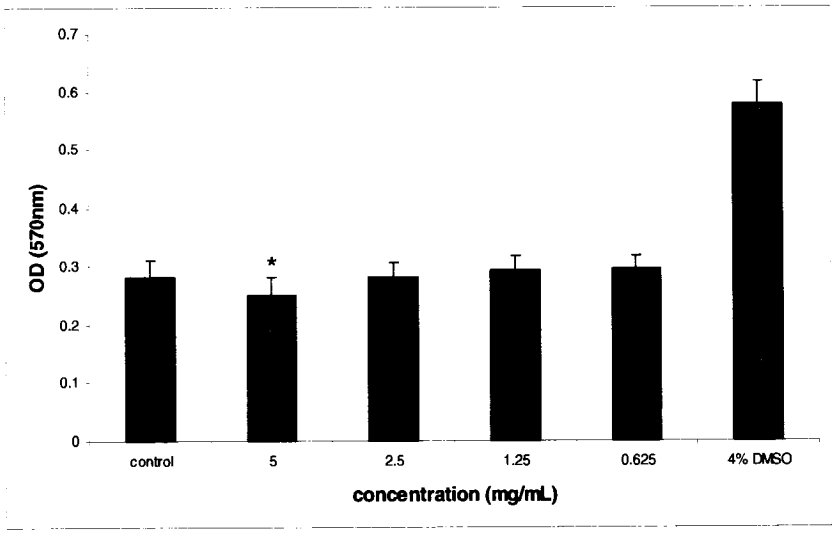

Graph 5.7: Cryotoxicity of analogue 74 to human embryonic liver cells at -25 °C

Analogue **76** showed greater cryotoxicity. Only 55 % cells were viable at 5 mg/mL (Graph 5.8). With compound **76**, a significant difference ($P<0.05$) in cell viability was seen at concentration of 2.25 mg/mL, however, at lower concentrations (1.25 and 0.625 mg/mL) there was no significant difference ($P>0.05$) in cell viability.

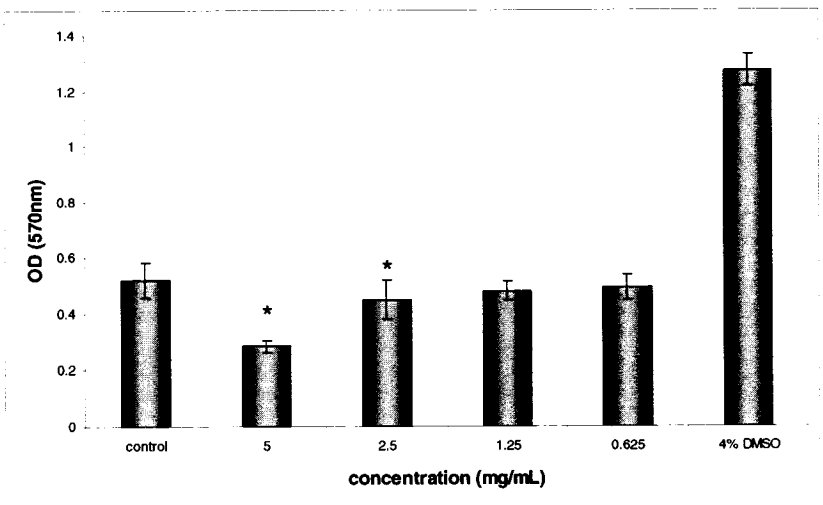

Graph 5.8: Cryotoxicity of analogue 76 to human embryonic liver cells at -25 °C

This result was not expected as this compound had the highest RI and the lowest TH activity (0.10 °C) amongst the three compounds (**72**, **74** and **76**). This compound also shaped the ice to hexagon that remained until the entire solution was frozen.

In conclusion, from these series of experiments it is likely that cytotoxicity and cryotoxicity are two different phenomenon. All of these analogues demonstrated cryotoxicity at high concentrations. Analogue **74** was not cytotoxic at physiological temperature but it was found to be cryotoxic at high analogue concentration. This result allows us to hypothesize that cryotoxicity of these analogues is a result of dynamic ice shaping associated with TH activity. The interesting discoveries from these analogues were that even though the dynamic ice shaping associated with TH activity was thought to be a cause of cryotoxicity, the amount of cryotoxicity does not correlate with the degree of TH gap and shape of the ice crystals. Analogue **76** had the lowest TH activity of 0.10 °C amongst the three (**72**, **74** and **76**) analogues and showed the highest level of cryotoxicity. Similarly, compound **72** had the highest TH activity of 0.17 °C and displayed medium cryotoxicity amongst the three compounds. In addition, analogue **74** had medium TH activity of 0.12 °C amongst the three compounds and showed the lowest cryotoxicity to the human liver cells. Thus, it seems that the amounts of cryotoxicity induced by each of these analogues were specific to the individual compounds. However, these analogues were not detrimental to the human liver cell lines both at physiological as well as cryogenic temperatures when applied at lower analogue concentrations.

References

[1] Yang, D. S. C., Sax, M., Chakarbartty, A., Hew, C. L. *Nature* **1988,** 333, 232-237.

[2] Quinn, P. J. *Cryobiology* **1985,** *22*, 128.

[3] Rubinsky, B.A., Arav, A., Mattioli, M., Devries, A. L.*Biochem. Biophys. Res. Comm.* **1990**, *173*, 1369-1374.

[4] Mosmann, T. *J. Immunol. Methods* **1983**, *65*, 55-63.

[5] Slater, T. F., Sawyer, B., Strauli, U. *Biochim. Biophys. Acta* **1963**, *77*, 383-393.

[6] Liu, S. Ph. D. Thesis, University of Ottawa, 2006.

[7] Hincha, D. K., Devries, A. L., Schmitt, J. M. *Biochem. Biophysics. Acta* **1993**, *1146,* 258-264

[8] Mugnano, J. A., Wang, T., Layne, J. R., Jr., Devries, A. L., Lee, R. E. *Cryobiology* **1995**, *32*, 556-557.

[9] Davies, P. L., Hew, C. L. *FASEB. J.* **1990**, *4*, 2460-2468.

[10] Raymond, J. A., Fritsen, C. H. *Cryobiology*, **2001**, *43*, 63.

[11] Pham, L., Dahiya, R., Rubinsky, B. *Cryosurgery* **1999**, *38*, 169.

[12] Mosmann, T. *J. Immunol. Methods* **1983**, *65*, 55-63.

Chapter 6

6.0 Experimental: Materials and Methods

General

Infrared (IR) spectra were recorded using a FTIR-8400 S, Furier Transform Infra Red Spectrophotometer (Simadzu) and Arid Zone™ MB Series ABB Bomen interfaced with a Dell computer. ^{1}H and ^{13}C NMR experiments were performed using a Bruker Avance 300 MHz, Bruker Avance 400 MHz, Bruker Avance 500 MHz or INOVA 500 MHz spectrometers. Deuterated chloroform was used for NMR experiments, unless otherwise stated. Chemical shifts are reported in ppm and were corrected using the chloroform trace as a reference. ^{1}H NMR signal patterns are abbreviated as follows: s-singlet, d-doublet, t-triplet, q-quartet, m-multiplet, br s-broad singlet, dd-doublet of doublet. Mass spectra were recorded using Matrix Assisted Laser Desorption Ionization spectrometers (MALDI-TOF) and Electrospray mass spectrometer.

Dichloromethane was distilled over calcium hydride and tetrahydrofuran, and benzene were distilled over sodium-benzophenone immediately before use. N,N-dimethylformamide (DMF) was dried with activated molecular sieves and stored under argon atmosphere. All solution phase reactions were performed under an argon atmosphere unless otherwise stated. Solution phase reactions were monitored by thin layer chromatography (TLC), and visualized with UV lamp (254 nm) and stained with i) ceric ammonium molybdate (CAM), and ii) dinitrophenyl hydrazone (DNPH). Flash chromatography was performed using silica gel (Natland Organic) of mesh size 200-400. All reverse phase HPLC purifications were done by using Varian (model 330) HPLC system equipped with a variable wavelength UV detector. C-18 analytical and preparatory columns were used for reverse phase HPLC purifications.

Solid phase syntheses were performed using Wang Fmoc-glycine resin (Nova Biochem) and reactions were monitored with Kaiser and TNBS tests in the following manner.

Kaiser test: Two drops from each of the following solutions was added to a sample of a few dry resin beads in a vial:

1) 5g of ninhydrin in 100 mL of ethanol

2) 80 g of phenol in 20 mL of ethanol

3) 2 mL of .001M aqueous solution of potassium cyanide in 98 mL of pyridine

The vial was put in the oven at 120 °C for 5 minutes. A positive test was indicated by the dark blue color of the solution and beads.

TNBS test: One drop from each of the following solutions was added to a sample of a few dry resin beads in a vial.

1) 10 % DIPEA in DMF

2) 1 % TNBS in DMF

The vial was shaken and left standing at room temp for 5 minutes. The solution was diluted with 1mL of DMF. A positive test was indicated by the dark orange color of the beads.

6.1 Preparation of the Carbohydrate Components

Protocol for the Preparation of 2,3,4,6-Tetra-*O*-acetyl-*α*-D-galactopyranosyl bromide (45)

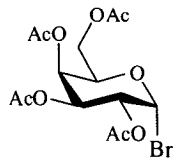

45

Commercial *β*-D-galactose-pentaacetate (5 g, 12.79 mmol) was stirred for one hour in a solution of 30 % HBr in AcOH (25 mL). The solution was diluted with 40 mL of dichloromethane and poured into a separatory funnel containing crushed ice. The organic layer was washed repeatedly with water until the aqueous phase was no longer acidic. The organic layer was dried over $MgSO_4$ and concentrated under reduced pressure. The title compound **45** was obtained as a white powder (4.71 g, 90 %) after recrystallization from diethyl ether.

^{1}H NMR (300 MHz, $CDCl_3$), δ: 6.69 (1H, d, J = 3.9 Hz), 5.51 (1H, d, J = 2.4 Hz), 5.38 (1H, dd, J = 3.3, 10.8 Hz), 5.03 (1H, dd, J = 3.9, 10.5 Hz), 4.50-4.46 (1H, m), 4.21-4.07 (2H, m), 2.14 (3H, s), 2.11 (3H, s), 2.05 (3H, s), 2.00 (3H, s);

^{13}C NMR (300 MHz, $CDCl_3$), δ: 170.1, 169.8, 169.6, 169.5, 87.9, 70.8, 67.7, 67.5, 66.7, 60.6, 20.5, 20.4, 20.4, 20.3;

MS (ESI, MeCN) calcd. for $C_{14}H_{19}BrO_9$, *m/z*: (M^+) 410.02, found 429.9 [$(M + NH_4)^+$]

Protocol for the Preparation of 2,3,4,6-Tetra-*O*-acetyl-1-allyl-*α*-D-galactopyranoside (46)[1]

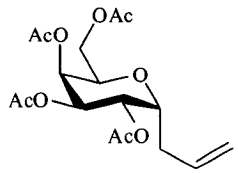

46

To a solution of 2,3,4,6-Tetra-*O*-acetyl-*α*-D-galactopyranosyl bromide **45** (1.27 g, 3.04 mmol) in distilled benzene (15.4 mL, 172.64 mmol) were added Allyl-phenyl-sulfone (1.418 mL, 7.79 mmol), *bis*-tri-*n*-butyl-tin (2.16 mL, 4.32 mmol) and the solution was sonicated with argon bubbling through. After 30 minutes the flask was sealed and irradiated with 450W mercury lamp for 12 hours. The progress of reaction was monitored by TLC every 3 hours. The reaction mixture was then loaded directly onto a silica gel column packed with hexanes. The organo tin was removed by elution with hexanes. A solution of 5:1 hexane/ethylacetate was used to elute unreacted sulfone. Further elution with a solution of 3:1 hexane/ethylacetate followed by concentration under reduced pressure, furnished allylated derivative **46** (1 g, 2.69 mmol) as a clear colourless viscous oil in 87 % yield.

^{1}H NMR (300 MHz, $CDCl_3$), δ: 5.74-5.65 (1H, m), 5.40 (1H, t, J = 2.7), 5.22-5.15 (2H, m), 5.12-5.09 (2H, m), 4.30-4.02 (4H, m), 2.49-2.38 (1H, m), 2.26-2.21 (1H, m), 2.08, (3H, s), 2.03 (3H, s), 2.00 (3H, s), 1.99 (3H, s);

^{13}C NMR (300 MHz $CDCl_3$) δ: 170.4, 169.9, 169.8, 169.7, 133.2, 117.5, 71.3, 68.0, 67.7, 67.4, 61.3, 30.7, 20.7, 20.6, 20.5;

MS (ESI, MeCN) calcd. for $C_{17}H_{24}O_9$, *m/z*: (M^+) 372.14, found 395 [$(M + Na)^+$]

---

[1] Magnusson, G., Ponte'n, F. *J. Org. Chem.* **1996**, *61*, 7463-7466.

Protocol for the Preparation of 2,3,4,6-Tetra-*O*-acetyl-1-acetaldehyde-α-D-galactopyranoside (47).[2]

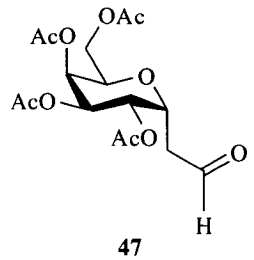

47

Ozone gas was bubbled through a solution of 2,3,4,6-Tetra-*O*-acetyl-1-allyl-α-D-galactopyranoside **46** (2.04 g, 5.48 mmol) in dry dichloromethane (20 mL) at -78 °C until the colour of the solution turned blue. Nitrogen gas was bubbled through the solution until the solution became colourless and triphenylphospine (3.59 g, 13.71 mmol) was subsequently added to the solution. The solution was allowed to warm up to room temperature and stirred overnight under nitrogen. The reaction mixture was concentrated and purified by flash column chromatography (4:1 toluene/acetone) to give the title compound **47** (1.98 g, 97 %).

^{1}H NMR (300 MHz, $CDCl_3$) δ: 9.71 (1H, dd, J = 1.5, J = 2.4 Hz), 5.415 (1H, t, J = 3.3 Hz), 5.28 (1H, dd, J = 4.8, 8.7 Hz), 5.18-5.16 (1H, m), 4.89-4.83 (1H, m), 4.35-4.28 (1H, m), 4.12-4.04 (2H, m), 2.73-2.68 (2H, m), 2.34 (1H, s), 2.11 (3H, s), 2.06 (3H, s), 2.04 (6H, s);

^{13}C NMR (300 MHz, $CDCl_3$) δ: 198.7, 171.0, 170.2, 170.1, 170.0, 70.0, 68.1, 68.0, 67.2, 67.0, 61.2, 42.2, 21.0, 21.0, 21.0;

---

[2] Ben, R., Eniade, A., Murphy, A. V., Landreau, G.*Bioconjugate Chem.* **2001**, *12*, 817-823.

MS (ESI, MeCN) calcd. for $C_{16}H_{22}O_{10}$, *m/z*: (M^+) 374.12, found 392.1 [$(M + NH_4)^+$]

Protocol for the Preparation of 1-(2,3,4,6-Tetra-*O*-acetyl-*α*-D-galactopyranosyl)-acetic acid (48).

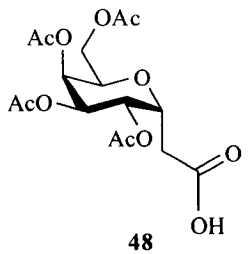

48

To a solution of 2,3,4,6-Tetra-*O*-acetyl-1-acetaldehyde-*α*-D-galactopyranoside **47** (1.5 g, 4.01mmol) in a mixture of *tert*-butyl alcohol (5.7 mL, 60.16 mmol) and 2-methyl-2-butene (5.5 mL, 52.13 mmol) at 0 °C were added a sonicated aqueous solution of potassium dihydrogen phosphate (5.45 g, 40.10 mmol) and sodium chlorite, (3.62 g, 40.10 mmol) in distilled water (10 mL). The mixture was stirred vigorously at 0 °C for 7 hours, and was extracted with ethyl acetate (50 mL). The organic phase was washed with water (100 mL), brine (50 mL), dried and concentrated to afford the title compound **48** (1.53 g, 98 %).

^{1}H NMR (300 MHz, $CDCl_3$) δ: 5.38 (1H, t, J = 2.7 Hz), 5.377-5.370 (1H, m), 5.17 (1H, dd, J = 3.3, 8.7 Hz), 4.66-4.64 (1H, m), 4.18-4.08 (3H, m), 2.71-2.61 (2H, m), 2.07 (3H, s), 2.01 (3H, s), 1.99 (6H, br s);

^{13}C NMR (300 MHz, $CDCl_3$) δ: 175.5, 170.7, 170.1, 169.9, 169.6, 69.4, 68.8, 67.8, 67.5, 67.1, 61.1, 33.1, 20.7, 20.7;

IR (CH_2Cl_2) cm^{-1}: 3600-3400, 1750;

MS (ESI, MeCN) calcd. for $C_{16}H_{22}O_{11}$, *m/z*: (M^+) 390.12, found 408.0 [$(M + NH_4)^+$]

6.2 Preparation of the Peptide Components

Protocol for the Preparation of Benzyl Fluorenylmethoxycarbonyl-L-lysine(*tert*-butyloxycarbonyl) (50).

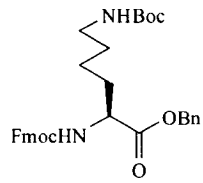

50

To a solution of commercial Fmoc-Lys(Boc)-OH (2.5 g, 5.33 mmol) in 45 mL DCM was added CDI (0.95 g, 5.86 mmol), and stirred at room temperature for 40 minutes. The benzyl alcohol (0.6 mL, 5.33 mmol) was added and allowed to stir at room temperature for overnight. The product was extracted with DCM and washed successively with a saturated ammonium chloride solution (100 mL), water (100 mL) and brine (100 mL). The organic phase was dried and concentrated. Flash column chromatography (50:1, DCM/methanol), afforded the title compound **50** (2.43 g, 82 %).

^{1}H NMR (300 MHz, $CDCl_3$) δ: 7.76 (2H, d, J = 7.5 Hz), 7.6 (2H, d, J = 7.5 Hz), 7.42-7.28 (9H, m), 5.41 (1H, d, J = 7.8 Hz), 5.23-5.13 (2H, m), 4.45-4.33 (4H, m), 4.23-4.19 (1H, m), 3.06 (2H, br s), 1.92-1.81 (1H, m), 1.76-1.64 (1H, m), 1.43 (10H, s), 1.38-1.22 (3H, m).

^{13}C NMR (300 MHz, $CDCl_3$) δ: 172.2, 156.0, 143.8, 143.6, 141.2, 135.1, 128.6, 128.3, 127.6, 127.0, 125.0, 119.9, 79.1, 66.9, 53.7, 47.1, 40.0, 32.1, 29.5, 28.3, 22.2;

MS (ESI, MeCN) calcd. for $C_{33}H_{38}N_2O_6$, *m/z*: (M^+) 558.27, found 559.1 [$(M + H)^+$]

Protocol for the Preparation of Benzyl Fluorenylmethoxycarbonyl-L-ornithine-(*tert*-butyloxycarbonyl) (53):

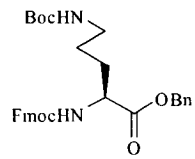

53

A solution of Fmoc-Orn(Boc)-OH (2.5 g, 5.5 mmol) and CDI (0.98 g, 0.061 mmol) in dry DCM (45 mL) was stirred at room temperature for 40 minutes. The rest of the procedure was the same as for compound **50** to afford the title compound **53** (2.69 g, 90 %).

^{1}H NMR (300 MHz, $CDCl_3$), δ: 7.67 (2H, d, J = 7.5 Hz), 7.51 (2H, d, J = 7.2 Hz), 7.43-7.26 (9H, m), 5.58 (1H, d, J = 7.5 Hz), 5.22-5.13 (2H, m), 4.41-4.39 (3H, m), 4.23-4.18 (1H, m), 3.08 (2H, br s), 1.94-1.82 (1H, m), 1.74-1.61 (1H, m), 1.35 (12H, br s);

^{13}C NMR (300 MHz, $CDCl_3$), δ: 172.0, 155.9, 143.8, 143.6, 141.2, 140.8, 135.1, 128.5, 128.4, 128.2, 127.6, 127.4, 126.9, 126.8, 125.0, 119.8, 79.2, 67.1, 66.8, 65.1, 53.6, 47.0, 39.8, 29.6, 28.3, 25.9;

MS (ESI, MeCN) calcd. for $C_{32}H_{36}N_2O_6$, *m/z*: (M^+) 544.26, found 545.1 [$(M + H)^+$]

Protocol for the Preparation of Benzyl Fluorenylmethoxycarbonyl-L-lysine (51):

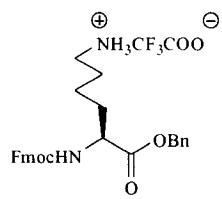

51

Compound **50** (1.845 g, 4.028 mmol) was dissolved in a solution of DCM and TFA (1:1) and was allowed to stir at room temperature for 40 minutes. Solvent was removed under reduced pressure to yield the title compound **51** (1.84 g; 100 %), which was used directly in the next step.

Protocol for the Preparation of Benzyl Fluorenylmethoxycarbonyl-L-ornithine (54):

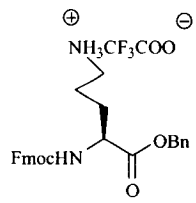

54

A solution of **53** (0.55 g, 1.01 mmol) was treated in a similar manner as for compound **50** to afford **54** (0.44 g, 100 %). This intermediate was used directly for the next coupling step.

6.3 General Protocol for the Preparation of Building Blocks

a) Preparation of Benzyl Fluorenylmethoxycarbonyl-L-lysine-1-(2,3,4,6-tetra-*O*-acetyl-*α*-D-galactopyranoside) (56).

b) Preparation of Benzyl Fluorenylmethoxycarbonyl-L-ornithine-1-(2,3,4,6-tetra-*O*-acetyl-*α*-D-galactopyranoside) (55).

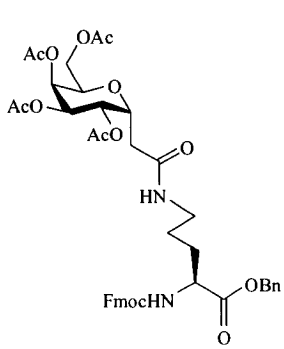

55

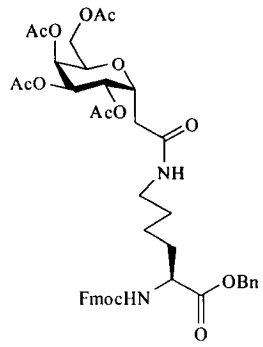

56

Compound 1-(2,3,4,6-Tetra-*O*-acetyl-α-D-galactopyranosyl)-acetic acid **48** (1.29 g, 3.307 mmol) was activated with HBTU (1.18 g, 2.97 mmol) in dry DCM (20 mL) at room temperature for 20 minutes. A solution of **51** (1.514 g, 3.30 mmol) or **54** (1.47 g, 3.30 mmol) in dry dichloromethane (20 mL) was then transferred into the activated carboxylic acid **48,** followed by the addition of diisopropylethylamine (0.6 mL, 3.3 mmol). The reaction mixture was allowed to stir overnight and was extracted with DCM (50 mL), washed successively with saturated ammonium chloride, water and brine. The organic layer was dried and concentrated. The crude product was purified with silica gel flash chromatography (50:1, DCM/methanol) to afford the title compound **56** and **55** (2.08 g, 76 % and 2.23 g, 83 %) respectively. However, we observed a peak for urea derivative (tetramethyl urea) in the NMR along with these compounds and were able to completely purify in the following step.

a) Compound (56):

^{1}H NMR (300 MHz, $CDCl_3$) δ: 7.75 (2H, d, J = 7.5Hz), 7.57 (2H, d, J = 7.2 Hz), 7.42-7.26 (9H, m), 6.12 (1H, t, J = 5.4Hz), 5.49 (1H, d, J = 7.8 Hz), 5.37 (1H, s), 5.27-5.23 (1H, m), 5.18-5.10 (3H, m), 4.67-4.61 (1H, m), 4.43-4.32 (3H, m), 4.23-4.19 (2H, m), 4.10 (2H, s), 3.26-3.12 (2H, m), 2.56-2.46 (1H, m), 2.39-2.33 (1H, m), 2.09 (3H, s), 2.02

(6H, s), 2.0 (3H, s), 1.92-1.81 (1H, m), 1.72-1.66 (1H, m), 1.53-1.43 (2H, m), 1.32-1.24 (2H, m);

^{13}C NMR (300 MHz, $CDCl_3$) δ: 172.1, 170.4, 169.8, 169.7, 169.4, 169.1, 155.9, 143.7, 141.1, 135.1, 128.5, 127.6, 126.9, 124.9, 124.9, 119.9, 69.1, 68.8, 67.7, 67.6, 67.0, 66.8, 61.1, 53.5, 46.9, 38.4, 34.2, 32.0, 28.8, 22.3, 20.6, 20.5;

IR (CH_2CL_2) cm^{-1}: 3313, 1749, 1649l;

MS (ESI, MeCN) calcd. for $C_{44}H_{50}N_2O_{14}$, *m/z*: (M^+) 830.33, found 831.1 [$(M + H)^+$]

b) Compound (55):

^{1}H NMR (300 MHz, $CDCl_3$) δ: 7.76 (2H, d, J = 7.5 Hz), 7.59 (2H, d, J = 7.21 Hz), 7.42-7.28 (9H, m), 6.12 (1H, br s), 5.55 (1H, d, J = 8.40), 5.40 (1H, t, J = 3.3 Hz), 5.29-5.23 (1H, m), 5.17-5.12 (3H, m), 4.67-4.61 (1H, m), 4.46-4.34 (3H, m), 4.25-4.19 (2H, m), 4.15-4.09 (2H, m), 3.29-3.23 (2H, m), 2.57-2.47 (1H, m), 2.41-2.34 (1H, m), 2.10 (3H, s), 2.05 (3H, s), 2.04 (3H, s), 2.0 (3H, s), 1.93-1.82 (1H, m), 1.73-1.47 (3H,m);

^{13}C NMR (300 MHz, $CDCl_3$), δ: 171.9, 170.5, 169.9, 169.7, 169.5, 169.2, 156.0, 14.6, 141.2, 135.0, 128.6, 128.5, 128.3, 127.7, 127.0, 125.0, 119.9, 69.4, 68.7, 67.8, 67.7, 67.2, 67.0, 66.8, 61.0, 53.5, 47.0, 38.6, 34.4, 30.0, 25.3, 20.7, 20.6;

MS (ESI, MeCN) calcd. for $C_{43}H_{48}N_2O_{14}$, *m/z*: (M^+) 816.31, found 817.0 [$(M + H)^+$], 840.1 [$(M+Na)^+$]

Protocol for the Preparation of Fluorenylmethoxycarbonyl-L-lysine-1-(2,3,4,6-tetra-*O*-acetyl-*α*-D-galactopyranoside) (57).

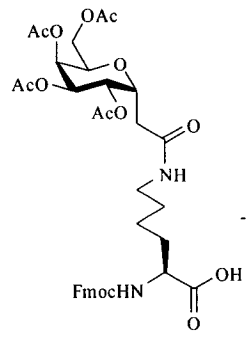

57

Compound **56** (1.3 g, 1.56 mmol) was dissolved in ethanol (20 mL) and catalytic palladium on charcoal (10 % w/w) was added. The reaction mixture was stirred under hydrogen atmosphere for 24 hours. The catalyst was filtered through a celite pad and washed with methanol. Excess solvent was removed and the crude product was purified through flash chromatography in 50:1, DCM/methanol and 10:1, DCM/methanol successively to furnish the title compound **57** (0.98 g, 85 %).

^{1}H NMR (300 MHz, $CDCl_3$) δ: 7.76 (2H, d, J = 7.2 Hz), 7.60 (2H, d, J = 6Hz), 7.42-7.37 (2H, m), 7.33-7.28 (2H, m), 6.25 (1H, br s), 5.6 (1H, d, J = 7.5 Hz), 5.39 (1H, t, J = 3.3), 5.27-5.23 (1H, m), 5.16-5.12 (1H, m), 4.68-4.63 (1H, m), 4.39 (2H, d, J = 6.6 Hz), 4.33-4.27 (1H, m), 4.24-4.19 (1H, m), 4.1 (2H, m), 3.28 (2H, m), 2.58-2.38 (2H, m), 2.11 (3H, br s), 2.04 (9H, br s), 1.85 (2H, m), 1.56 (2H, m), 1.42 (3H, m);

^{13}C NMR (300 MHz $CDCl_3$) δ: 174.4, 172.4, 170.9, 170.4, 170.0, 169.8, 156.1, 143.6, 141.2, 127.7, 127.0, 125.0, 119.9, 69.1, 68.9, 67.8, 67.7, 66.9, 61.2, 53.4, 50.6, 47.0, 39.1, 34.1, 31.7, 28.6, 22.1, 20.7;

IR (CH_2Cl_2) cm^{-1}: 3367, 1748;

MS (ESI, MeCN) calcd. for $C_{37}H_{44}N_2O_{14}$, *m/z*: (M^+) 740.28, found 741.1 [$(M + H)^+$], 763.1[$(M + Na)^+$]

Protocol for the Preparation of Fluorenylmethoxycarbonyl-L-ornithine-1-(2,3,4,6-tetra-*O*-acetyl-*α*-D-galactopyranoside) (58).

The compound **55** (1.3 g, 1.59 mmol) was dissolved in 1:1ethanol/ethylacetate to yield the title compound **58** (0.96 g, 84 %) using the same procedure as for compound **57**.

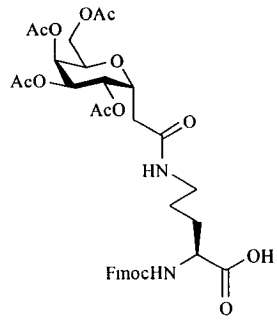

58

^{1}H NMR (300 MHz, $CDCl_3$), δ: 7.75 (2H, d, *J* = 7.5 Hz), 7.6 (2H, m), 7.41-7.36 (2H, m), 7.32-7.27 (2H, m), 6.57 (1H, br s), 5.76 (1H, d, *J* = 7.8), 5.40 (1H, t, *J* = 3 Hz), 5.27-5.22 (1H, m), 5.18-5.14 (1H, m), 4.69-4.63 (1H, m), 4.45-4.38 (3H, m), 4.31-4.08 (3H, m), 3.36-3.27 (2H, m), 2.64-2.55 (1H, m), 2.47-2.41 (1H, m), 2.11 (3H, s), 2.05 (3H, s), 2.04 (3H, s), 2.02 (3H, s), 1.76-1.61 (4H, m);

^{13}C NMR (300 MHz, $CDCl_3$), δ: 174.0, 170.9, 170.4, 170.1, 169.9, 169.7, 156.1, 143.6, 141.2, 127.7, 127.0, 125.0, 120.0, 69.4, 67.9, 67.7, 67.0, 66.8, 66.8, 61.2, 53.1, 47.0, 39.0, 34.4, 31.0, 29.7, 25.2, 20.7, 20.7, 20.6;

MS (ESI, MeCN) calcd. for $C_{36}H_{42}N_2O_{14}$, *m/z*: (M^+) 726.26, found 727 [$(M + H)^+$], 749.0 [$(M + Na)^+$]

Protocol for the Preparation of Fluorenylmethoxycarbonyl-L-lysine-1-[(2,3,4,6-tetra-*O*-acetyl-*α*-D-galactopyranosyl)] diazoketone (64).

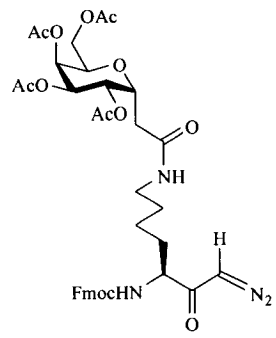

64

Method A: To a solution of **57** (0.2 g, 0.27 mmol) in DCM (5mL) was added freshly distilled thionyl chloride (0.2 mL, 0.27 mmol) and the solution was refluxed under nitrogen at 70 °C for 2 hours. Excess thionyl chloride was removed under reduced pressure. The acid chloride was then dissolved in dry dichloromethane (10 mL) and transferred dropwise to a stirred solution of 0.7M dry diazomethane in dichloromethane under argon at 0 °C. The reaction mixture was allowed to warm up to room temperature for 4 hours and was quenched with 5 % aqueous acetic acid solution. The solution was diluted with dichloromethane and washed successively with a saturated solution of sodium bicarbonate, 1N HCl and brine. The organic phase was dried, filtered, and concentrated under reduced pressure at room temperature. The crude product was purified through silica gel neutralized with 2 % triethylamine (60:1, DCM/methanol) to afford **64** as a yellow solid (0.065 g, 30 %).

Method B: To a solution of **57** (0.99 g, 1.33 mmol) in dry THF (15 mL) at -20 °C, added isobutyl chloroformate (0.18 mL, 1.39 mmol) followed by N-methyl morpholine (0.15 mL, 1.39 mmol) and stirred for 30 minutes. The resulting solution was allowed to

warm to -5 °C and a solution of dry diazomethane (0.7M) in diethyl ether was added until a rich yellow colour was persisted. The solution was allowed to warm to room temperature and stirred for 2 hours. Excess diazomethane was destroyed by dropwise addition of 5 % acetic acid solution. The product was extracted with diethylether and washed successively with a solution of saturated sodium bicarbonate, 1N HCl and brine. The organic layer was dried over magnesium sulfate, filtered and concentrated under reduced pressure to produce clear yellow oil. The crude product was purified by flash chromatography with silica gel (neutralized with 2% triethylamine) packed on dichloromethane (25:1, DCM/methanol) to afford the title compound **64** as a yellow solid (85 %, 0.86 g).

^{1}H NMR (400 MHz $CDCl_3$) δ: 7.76 (2H, d, J = 8 Hz), 7.60-7.58 (2H, m), 7.42-7.37 (2H, m), 7.33-7.28 (2H, m), 6.18 (1H, s), 5.62 (1H, d, J = 7.8 Hz), 5.38 (2H, br s), 5.28-5.22 (1H, m), 5.14-5.10 (1H, m), 4.68-4.62 (1H, m), 4.51-4.36 (2H, m), 4.25-4.18 (3H, m), 4.14-4.07 (2H, m), 3.27-3.19 (2H, m), 2.57-2.34 (1H, m), 2.3-2.0 (1H, m), 2.09 (3H, s), 2.02 (9H, br s), 1.18 (1H, m), 1.52 (3H, m), 1.35 (2H, m);

^{13}C NMR (400 MHz, $CDCl_3$) δ: 193.5, 170.6, 170.0, 169.8, 169.6, 169.4, 156.1, 143.8, 141.4, 127.8, 127.1, 125.1, 125.0, 120.1, 69.4, 67.9, 67.8, 67.0, 66.8, 61.2, 57.6, 54.1, 47.3, 39.0, 34.5, 31.8, 29.0, 22.4, 20.8, 20.8, 20.7, 20.7;

IR (CH_2Cl_2) cm^{-1}: 3362, 2109, 1749, 1649;

MS (ESI, MeCN) calcd. for $C_{38}H_{44}N_4O_{13}$, *m/z*: (M^+) 765.3, found 765.3. M^+; 787.3 [$(M + Na)^+$]

Protocol for the Preparation of Fluorenylmethoxycarbonyl-L-ornithine-1-[(2,3,4,6-tetra-*O*-acetyl-*α*-D-galactopyranosyl)] diazoketone (69).

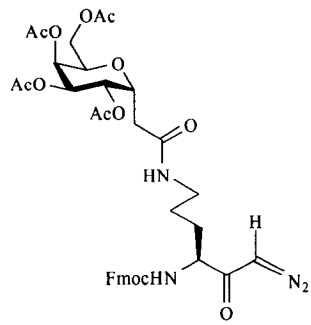

69

A solution of **58** (0.99 g, 1.36 mmol) in dry THF (15 mL) was used. The rest of the procedure was similar as method B for compound **64**. The title compound **69** was isolated as a yellow solid (0.90 g, 89 %).

^{1}H NMR (300 MHz, $CDCl_3$) δ: 7.75 (2H, d, J = 7.2 Hz), 7.5 (2H, m), 7.41-7.36 (2H, m), 7.32-7.27 (2H, m), 6.31 (1H, br s), 5.79 (1H, d, J = 7.8 Hz), 5.44 (1H, s), 5.39 (1H, br s), 5.24 (2H, m), 5.16-5.12 (1H, m), 4.69-4.63 (1H, m), 4.50-4.36 (2H, m), 4.27-4.08 (4H, m), 3.27 (2H, br s), 2.59-2.51 (1H, m), 2.42-2.35 (1H, m), 2.10 (3H, s), 2.04 (3H, s), 2.03 (3H, s), 2.00 (3H, s), 1.81 (1H, m), 1.54 (3H, br s);

^{13}C NMR (300 MHz $CDCl_3$) δ: 193.3, 170.5, 169.9, 169.7, 169.6, 169.4, 156.1, 143.6, 141.2, 127.6, 127.0, 125.0, 124.9, 119.9, 69.3, 68.7, 67.8, 67.6, 66.7, 66.6, 61.0, 57.2, 54.0, 53.4, 47.1, 38.8, 34.4, 29.6, 25.5, 20.6, 20.6;

IR (CH_2Cl_2) cm^{-1}: 3339, 2109, 1751, 1655;

MS (ESI, MeCN) calcd. for $C_{37}H_{42}N_4O_{13}$, *m/z*: (M^+) 751.28, found 773.0 [$(M + Na)^+$]

Protocol for the Preparation of Fluorenylmethoxycarbonyl-*β*-L-lysine-1-[(2,3,4,6-tetra-*O*-acetyl-*α*-D-galactopyranoside)] (65).

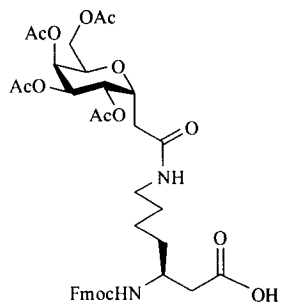

65

To a solution of diazoketone **64** (0.631 g, 0.827 mmol) in 2:1 dioxane/water (15 mL) was added a catalytic amount of silver benzoate. The solution was refluxed under nitrogen at 70 °C for 6 hours. The catalyst was removed by filtration through a celite pad and the bulk of the filtrate was concentrated under reduced pressure. The residue was diluted with saturated sodium bicarbonate solution and stirred for 10 minutes. The mixture was then extracted with diethyl ether (3 x 20 ml). The aqueous phase was acidified with 1N HCl to pH 2 and was extracted with ethyl acetate (3 x 15 mL). The organic phase was dried over sodium sulfate, filtered and concentrated under reduced pressure. The crude product was purified by flash chromatography with silica gel column packed with dichloromethane (eluted in 50:1, DCM/methanol to flush the unreacted diazoketone) and (10:1, DCM/methanol) to collect the title compound **65** as a white solid (0.53 g, 85 %).

^{1}H NMR (300 MHz $CDCl_3$), δ: 7.75 (2H, d, J = 6 Hz), 7.5 (2H, d, J = 7.2), 7.41-7.36 (2H, m), 7.36-7.27 (2H, m), 6.37 (1H, br, s), 5.49 (1H, d, J = 8.7 Hz), 5.37 (1H, br s), 5.28-5.23 (2H, m), 5.16-5.12 (1H, m), 4.69-4.63 (1H, m), 4.38-4.36 (2H, m), 4.25-3.96 (

4H, m), 3.23 (2H, br s), 2.58-2.50 (3H, m), 2.43-2.37 (1H, m), 2.09 (3H, s), 2.02 (9H, br s), 1.57-1.50 (4H, m), 1.38 (2H, m);

^{13}C NMR (300 MHz, $CDCl_3$), δ: 174.6, 170.7, 169.9, 179.0, 169.9, 169.7, 169.7, 156.1, 143.7, 141.2, 127.7, 127.0, 125.0, 119.9, 69.1, 67.7, 66.9, 66.6, 61.3, 47.1, 39.0, 34.1, 33.5, 28.6, 23.0, 20.7, 20.7, 20.6;

IR (CH_2Cl_2) cm^{-1}: 3386-3299, 1739, 1643, 1217;

MS (ESI, MeCN) calcd. for $C_{38}H_{46}N_2O_{14}$, *m/z*: (M^+) 754.29, found 755.2 [$(M + H)^+$]

Protocol for the Preparation of Fluorenylmethoxycarbonyl-β-L-ornithine-1-[(2,3,4,6-tetra-*O*-acetyl-α-D-galactopyranoside)] (70).

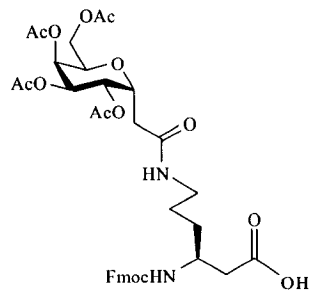

70

A protocol analogous to the preparation of **65** was followed to obtain the title compound **70** as a white solid (0.48 g, 80 %) from **69** (0.613 g, 0.817 mmol).

^{1}H NMR (300 MHz, $CDCl_3$), δ: 7.75 (2H, d, J = 7.2 Hz), 7.58 (2H, d, J = 7.2 Hz), 7.41-7.36 (2H, m), 7.32 -7.26 (2H, m), 6.48 (1H, br s), 5.53 (1H, d, J = 9 Hz)), 5.39 (1H, s), 5.27-5.24 (2H, m), 5.18-5.14 (1H, m), 4.70-4.64 (1H, m), 4.39 (2H, d, J = 6.6 Hz), 4.29-4.05 (4H, m), 3.99 (1H, m), 3.28 (2H, br s), 2.61-2.53 (3H, m), 2.47-2.40 (1H, m), 2.10 (3H, s), 2.04 (3H, s), 2.03 (3H, s), 2.01 (3H, s), 1.57 (4H, br s);

^{13}C NMR (300 MHz, $CDCl_3$), δ: 174.2, 170.6, 169.8, 169.7, 169.6, 169.5, 156.0, 143.6, 141.0, 127.4, 126.8, 124.8, 119.7, 68.9, 68.7, 68.7, 67.5, 66.7, 66.4, 60.9, 53.2, 46.9, 38.9, 38.8, 38.7, 38.7, 34.0, 31.3, 25.6, 20.5, 20.4;

IR (CH_2Cl_2) cm^{-1}: 3357, 1739, 1643;

MS (ESI, MeCN) calcd. for $C_{37}H_{44}N_2O_{14}$, *m/z*: (M^+) 740.28, found 741.4 [$(M + H)^+$]

6.4 Solid Phase Synthesis of AFGP Analogues

General Protocol for the Preparation of [β-Lysine (Galactose)-Glycine-Glycine]$_4$ Glycine-Acetate (73).

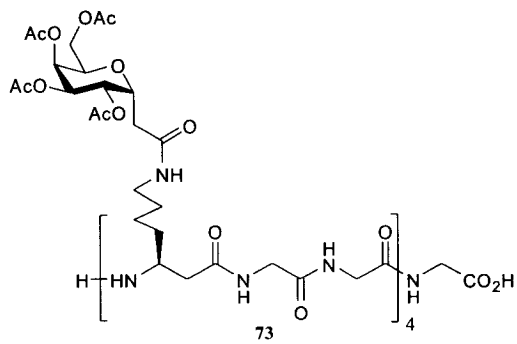

73

Wang resin preloaded with Fmoc-glycine (0.1 g, 0.06 mmol active site) was swollen in dry DMF (10 mL) in a manual solid phase peptide synthesizer for 1 hour. The solvent was drained and 10 mL of 20 % piperidine in DMF was added to the resin. The solution was allowed to stir for 2 hours. Positive Kaiser and TNBS test were found. The resin was washed with dry DMF three times. Commercial Fmoc-glycine-OH (53.5 mg, 0.18 mmol) was pre activated with HBTU (68 mg, 0.18 mmol) and DIPEA (0.032 ml, 0.18 mmol) in 5 mL dry DMF for 40 minutes and transferred into the solid phase synthesizer containing resin bound amino acid. Dry DMF (5 mL) was added and the

resin was allowed to stir for 24 hours. After 24 hours the beads were tested for negative Kaiser and TNBS test. The resin was washed with dry DMF three times and the same loading sequence was followed for the second commercial Fmoc-glycine-OH. The third coupling was done with building block **65** (58 mg, 0.078 mmol). After 48 hours coupling, the entire reaction sequence was repeated three times. After the final coupling of the building block was completed, a solution of 20 % piperidine in DMF was added and the solution was stirred for 2 hours. The resin was washed successively with DMF, DCM and methnol and dried over potassium hydroxide pellets under vacuum for 6 hours. The resin was treated with a 1:1 mixture of DCM/TFA for 1 hour. The solution was drained and the resin was washed successively with DCM and TFA. The filtrate was concentrated and diethyl ether was added to precipitate yellow glycopolymer **73** (0.139 g, 90 %).

^{1}H NMR (500 MHz, MeOH D4), δ: 5.31 (2H, m), 5.15 (5H, m), 4.58 (1H, m), 4.16-4.02 (12H, m), 3.85-3.76 (18H, m), 3.21 (6H, m), 3.10 (8H, m), 2.60 (3H, m), 2.40 (8H, m), 2.02 (12H, s), 1.95, 1.92, 1.90 (3H each, s, 36 total), 1.61 (2H, m), 1.47 (17H, m), 1.28 (7H, m);

^{13}C NMR (500 MHz, MeOH, D4), 172.9, 170.7, 170.6, 170.3, 170.0, 169.9, 157.6, 175.2, 115.6, 113.3, 69.8, 68.5, 67.8, 67.5, 65.3, 61.0, 60.8, 44.3, 43.8, 43.4, 42.7, 37.7, 37.0, 35.2, 34.9, 34.9, 33.4, 30.2, 30.0, 24.3, 23.6, 20.8, 20.7, 20.6, 20.6;

MS (MALDI, MeOH, negative ion) calcd. for $C_{110}H_{165}N_{17}O_{54}$, *m/z*: ($M^+$) 2588.07, found 2586.88 [$(M - H)^+$] ;

Protocol for the Preparation of [β-Lysine(Galactose)-Glycine-Glycine]$_4$ Glycine (74):

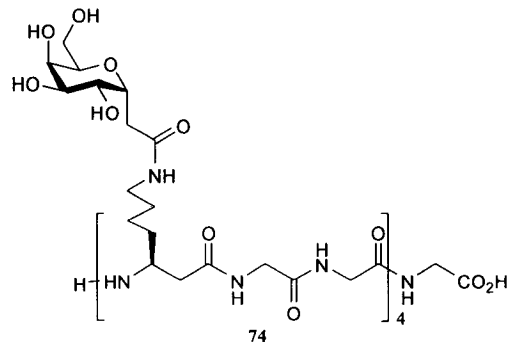

74

Compound **73** (33.4 mg, 0.012 mmol) was dissolved in 10 mL methanol with a catalytic amount of sodium metal at pH 10-11. 2 mL water was added to the reaction mixture and was allowed to stir for overnight. The reaction mixture was neutralized with acidic amberlite IR-120 resin and filtered. A bulk of the solvent was removed under vacuum and, water was added, lyophilized and purified by reversed phase HPLC using 0.1% TFA water/acetonitrile and lyophilized to afford the title glycopolymer **74** as a white solid (22.9 mg, 100 %).

^{1}H NMR (500 MHz, D_2O), δ: 4.35 (1H, s), 4.06 (1H, s), 3.86-3.55 (7H, m), 3.05 (2H, s), 2.66-2.33 (3H, m), 1.58-1.20 (4H, m);

^{13}C NMR (500 MHz, D_2O), δ: 174.2, 173.3, 173.2, 171.8, 171.6, 170.6, 163.0, 72.8, 72.3, 69.5, 68.6, 67.4, 60.7, 60.6, 48.5, 47.1, 42.6, 42.5, 42.3, 42.1, 41.1, 40.9, 39.1, 38.8, 36.5, 33.0, 32.2, 31.4, 27.8, 27.8, 22.4, 21.6;

IR (neat) cm^{-1}: 3307-3261, 1635;

MS (MALDI, H_2O, positive ion) calcd. for $C_{78}H_{133}N_{17}O_{38}$, *m/z*: ($M^+$) 1915.90, found 1917.0 [$(M + H)^+$], 1938.53 [$(M + Na)^+$], 1950.57 [$(M + K)^+$]

General Protocol for the Preparation of [(β-Lysine(Galactose)-Alanine-Alanine)]$_4$ Glycine-Acetate (71):

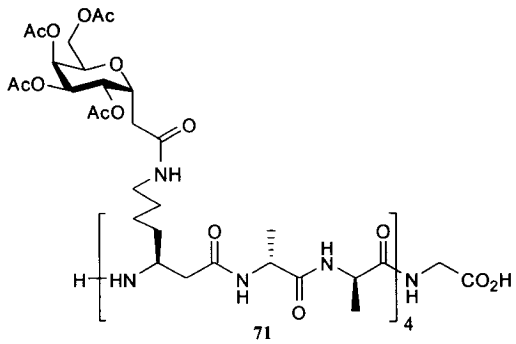

71

A protocol analogous to the preparation of **73** was followed to furnish a yellow solid **71** (146 mg, 90 %).

^{1}H NMR (500 MHz, MeOH D_4), δ: 5.30 (2H, s), 5.14 (7H, s), 4.57 (4H, s), 4.14-3.82 (26H, m), 3.82 (2H, m), 3.57-3.45 (5H, m), 3.20 (7H, s), 3.06 (9H, m), 2.59 (5H, m), 2.42 (6H, m), 2.31 (5H, m), 2.01, 1.94, 1.91, 1.89 (12H, each, 48 total), 1.60-1.29 (51H, m);

^{13}C NMR (500 MHz, MeOH, D_4), δ: 173.3, 170.6, 170.3, 169.9, 169.8, 159.3, 116.0, 114.2, 71.9, 69.7, 68.5, 67.8, 67.5, 60.7, 60.0, 38.9, 33.3, 28.5, 22.9, 19.1, 16.2;

MS (MALDI, MeOH, positive ion) calcd. for $C_{118}H_{181}N_{17}O_{54}$, *m/z*: $(M)^+$ 2701.0, found 2701.0 $(M)^+$

Protocol for the Preparation of [β-Lysine(Galactose)-Alanine-Alanine)]$_4$ Glycine (72):

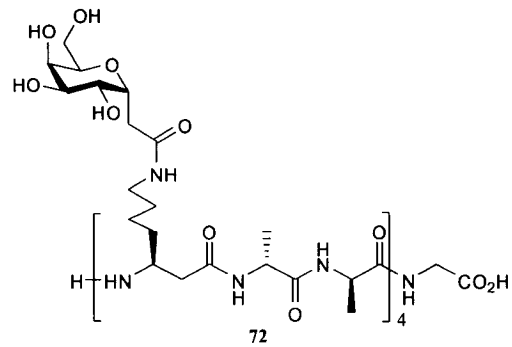

72

A protocol analogous to the preparation of **74** was followed to furnish the title compound **72** as a white solid in 100 % yield.

^{1}H NMR (500 MHz, D_2O), δ: 7.97-7.9 (1H, m), 7.75-7.72 (1H, m), 4.31 (1H, m), 4.19-3.96 (2H, m), 3.87-3.81 (1H, m), 3.65-3.62 (1H, m), 3.58-3.52 (1H, m), 3.52-3.51 (1H, m), 2.99 (1H, m), 2.49-2.21 (4H, m), 1.50-1.10 (8H, m);

^{13}C NMR (500 MHz, D_2O), δ: 174.7, 174.3, 173.5, 172.7, 171.9, 163.3, 146.8, 138.7, 130.2, 129.2, 125.9, 73.1, 72.5, 69.8, 68.9, 67.7, 60.9, 53.0, 49.9, 49.6, 48.8, 47.2, 41.2, 39.4, 33.5, 32.4, 31.7, 28.1, 26.6, 22.6, 21.9, 16.7;

IR (neat) cm^{-1}: 3330, 1637;

MS (MALDI, H_2O, positive ion) calcd. for $C_{86}H_{149}N_{17}O_{38}$, *m/z*: ($M^+$) 2028.0, found 2051.10 [$(M + Na)^+$]

Protocol for the Preparation of [β-Ornithine(Galactose)-Glycine-Glycine]$_4$ Glycine-Acetate (75):

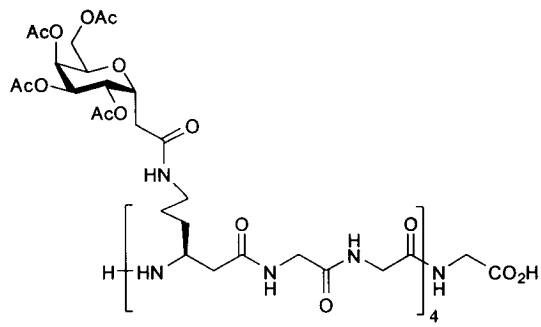

75

A protocol analogous to the preparation of **73** was followed to furnish the title compound **75** a yellow solid (141 mg, 93 %).

^{1}H NMR (500 MHz, MeOH, D_4), δ: 5.19 (4H, s), 5.02 (9H, m), 4.45 (3H, s), 4.03-3.91 (17H, m), 3.73-3.63 (22H, m), 3.0-2.97 (13H, m), 2.47 (6H, m), 2.27 (12H, m), 1.89, 1.83, 1.80, 1.78 (12H each, s 48 total), 1.35 (17H, br s);

^{13}C NMR (500 MHz, MeOH, D_4), δ: 172.1, 172.0, 171.9, 171.7, 171.6, 171.2, 171.2, 71.0, 69.7, 69.0, 68.7, 62.2, 54.9, 54.5, 43.5, 41.6, 39.8, 34.6, 32.6, 26.7, 26.1, 20.5, 20.5, 20.4, 20.3;

MS (MALDI, MeOH, negative ion) calcd. for $C_{106}H_{157}N_{17}O_{54}$, *m/z*: ($M^+$) 2533.41, found 2532.0 [$(M - H)^+$]

Protocol for the Preparation of [β-Ornithine(Galactose)-Glycine-Glycine]$_4$ Glycine (76):

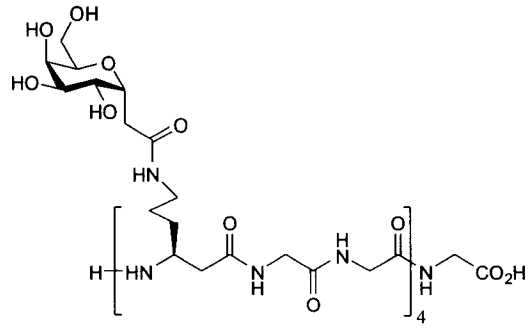

76

A protocol analogous to the preparation of **74** was followed to furnish a white solid **76** in 100 % yield.

^{1}H NMR (500 MHz, D_2O), δ: 4.16 (1H, br s), 3.99-3.84 (6H, m), 3.77 (1H, m), 3.71-3.63 (3H, m), 3.20-3.14 (2H, m), 2.66-2.59 (4H, m), 2.55-2.49 (2H, m), 2.42 (1H, m), 1.66 (1H, m), 1.56 (1H, m), 1.45 (2H, m);

^{13}C NMR (500 MHz, D_2O), δ: 176.5, 175.8, 174.3, 173.1, 165.6, 165.4, 128.0, 117.6, 75.3, 74.8, 71.9, 71.1, 69.8, 63.2, 49.5, 44.9, 44.8, 43.3, 41.3, 41.1, 36.8, 34.7, 33.3, 27.3;

IR: (neat) cm^{-1}: 3315-3265, 1635;

MS (MALDI, H_2O, positive ion) calcd. for $C_{74}H_{125}N_{17}O_{38}$, *m/z*: ($M^+$) 1859.87, found 1882.94 [$(M + Na)^+$]

CLAIMS TO ORIGINAL RESEARCH

1. Glycosylated building blocks containing β-amino acids were synthesized via modified Arndt-Eistert homologation. These building blocks were then used to assemble a series of new *C*-linked AFGP analogues containing β-amino acids.
2. Antifreeze-specific activity was assessed using a thermal hysteresis (TH) assay and recrystallization inhibition (RI) assay. All of the new analogues displayed a significant degree of TH activity, dynamic ice shaping as well as genuine RI activity.
3. The solution conformation of these new analogues was analyzed using circular dichroism (CD) spectroscopy. The overall conformation was mainly random coil accompanied by some β-turns, α-helix and β-sheets secondary structures.
4. *In vitro* cytotoxicity studies of these analogues were performed on human embryonic liver cell lines. The analogue **74** was not found to be cytotoxic at a physiological temperature, whereas analogues **72** and **76** were found to be cytotoxic only at high concentrations. However, all of these analogues were found to be cryotoxic at high concentrations and none of them were found to be cytotoxic or cryotoxic at lower analogue concentrations.

APPENDIX:

^{1}H and ^{13}C NMR Spectra

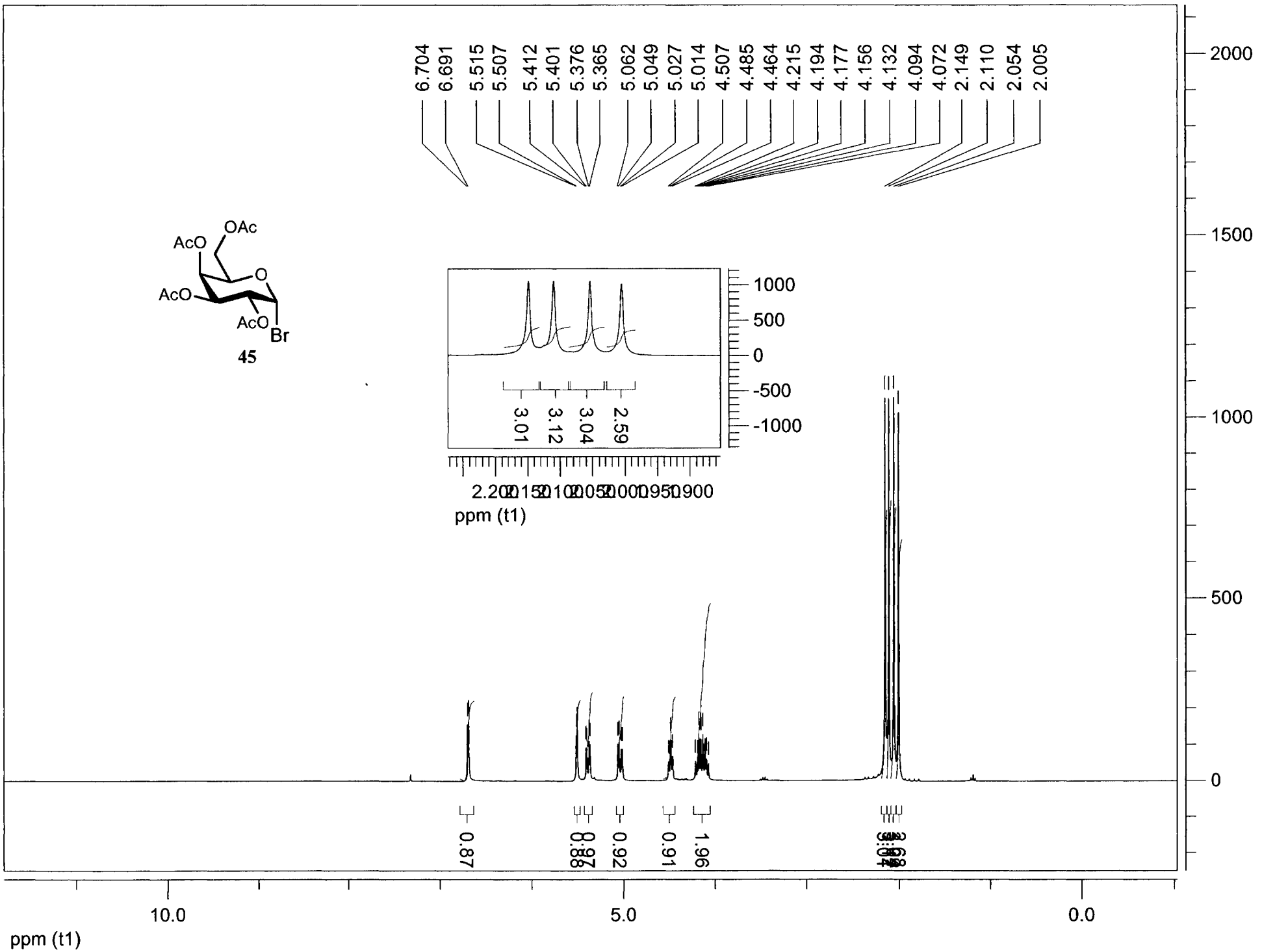
6.704
6.691
5.515
5.507
5.412
5.401
5.376
5.365
5.062
5.049
5.027
5.014
4.507
4.485
4.464
4.215
4.194
4.177
4.156
4.132
4.094
4.072
2.149
2.110
2.054
2.005
OAc
AcO
AcO
AcO
O
Br
45
3.01
3.12
3.04
2.59
ppm (t1)
0.87
0.88
0.92
0.91
1.96
10.0
5.0
0.0
ppm (t1)

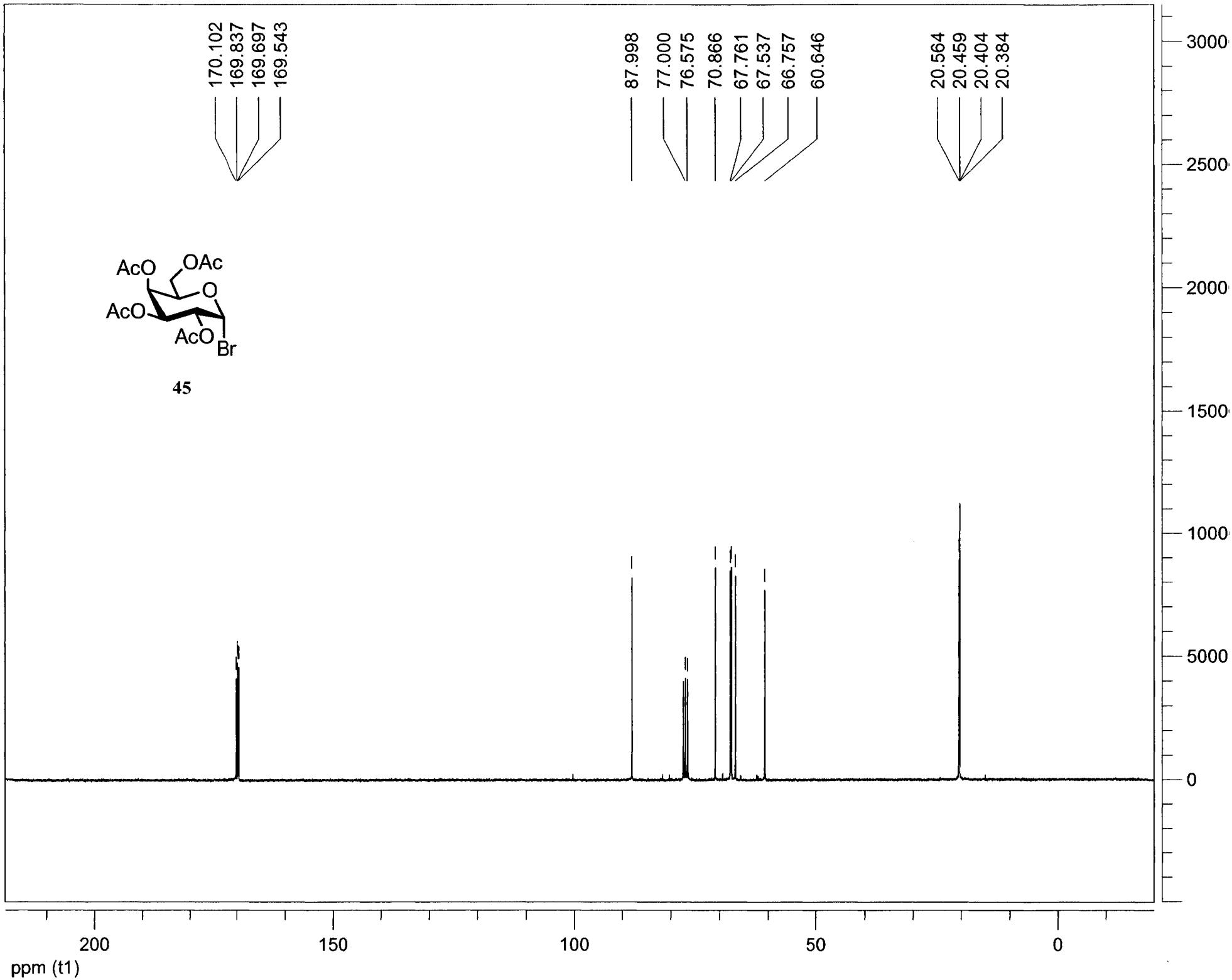
170.102
169.837
169.697
169.543
87.998
77.000
76.575
70.866
67.761
67.537
66.757
60.646
20.564
20.459
20.404
20.384
AcO
OAc
O
AcO
AcO
Br
3000
2500
2000
1500
1000
5000
0
200
150
100
50
0
ppm (t1)

45

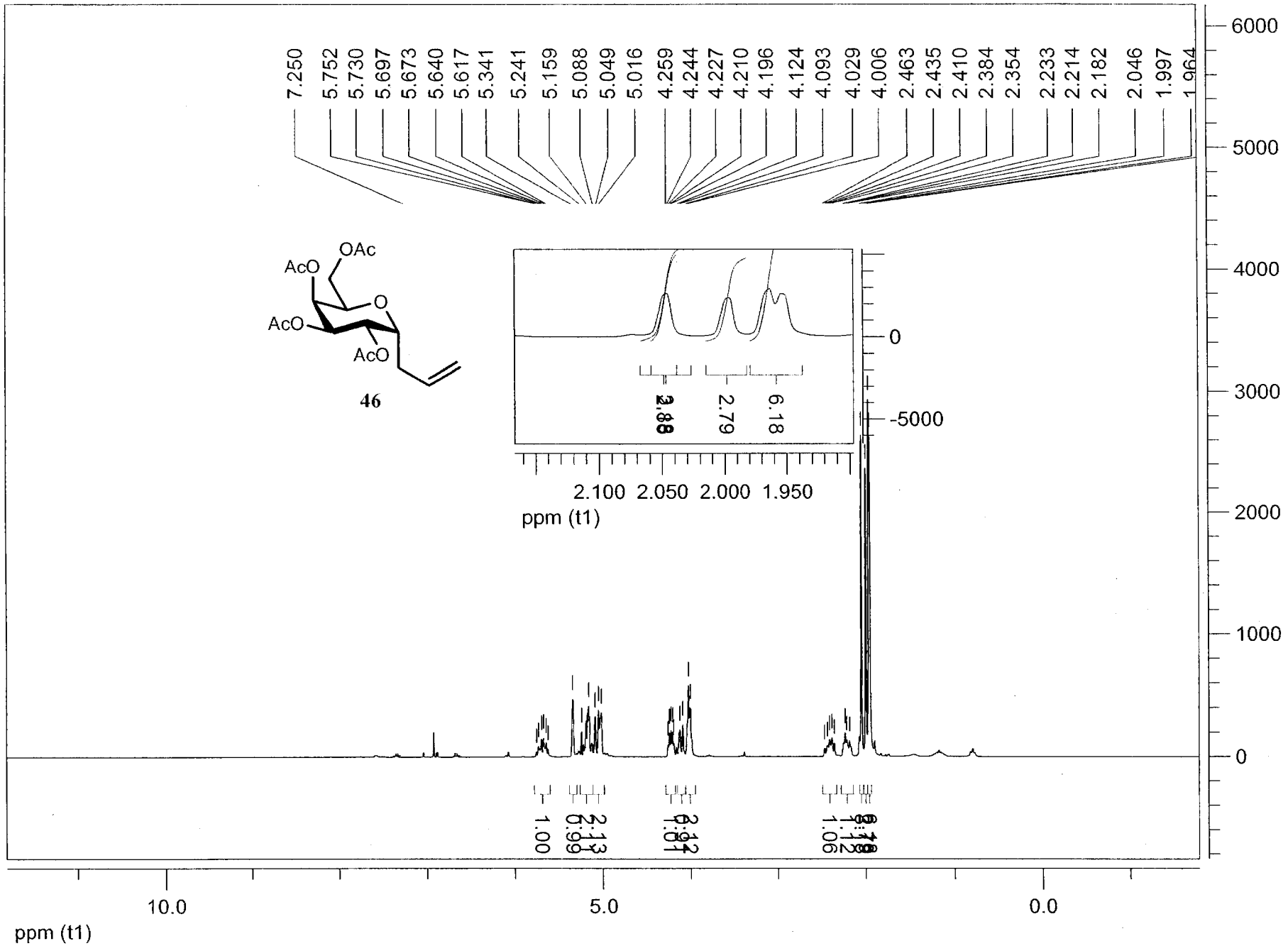
7.250
5.752
5.730
5.697
5.673
5.640
5.617
5.341
5.241
5.159
5.088
5.049
5.016
4.259
4.244
4.227
4.210
4.196
4.124
4.093
4.029
4.006
2.463
2.435
2.410
2.384
2.354
2.233
2.214
2.182
2.046
1.997
1.964
AcO
OAc
AcO
O
AcO
46
2.79
6.18
2.100 2.050 2.000 1.950
ppm (t1)
6000
5000
4000
3000
2000
1000
0
-5000
1.00
2.13
1.01
1.06
10.0
5.0
0.0
ppm (t1)

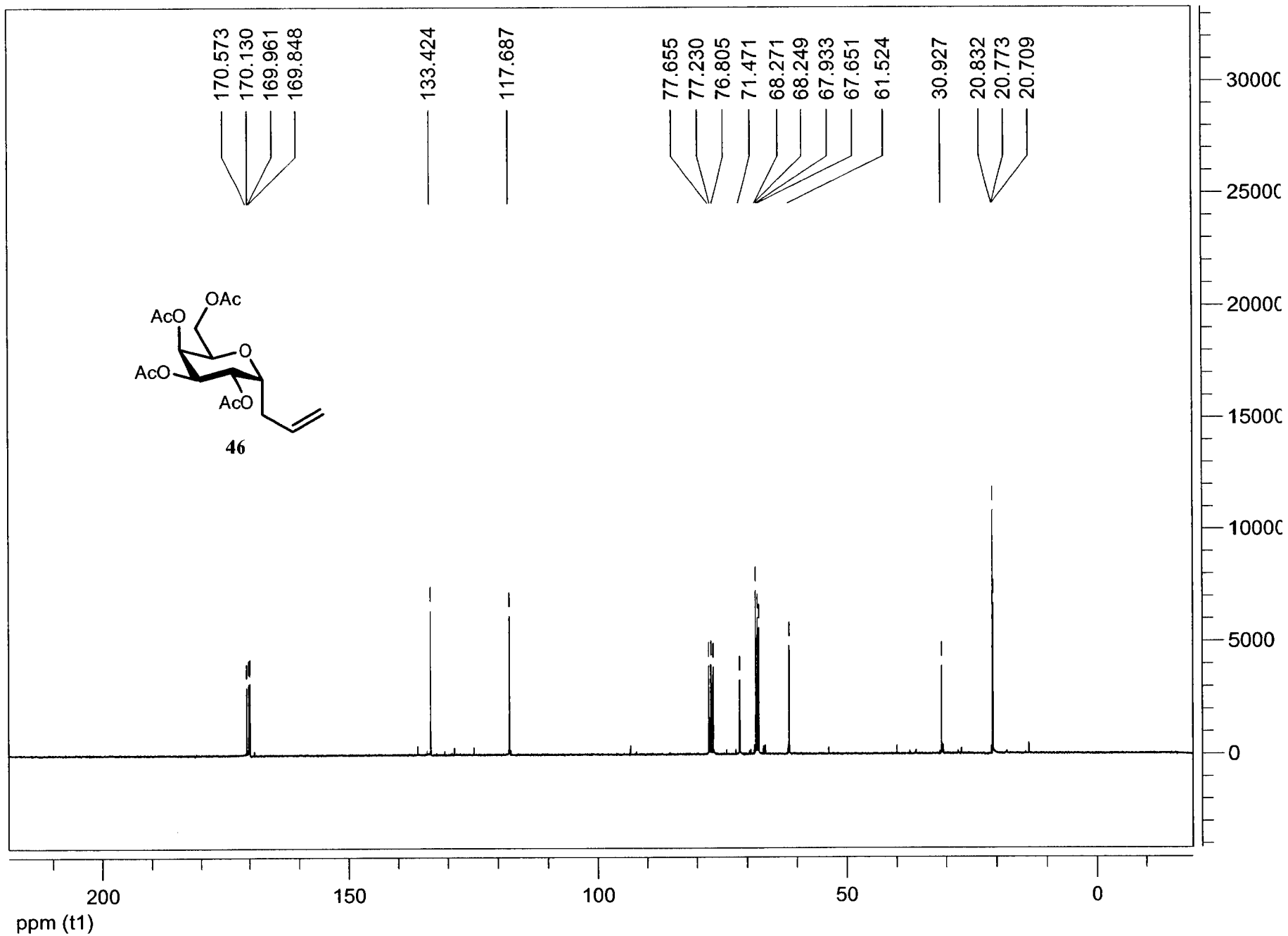
170.573
170.130
169.961
169.848
133.424
117.687
77.655
77.230
76.805
71.471
68.271
68.249
67.933
67.651
61.524
30.927
20.832
20.773
20.709
OAc
AcO
AcO
AcO
O
46
3000
2500
2000
1500
1000
5000
0
200
150
100
50
0
ppm (t1)

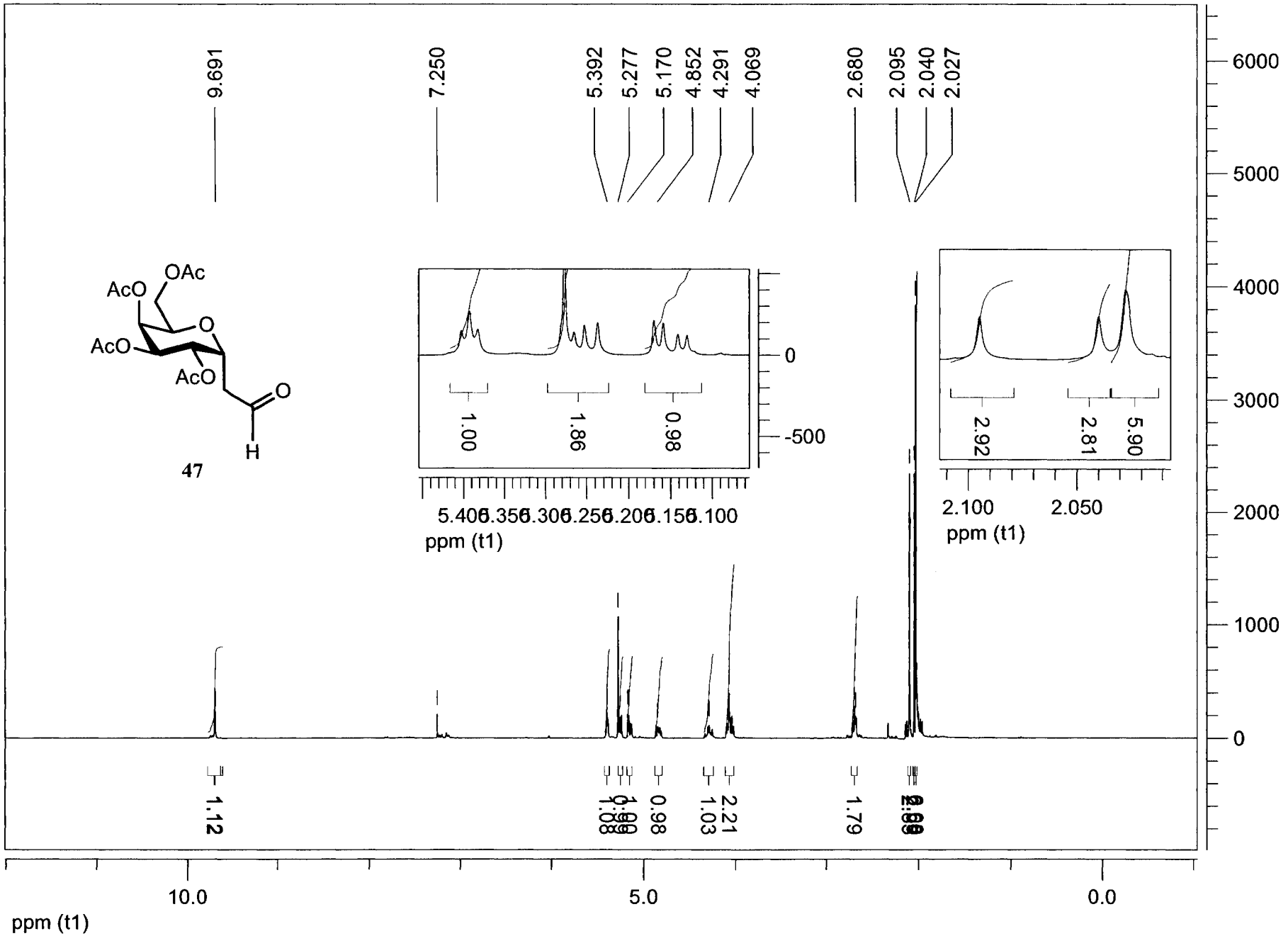
9.691
7.250
5.392
5.277
5.170
4.852
4.291
4.069
2.680
2.095
2.040
2.027
OAc
AcO
AcO
AcO
O
O
H
47
1.00
1.86
0.98
0
-500
5.40 6.35 6.30 6.25 6.20 6.15 6.10
ppm (t1)
2.92
2.81
5.90
2.100
2.050
ppm (t1)
1.12
1.08
0.98
1.03
2.21
1.79
6000
5000
4000
3000
2000
1000
0
10.0
5.0
0.0
ppm (t1)

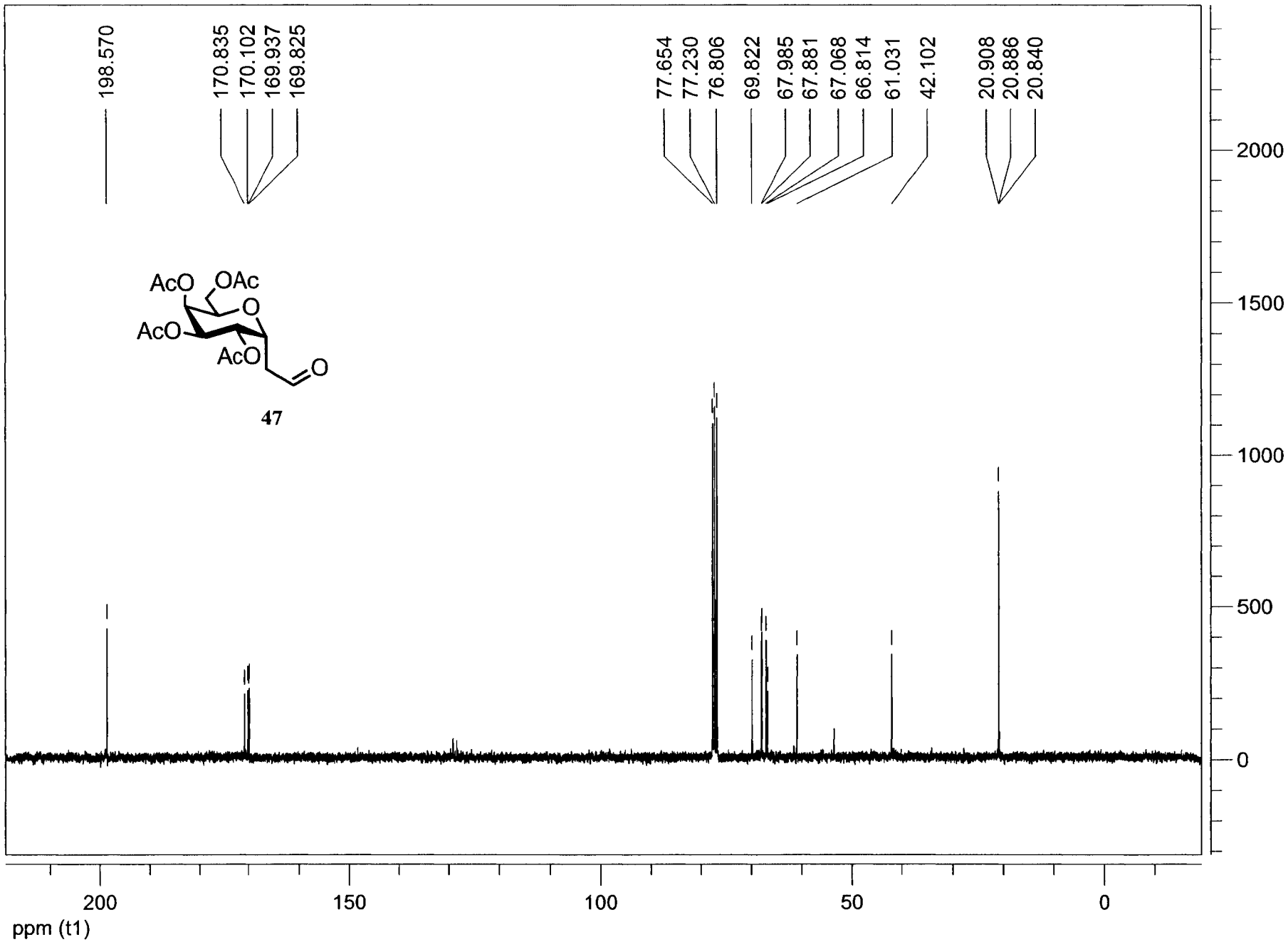
198.570
170.835
170.102
169.937
169.825
77.654
77.230
76.806
69.822
67.985
67.881
67.068
66.814
61.031
42.102
20.908
20.886
20.840
AcO
OAc
O
AcO
AcO
O
47
2000
1500
1000
500
0
200
150
100
50
0
ppm (t1)

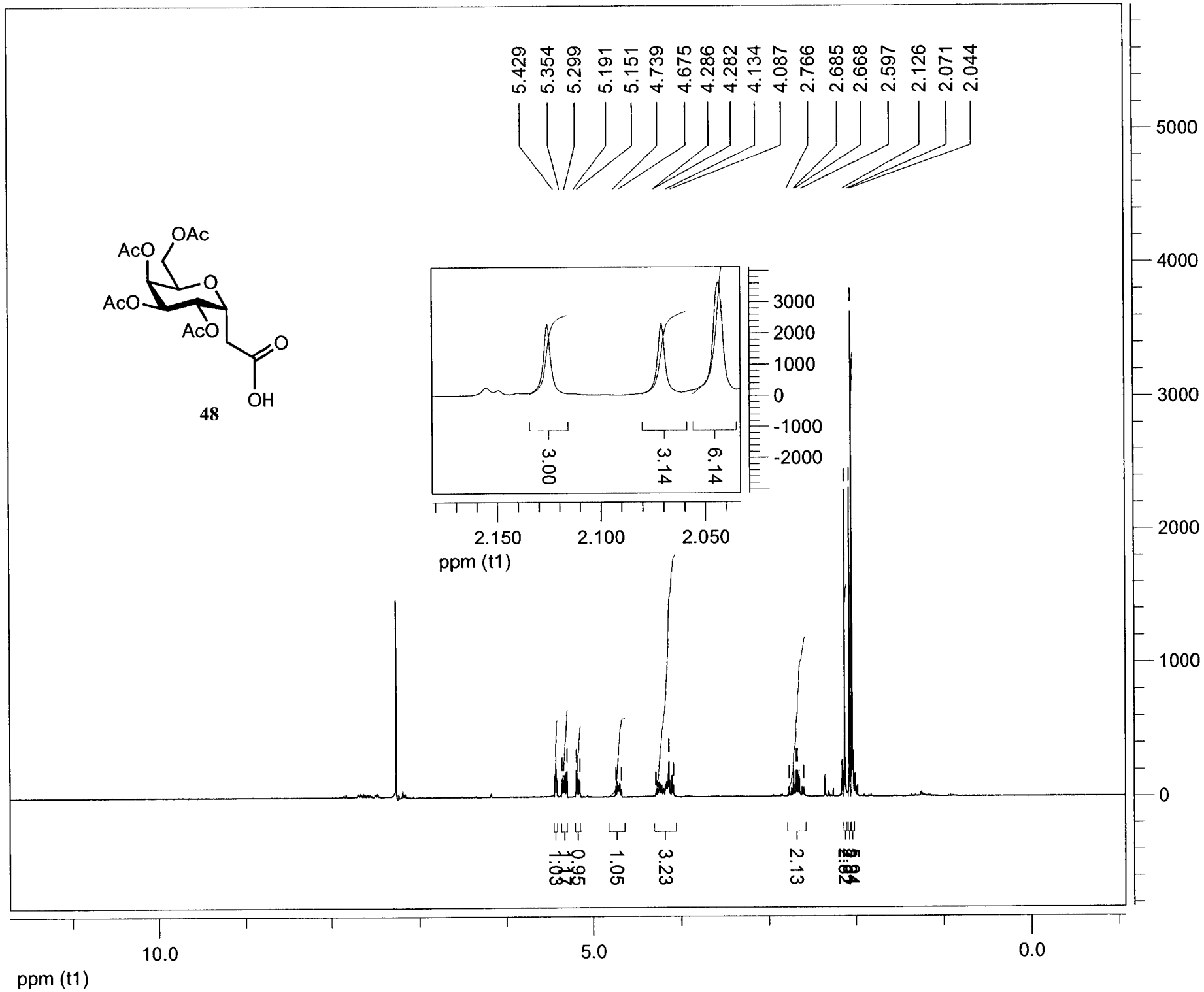
5.429
5.354
5.299
5.191
5.151
4.739
4.675
4.286
4.282
4.134
4.087
2.766
2.685
2.668
2.597
2.126
2.071
2.044
OAc
AcO
AcO
AcO
O
O
OH
48
3.00
3.14
6.14
2.150
2.100
2.050
ppm (t1)
1.03
0.95
1.05
3.23
2.13
10.0
5.0
0.0
ppm (t1)

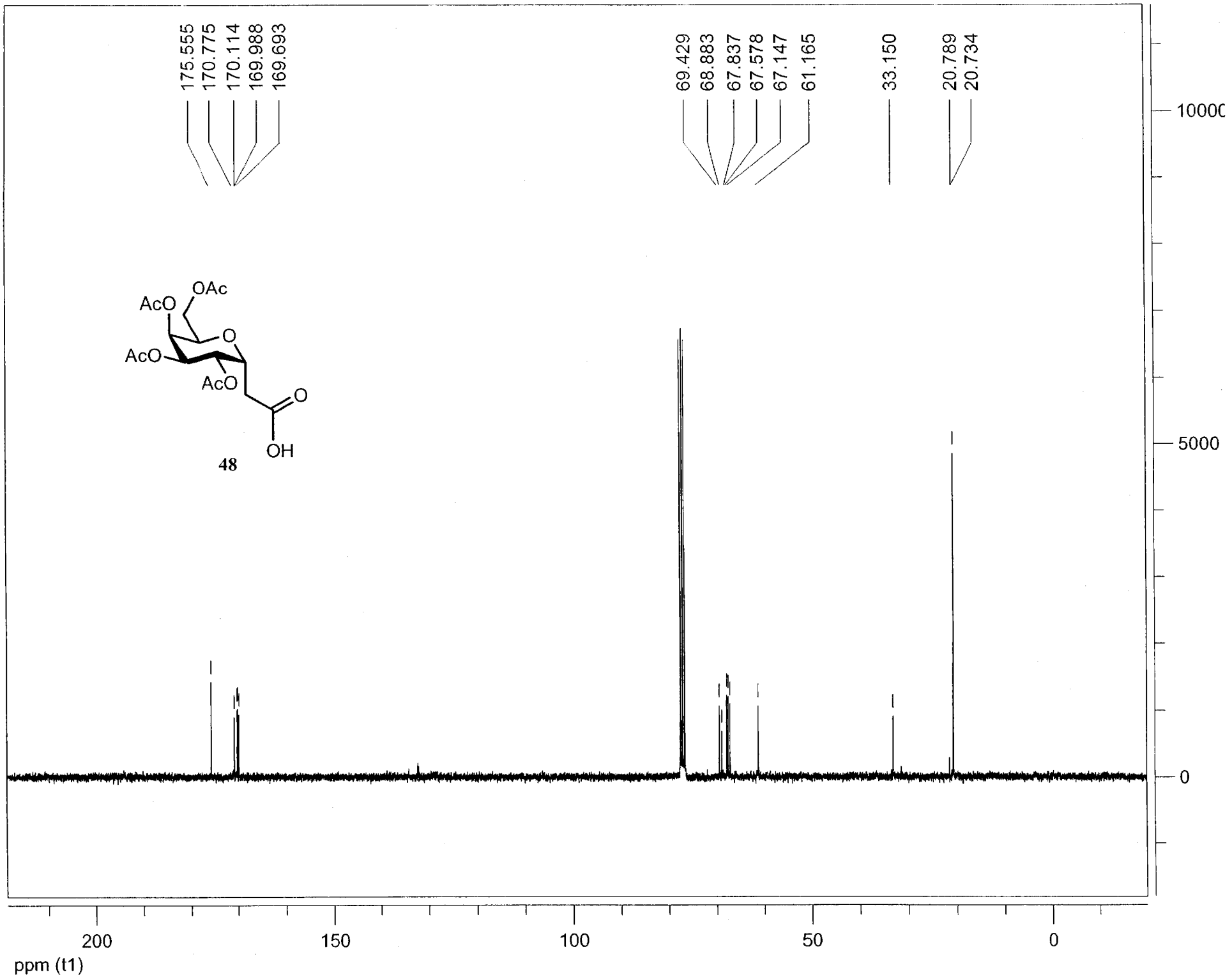
175.555
170.775
170.114
169.988
169.693
69.429
68.883
67.837
67.578
67.147
61.165
33.150
20.789
20.734
OAc
AcO
AcO
AcO
O
O
OH
48
10000
5000
0
200
150
100
50
0
ppm (t1)

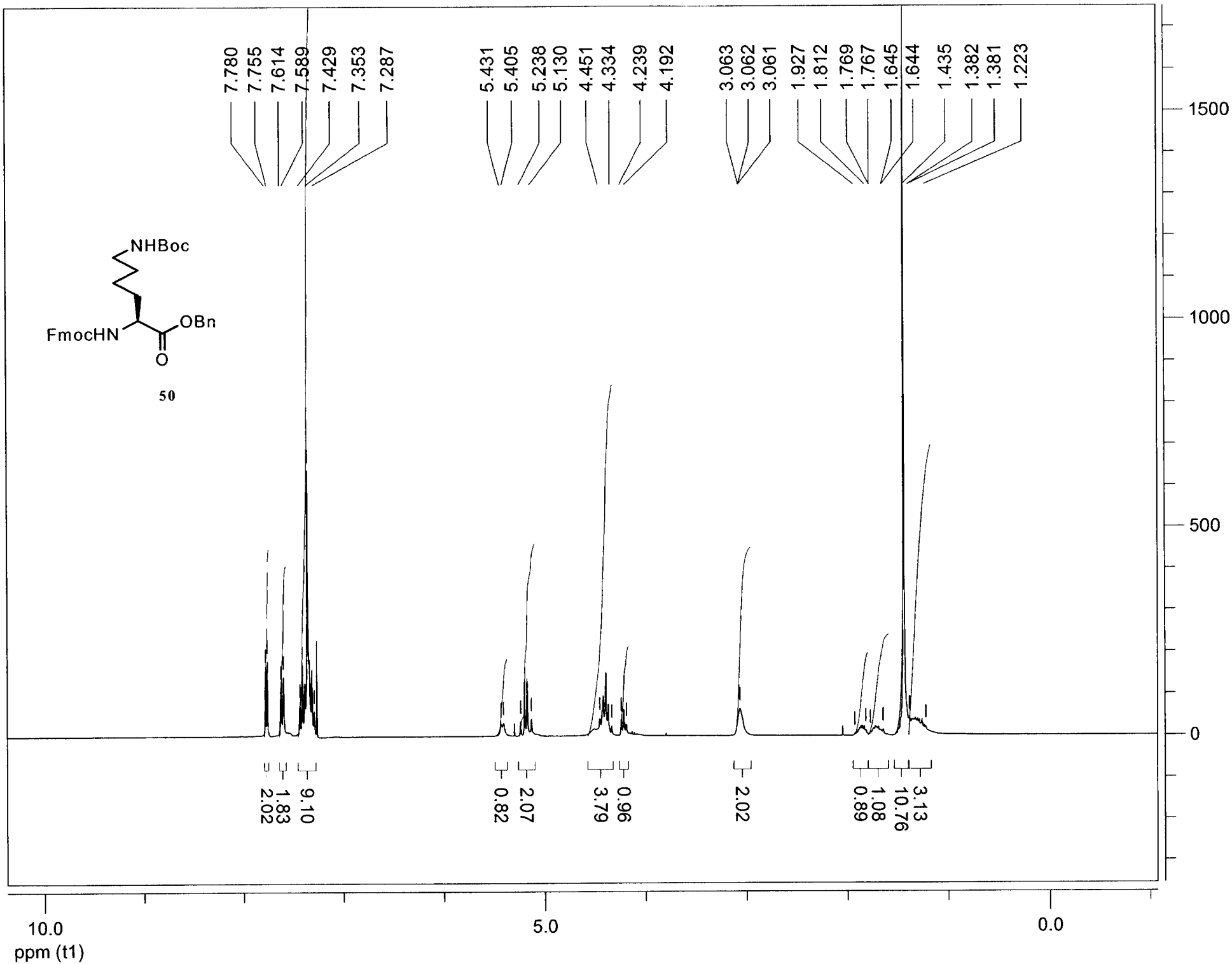
7.780
7.755
7.614
7.589
7.429
7.353
7.287
5.431
5.405
5.238
5.130
4.451
4.334
4.239
4.192
3.063
3.062
3.061
1.927
1.812
1.769
1.767
1.645
1.644
1.435
1.382
1.381
1.223
NHBoc
FmocHN
OBn
O
50
2.02
1.83
9.10
0.82
2.07
3.79
0.96
2.02
0.89
1.08
10.76
3.13
1500
1000
500
0
10.0
5.0
0.0
ppm (t1)

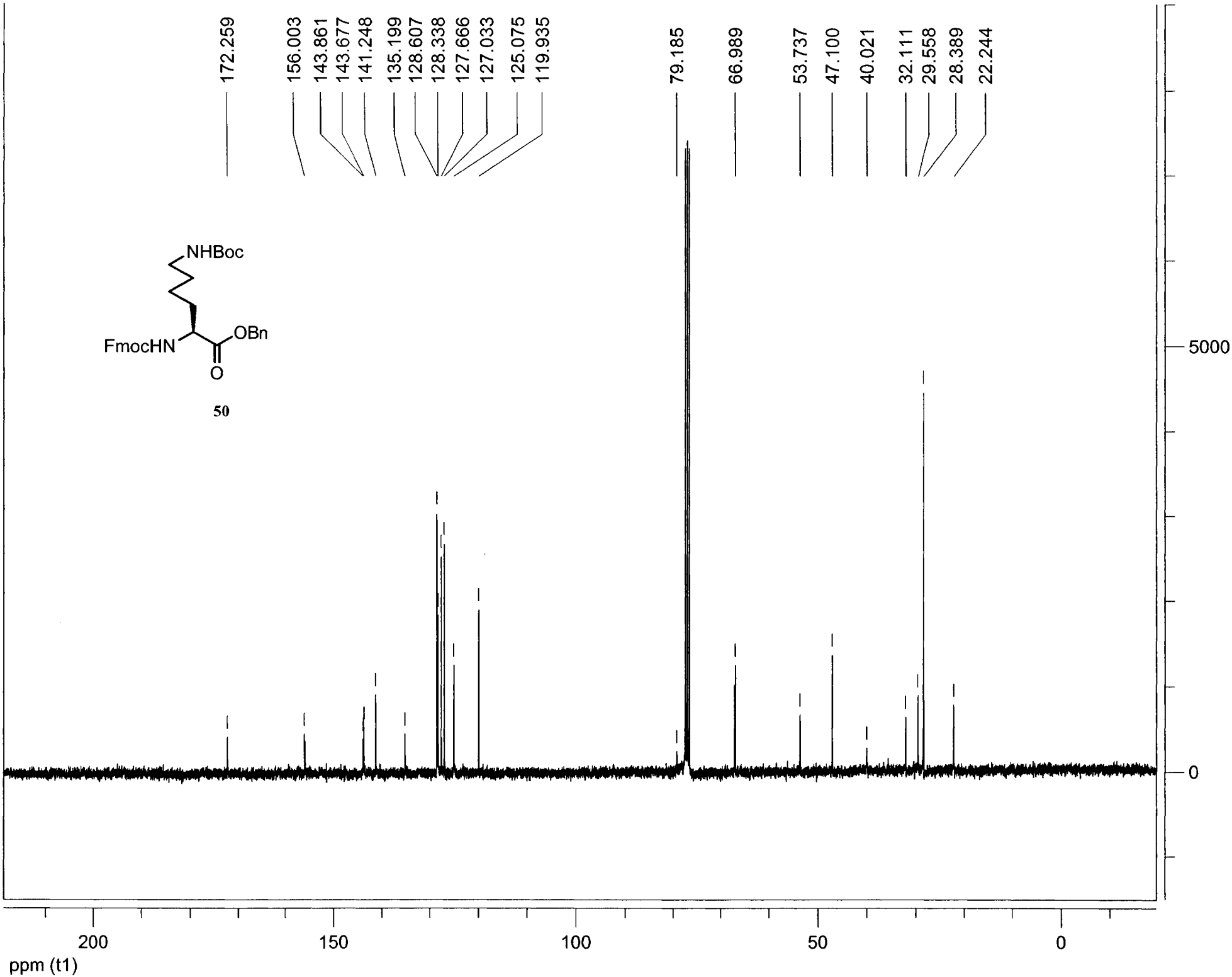
172.259
156.003
143.861
143.677
141.248
135.199
128.607
128.338
127.666
127.033
125.075
119.935
79.185
66.989
53.737
47.100
40.021
32.111
29.558
28.389
22.244
NHBoc
FmocHN
OBn
O
50
5000
0
200
150
100
50
0
ppm (t1)

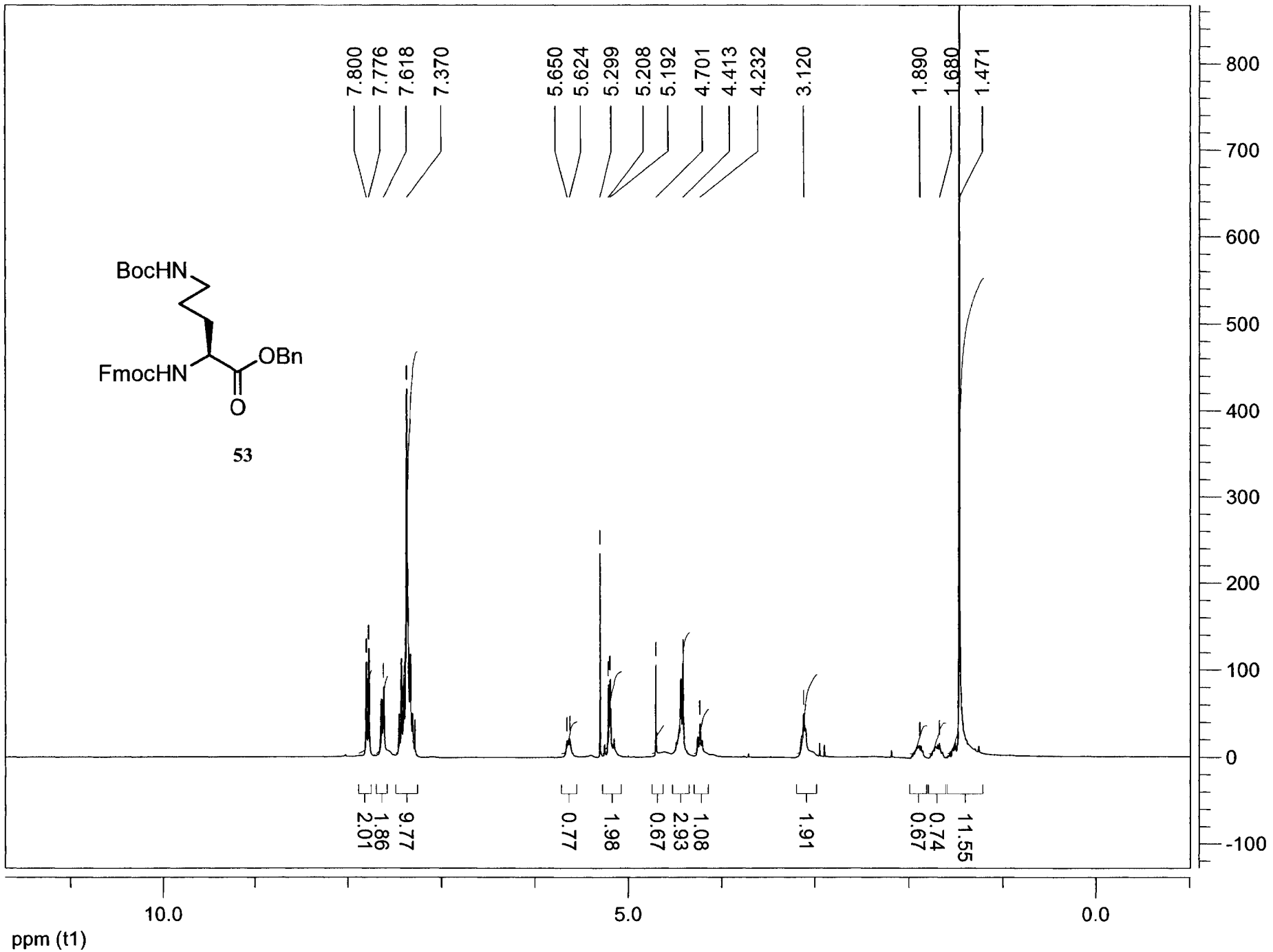
7.800
7.776
7.618
7.370
5.650
5.624
5.299
5.208
5.192
4.701
4.413
4.232
3.120
1.890
1.680
1.471
BocHN
FmocHN
OBn
O
53
2.01
1.86
9.77
0.77
1.98
0.67
2.93
1.08
1.91
0.67
0.74
11.55
800
700
600
500
400
300
200
100
0
-100
10.0
5.0
0.0
ppm (t1)

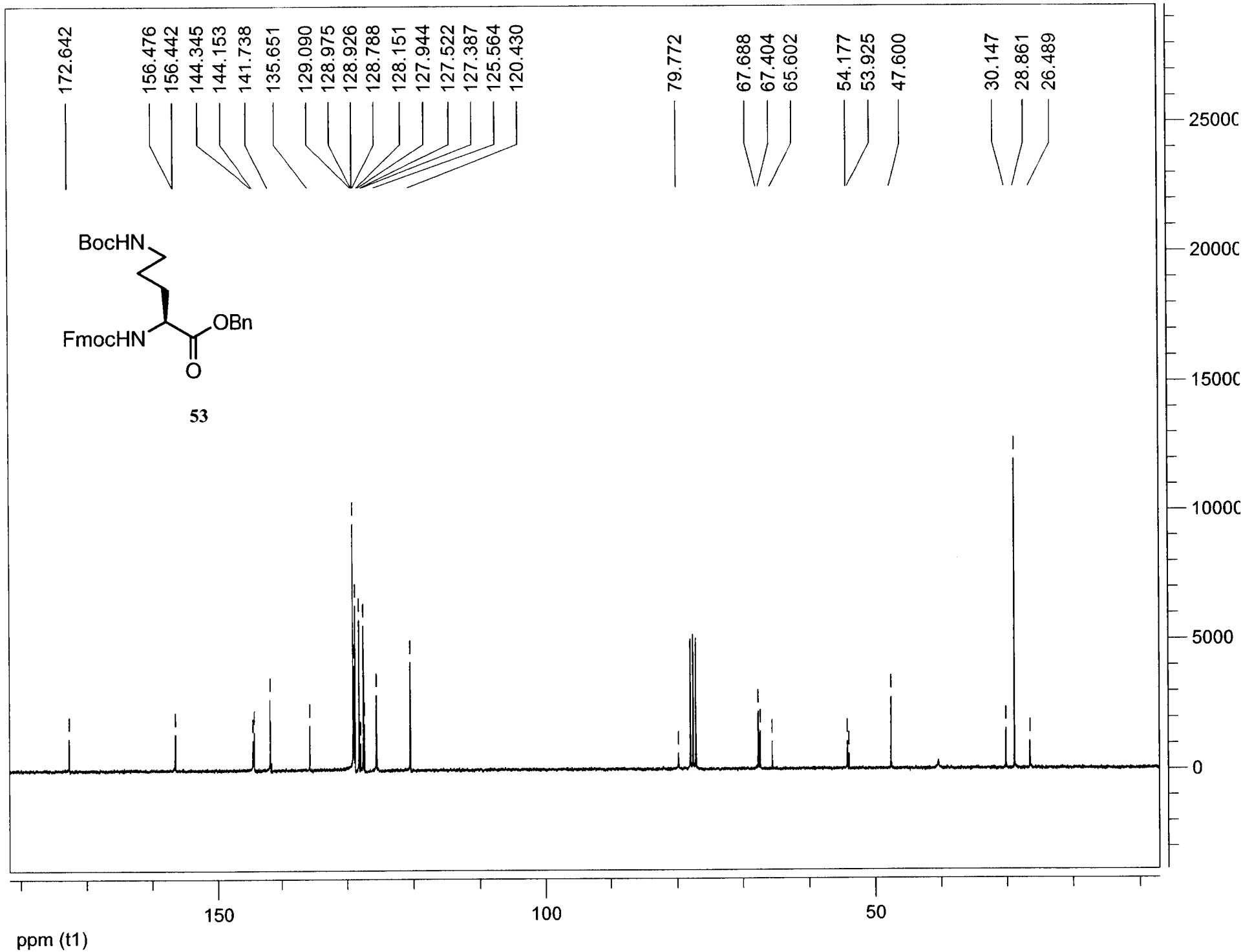
172.642
156.476
156.442
144.345
144.153
141.738
135.651
129.090
128.975
128.926
128.788
128.151
127.944
127.522
127.387
125.564
120.430
79.772
67.688
67.404
65.602
54.177
53.925
47.600
30.147
28.861
26.489
BocHN
FmocHN
OBn
O
53
25000
20000
15000
10000
5000
0
150
100
50
ppm (t1)

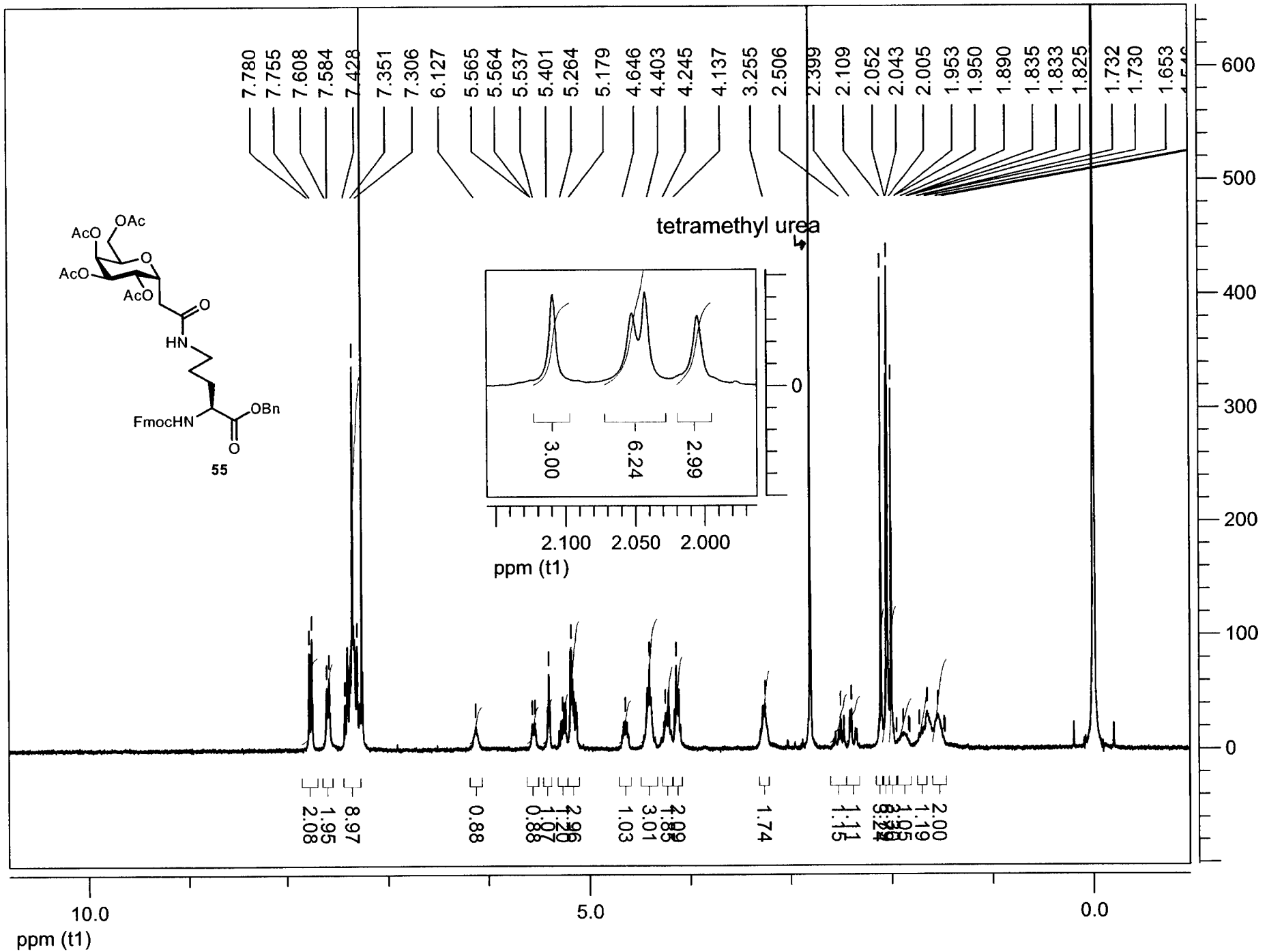
7.780
7.755
7.608
7.584
7.428
7.351
7.306
6.127
5.565
5.564
5.537
5.401
5.264
5.179
4.646
4.403
4.245
4.137
3.255
2.506
2.399
2.109
2.052
2.043
2.005
1.953
1.950
1.890
1.835
1.833
1.825
1.732
1.730
1.653
tetramethyl urea
AcO
OAc
AcO
AcO
O
HN
FmocHN
OBn
O
O
55
3.00
6.24
2.99
2.100
2.050
2.000
ppm (t1)
2.08
1.95
8.97
0.88
0.88
1.07
2.96
1.03
3.01
2.89
1.74
1.15
1.11
1.19
2.00
600
500
400
300
200
100
0
10.0
5.0
0.0
ppm (t1)

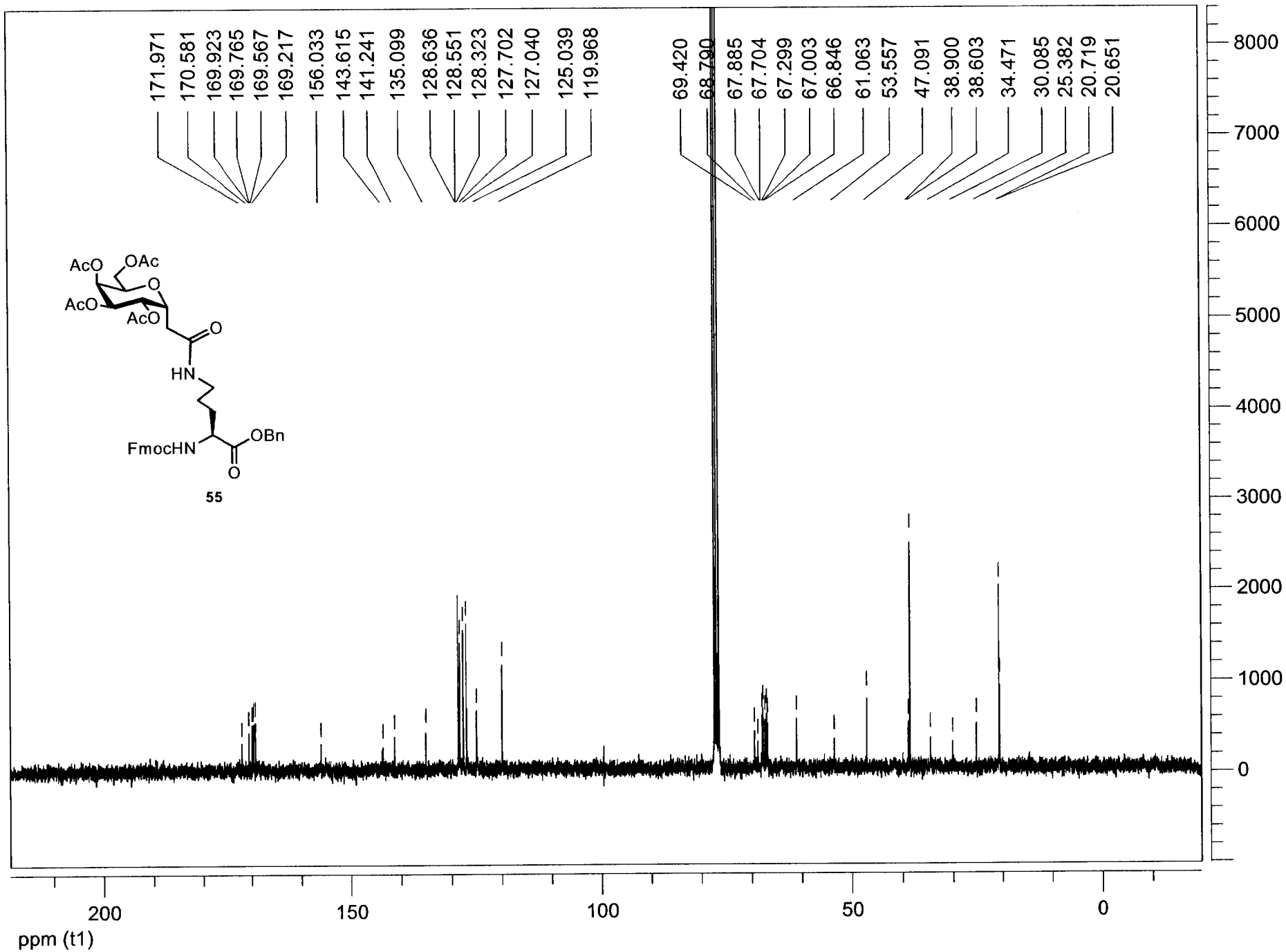
171.971
170.581
169.923
169.765
169.567
169.217
156.033
143.615
141.241
135.099
128.636
128.551
128.323
127.702
127.040
125.039
119.968
69.420
68.790
67.885
67.704
67.299
67.003
66.846
61.063
53.557
47.091
38.900
38.603
34.471
30.085
25.382
20.719
20.651
AcO
OAc
AcO
AcO
O
HN
O
FmocHN
OBn
O
55
8000
7000
6000
5000
4000
3000
2000
1000
0
200
150
100
50
0
ppm (t1)

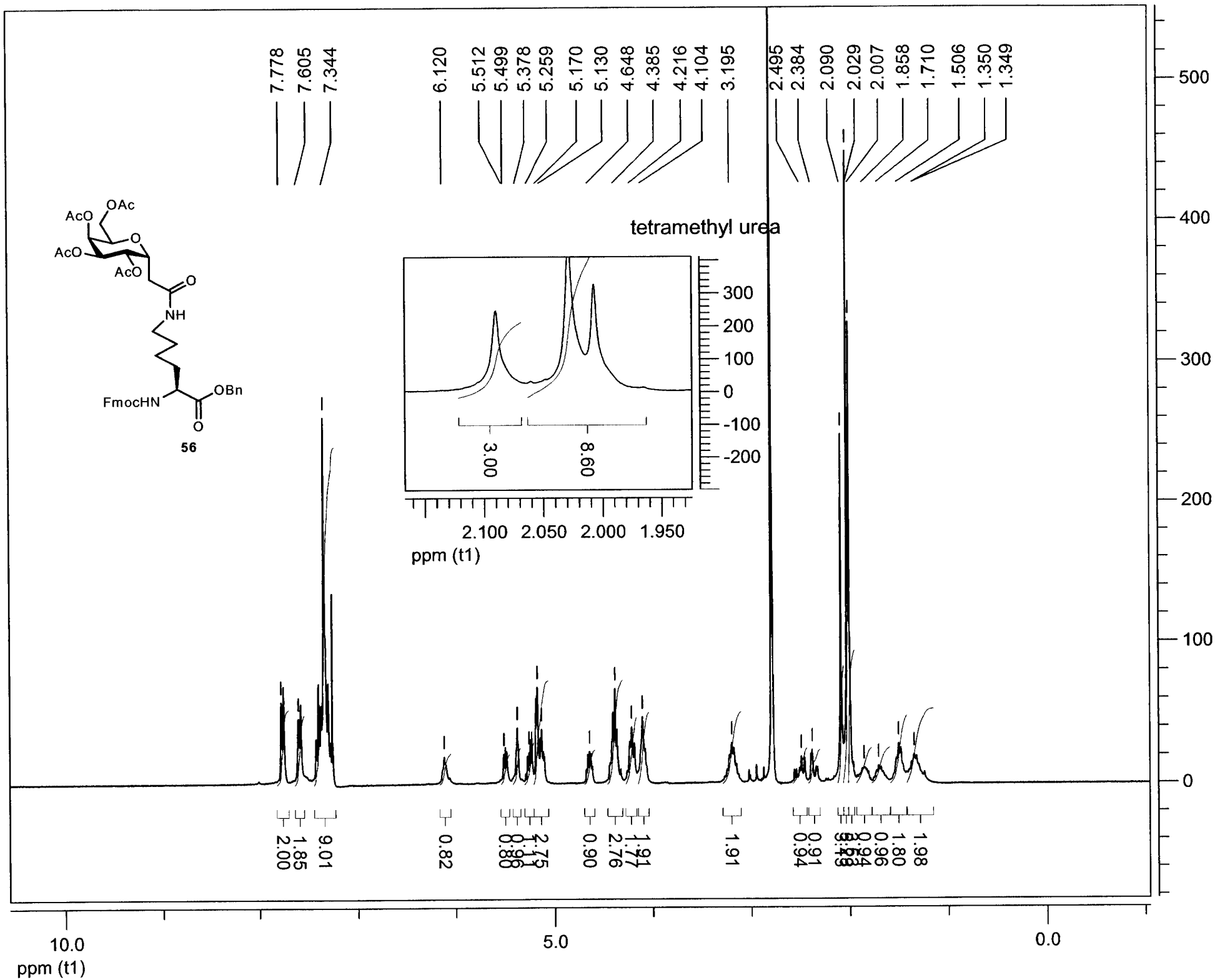
7.778
7.605
7.344
6.120
5.512
5.499
5.378
5.259
5.170
5.130
4.648
4.385
4.216
4.104
3.195
2.495
2.384
2.090
2.029
2.007
1.858
1.710
1.506
1.350
1.349
tetramethyl urea
AcO
OAc
AcO
AcO
O
NH
FmocHN
OBn
O
O
56
3.00
8.60
2.100 2.050 2.000 1.950
ppm (t1)
2.00
1.85
9.01
0.82
0.90
1.91
1.91
2.76
1.80
1.98
10.0
5.0
0.0
ppm (t1)

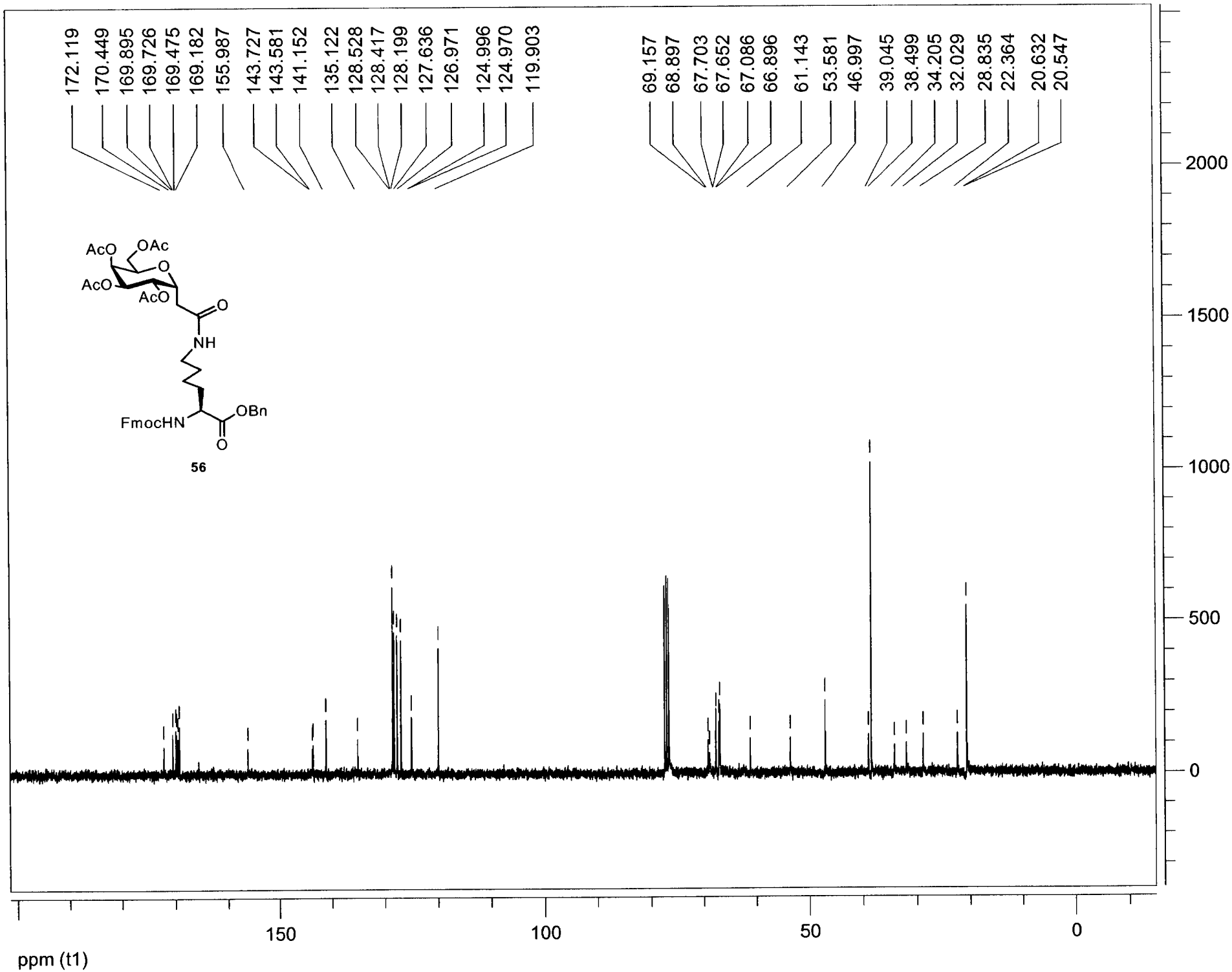
172.119
170.449
169.895
169.726
169.475
169.182
155.987
143.727
143.581
141.152
135.122
128.528
128.417
128.199
127.636
126.971
124.996
124.970
119.903
69.157
68.897
67.703
67.652
67.086
66.896
61.143
53.581
46.997
39.045
38.499
34.205
32.029
28.835
22.364
20.632
20.547
AcO
OAc
AcO
AcO
O
NH
FmocHN
OBn
O
O
56
2000
1500
1000
500
0
150
100
50
0
ppm (t1)

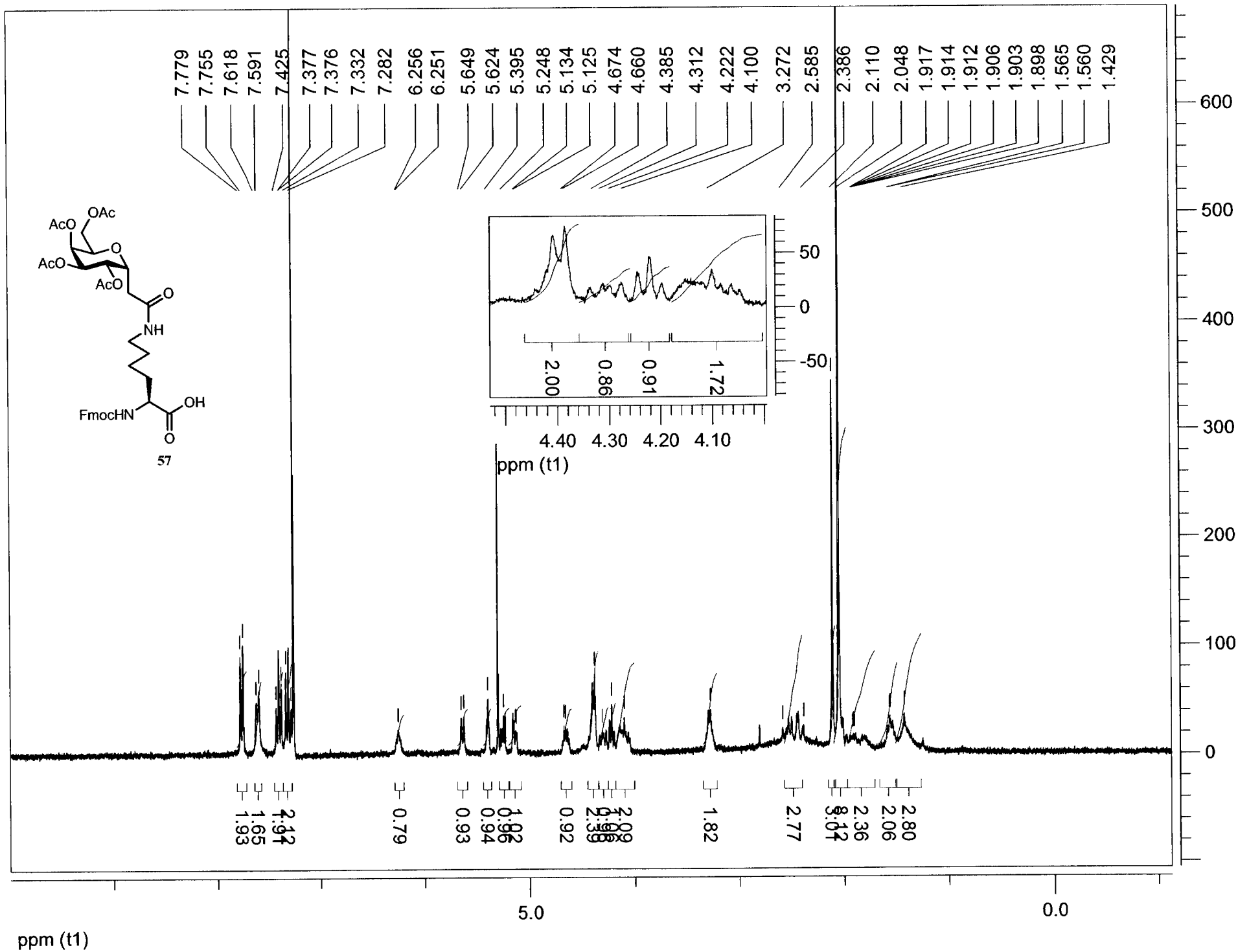
7.779
7.755
7.618
7.591
7.425
7.377
7.376
7.332
7.282
6.256
6.251
5.649
5.624
5.395
5.248
5.134
5.125
4.674
4.660
4.385
4.312
4.222
4.100
3.272
2.585
2.386
2.110
2.048
1.917
1.914
1.912
1.906
1.903
1.898
1.565
1.560
1.429
AcO
OAc
AcO
AcO
O
NH
O
FmocHN
OH
O
57
2.00
0.86
0.91
1.72
4.40
4.30
4.20
4.10
ppm (t1)
50
0
-50
600
500
400
300
200
100
0
1.93
1.65
2.12
0.79
0.93
0.94
0.92
1.82
2.77
2.36
2.06
2.80
5.0
0.0
ppm (t1)

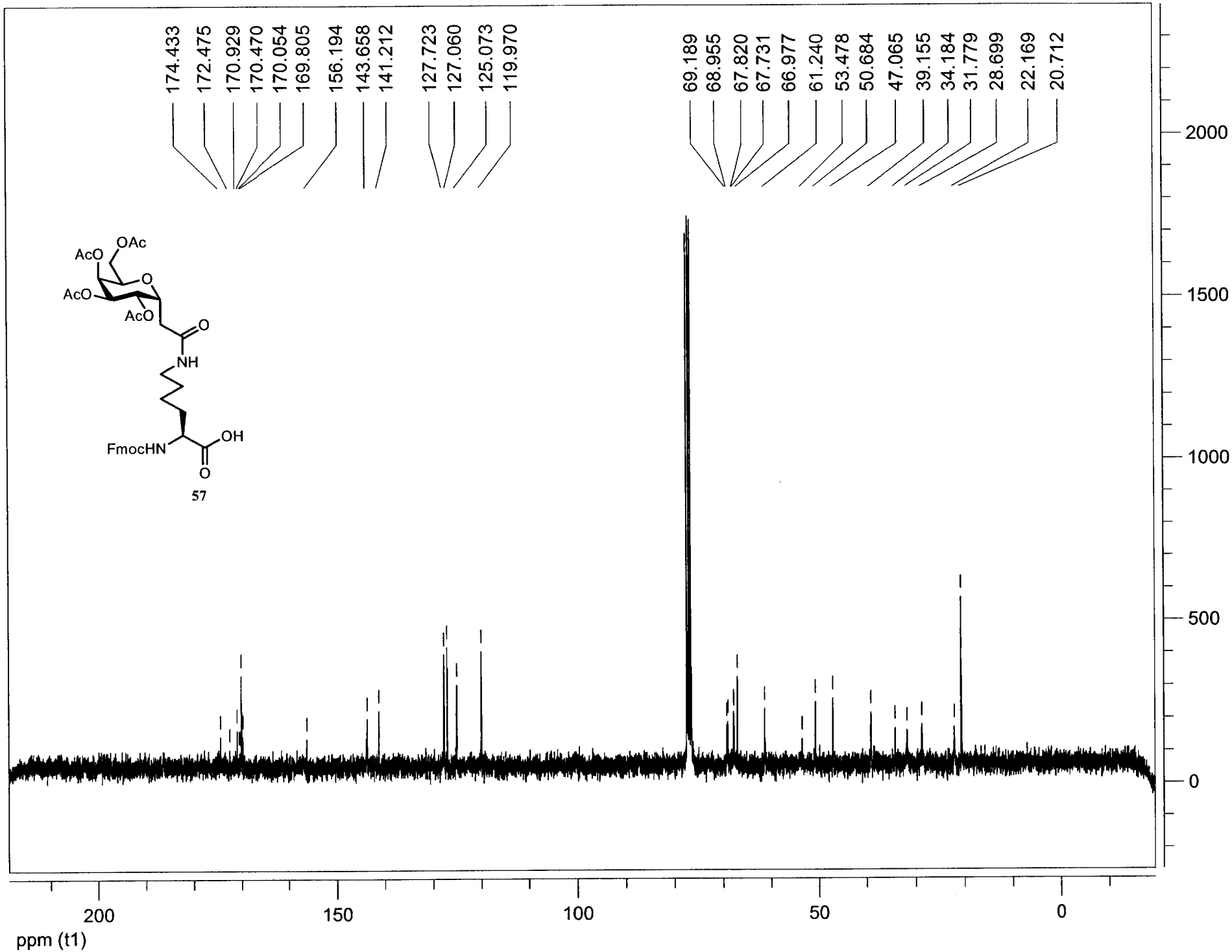
174.433
172.475
170.929
170.470
170.054
169.805
156.194
143.658
141.212
127.723
127.060
125.073
119.970
69.189
68.955
67.820
67.731
66.977
61.240
53.478
50.684
47.065
39.155
34.184
31.779
28.699
22.169
20.712
AcO
OAc
AcO
AcO
O
NH
FmocHN
OH
O
57
2000
1500
1000
500
0
200
150
100
50
0
ppm (t1)

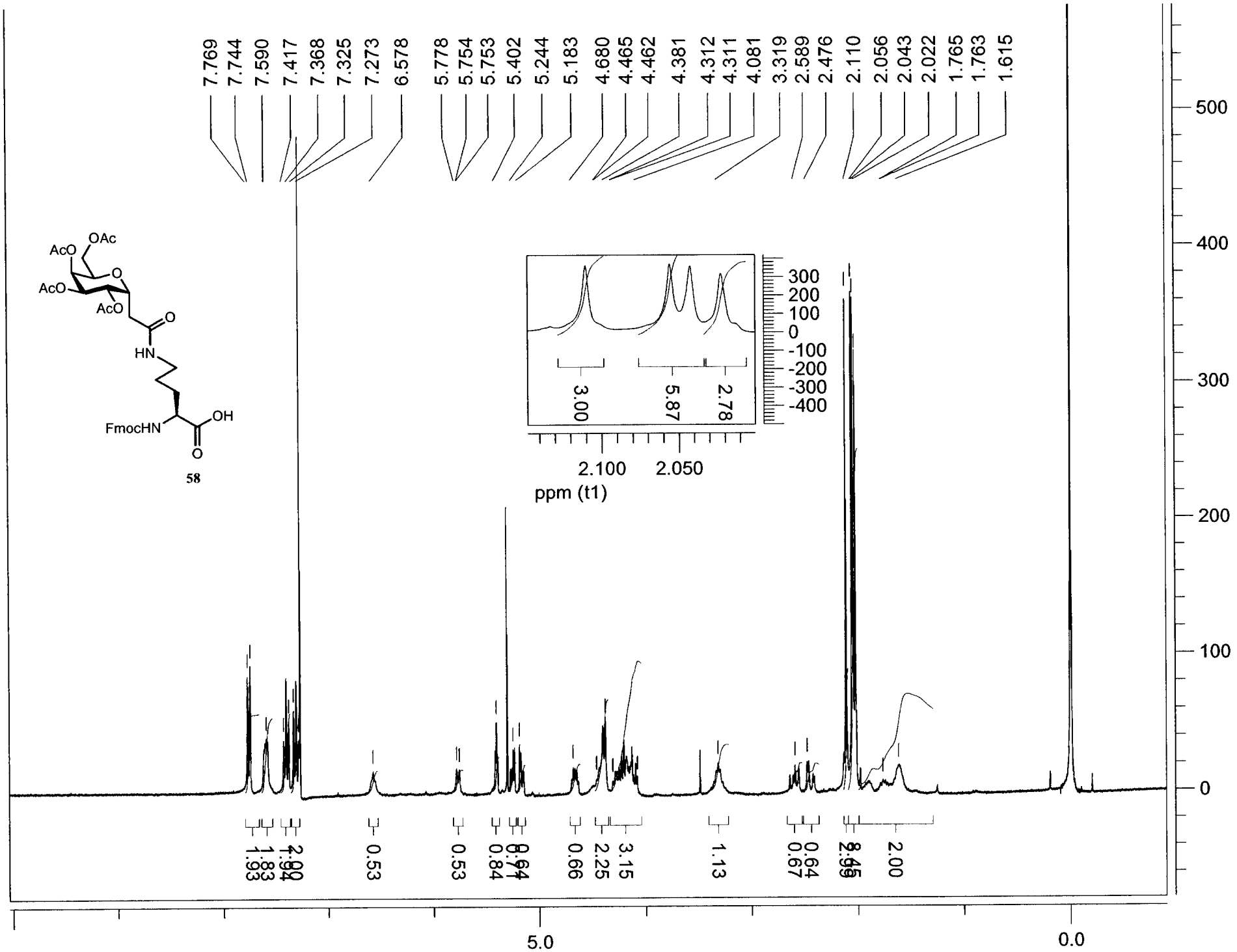
7.769
7.744
7.590
7.417
7.368
7.325
7.273
6.578
5.778
5.754
5.753
5.402
5.244
5.183
4.680
4.465
4.462
4.381
4.312
4.311
4.081
3.319
2.589
2.476
2.110
2.056
2.043
2.022
1.765
1.763
1.615
AcO
OAc
AcO
AcO
O
HN
O
FmocHN
OH
O
58
3.00
5.87
2.78
2.100
2.050
ppm (t1)
300
200
100
0
-100
-200
-300
-400
500
400
300
200
100
0
1.93
1.83
0.53
0.53
0.84
0.66
2.25
3.15
1.13
0.67
0.64
2.00
5.0
0.0
ppm (t1)

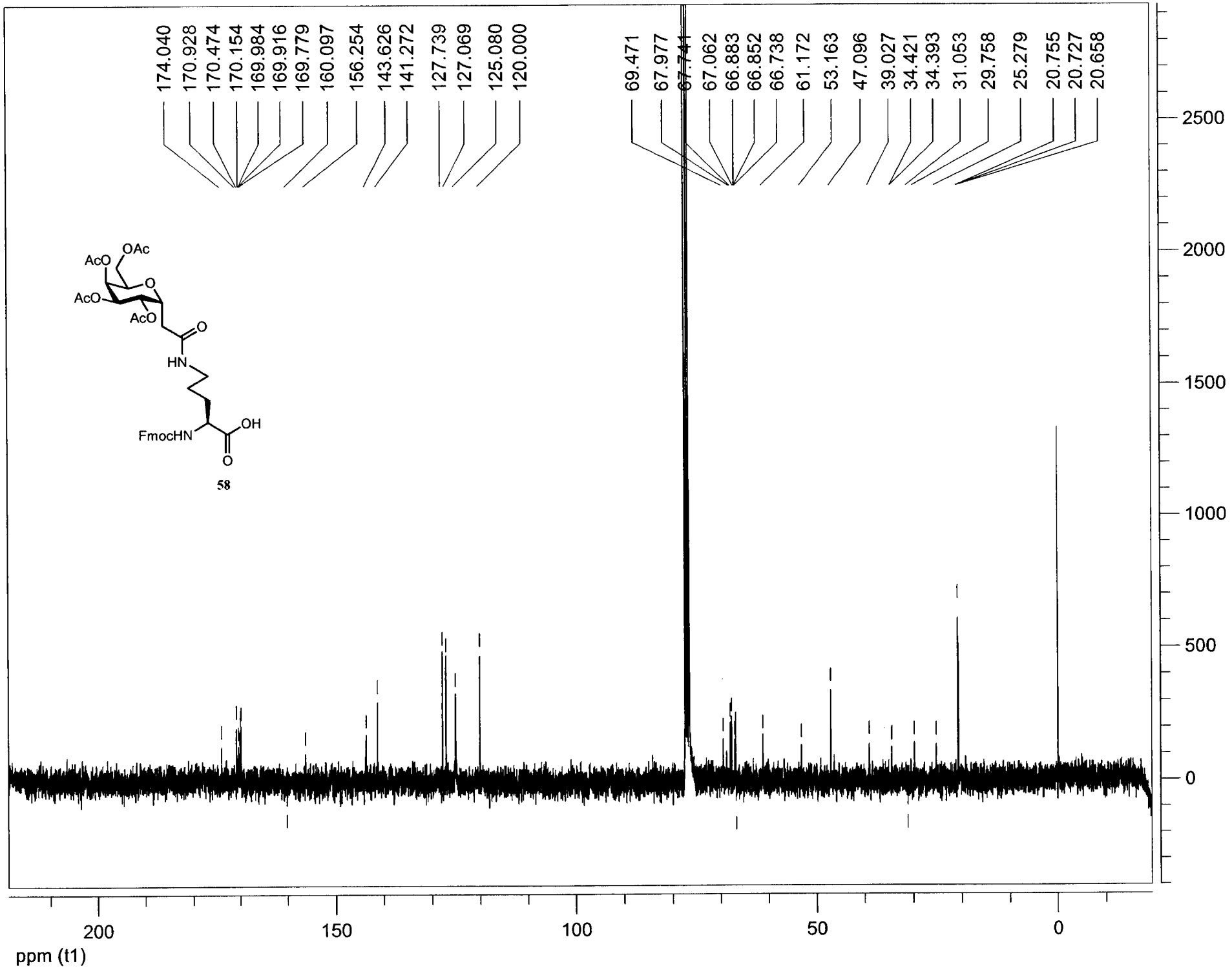
174.040
170.928
170.474
170.154
169.984
169.916
169.779
160.097
156.254
143.626
141.272
127.739
127.069
125.080
120.000
69.471
67.977
67.741
67.062
66.883
66.852
66.738
61.172
53.163
47.096
39.027
34.421
34.393
31.053
29.758
25.279
20.755
20.727
20.658
AcO
OAc
AcO
AcO
O
HN
O
FmocHN
OH
O
58
2500
2000
1500
1000
500
0
200
150
100
50
0
ppm (t1)

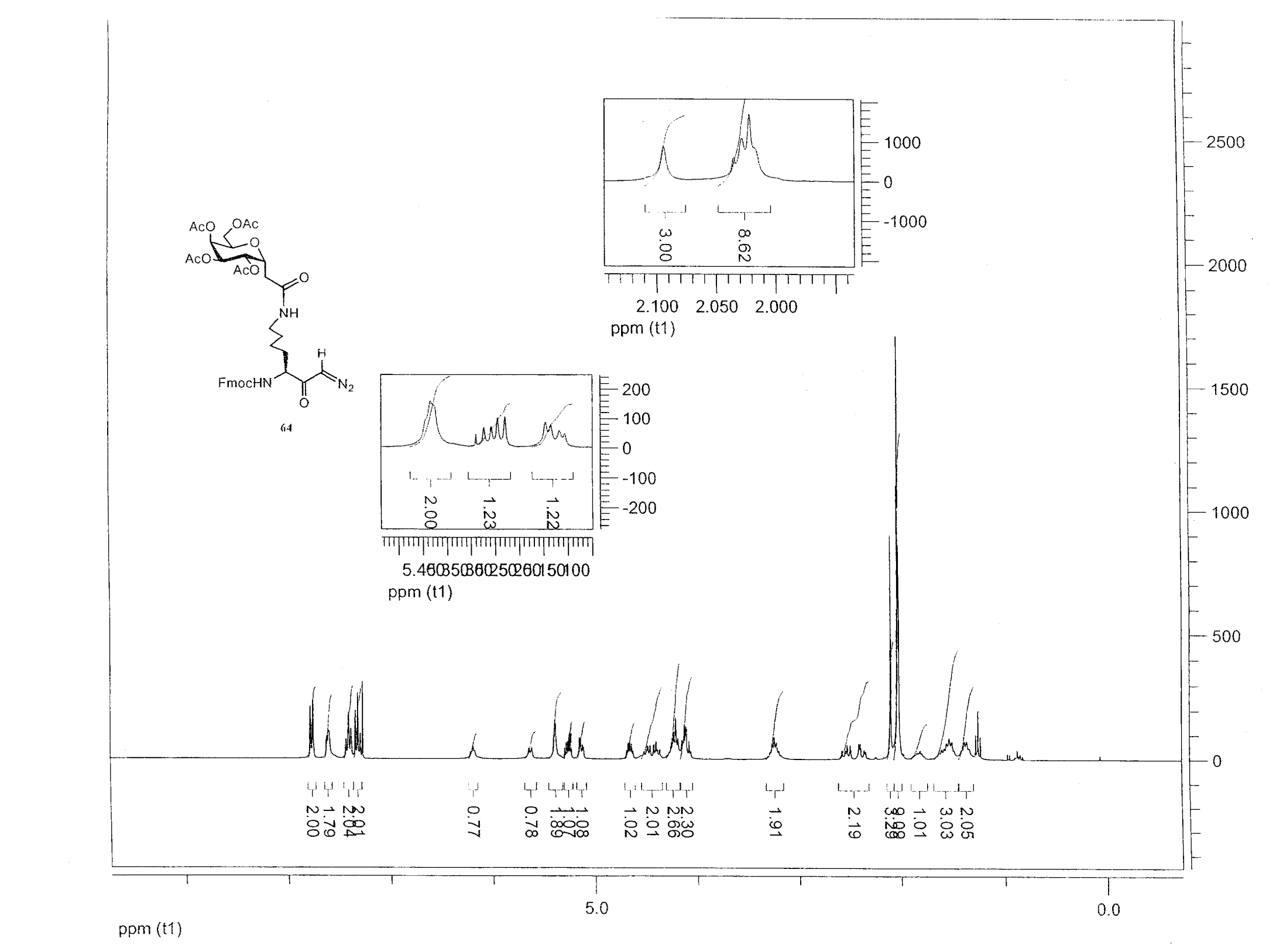
AcO
OAc
AcO
AcO
O
NH
O
FmocHN
H
N2
O
64
3.00
8.62
1000
0
-1000
2.100
2.050
2.000
ppm (t1)
2.00
1.23
1.22
200
100
0
-100
-200
ppm (t1)
2500
2000
1500
1000
500
0
2.00
1.79
2.01
0.77
0.78
1.89
1.02
2.01
1.91
2.19
1.01
3.03
2.05
5.0
0.0
ppm (t1)

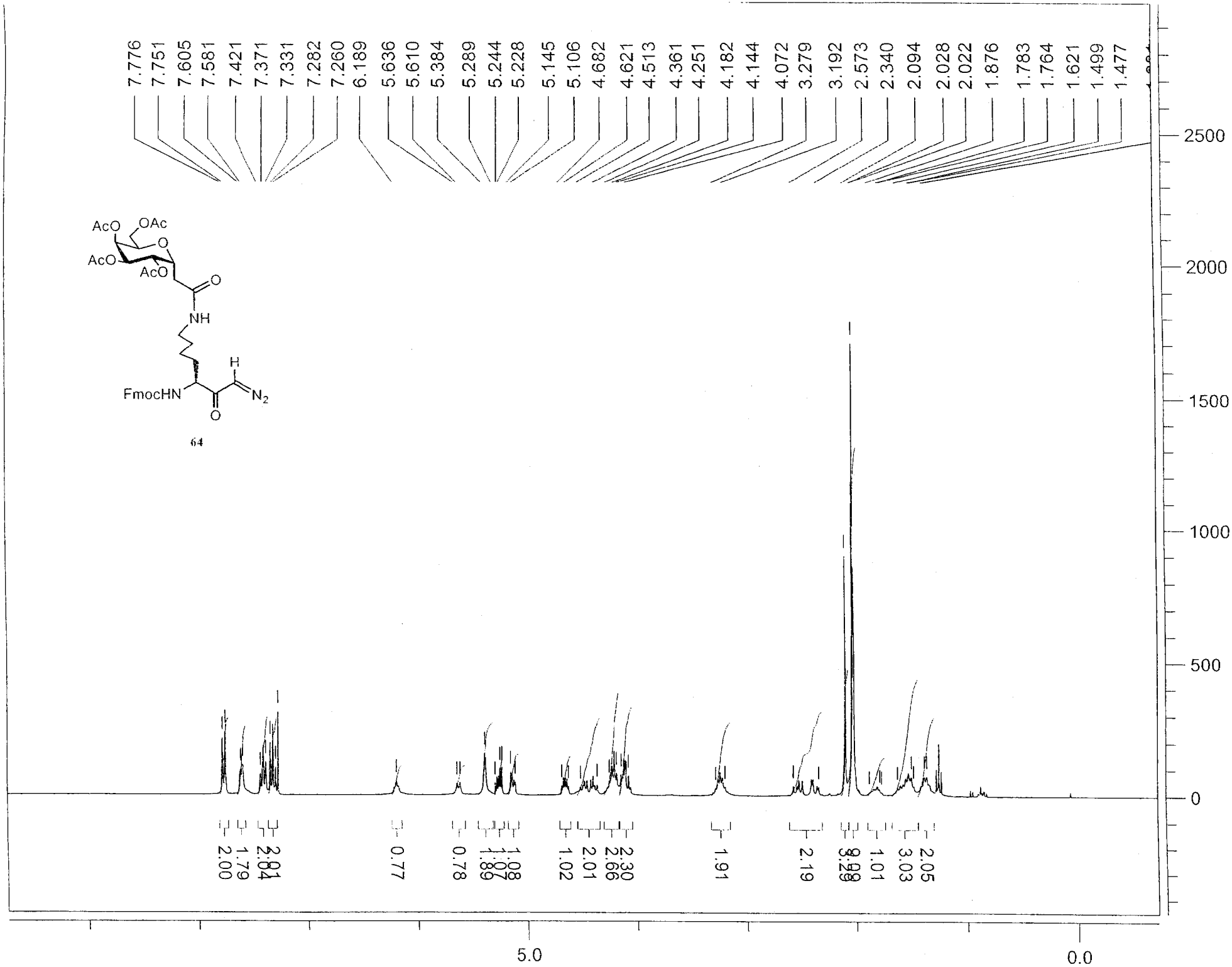
7.776
7.751
7.605
7.581
7.421
7.371
7.331
7.282
7.260
6.189
5.636
5.610
5.384
5.289
5.244
5.228
5.145
5.106
4.682
4.621
4.513
4.361
4.251
4.182
4.144
4.072
3.279
3.192
2.573
2.340
2.094
2.028
2.022
1.876
1.783
1.764
1.621
1.499
1.477
AcO
OAc
AcO
AcO
O
NH
FmocHN
N_2
O
64
2500
2000
1500
1000
500
0
2.00
1.79
2.04
0.77
0.78
1.86
1.08
1.02
2.01
2.66
2.30
1.91
2.19
1.01
3.03
2.05
5.0
0.0
ppm (t1)

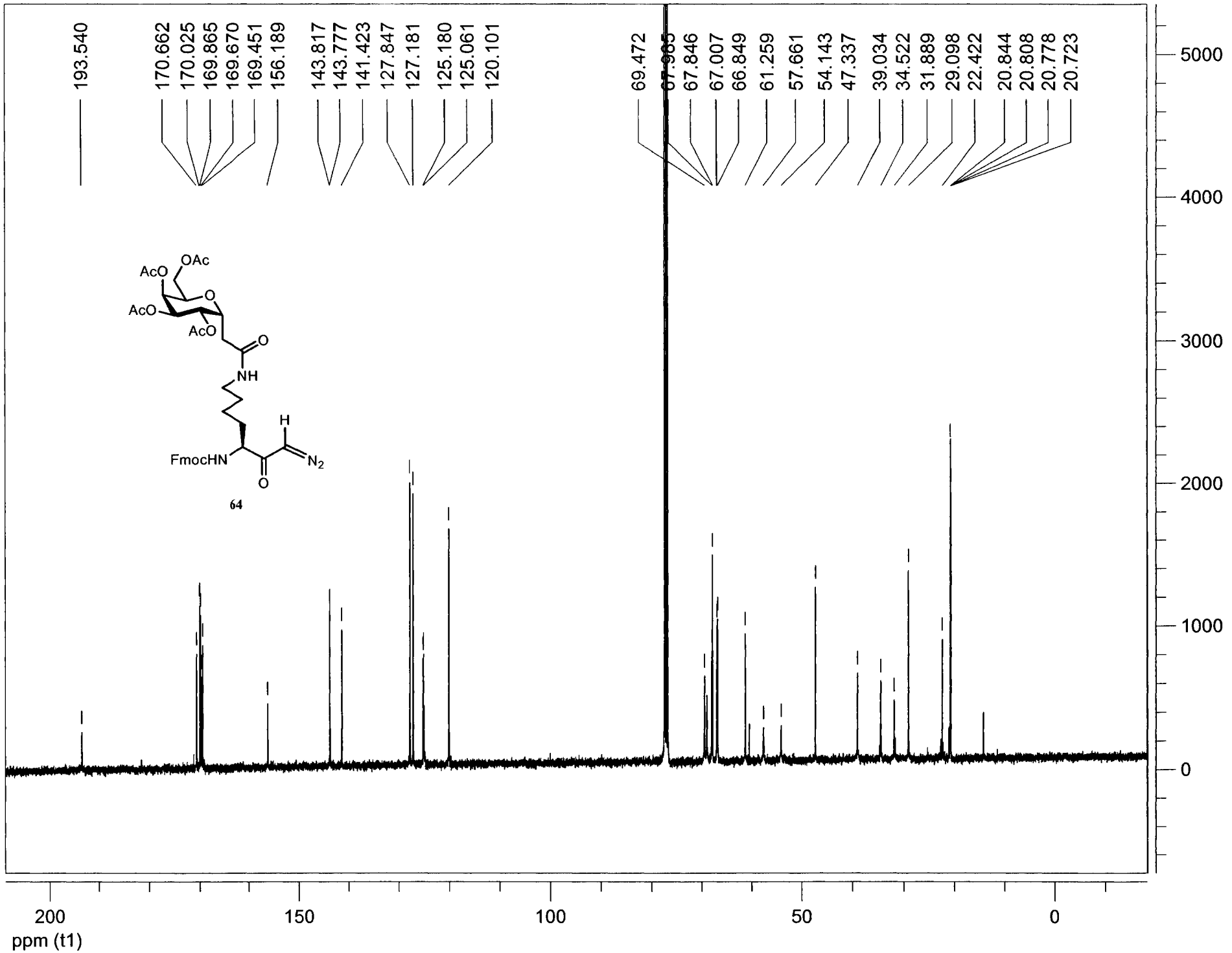
193.540
170.662
170.025
169.865
169.670
169.451
156.189
143.817
143.777
141.423
127.847
127.181
125.180
125.061
120.101
69.472
67.965
67.846
67.007
66.849
61.259
57.661
54.143
47.337
39.034
34.522
31.889
29.098
22.422
20.844
20.808
20.778
20.723
AcO
OAc
AcO
AcO
O
NH
H
FmocHN
N_2
O
O
64
5000
4000
3000
2000
1000
0
200
150
100
50
0
ppm (t1)

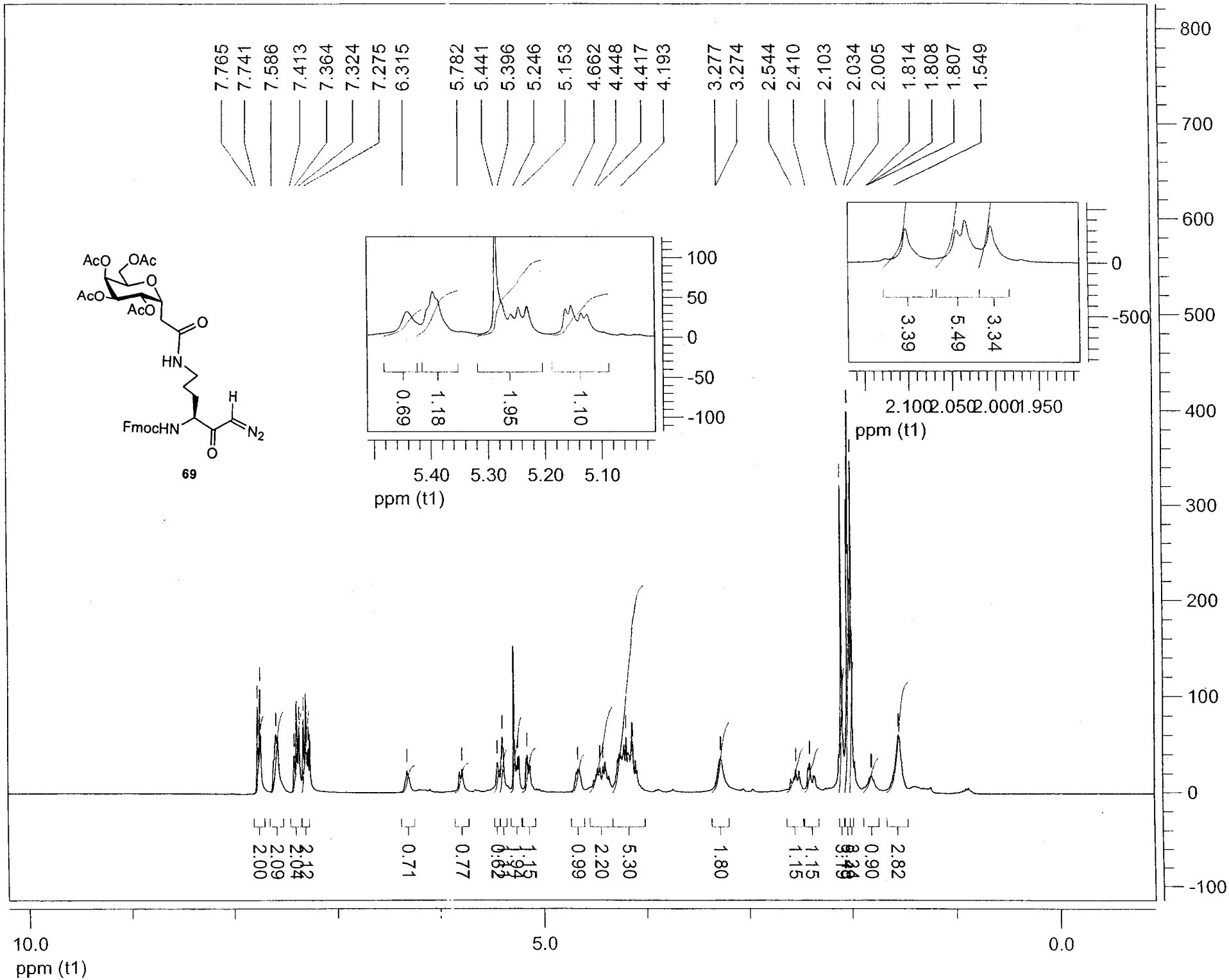
7.765
7.741
7.586
7.413
7.364
7.324
7.275
6.315
5.782
5.441
5.396
5.246
5.153
4.662
4.448
4.417
4.193
3.277
3.274
2.544
2.410
2.103
2.034
2.005
1.814
1.808
1.807
1.549
AcO
OAc
AcO
AcO
O
HN
H
FmocHN
N2
O
O
69
0.69
1.18
1.95
1.10
5.40
5.30
5.20
5.10
ppm (t1)
3.39
5.49
3.34
2.100
2.050
2.000
1.950
ppm (t1)
2.00
2.09
0.71
0.77
0.99
2.20
5.30
1.80
1.15
0.90
2.82
10.0
5.0
0.0
ppm (t1)

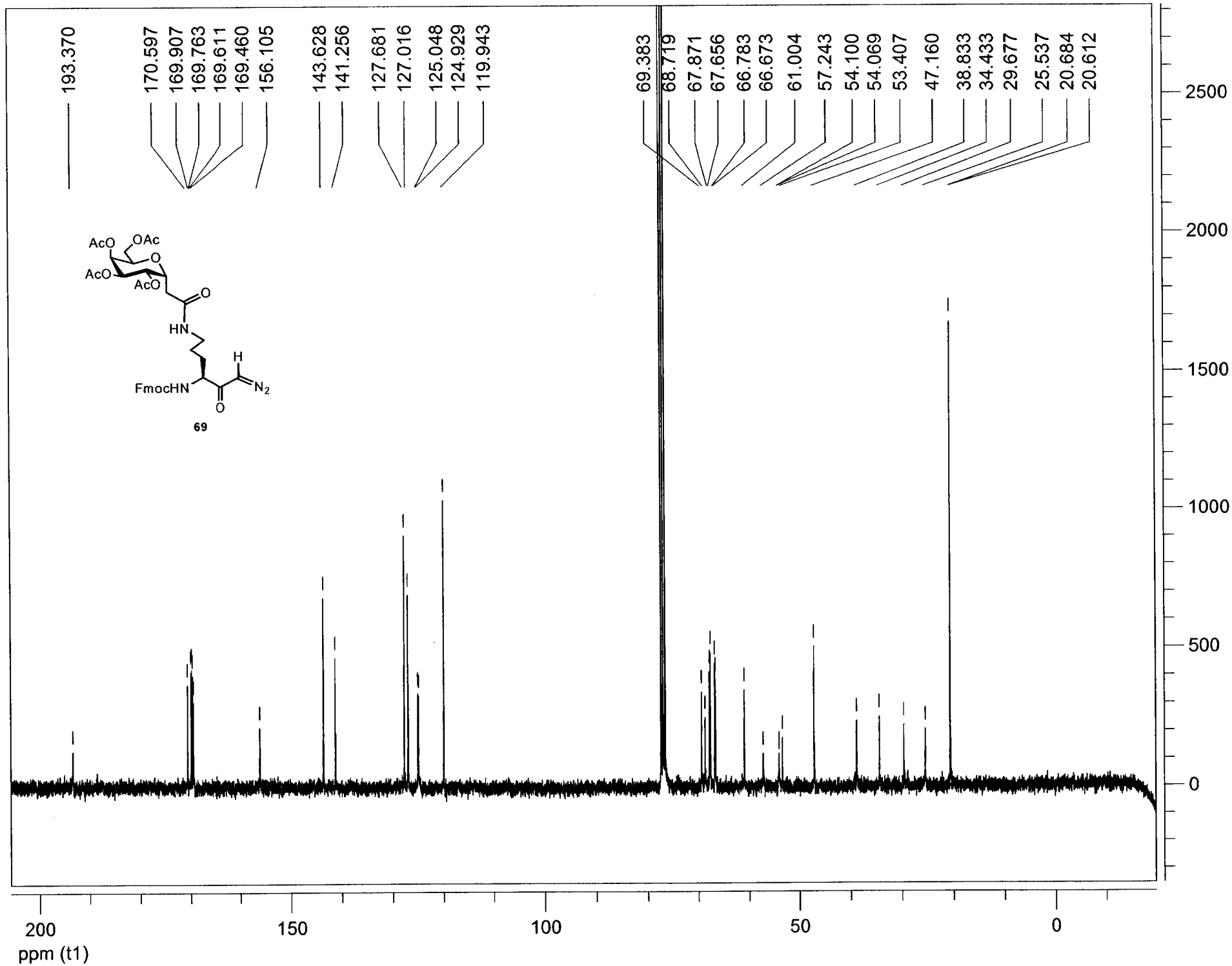
193.370
170.597
169.907
169.763
169.611
169.460
156.105
143.628
141.256
127.681
127.016
125.048
124.929
119.943
69.383
68.719
67.871
67.656
66.783
66.673
61.004
57.243
54.100
54.069
53.407
47.160
38.833
34.433
29.677
25.537
20.684
20.612
AcO
OAc
AcO
AcO
O
HN
H
FmocHN
N2
O
69
2500
2000
1500
1000
500
0
200
150
100
50
0
ppm (t1)

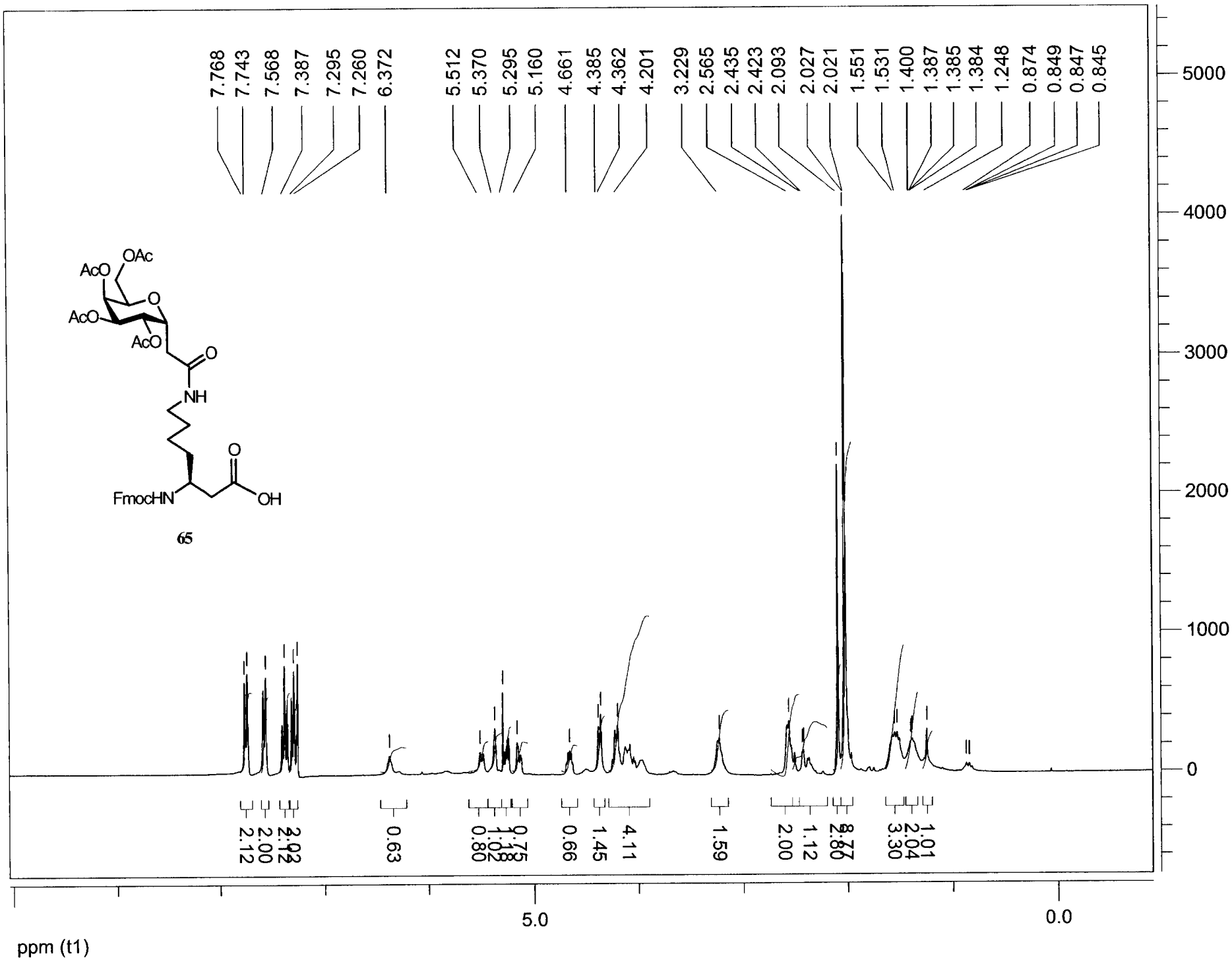
7.768
7.743
7.568
7.387
7.295
7.260
6.372
5.512
5.370
5.295
5.160
4.661
4.385
4.362
4.201
3.229
2.565
2.435
2.423
2.093
2.027
2.021
1.551
1.531
1.400
1.387
1.385
1.384
1.248
0.874
0.849
0.847
0.845
5000
4000
3000
2000
1000
0
2.12
2.00
0.63
0.80
0.99
1.45
4.11
1.59
2.00
1.12
3.30
5.0
0.0
ppm (t1)

65

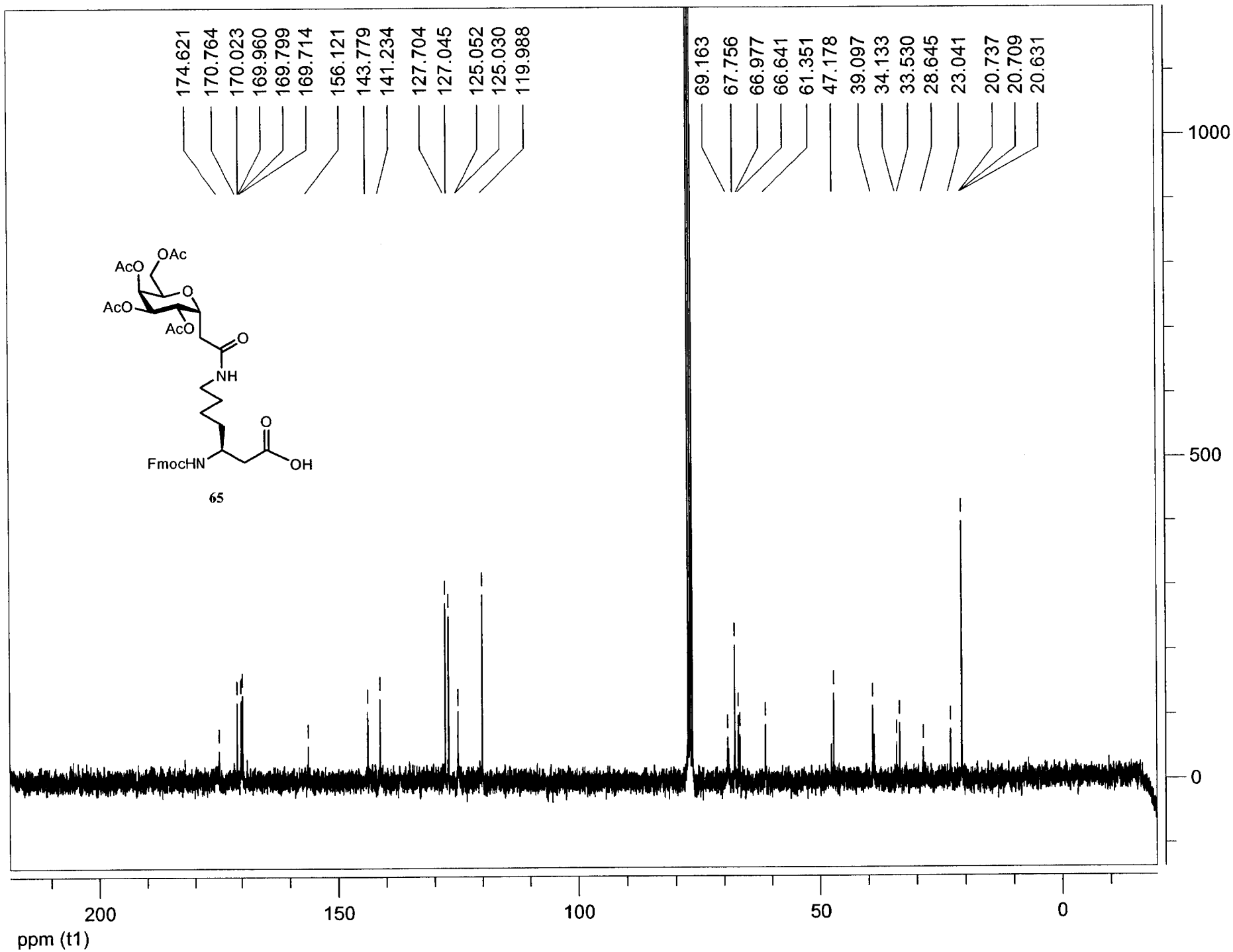
174.621
170.764
170.023
169.960
169.799
169.714
156.121
143.779
141.234
127.704
127.045
125.052
125.030
119.988
69.163
67.756
66.977
66.641
61.351
47.178
39.097
34.133
33.530
28.645
23.041
20.737
20.709
20.631
AcO
OAc
AcO
AcO
O
O
NH
O
FmocHN
OH
1000
500
0
200
150
100
50
0
ppm (t1)

65

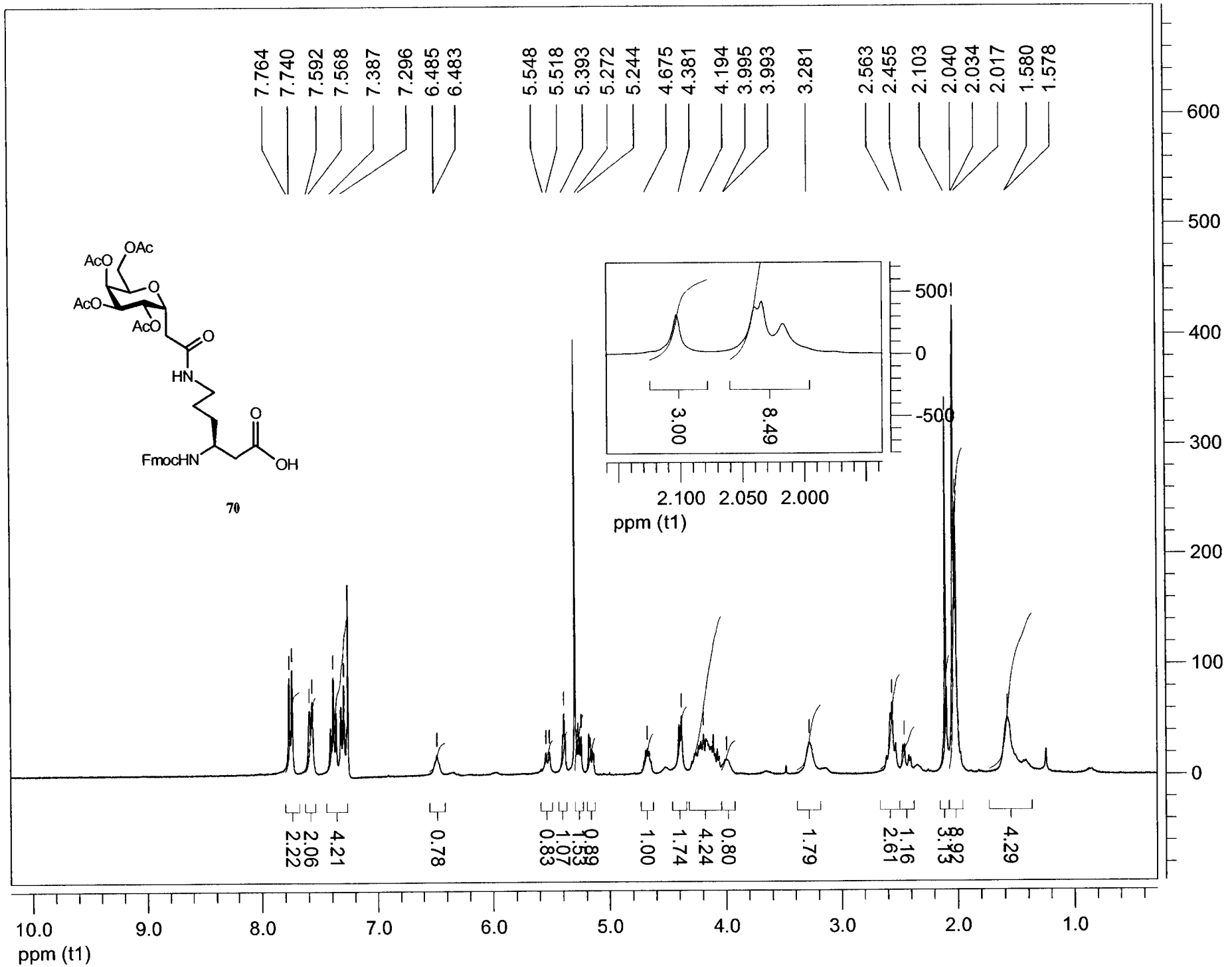
7.764
7.740
7.592
7.568
7.387
7.296
6.485
6.483
5.548
5.518
5.393
5.272
5.244
4.675
4.381
4.194
3.995
3.993
3.281
2.563
2.455
2.103
2.040
2.034
2.017
1.580
1.578
AcO
OAc
AcO
AcO
O
HN
O
O
FmocHN
OH
70
3.00
8.49
2.100 2.050 2.000
ppm (t1)
2.22
2.06
4.21
0.78
0.83
1.07
1.53
0.89
1.00
1.74
4.24
0.80
1.79
2.61
1.16
3.13
8.92
4.29
10.0 9.0 8.0 7.0 6.0 5.0 4.0 3.0 2.0 1.0
ppm (t1)

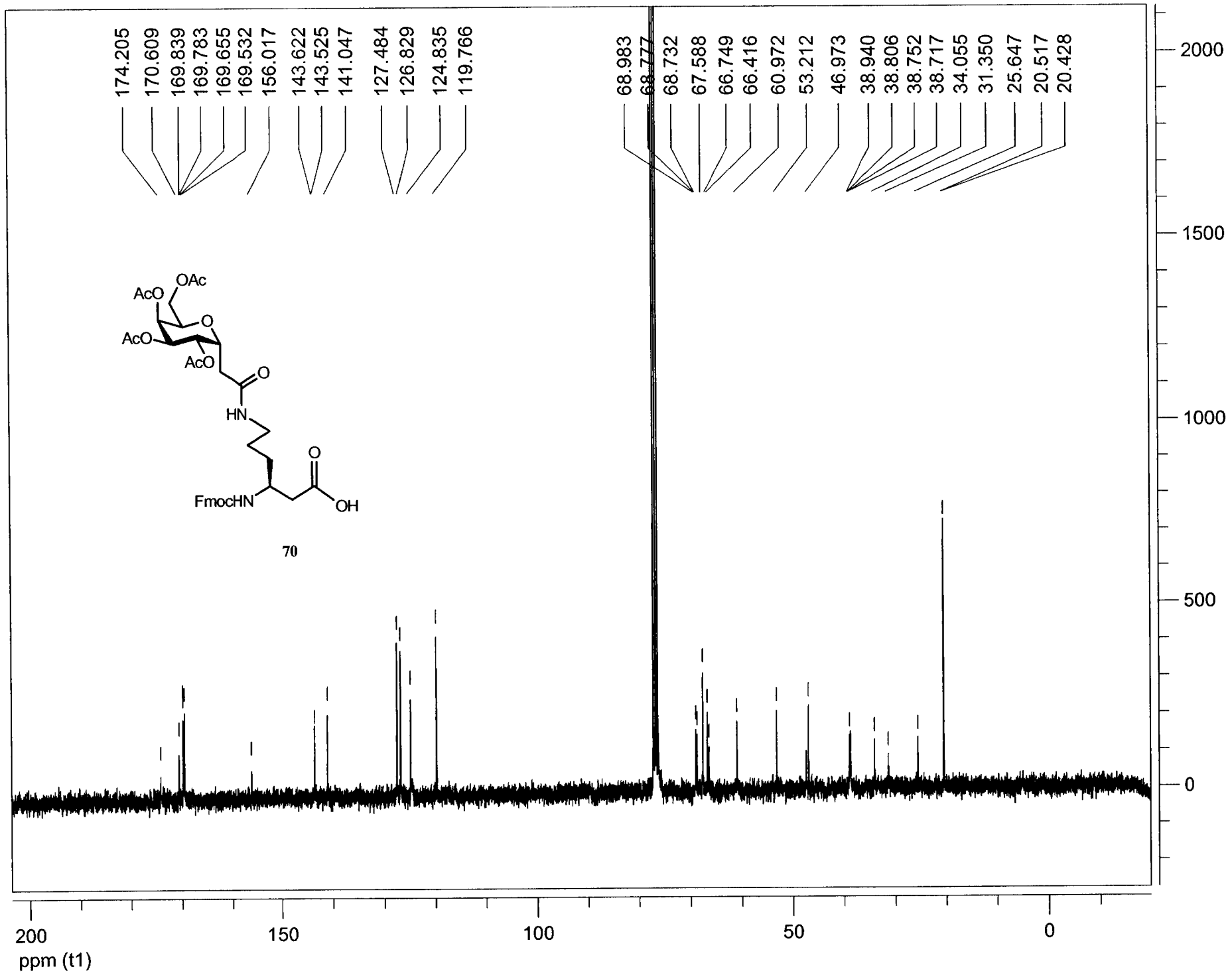
174.205
170.609
169.839
169.783
169.655
169.532
156.017
143.622
143.525
141.047
127.484
126.829
124.835
119.766
68.983
68.777
68.732
67.588
66.749
66.416
60.972
53.212
46.973
38.940
38.806
38.752
38.717
34.055
31.350
25.647
20.517
20.428
OAc
AcO
AcO
AcO
O
O
HN
O
FmocHN
OH
2000
1500
1000
500
0
200
150
100
50
0
ppm (t1)

70

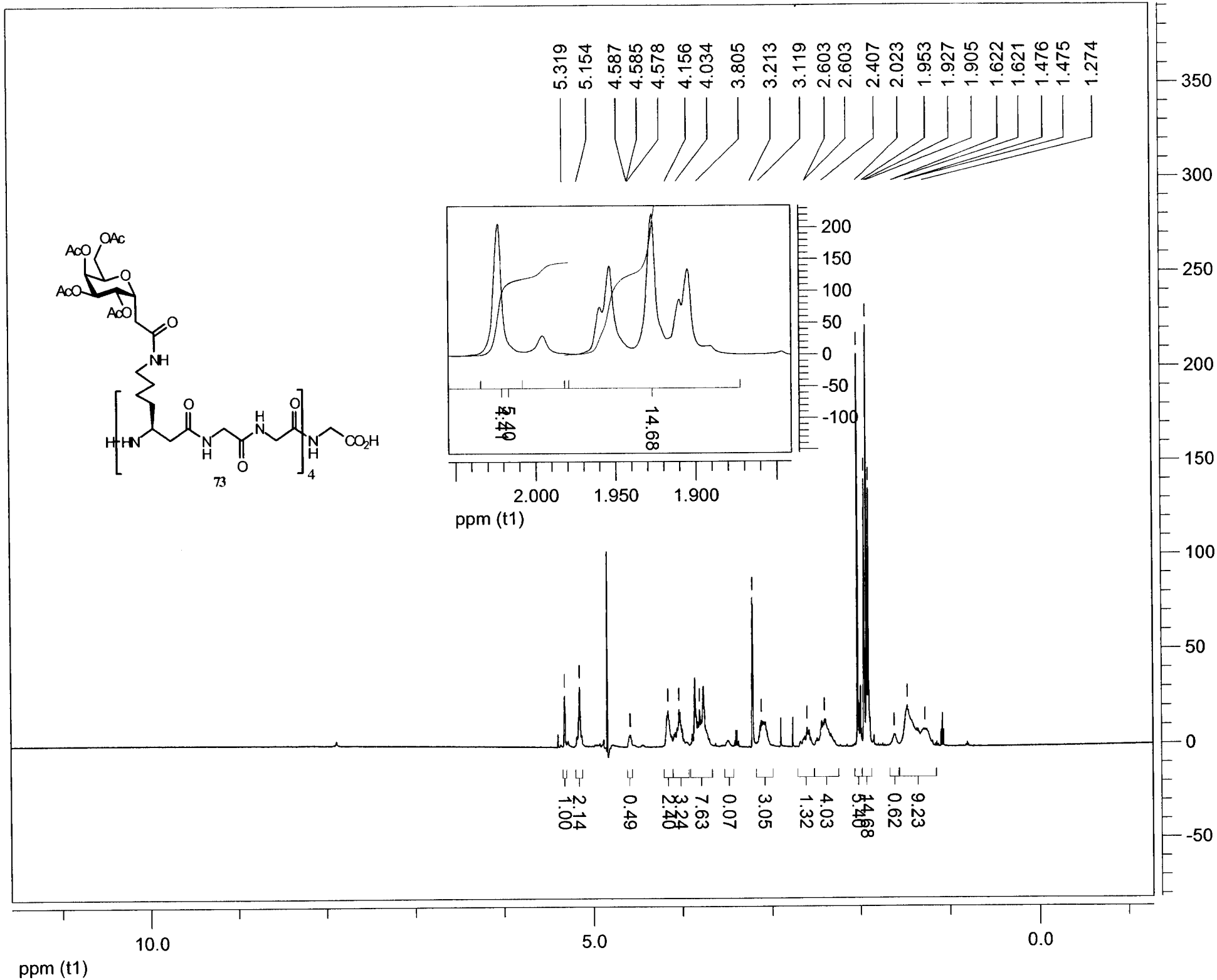
5.319
5.154
4.587
4.585
4.578
4.156
4.034
3.805
3.213
3.119
2.603
2.603
2.407
2.023
1.953
1.927
1.905
1.622
1.621
1.476
1.475
1.274
AcO
OAc
AcO
AcO
O
NH
HN
O
N
H
O
N
H
O
CO2H
73
4
5.40
14.68
2.000
1.950
1.900
ppm (t1)
1.00
2.14
0.49
2.40
3.24
7.63
0.07
3.05
1.32
4.03
5.40
14.68
0.62
9.23
10.0
5.0
0.0
ppm (t1)

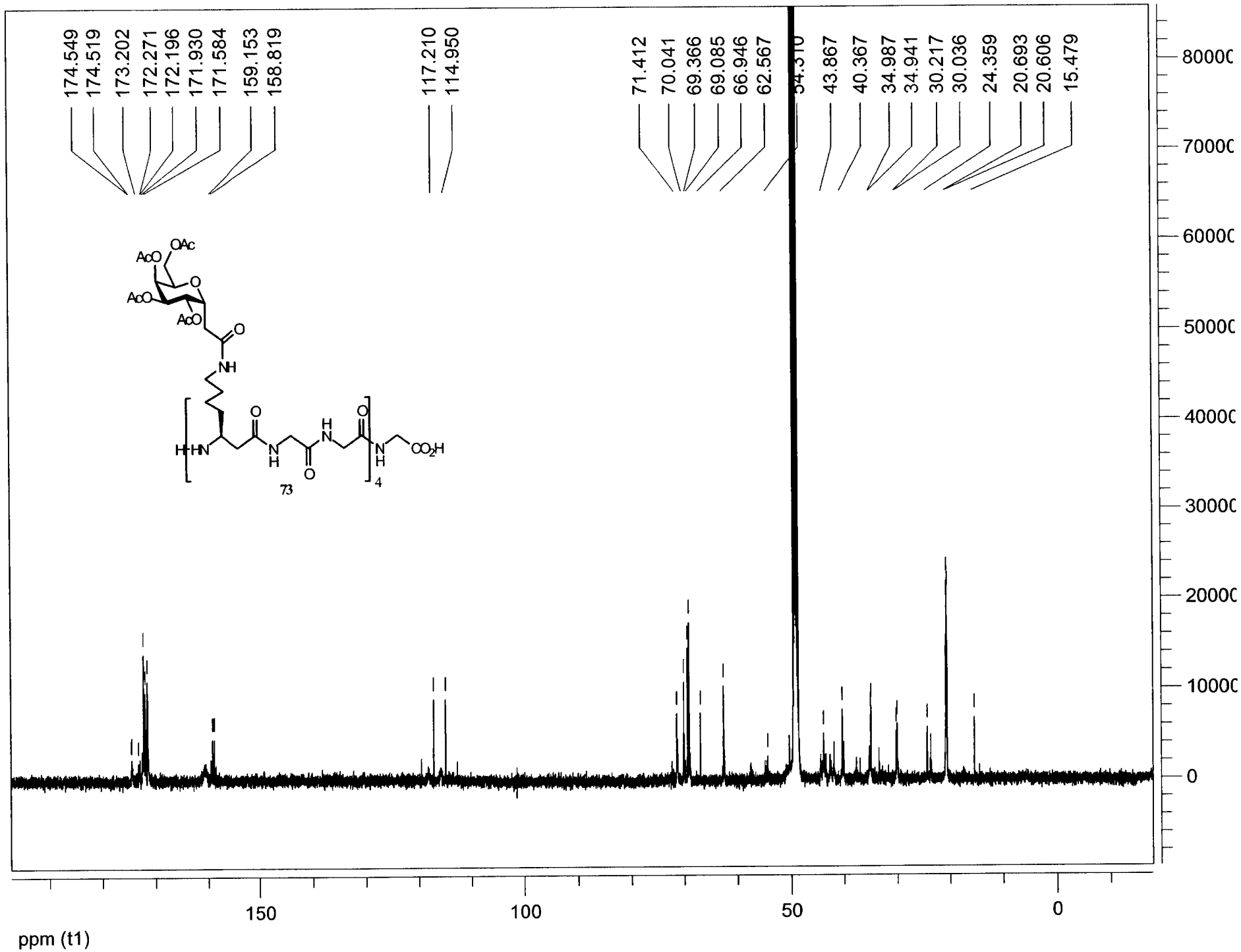
174.549
174.519
173.202
172.271
172.196
171.930
171.584
159.153
158.819
117.210
114.950
71.412
70.041
69.366
69.085
66.946
62.567
54.310
43.867
40.367
34.987
34.941
30.217
30.036
24.359
20.693
20.606
15.479
AcO
OAc
AcO
AcO
O
NH
HN
H
N
O
CO2H
4
73
8000
7000
6000
5000
4000
3000
2000
1000
0
150
100
50
0
ppm (t1)

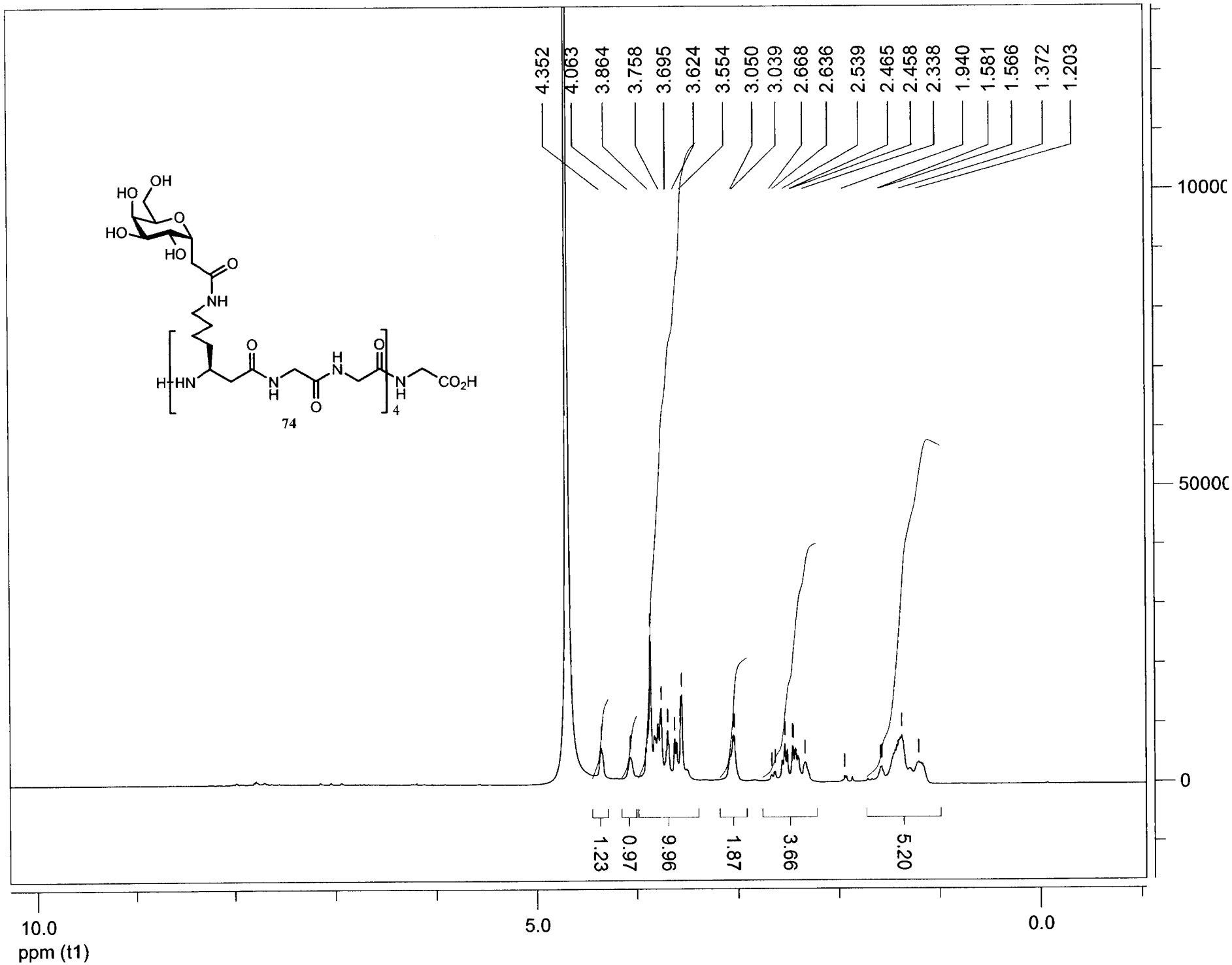
4.352
4.063
3.864
3.758
3.695
3.624
3.554
3.050
3.039
2.668
2.636
2.539
2.465
2.458
2.338
1.940
1.581
1.566
1.372
1.203
10000
50000
0
1.23
0.97
9.96
1.87
3.96
5.20
10.0
5.0
0.0
ppm (t1)
74

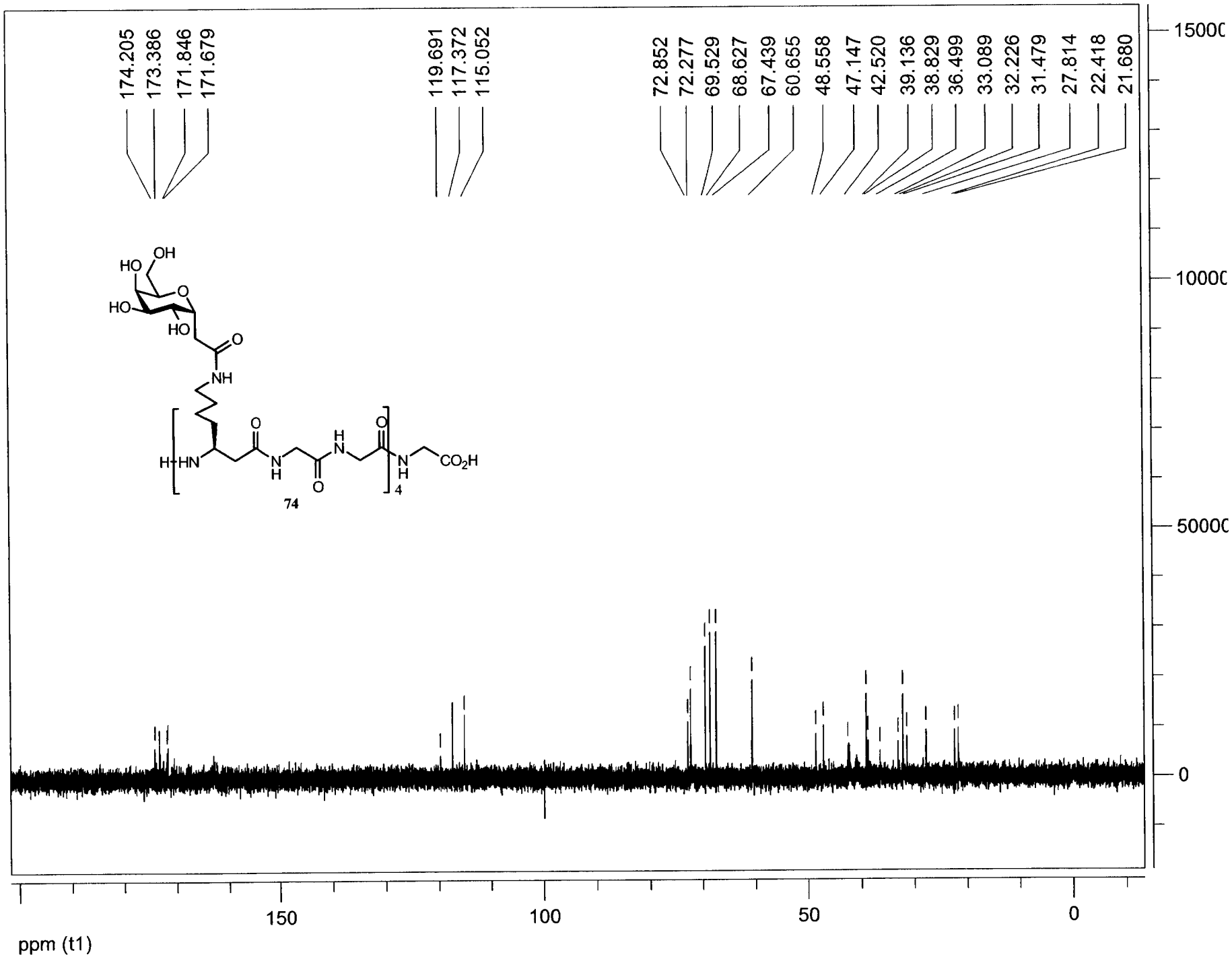
174.205
173.386
171.846
171.679
119.691
117.372
115.052
72.852
72.277
69.529
68.627
67.439
60.655
48.558
47.147
42.520
39.136
38.829
36.499
33.089
32.226
31.479
27.814
22.418
21.680
HO
OH
HO
O
HO
O
NH
H
HN
O
N
H
O
H
N
O
N
H
4
CO2H
74
150
100
50
0
ppm (t1)

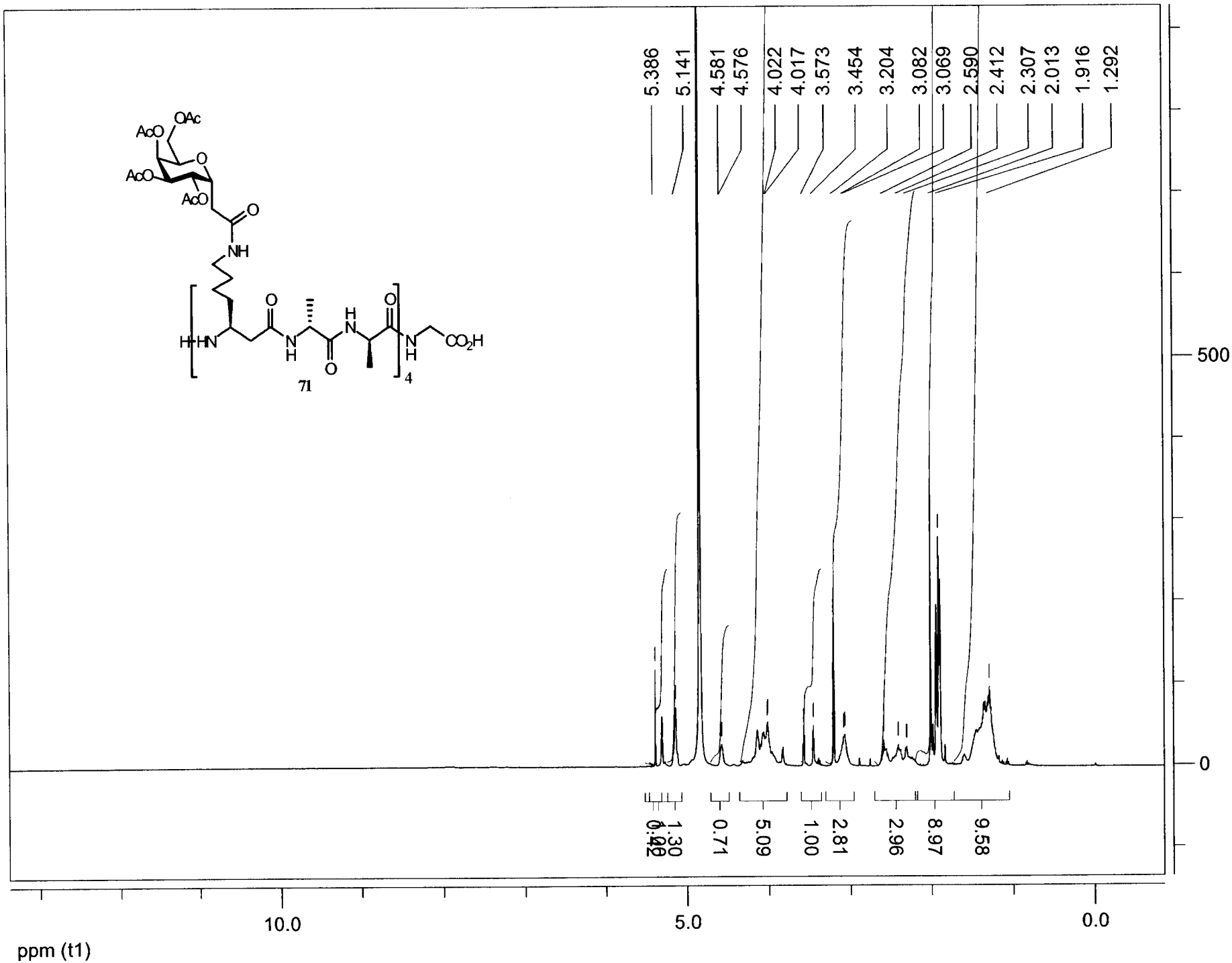
5.386
5.141
4.581
4.576
4.022
4.017
3.573
3.454
3.204
3.082
3.069
2.590
2.412
2.307
2.013
1.916
1.292
500
0
1.30
0.71
5.09
1.00
2.81
2.96
8.97
9.58
10.0
5.0
0.0
ppm (t1)
71

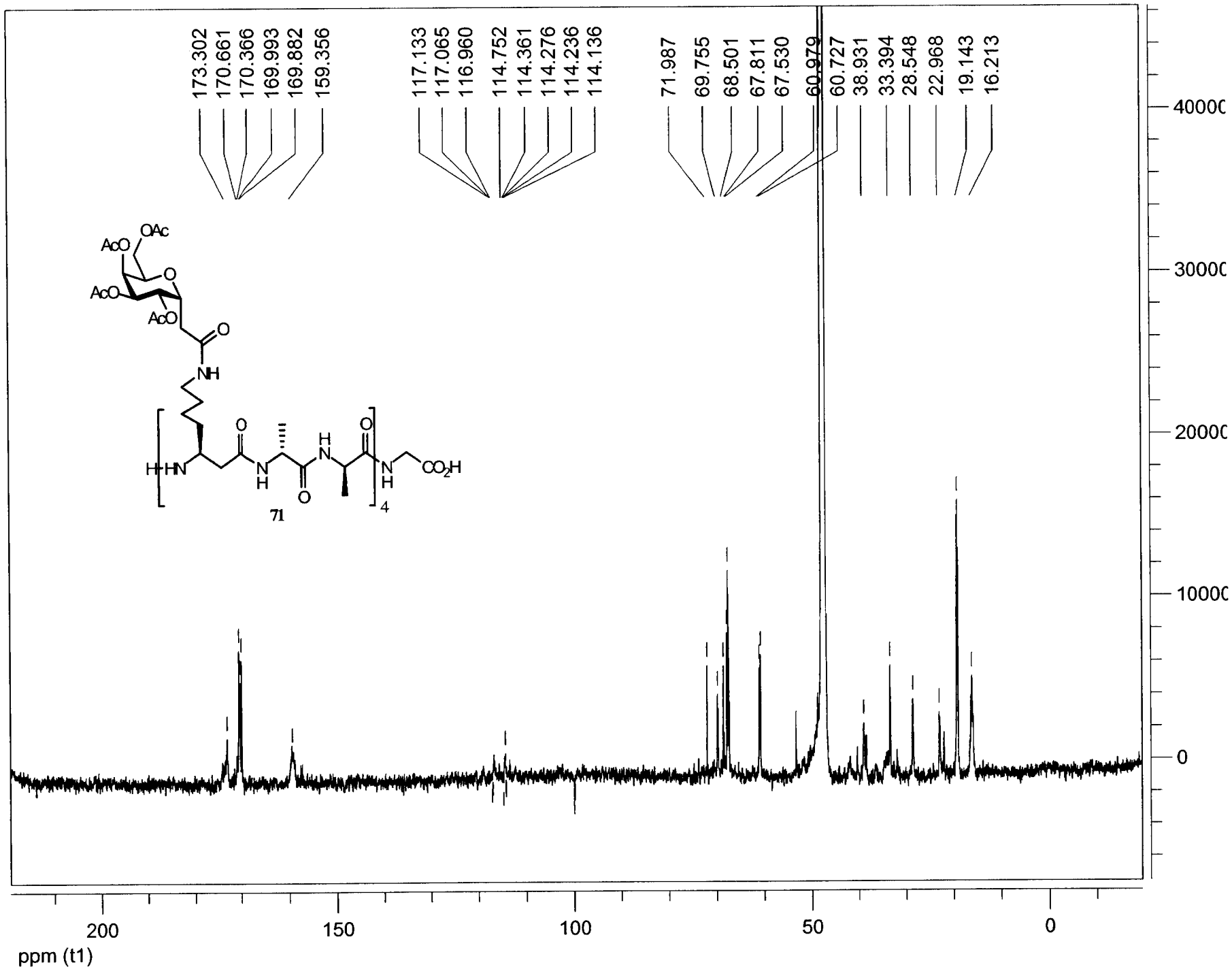
173.302
170.661
170.366
169.993
169.882
159.356
117.133
117.065
116.960
114.752
114.361
114.276
114.236
114.136
71.987
69.755
68.501
67.811
67.530
60.979
60.727
38.931
33.394
28.548
22.968
19.143
16.213
4000
3000
2000
1000
0
200
150
100
50
0
ppm (t1)
71

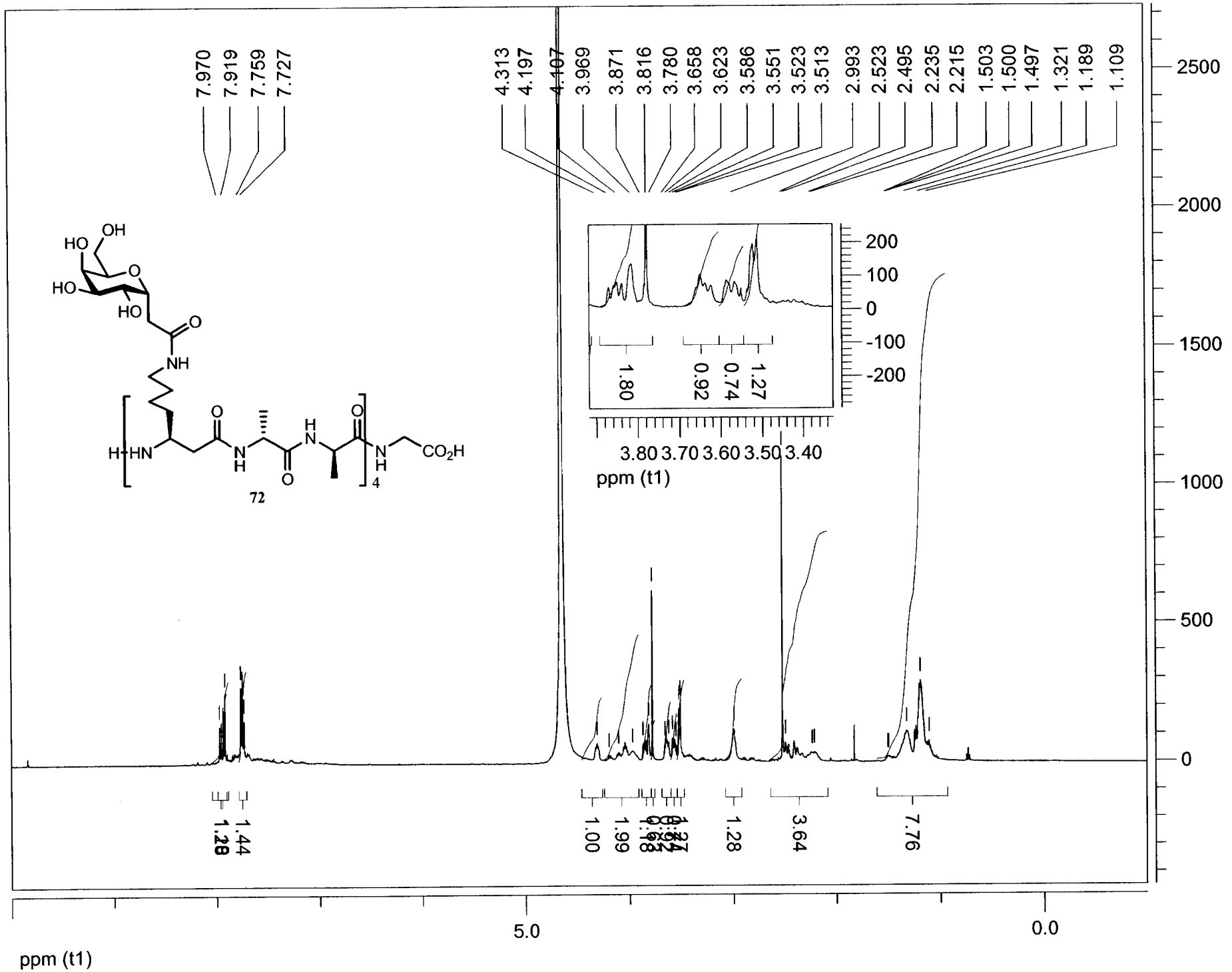
7.970
7.919
7.759
7.727
4.313
4.197
4.107
3.969
3.871
3.816
3.780
3.658
3.623
3.586
3.551
3.523
3.513
2.993
2.523
2.495
2.235
2.215
1.503
1.500
1.497
1.321
1.189
1.109
HO
OH
HO
O
HO
O
NH
H-HN
O
N
H
O
N
H
O
N
H
CO2H
4
72
1.80
0.92
0.74
1.27
3.80 3.70 3.60 3.50 3.40
ppm (t1)
200
100
0
-100
-200
2500
2000
1500
1000
500
0
1.28
1.44
1.00
1.99
1.28
3.64
7.76
5.0
0.0
ppm (t1)

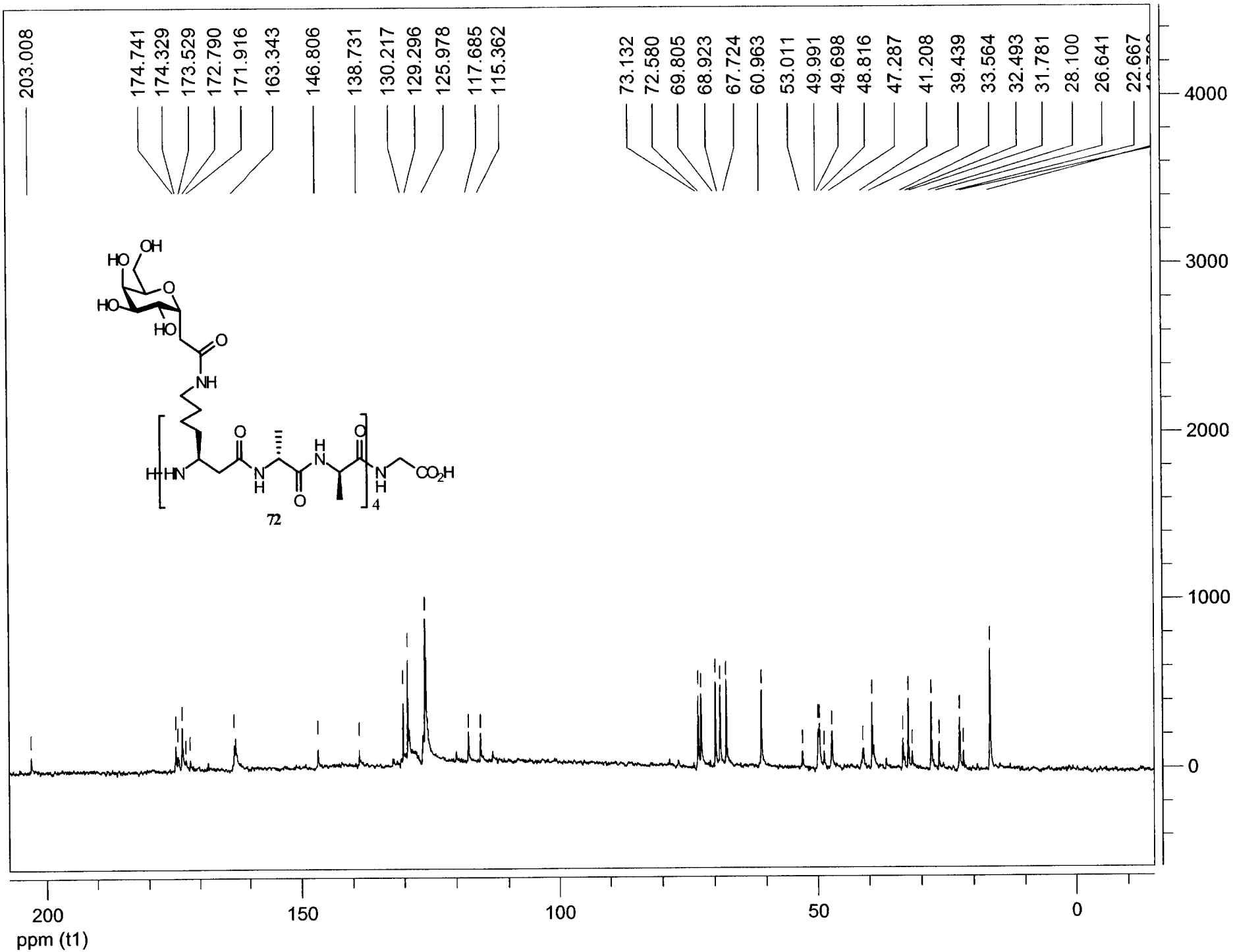
203.008
174.741
174.329
173.529
172.790
171.916
163.343
146.806
138.731
130.217
129.296
125.978
117.685
115.362
73.132
72.580
69.805
68.923
67.724
60.963
53.011
49.991
49.698
48.816
47.287
41.208
39.439
33.564
32.493
31.781
28.100
26.641
22.667
4000
3000
2000
1000
0
200
150
100
50
0
ppm (t1)

72

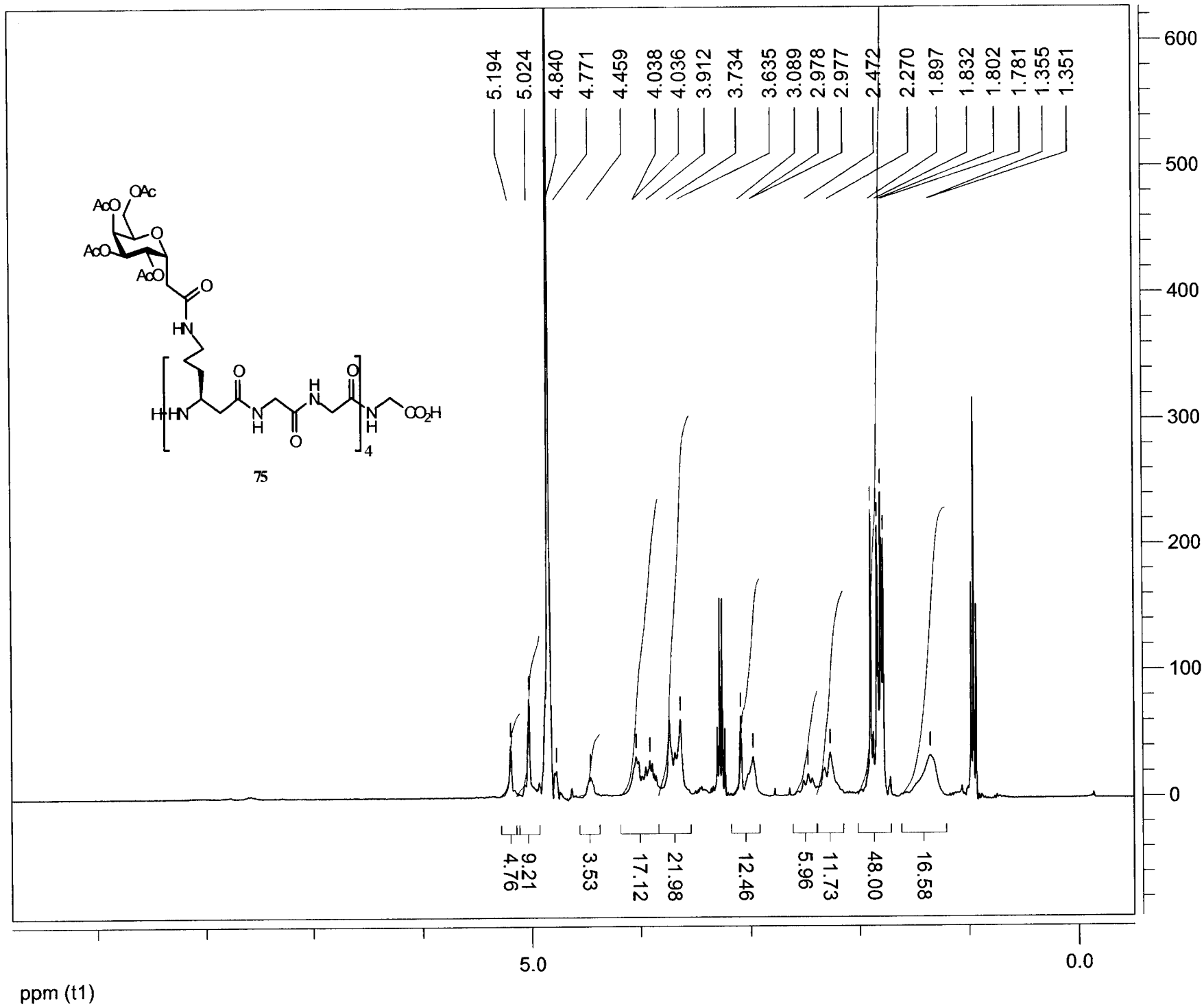
5.194
5.024
4.840
4.771
4.459
4.038
4.036
3.912
3.734
3.635
3.089
2.978
2.977
2.472
2.270
1.897
1.832
1.802
1.781
1.355
1.351
4.76
9.21
3.53
17.12
21.98
12.46
5.96
11.73
48.00
16.58
600
500
400
300
200
100
0
5.0
0.0
ppm (t1)

75

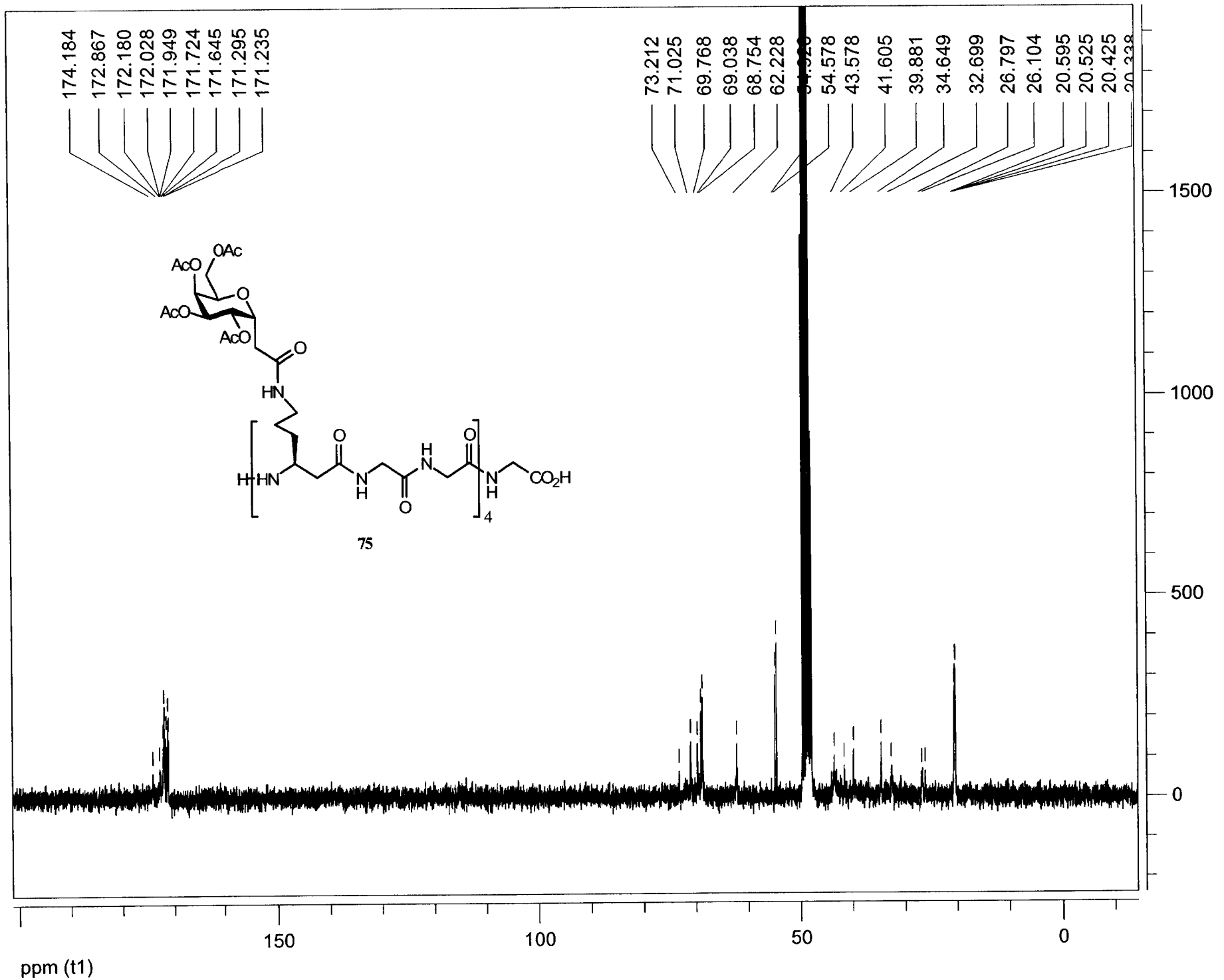
174.184
172.867
172.180
172.028
171.949
171.724
171.645
171.295
171.235
73.212
71.025
69.768
69.038
68.754
62.228
54.578
43.578
41.605
39.881
34.649
32.699
26.797
26.104
20.595
20.525
20.425
1500
1000
500
0
150
100
50
0
ppm (t1)
AcO
OAc
AcO
AcO
O
HN
O
H
HN
N
H
O
N
H
O
4
CO2H

75

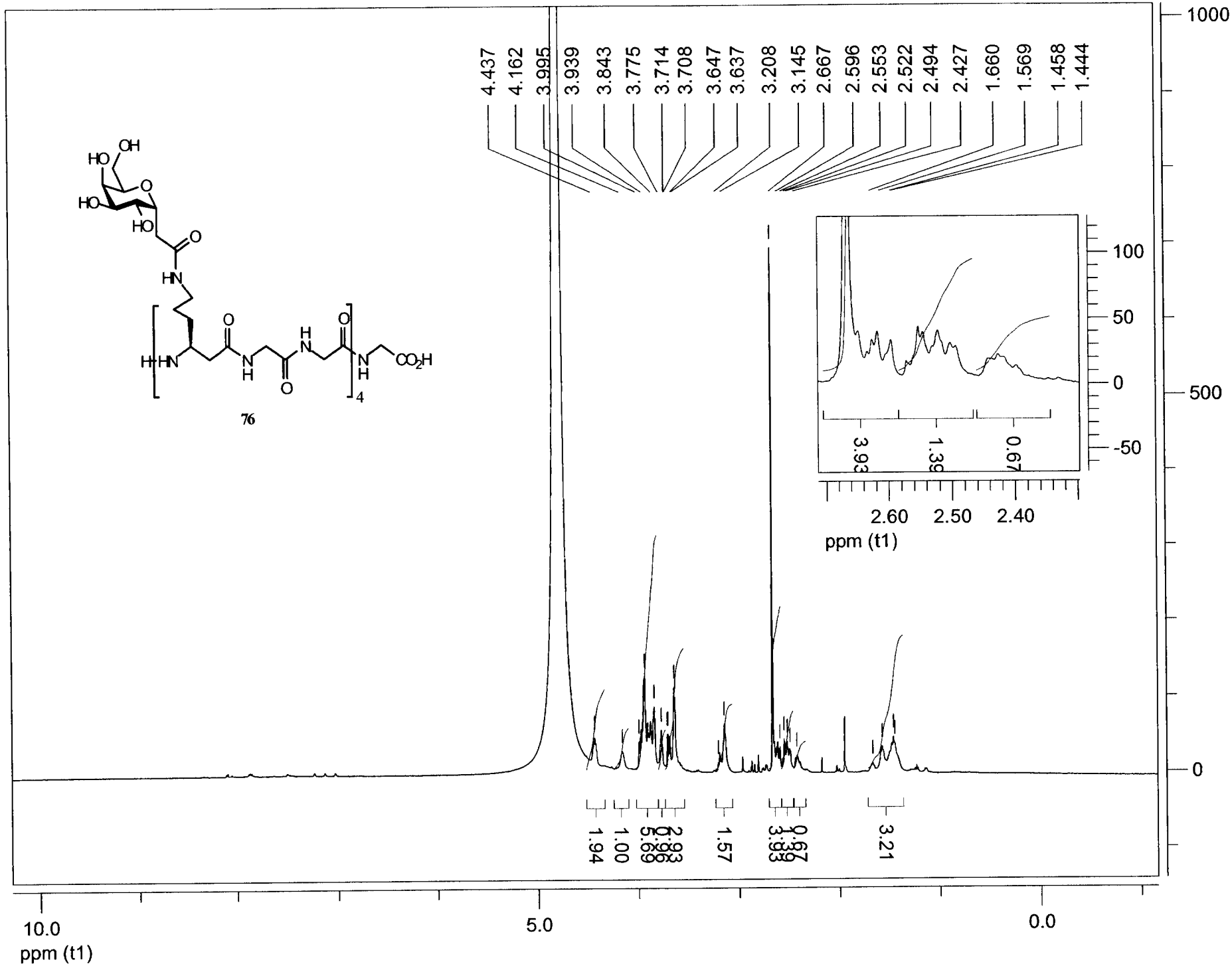
4.437
4.162
3.995
3.939
3.843
3.775
3.714
3.708
3.647
3.637
3.208
3.145
2.667
2.596
2.553
2.522
2.494
2.427
1.660
1.569
1.458
1.444
1000
500
0
100
50
0
-50
3.93
1.39
0.67
2.60
2.50
2.40
ppm (t1)
1.94
1.00
5.66
2.93
1.57
3.93
0.67
3.21
10.0
5.0
0.0
ppm (t1)

76

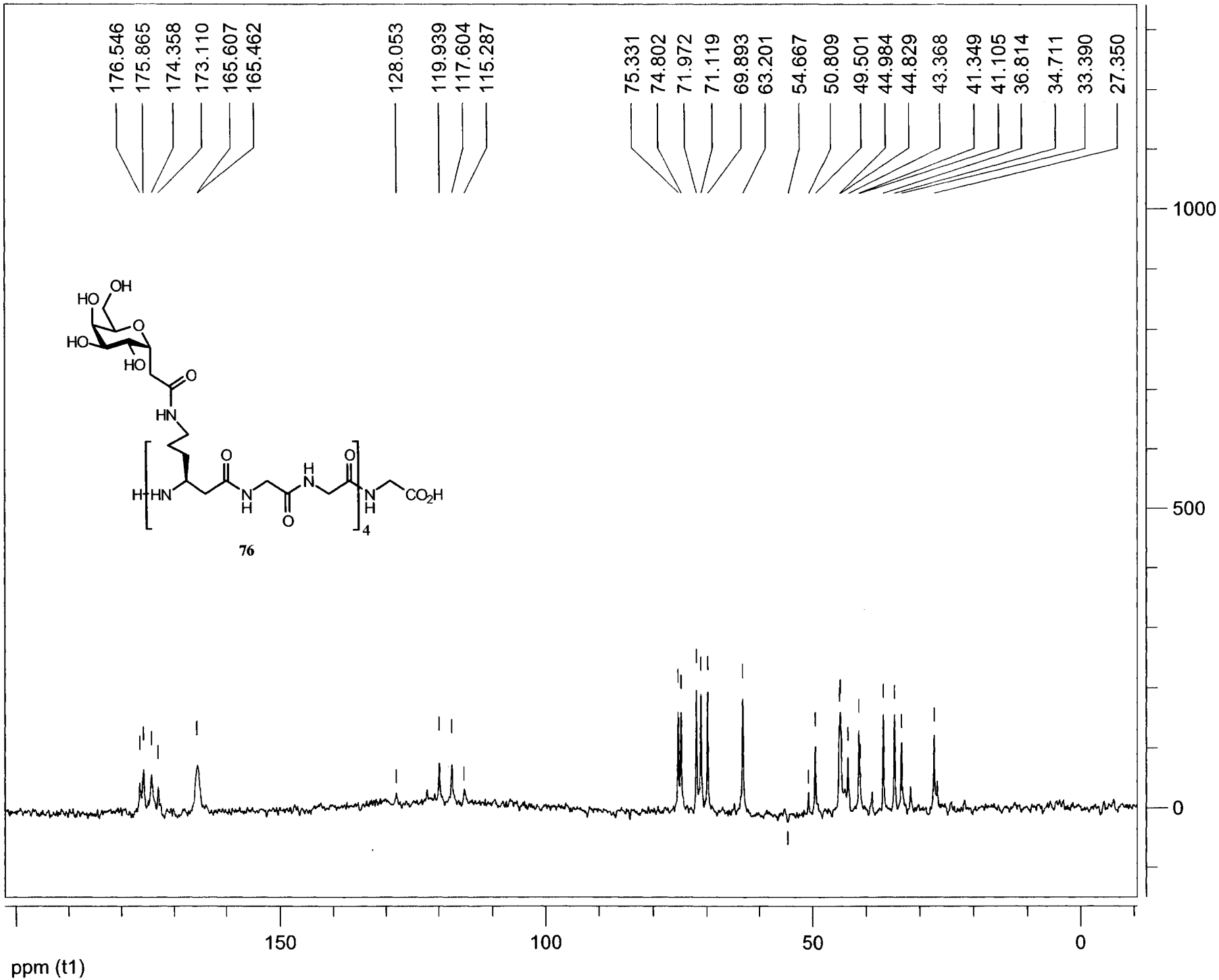
176.546
175.865
174.358
173.110
165.607
165.462
128.053
119.939
117.604
115.287
75.331
74.802
71.972
71.119
69.893
63.201
54.667
50.809
49.501
44.984
44.829
43.368
41.349
41.105
36.814
34.711
33.390
27.350
1000
500
0
150
100
50
0
ppm (t1)

76